UNIVERSITAT POLITÈCNICA DE VALÈNCIA

INSTITUTO DE RECONOCIMIENTO MOLECULAR Y DESARROLLO TECNOLÓGICO

Tesis Doctoral

Desarrollo de métodos integrados para la determinación de biomarcadores genéticos

Presentada por **Sara Martorell Tejedor** para optar al grado de Doctor en Técnicas Experimentales en Química por la Universitat Politècnica de València

Directores

Dr. Ángel Maquieira Catalá

Dr. Luis Antonio Tortajada Genaro

Septiembre de 2021

CERTIFICADO IDM

D. Ángel Maquieira Catalá, Catedrático de Universidad del Departamento de Química de la Universitat Politècnica de València.

D. Luis Antonio Tortajada Genaro, Profesor Titular del Departamento de Química de la Universitat Politècnica de València.

CERTIFICAN:

Que el trabajo que presenta Sara Martorell Tejedor en esta memoria, con el título "Desarrollo de métodos integrados para la determinación de biomacadores genéticos" ha sido realizado bajo nuestra dirección en el Instituto de Reconocimiento Molecular y Desarrollo Tecnológico (IDM) para optar al grado de Doctor por la Universitat Politècnica de València.

Para que así conste, firman el presente certificado en Valencia, a 21 de Junio de 2021.

Dr. Ángel Maquieira Catalá

Dr. Luis Antonio Tortajada Genaro

AGRADECIMIENTOS

"Nada en la vida es para ser temido, es sólo para ser comprendido. Ahora es el momento de entender más, de modo que podamos temer menos". Marie Curie (1867-1934).

Todavía recuerdo el primer día que llegué al grupo SyM y ya han pasado unos cuantos años desde entonces, pero para mí, ir al laboratorio sigue siendo como estar en casa. A lo largo de esta etapa he conocido a muchas personas y algunas de ellas van a formar parte de mí para siempre.

Quería agradecer en primer lugar a mis tutores de tesis. A Ángel, por todo el apoyo y dedicación que me ha ofrecido durante estos años. Desde el inicio, por haber confiado en mí y haberme dado la oportunidad de formar parte de su equipo. Por su amabilidad, su buen hacer y su sabiduría, por orientarme y ayudarme en todo este proceso de tesis doctoral. A Luis, por darme infinitas directrices en el mundo de la investigación. Por su visión y enfoque científicos, por las ideas desarrolladas, la creatividad y el aprendizaje constante. He sido una afortunada, puesto que he tenido a dos grandes tutores de tesis como referentes, que me han enseñado a descubrir, pensar, experimentar y reflexionar mejor. Gracias a ambos por impulsarme a crecer.

A Sergi, por su apoyo incondicional, por darme alas y voluntad para creer en mi misma. Su visión de la vida y su dedicación han sido y son, una piedra angular para mí. A Mª José Bañuls, por ser siempre tan amable y tener siempre una sonrisa dibujada. A Miguel Ángel, por ayudarme en los experimentos, por su simpatía y sus anécdotas siempre divertidas. A David, por su ingenio y su risa contagiosa. También quería agradecer a Nuria, Patricia y Pilar por los momentos compartidos. A Rosa, por su ejemplo, a Marichu y Júlia por ser tan amables y proveernos siempre de dulces en el seminario. A todos los demás miembros de la unidad docente que han compartido momentos conmigo. Gracias a todos, sois unos grandes profesionales y me habéis hecho sentir en casa.

A mis compis del lab, no podría sentirme más dichosa. Sin ellos, nada habría sido lo mismo. Más que compañeros, son amigos y todos unos cracks. A todos los quiero mucho, tanto a los que están conmigo desde el inicio, los que llegaron hace poco, como a los que se fueron. Gracias a Maribel, Vicky, Edurne, Pilar, Pedro, William, Cintia, Yeray, Amadeo, Gabi, Salva, Mjota, Dani, Eric, Zeneida, Noelle, Estrella, Andy, Aitor, sois geniales! Gracias a Paola y Julieth, llegasteis cuando yo ya estaba de partida, pero me habría gustado compartir más tiempo con vosotras, sois maravillosas. A Miquel y Augusto, por ser tan bonicos de corazón, por ayudarme siempre que lo he necesitado. Y, por último, a Ana, a mi querida Anis, porque eres un sol de persona, mi compañera de ADN, mi amiga y confidente, gracias por tus valores, tu cariño, gracias por todos los abrazos. Me siento profundamente agradecida de haber invertido mi tiempo y esfuerzo en formar parte de este equipo multidisciplinar lleno de gente interesante e inteligente.

A mis padres, por impulsarme, por darme la mano siempre que me caigo, por cuidarme día a día, por su bondad. A mi tía Guiller, por darme las herramientas que necesito para enfrentarme a los obstáculos, por su esfuerzo y trabajo, por ser ejemplo. A mis tías y tíos, a mis primas y primos, por su cariño. A los que ya no están, pero siguen estando presentes. En especial a mi abuela Guillermina, por ser ejemplo de superación y bondad. Por inculcarme sus valores y principios. Gracias a toda mi familia.

A mis amigas y amigos, a todos ellos, empezando por mis amigas de la universidad, que son ya mi familia, y que están apoyándome día a día en todo este proceso, en especial quería agradecer a Maite, por estar siempre, a Mara, Rubén y Maricruz por estar en el día a día y por ser un referente, también a Mari y Miriam. A las amigas que la vida me ha ido poniendo en el camino, especialmente quiero agradecer a Sandra, Ana y Vanesa, por estar conmigo en casa tras salir del lab y apoyarnos mutuamente. A mis amigas y amigos de toda la vida, a Miriam, Erika, Celina, Miguel Ángel, Mjota, María, Emma, Belén, Mela, Blanqui, Fina, Nuria, MNieves, Alejandro, Pedro, Víctor, a todos mis amigos de Tous. En especial quería agradecer a Clara y Mabel por estar siempre, por darme la mano día a día. Y como no, a Aurora, ella hace mi mundo más significativo, por su carisma y su nobleza. Más que amigas, sois hermanas.

También quería agradecer a todas las mujeres que con su esfuerzo y perseverancia han sido ejemplo de lucha en el ámbito científico, filosófico y social. En especial me gustaría nombrar a Marie Curie, Angela Davis, Simone de Beauvoir, Simone Weil, Virginia Woolf, Mary Wollstonecraft, Frida Kalho y Vandana Shiva. Las lecturas de sus ensayos han sido imprescindibles en este proceso de tesis. Gracias Pablo, por impulsarme y por creer en mí.

Por último, quería agradecer a los profesores de mi vida, porque la labor de ellos ha sido esencial en mi desarrollo y curiosidad. En especial, a Pepita de la guarde, a doña Lola, doña Tere, Miguel Ángel y don Fernando de Tous, por creer tanto en mí y motivarme desde pequeña. A Mati y Mari Carmen del insti, a Nico, Maria José y Sara de la uni, a Carmen y María del máster y a Laura del posgrado. Gracias, todos habéis aportado un granito de arena para que hoy pueda defender la tesis.

¡Gracias a todos!

RESUMEN

La detección selectiva y sensible de variaciones de nucleótido único es fundamental para el diagnóstico precoz, la terapia individualizada y el pronóstico de enfermedades. Algunas de estas mutaciones puntuales están implicadas en el síndrome respiratorio agudo severo (SARS) y en el desarrollo de diversos tipos de cáncer. La pandemia SARS-CoV-2 ha puesto de manifiesto la necesidad acuciante de desarrollar métodos de detección fiables, rápidos y sencillos para el diagnóstico masivo. Asimismo, existe una demanda creciente de biosensores genómicos que sean selectivos, multianalito y de bajo coste y permitan detectar e identificar ciertos biomarcadores oncológicos.

La presente tesis doctoral se ha centrado en el desarrollo de sistemas integrados de amplificación isoterma, hibridación selectiva y biosensado óptico para la detección de mutaciones puntuales en los genes *PIK3CA, KRAS y BRAF* asociadas al cáncer colorectal. Estos biomarcadores predictivos se relacionan con un incremento de la proliferación celular, apoptosis y resistencia a tratamientos con anticuerpos monoclonales (Cetuximab y Panitumumab). En concreto, las mutaciones del gen *KRAS* tienen una prevalencia del 40-50%, mientras que las mutaciones en los genes *PIK3CA* y *BRAF* presentan una prevalencia del 18 y del 5%, respectivamente.

Desde el punto de vista analítico, se ha abordado la discriminación de estas mutaciones puntuales, lo cual supone un gran reto debido a la heterogeneidad de la muestra y a la reducida proporción de ADN mutante con respecto al ADN nativo. De hecho, existen pocas técnicas capaces de lograr la detección de mutaciones puntuales, destacando la secuenciación y la PCR a tiempo real. Sin embargo, nos encontramos ante el desafío científico-técnico de desarrollar nuevos métodos que presenten mejores prestaciones como una elevada selectividad, sensibilidad, respuesta rápida y, especialmente, que no requieran infraestructuras complejas.

En este contexto, se han explorado los métodos isotermos de amplificación de ADN, dado que son particularmente adecuados para el desarrollo de una nueva generación de dispositivos de diagnóstico dirigidos a apoyar la medicina de precisión. En concreto, se ha seleccionado la amplificación isoterma por recombinasa-polimerasa (RPA) como una alternativa a los métodos de detección que requieren de infraestructuras singulares, así como de personal cualificado. Además, se ha investigado su integración con plataformas bioanalíticas, lo que supone un gran avance para la simplificación de los procesos de biorreconocimiento y su detección óptica. Esta metodología ha presentado ventajas frente a otros sistemas de detección de ADN, en términos de portabilidad y equipos, así como reducción de tiempos de ensayo y la posibilidad de realizar las pruebas de diagnóstico fuera del laboratorio.

La presente tesis doctoral, enmarcada en este contexto, se estructura en los siguientes capítulos.

En el **capítulo 1** se presenta una nueva variante de la amplificación por recombinasa-polimerasa, denominada RPA-bloqueada. Su mecanismo se basa en el enriquecimiento de alelos minoritarios mediante de la introducción de un agente bloqueante en la amplificación isoterma de la RPA. La adición de este oligonucleótido, complementario a la secuencia nativa, hace que se forme un complejo más estable con la variante nativa que con la variante mutante, controlando el proceso de elongación de modo más selectivo. Con este método, se ha conseguido superar el reto de amplificar selectivamente los alelos minoritarios en muestras reales donde existe una baja concentración de ADN tumoral, a temperatura constante (37 °C) y sin la necesidad de emplear equipos sofisticados.

Además, en esta investigación se ha desarrollado un soporte analítico formado por un chip de policarbonato con sondas alelo-específicas ancladas covalentemente, con el objetivo de detectar selectivamente el producto post-amplificado, procedente de RPA-bloqueada, mediante un ensayo de hibridación. En concreto, este tipo de plataformas bioanalíticas resultan altamente interesantes, puesto que poseen propiedades

superficiales y ópticas óptimas para la fabricación de biosensores y para aplicaciones microfluídicas. La integración del método ha permitido desarrollar un sistema portátil para el genotipado simultáneo de mutaciones en los exones 9 y 20 del gen *PIK3CA* en líneas celulares y en tejidos tumorales de pacientes oncológicos.

En el **capítulo 2**, se describe el desarrollo de un genosensor que incorpora partículas magnéticas conjugadas a sondas alelo-específicas para la concentración y detección del producto de amplificación selectivo derivado de la RPA-bloqueada. Con este genosensor, de formato homogéneo, se han reducido los tiempos de hibridación y los volúmenes de reacción, así como las interacciones inespecíficas, sin disminuir la sensibilidad alcanzada en el formato heterogéneo. Para mejorar la automatización, el ensayo se ha integrado en chips termoplásticos transparentes de cicloolefina con canales microfluídicos, mientras que las partículas magnéticas se han controlado mediante imanes permanentes ubicados en una plataforma construida mediante impresión 3D. Esta aproximación se ha concretado en un sistema portátil y de bajo coste para el genotipado del gen *KRAS* (codón 12), aplicable a muestras de tumores procedentes de tejido parafinado.

Los **capítulos 3 y 4** se centran en el desarrollo de superficies termoplásticas para el anclaje covalente de sondas alelo-específicas mediado por nanomateriales, con el objetivo de incrementar la densidad de inmovilización y por ende la sensibilidad del sistema. Así, se ha estudiado el anclaje covalente a superficies termoplásticas de policarbonato y cicloolefina activadas, de sondas alelo-específicas, mediado por dendrímeros carboxílicos mediante la química de la carbodiimida y por dendrones mediante la reacción quimioselectiva del grupo tiol-ino.

En estos capítulos, se ha demostrado que las plataformas termoplásticas 3D con híbridos ADN/dendrímero y ADN/dendrón presentan mejores prestaciones analíticas que los sistemas lineales, debido al gran número de sitios de unión por unidad de superficie, la gran flexibilidad de las ramas que conforman su estructura, la reducción de impedimentos estéricos y la distancia superficie-sonda. La combinación del método

de amplificación isotermo de la RPA-bloqueada con la hibridación llevada a cabo en las plataformas bioanalíticas desarrolladas ha permitido crear un genosenor efectivo y multiplexado para el genotipado del codón V600 del gen *BRAF* y el codón H1047 del gen *PIK3CA,* en muestras de tejido biopsiado. Trabajando en condiciones restrictivas, se ha logrado una hibridación alelo selectiva puesta de manifiesto mediante detección colorimétrica, obteniendo un perfil molecular característico que permite su clasificación en el correspondiente grupo poblacional. Los resultados obtenidos concuerdan con los del método de secuenciación masiva que es el de referencia.

Las investigaciones desarrolladas en la presente tesis han dado lugar a nuevas aportaciones metodológicas de interés basadas en la obtención de sistemas biosensores integrados. Estas plataformas, junto con los rápidos avances en el campo de la tecnología digital y la "salud móvil", contribuirán al desarrollo de herramientas de diagnóstico masivo, cumpliendo con las características establecidas por la OMS para sistemas ASSURED (sensibles, específicos, fáciles de usar, rápidos y robustos, sin equipos, con conectividad a tiempo real, de fácil muestreo y disponibles para los usuarios finales). Estos sistemas permiten abordar prioridades como el control de enfermedades, fortalecer la eficiencia de los sistemas de atención médica y pueden dar respuesta a la demanda de genosensores de diagnóstico masivo.

RESUM

La detecció selectiva i sensible de variacions de únic nucleòtid és fonamental per al diagnòstic precoç, la teràpia individualitzada i el pronòstic de malalties. Algunes d'aquestes mutacions puntuals estan implicades en el síndrome respiratòri agut sever (SARS) i en el desenvolupament de diversos tipus de càncer. La pandèmia SARS-CoV-2 ha posat de manifest la necessitat apressant de desenvolupar mètodes de detecció fiables, ràpids i senzills per al diagnòstic massiu. Així mateix, existeix una demanda creixent de biosensors genòmics que siguen selectius, multianàlit i de baix cost i que permeten detectar i identificar certs biomarcadors oncològics.

La present tesi doctoral s'ha centrat en el desenvolupament de sistemes integrats d'amplificació isoterma, hibridació selectiva i biosensat òptic per a la detecció de mutacions puntuals en els gens *PIK3CA, KRAS* i *BRAF* associades al càncer colorectal. Aquests biomarcadors predicitius es relacionen amb un increment de la proliferació cel·lular, apoptosi i resistència a tractaments amb anticossos monoclonals (Cetuximab i Panitumumab). En concret, les mutacions del gen *KRAS* tenen una prevalença del 40-50%, mentre que les mutacions en els gens *PIK3CA* i *BRAF* presenten una prevalença del 18 i del 5%, respectivament.

Des del punt de vista analític, s'ha abordat la discriminació d'aquestes mutacions puntuals, la qual cosa suposa un gran repte degut a la heterogeneitat de la mostra i a la reduïda proporció d'ADN mutant respecte a l'ADN natiu. De fet, existeixen poques tècniques capaces d'aconseguir la detecció de mutacions puntuals, destacant la seqüenciació i la PCR a temps real. No obstant això, ens trobem davant el desafiament cientific-tècnic de desenvolupar nous mètodes que presenten millors prestacions com una elevada selectivitat, sensibilitat, resposta ràpida i, especialment, que no requerisquen infraestructures complexes.

En aquest context, s'han explorat els mètodes isoterms d'amplificació d'ADN, atés que són particularment adequats per al desenvolupament d'una nova generació de

dispositius de diagnòstic dirigits a donar suport a la medicina de precisió. En concret, s'ha seleccionat l'amplificació isoterma per recombinasa-polimerasa (RPA) com una alternativa als mètodes de detecció que requereixen d'infraestructures singulars, així com de personal qualificat. A més, s'ha investigat la seua integració amb plataformes bioanalítiques, la qual cosa suposa un gran avanç per a la simplificació dels processos de bioreconeiximent i la seua detecció òptica. Aquesta metodologia ha presentat avantatges enfront d'altres sistemes de detecció d'ADN, en termes de portabilitat i equips, així com reducció de temps d'assaig i la possibilitat de realitzar les proves de diagnòstic fora del laboratori.

La present tesi doctoral, emmarcada en aquest context, s'estructura en els següents capítols.

En el **capítol 1** es presenta una nova variant de l'amplificació per recombinasa-polimerasa, denominada RPA-bloquejada. El seu mecanisme es basa en l'enriquiment d'al·lels minoritaris mitjançant de la introducció d'un agent bloquejant en l'amplificació isoterma de la RPA. L'addició d'aquest oligonucleótid, complementari a la seqüència nativa, fa que es forme un complex més estable amb la variant nativa que amb la variant mutant, controlant el procés d'elongació de manera més selectiva. Amb aquest mètode, s'ha aconseguit superar el repte d'amplificar selectivament els al·lels minoritaris en mostres reals on existeix una baixa concentració d'ADN tumoral, a temperatura constant (37 °C) i sense la necessitat d'emprar equips sofisticats.

A més, en aquesta investigació s'ha desenvolupat un suport analític format per un xip de policarbonat amb sondes al·lel-específiques ancorades covalentement, amb l'objectiu de detectar selectivament el producte post-amplificat, procedent de RPA-bloquejada, mitjançant un assaig d'hibridació. En concret, aquest tipus de plataformes bioanalitiques resulten altament interessants, ja que posseeixen propietats superficials i òptiques òptimes per a la fabricació de biosensors i per a aplicacions microfluidiques. La integració del mètode ha permés desenvolupar un sistema portàtil per al genotipat

simultani de mutacions en els exons 9 i 20 del gen *PIK3CA* en línies cel·lulars i en teixits tumorals de pacients oncològics.

En el **capítol 2**, es descriu el desenvolupament d'un genosensor que incorpora partícules magnètiques conjugades a sondes al·lel-específiques per a la concentració i detecció del producte d'amplificació selectiu derivat de la RPA-bloquejada. Amb aquest genosensor, de format homogeni, s'han reduït els temps d'hibridació i els volums de reacció, així com les interaccions inespecífiques, sense disminuir la sensibilitat aconseguida en el format heterogeni. Per a millorar l'automatització, l'assaig s'ha integrat en xips termoplàstics transparents de cicloolefina amb canals microfluidics, mentre que les partícules magnètiques s'han controlat mitjançant imants permanents ubicats en una plataforma construïda amb impressió 3D. Aquesta aproximació s'ha concretat en un sistema portàtil i de baix cost per al genotipat del gen *KRAS* (codò 12), aplicable a mostres de tumors procedents de teixit parafinat.

Els capítols **3 i 4** se centren en el desenvolupament de superfícies termoplàstiques per a l'ancoratge covalent, de sondes al·lel-específiques, mediat per nanomaterials, amb l'objectiu d'incrementar la densitat d'immobilització i per tant la sensibilitat del sistema. Així, s'ha estudiat l'ancoratge covalent a superfícies termoplàstiques de policarbonat i cicloolefina activades a sondes al·lel-específiques mediat per dendrimers csarboxílics mitjançant la química de la carbodiimida i per dendrons mitjançant la reacció quimioselectiva del grup tiol-ino.

En aquests capítols, s'ha demostrat que les plataformes termoplàstiques 3D amb híbrids ADN/dendrimer i ADN/dendró presenten millors prestacions analítiques que els sistemes lineals, a causa del gran nombre de llocs d'unió per unitat de superfície, la gran flexibilitat de les branques que conformen la seua estructura, la reducció d'impediments estèrics i la distancia superfície-sonda. La combinació del mètode d'amplificació isoterm de la RPA-bloquejada amb la hibridació duta a terme en les plataformes bioanalítiques desenvolupades ha permés crear un genosenor efectiu i multiplexatge per al genotipat del codó V600 del gen *BRAF* i el codó H1047 del gen *PIK3CA*, en mostres de teixit

biopsiat. Treballant en condicions restrictives, s'ha aconseguit una hibridació al·lel selectiva posada de manifest mitjançant detecció colorimètrica, obtenint un perfil molecular característic que permet la seua classificació en el corresponent grup poblacional. Els resultats obtinguts concorden amb els del mètode de seqüenciació massiva que és el de referència.

Les investigacions desenvolupades en la present tesi han donat lloc a noves aportacions metodològiques d'interés basades en l'obtenció de sistemes biosensors integrats. Aquestes plataformes, juntament amb els ràpids avanços en el camp de la tecnologia digital i la "salut mòbil", contribuiran al desenvolupament d'eines de diagnòstic massiu, complint amb les característiques establides per l'OMS per a sistemes ASSURED (sensibles, específics, fàcils d'usar, ràpids i robustos, sense equips, amb connectivitat a temps real, de fàcil mostreig i disponibles per als usuaris finals). Aquests sistemes permeten abordar prioritats com el control de malalties, enfortir l'eficiència dels sistemes d'atenció mèdica i poden donar resposta a la demanda de genosensors de diagnòstic massiu.

ABSTRACT

The selective and sensitive detection of single nucleotide variations is essential for early diagnosis, individualized therapy, and prognosis of diseases. Some of these point mutations are involved in severe acute respiratory syndrome (SARS) and in the development of various types of cancer. The SARS-CoV-2 pandemic has highlighted the pressing need to develop reliable, fast and simple detection methods for mass diagnosis. Likewise, there is a growing demand for genomic biosensors that are selective, multi-analyte and low-cost and that allow the detection and identification of certain oncological biomarkers.

This doctoral thesis has focused on the development of integrated systems for isothermal amplification, selective hybridization and optical biosensing for the detection of point mutations in the *PIK3CA, KRAS* and *BRAF* genes associated with colorectal cancer. These predictive biomarkers are related to increased cell proliferation, apoptosis, and resistance to monoclonal antibody treatments (Cetuximab and Panitumumab). Specifically, mutations in the *KRAS* gene have a prevalence of 40-50%, while mutations in the *PIK3CA* and *BRAF* genes have a prevalence of 18 and 5%, respectively.

From an analytical point of view, the discrimination of these point mutations has been addressed, which is a great challenge due to the heterogeneity of the sample and the reduced proportion of mutant DNA with respect to native DNA. In fact, there are few techniques capable of achieving the detection of point mutations, highlighting sequencing and real-time PCR. However, we are faced with the scientific-technical challenge of developing new methods that present better benefits such as high selectivity, sensitivity, rapid response and, especially, that do not require complex infrastructures.

In this context, isothermal DNA amplification methods have been explored, as they are particularly suitable for the development of a new generation of diagnostic

devices aimed at supporting precision medicine. Specifically, isothermal amplification by recombinase-polymerase (RPA) has been selected as an alternative to detection methods that require unique infrastructures, as well as qualified personnel. In addition, its integration with bioanalytical platforms has been investigated, which represents a great advance for the simplification of biorecognition processes and their optical detection. This methodology has presented advantages over other DNA detection systems, in terms of portability and equipment, as well as reduction of test times and the possibility of performing diagnostic tests outside the laboratory.

This doctoral thesis, framed in this context, is structured in the following chapters.

Chapter 1 presents a new variant of recombinase-polymerase amplification, called RPA-blocked. Its mechanism is based on the enrichment of minority alleles by introducing a blocking agent in the isothermal amplification of RPA. The addition of this oligonucleotide, complementary to the native sequence, causes a more stable complex to be formed with the native variant than with the mutant variant, controlling the elongation process more selectively. With this method, it has been possible to overcome the challenge of selectively amplifying minority alleles in real samples where there is a low concentration of tumor DNA, at a constant temperature (37 ° C) and without the need for sophisticated equipment.

Furthermore, in this research, an analytical support consisting of a polycarbonate chip with covalently anchored allele-specific probes has been developed, with the aim of selectively detecting the post-amplified product, from RPA-blocked, by means of a hybridization assay. Specifically, this type of bioanalytical platforms is highly interesting, since they have optimal surface and optical properties for the manufacture of biosensors and for microfluidic applications. The integration of the method has made it possible to develop a portable system for the simultaneous genotyping of mutations in exons 9 and 20 of the *PIK3CA* gene in cell lines and tumor tissues of cancer patients.

In **Chapter 2,** the development of a genosensor that incorporates magnetic particles conjugated to allele-specific probes for the concentration and detection of the selective amplification product derived from RPA-blocked is described. With this homogeneous format genosensor, hybridization times and reaction volumes have been reduced, as well as nonspecific interactions, reducing the sensitivity achieved in the heterogeneous format. To improve automation, the assay has been integrated into transparent cycloolefin thermoplastic chips with microfluidic channels, while the magnetic particles have been controlled with a permanent magnet platform built using 3D printing. This approach has resulted in a portable and low-cost system for genotyping the *KRAS* gene (codon 12), applicable to tumor samples from paraffin tissue.

Chapters 3 and 4 focus on the development of thermoplastic surfaces for the covalent anchoring of allele-specific probes mediated by nanomaterials, with the aim of increasing the immobilization density and therefore the sensitivity of the system. Thus, covalent anchorage to polycarbonate and cycloolefin thermoplastic surfaces activated to allele-specific probes mediated by carboxylic dendrimers through carbodiimide chemistry and by dendrons through the chemoselective reaction of the thiol-ino group has been studied.

In these chapters, it has been shown that 3D thermoplastic platforms with DNA / dendrimer and DNA / dendron hybrids have better analytical performance than linear systems, due to the large number of binding sites per unit area, the great flexibility of the branches that make up its structure, the reduction of steric hindrances and the surface-probe distance. The combination of the RPA-blocked isothermal amplification method with the hybridization carried out in the developed bioanalytical platforms has allowed the creation of an effective and multiplexed genosenor for the genotyping of the *V600* codon of the *BRAF* gene and the *H1047* codon of the *PIK3CA* gene, in samples. of biopsied tissue. Working under restrictive conditions, a selective allele hybridization has been achieved, revealed by colorimetric detection, obtaining a characteristic molecular profile that allows its classification in the corresponding population group. The results obtained agree with those of the sequencing method.

INDICE

RESULTADOS EXPERIMENTALES

LISTADO DE FIGURAS

Figuras introducción:

Figuras capítulo 1:

Figuras capítulo 2:

Figuras capítulo 3:

LISTADO DE TABLAS

Tablas introducción:

Tablas capítulo 1:

Tablas capítulo 3:

ABREVIATURAS

ADN	Ácido dexosirribonicléico
ARMS	Sistema de mutación refractario a la amplificación por PCR
ARN	Ácido ribonucleico
COP	Polímero de la cicloolefina
EGFR	Receptor del factor de crecimiento epidérmico
FFPE	Tejido fijado en formalina
FRET	Transferencia de energía de resonancia de Förster
HDA	Amplificación dependiente de helicasa
IA	Amplificación isoterma
LAMP	Amplificación isoterma mediada por bucle
LNA	Ácido nucleico bloqueado
LOD	Límite de detección
MNPs	Partículas magnéticas
NGS	Secuenciación de segunda generación
PC	Policarbonato
PCR	Amplificación en cadena de la polimerasa
PDMS	Polidimetilsiloxano
PNA	Ácido peptidonucleico
POCT	Pruebas de Laboratorio en el lugar de asistencia
RCA	Amplificación en círculo rodante
RPA	Amplificación por recombinasa-polimerasa
SDA	Amplificación por desplazamiento de hebra
SMRT	Secuenciación a tiempo real de una única molécula de AD
SNP	Polimorfismo de un único nucleótido
Tm	Temperatura de melting
µTAS	Sistemas para detección de ADN de análisis micro-totales

INTRODUCCIÓN

1. Biosensado de ADN

La detección y cuantificación de biomarcadores de ácidos nucleicos en muestras humanas permite definir el tipo, estado o progreso de la patología asociada, así como un correcto diagnóstico clínico y una terapia personalizada. Esta práctica se lleva a cabo generalmente en laboratorios centralizados y bien equipados. Sin embargo, existen otras alternativas interesantes para determinar los niveles de estos biomarcadores, utilizando ensayos en el lugar de atención (*point-of-care testing*, POCT) que permitan expandir su uso (Chen *et al.,* 2020).

Para ello, se pueden utilizar bioreceptores que muestren elevada selectividad en su interacción con determinadas moléculas. Esta capacidad de reconocimiento específico, inherente a muchas biomoléculas, tales como anticuerpos, enzimas, carbohidratos, lípidos y ácidos nucleicos entre otras, permite desarrollar dispositivos para la detección de biomarcadores (Jayanthi *et al.,* 2017).

Dentro de este tipo de sistemas analíticos, los biosensores de ácidos nucleicos ocupan una posición competitiva en el mercado del diagnóstico clínico. Un biosensor de ADN o genosensor es un dispositivo bioanalítico usado para conocer la naturaleza y/o concentración de ácidos nucleicos (Chen y Wang, 2020). Este biosensor es capaz de traducir la reacción de reconocimiento molecular del ligando con su receptor de ADN específico en una señal medible y cuantificable. Generalmente, el proceso de biosensado comprende varias etapas. En primer lugar, tiene lugar el biorreconocimiento, seguido de una traducción del evento de unión biológica en una señal fisicoquímica (transducción) y finalmente el procesamiento y transformación de la señal en información química (Perumal y Hashim, 2014) (**Figura 1**).

El fundamento del biosensado de ADN se basa generalmente en procesos de hibridación, mediante los cuales se combinan dos cadenas con secuencias de bases complementarias en una única molécula, formando una estructura de doble hélice. Para ello, se inmoviliza sobre un material un fragmento de ADN con una secuencia

complementaria a la del ADN diana sobre un material. Posteriormente, tiene lugar el biorreconocimiento que puede monitorizarse y traducirse en una señal analítica medible a partir del transductor empleado (Rashid y Yusof, 2017).

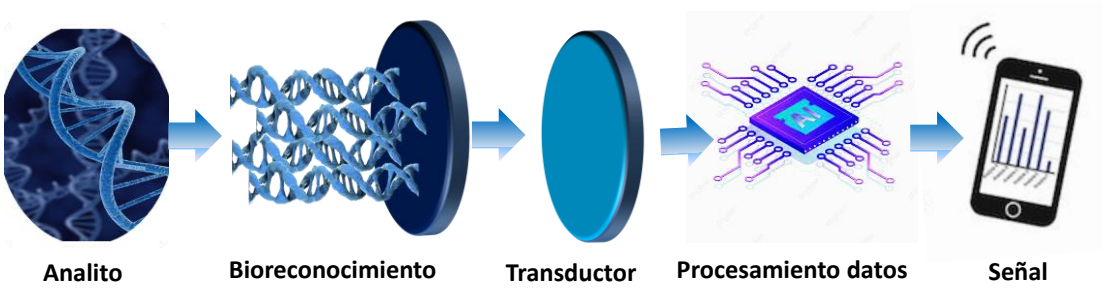

Figura 1. Esquema del funcionamiento de un biosensor de ADN.

Los transductores utilizados en biosensado de ADN pueden ser másicos (medición de cambios en masa), electroquímicos (registro de cambios de corriente, impedancia, etc.) (Díaz-Fernández *et al.,* 2020) u ópticos (medidas de las variaciones en las propiedades ópticas). Éstos a su vez pueden emplear formato con marcaje o sin marcaje, como los basados en fluorescencia o en resonancia de plasmón superficial (SPR), respectivamente (Nguyen *et al.,* 2019).

Los biosensores colorimétricos son un tipo de sensores ópticos que operan en el espectro de luz visible. Ciertos formatos permiten la observación directa del cambio de color cuando el analito problema está presente, evitando el uso de instrumentos analíticos para su lectura, lo cual favorece la detección *in situ* y a tiempo real (Du y Dong, 2017). Este tipo de sensado ofrece, además, una gran versatilidad puesto que permite determinar la concentración de ADN mediante el registro del cambio de color con aplicaciones para smartphones, escáner documental, disco compacto, etc. lo cual contribuye al desarrollo de biosensores portátiles, económicos, con respuesta rápida, integrando tecnología digital y lo que se denomina salud móvil (Mahato y Chandra, 2019), (Tortajada-Genaro *et al.,* 2019).

Las áreas de aplicación de los biosensores de ADN son muy diversas entre las que se destaca la farmacogenética, la industria alimentaria o el genotipado, entre otros.

Incluyen desde la detección de secuencias de decenas de nucleótidos hasta la identificación del nucleótido presente en cierta posición de interés. No obstante, la discriminación selectiva de la variación de una sola base en una secuencia genética, sigue siendo un gran desafío en el desarrollo de nuevos genosensores, especialmente cuando se requiere una detección robusta, rápida y cuantitativa de biomarcadores a concentraciones muy bajas (Wang *et al.,* 2020).

2. Problemática en la detección de mutaciones

Una mutación se refiere a un cambio en la estructura de un gen, lo que da como resultado una forma variante que puede transmitirse a las generaciones posteriores. Estas variaciones están causadas por la alteración de las bases del ADN (deleción, inserción, traslocación, reordenamiento o mutación puntual, entre otras). En concreto, una mutación puntual, se produce al cambiar en una posición concreta del genoma, siendo reemplazado el nucleótido nativo por uno de los otros tres posibles nucleótidos (G: guanina, C: citosina, A: adenina, T: timina). Algunas mutaciones puntales están asociadas con el desarrollo de diversos cánceres y, pueden emplearse como biomarcadores tumorales, en cáncer de pulmón, mama o colon, entre otros, ya que se relacionan con diferencias en la respuesta frente a tratamientos farmacológicos específicos (Lu *et al.,* 2020). La detección de estas variaciones nucleotídicas en muestras clínicas es difícil e implica un gran desafío, puesto que requiere de un método altamente sensible y selectivo (Matsuda, 2017).

Históricamente, el estudio genético de un tumor se lleva a cabo a partir de un extracto de muestras de tejido tumoral procedente de biopsia incluido en bloques de parafina y fijados con formalina (FFPE). Para ello, el servicio de anatomía patológica establece un flujo de trabajo que permite un diagnóstico totalmente integrado. En los estudios con base morfológica, como la inmunohistoquímica o FISH (hibridación in situ), el anatomopatólogo ha de distinguir entre estructuras neoplásicas y sanas para garantizar un diagnóstico molecular correcto (López-Ríos *et al.,* 2015). Para ello, se debe

seleccionar mediante microscopio óptico el área más representativa de la lesión tumoral, considerando que dichas muestras presentan un tamaño reducido y diferenciación divergente o heterogeneidad. En la fase preclínica, la toma de muestra tumoral ha de ser accesible y no representar riesgo para el paciente (Pirker *et al.,* 2010). Por su parte, la fijación y el tiempo de hipoxia del tejido, ha de ser lo más reducido posible, porque influye directamente en la calidad el ADN, además, la extracción ha de cumplir los parámetros de calidad y concentración establecidos (parámetro ratio 260/280>1.8). Las guías europeas recomiendan un mínimo del 50% de componente mutante, si se aplican técnicas de detección de baja sensibilidad como la secuenciación directa, o de un 10% si se van a aplicar técnicas de alta sensibilidad como las basadas en PCR de enriquecimiento de alelos (Gilson *et al.,* 2019).

Además, hay que considerar que las variaciones de un solo nucleótido son mucho más complejas de detectar que las variaciones de múltiples nucleótidos. Estas mutaciones están presentes en condiciones homocigotas o heterocigotas en la línea germinal, incluso en su forma heterocigótica, el nucleótido y su sustitución está presente en una proporción de 1:1 en las muestras analizadas. Por otro lado, la mutación en el tejido tumoral también está presente en condiciones homocigóticas o heterocigotas en el ADN de las células que forman este tejido; sin embargo, el porcentaje de células tumorales que tiene la mutación varía en comparación con la célula sana desde el momento del diagnóstico hasta después de la terapia (Rees y Liu, 2018).

Los principales parámetros de una técnica molecular de análisis genético son la especificidad para distinguir entre las posibles variantes en los codones de interés y la sensibilidad. Ambos parámetros son muy relevantes, dado que los tumores pueden ser muy heterogéneos, tanto en lo que respecta al porcentaje de células tumorales dentro del tejido biopsiado como a la heterogeneidad genética de las células que lo conforman. En este contexto, el reto científico-técnico se centra en desarrollar técnicas capaces de identificar los alelos minoritarios mutantes en una matriz compleja y heterogénea de ADN nativo (Milbury *et al.,* 2014).

3. Tecnologías para el análisis genético

3.1 Secuenciación

En 1977, Sanger y sus colaboradores desarrollaron la técnica que sería aplicada a lo largo de más de dos décadas para el diagnóstico molecular de mutaciones y que permite, además, conocer la secuencia concreta de los nucleótidos que componen cualquier ácido nucleico. Esta técnica de secuenciación considerada de primera generación y que lleva el nombre de su descubridor, se ha aplicado para la detección de variaciones de un nucleótido, inserciones o deleciones en uno o varios genes (Schuster, 2006). A pesar de ser la base de las técnicas actuales de secuenciación y poseer una elevada fiabilidad, presenta algunas desventajas como baja sensibilidad, puesto que detecta mutaciones a partir de muestras con concentraciones superiores al 20-25 %de ADN mutante. Además, en la práctica de laboratorio es un procedimiento complejo, lento y poco estandarizado (Morandi *et al.,* 2012).

Otra técnica empleada es la pirosecuenciación, cuyo procedimiento se basa en la detección quimioluminiscente. Concretamente, existen algunos kits disponibles en el mercado para la detección de las mutaciones más frecuentes basados en esta técnica, como es el ejemplo del *KRAS* Pyro Kit 24 (Qiagen), y el *RAS* Extension Pyro Kit 24 (therascreen® *KRAS* test), Ampliseq ™ (Life Technologies, Carlsbad, CA) o Idylla™ *KRAS* Mutation Test, el kit therascreen® RAS Extension Pyro (Qiagen), o el *KRAS, BRAF , PIK3CA* Array (Randox Molecular, Crumlin, Reino Unido) (Solassol *et al.,* 2016) validados por la FDA (Jo *et al.,* 2016).

Las técnicas de primera generación han resultado ser la base de la secuenciación, dando paso al desarrollo de las nuevas generaciones de secuenciación masiva (NGS) que han supuesto una revolución en el diagnóstico oncológico. Estas nuevas tecnologías de alto rendimiento facilitan la detección de diversas alteraciones genéticas y proporcionan información más extensa en la práctica clínica con menos material tumoral de partida (Lin *et al.,* 2014).

Dentro de las plataformas de secuenciación NGS de segunda generación encontramos 454 Life Sciencies (Roche), SOLID (Support Oligonucleotide Ligation Direction), Ion Torrent Personal Genome Machine (PGM) de Thermo Fisher Scientific y la plataforma NextSeq500 de Illumina, ésta última es la tecnología de secuenciación más utilizada debido a que ofrece plataformas efectivas (MiniSeq o HiSeq XTen, entre otras). Los métodos de secuenciación de tercera generación tienen como objetivo secuenciar moléculas largas de ADN y ARN.

Otra tecnología comercializada actualmente, líder en esta área, es la denominada (Singe Molecule RealTime (SMRT) de Pacific Biosciences, que permite secuenciar fragmentos muy largos de hasta 30-50 kb. Sin embargo, se requiere de una gran inversión inicial para adquirir y mantener estos equipos. Ello hace que únicamente laboratorios altamente cualificados y grandes hospitales puedan contar con este tipo de metodologías (Slatko *et al.,* 2018). Sin embargo, las técnicas de secuenciación están evolucionando continuamente, aumentando su capacidad de trabajo al utilizar equipos y medios robustos hasta conseguir que la secuenciación de ácidos nucleicos sea muy accesible técnica y económicamente.

3.2 Amplificación. Técnicas basadas en PCR

Entre las técnicas de amplificación de ácidos nucleicos basados en PCR (reacción en cadena de la polimerasa) destaca la variante en tiempo real o PCR cuantitativa. Esta reacción utiliza los mismos componentes que la PCR convencional o de punto final, excepto la adición de un marcador fluorescente, gracias al cual se produce la monitorización de los productos amplificados a medida que la reacción avanza. La respuesta se asocia a los ácidos nucleicos amplificados, de tal modo que el incremento de señal es proporcional a la cantidad de amplicón de ADN (Navarro *et al.,* 2015).

Dichos marcadores fluorescentes pueden ser específicos (sondas TaqMan) y no específicos (SYBR Green). Éste último, es un intercalante ampliamente utilizado y que presenta elevada afinidad por la doble hebra de ADN, sin embargo, presenta el inconveniente que puede generar resultados inespecíficos, puesto que puede intercalarse en cualquier molécula de ADN de doble cadena, p.e. dímeros de cebadores, y generar una señal no específica. Los métodos específicos se basan en el fenómeno FRET, el cual se fundamenta en la transferencia de energía de un agente dador o reportero fluorescente a un aceptor o 'quencher', unidos a una sonda TaqMan, la cual hibrida de manera específica con la secuencia diana. Tras el proceso de hibridación, la enzima Taq polimerasa, que sintetiza la nueva hebra, rompe la unión entre el reportero y el quencher, emitiendo fluorescencia que es detectable a tiempo real (Gilson *et al.,* 2019).

Existen multitud de métodos y kits basados en PCR que se utilizan para la detección de mutaciones puntuales del gen *KRAS,* a partir de ADN derivado de tejido FFPE tumoral de colon, como es, cobas® KRAS 4800 (Roche) (Lee *et al.,* 2012), QClamp ™ *KRAS* kit (Solassol *et al.,* 2016) y droplet PCR (Alcaide *et al.,* 2019). En este contexto, también encontramos la técnica de amplificación refractaria (ARMS), PCR de enriquecimiento mutante (EPCR), TaqMAMA que combina la amplificación a tiempo real con sondas TaqMan, sondas de hidrólisis específica de alelo o de hibridación dual, análisis de fusión de alta resolución (HRMA) o el análisis de alta resolución de fusión

(HRM) (Solassol *et al.,* 2011*),* basada en la comparación de curvas de fusión de las cadenas de ADN. También encontramos sistemas de mutación refractaria de amplificación (ARMS) (Milburi *et al.,* 2009), estrategias de reacción en cadena de la polimerasa en tiempo real (PCR), COLD-PCR y ICE-COLD-PCR, pirosecuenciación o secuenciación (NGS) (Jia *et al.,* 2014), descritos en el apartado anterior.

La mayoría de estos métodos pueden detectar ADN con una sola mutación, incluso cuando esta mutación está presente entre el 1% y el 5% en relación con la cantidad de ADN de tipo nativo en una muestra compleja. Algunas tecnologías más recientes, como la droplet PCR, alcanzan incluso concentraciones más bajas (0.05%). Sin embargo, estos métodos presentan limitaciones debidas a la necesidad de emplear instrumentos sofisticados y por no facilitar el enriquecimiento de los alelos mutantes que se encuentran en menor proporción (Fouz y Apella, 2020). En los últimos años, también se han desarrollado métodos basados en PCR de alta sensibilidad. Por ejemplo, se ha estudiado la limitación de la temperatura de desnaturalización de la PCR para enriquecer mutaciones conocidas (Zhou *et al.,* 2011) o métodos de PCR basados en técnicas de amplificación alelo-específicas (PCR-ASA) para el enriquecimiento de mutaciones (Tortajada-Genaro *et al.,* 2016; He *et al.,* 2020). En la **Tabla 1** se recogen las técnicas y características de las mismas, utilizadas para la detección de mutaciones puntuales.

Tabla 1. Técnicas de detección de mutaciones puntuales

Técnica	Sensibilidad (%DNA mutado)	Características
Secuenciación		Requiere una elevada cantidad de ADN mutante
Sanger	25	
Pirosecuenciación	5-10	Requiere de equipos sofisticados (Secuenciadores)
PCR cuantitativa en tiempo real		
TaqMAN PCR	10	Requiere de termociclador
ARMS	1	
Cobas	2.5-5	
Droplet PCR	0.05	
Técnicas de enriquecimiento de alelo mutado		Requiere de termociclador
PNA-LNA PCR clamp	0.1-1	
COLD-PCR	0.1-1	
PCR-RFLP	5	

Otra aproximación para la detección de mutaciones puntuales es la basada en PCR bloqueada que, mediante la adición de agentes bloqueantes, inhibe selectivamente la amplificación de las secuencias nativas (Fouz y Apella, 2020). Se basa en la superposición del cebador con el oligonucleótido bloqueante nativo, es decir, lograr la unión competitiva entre el bloqueante y el cebador por el alelo de tipo nativo y que no afecte la amplificación de los alelos mutantes. Dicha técnica ha sido aplicada para la detección de mutaciones puntuales en el gen *KRAS*, a partir de muestras incluidas en parafina, demostrando ser una herramienta muy interesante para la detección de cáncer colorectal (Huang *et al.,* 2015).

Para mejorar el bloqueo, se utilizan oligonucleótidos modificados, por ejemplo, los ácidos peptidonucleicos (PNA). Un PNA es un polímero sintético con estructura análoga al ADN, en la cual la cadena principal del fosfodiéster es reemplazada por una repetición similar a un péptido de la cadena de 2-aminoetilglicina. El híbrido de ADN/PNA formado durante la amplificación tiene una mayor estabilidad térmica que el híbrido de ADN/ADN correspondiente, puesto que el desajuste de un solo par de bases implica una disminución de la temperatura de fusión (Tm, *melting temperature*). El PNA hibridado con la secuencia diana puede inhibir la hibridación del cebador y por tanto el proceso de amplificación (Kim *et al.,* 2015). Además, puede existir competencia entre el PNA, complementario a la secuencia nativa y uno de los cebadores de PCR, complementario a la secuencia diana mutante, o viceversa (Fouz y Apella, 2020). Esta aproximación ha sido utilizada para la detección de mutaciones en el gen *EGFR* (Kim *et al.,* 2013), *KRAS, PIK3CA y BRAF* (Kwon *et al.,* 2011) presentes en cáncer de colon. Otras estructuras como las LNA (ácido nucleico bloqueado), quimeras LNA / ADN y combinaciones de éstas también han sido utilizadas para la detección de variaciones puntuales (Orum, 2000).

3.3 Técnicas basadas en amplificación isoterma

Las técnicas de amplificación isoterma surgen como respuesta a las limitaciones de la técnica convencional de PCR (**Tabla 1**). No dependen de ciclos precisos de amplificación, para ello emplean otras enzimas y proteínas presentes en la síntesis de ADN/ARN (Zhao *et al.,* 2015). Estos métodos se han establecido como alternativas altamente exitosas frente a la PCR convencional (Lobo-Castañón, 2016), especialmente para aplicaciones tipo *point-of-care* (Pumford *et al.,* 2020).

Estas metodologías logran la amplificación de los ácidos nucleicos diana a temperatura constante, lo cual simplifica el diseño y la operación del sistema. El rango de temperatura requerido se encuentra entre 37°C y 65°C, dependiendo de la variante de amplificación. Es decir, son inferiores a las temperaturas de trabajo de la PCR, lo cual resulta más adecuado para el desarrollo de biosensores integrados y portátiles (Giuffrida y Spoto, 2017).

El mercado global de esta tecnología se valoró en 1.600 millones de dólares en 2016 y se prevé una demanda creciente frente a otras técnicas de diagnóstico molecular (**Figura 2**). Además, las amplificaciones isotermas permiten el desarrollo de pruebas de diagnóstico dirigidas a entornos con recursos limitados o zonas remotas, combinando la reacción de amplificación con lectura óptica multiplexada en tiempos de reacción cortos (Craw y Balachandran, 2012).

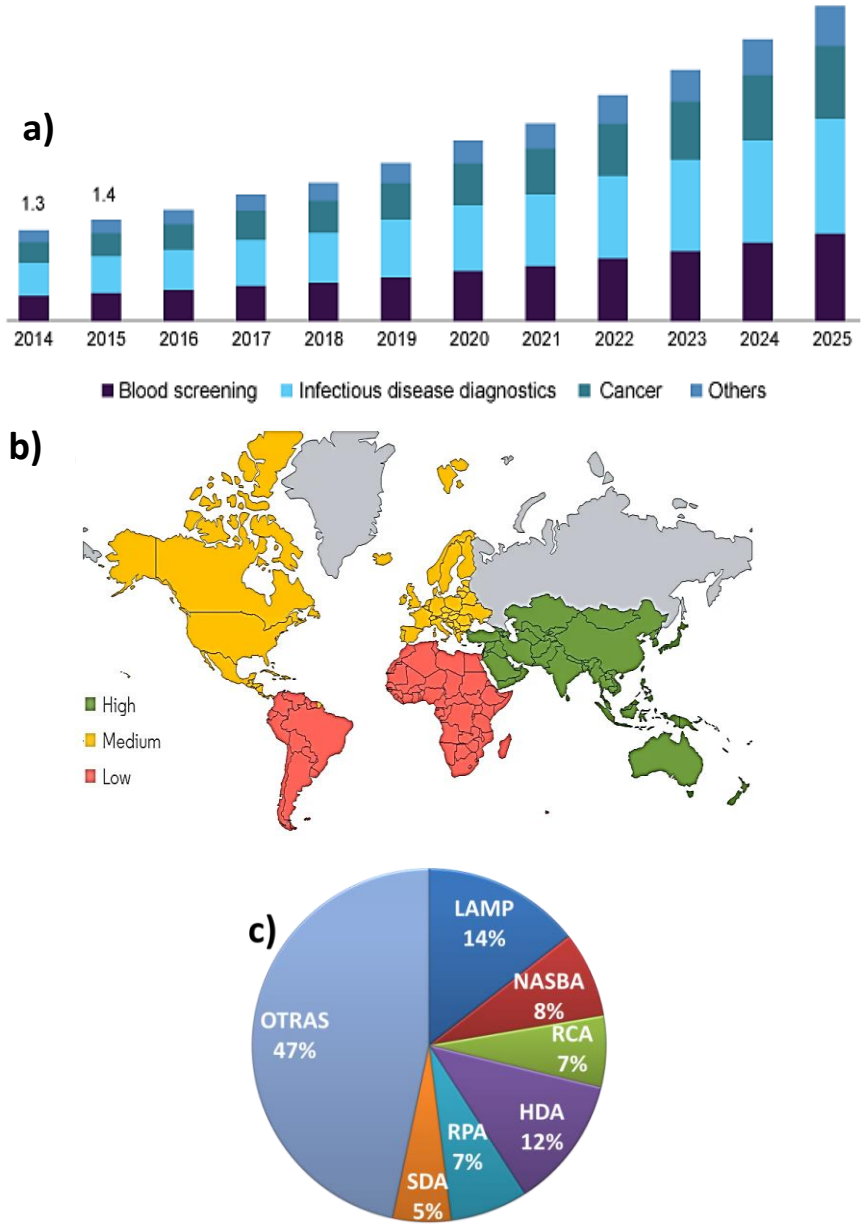

Figura 2. a) Mercado global de las tecnologías de amplificación isoterma en función de la aplicación (previsión hasta 2025). b) Tasas de crecimiento del mercado de las tecnologías de amplificación isoterma. c) Porcentaje de participación de mercado de las diferentes tecnologías de amplificación isoterma de ácidos nucleicos. Figuras originales extraídas del informe de mercado global de las tecnologías de amplificación isoterma, 2021.

3.3.1 Clasificación de las técnicas de amplificación isoterma

LAMP (amplificación isoterma mediada por bucle) es un método simple, rápido, consolidado (aprobado por la FDA) y de bajo coste que permite la amplificación isoterma específica de ADN (Yoo *et al.,* 2020). Fue descrita por primera vez por Notomi en el 2000 (Notomi *et al.,* 2000). El mecanismo se fundamenta en la síntesis de ADN por desplazamiento de cadena en presencia de la polimerasa de Bacillus stearothermophylus (Bst). Esta amplificación trabaja a temperatura constante de 60-65°C durante 45-60 minutos. En la reacción se introducen dos cebadores internos y dos externos, capaces de reconocer a seis secuencias distintas del ADN diana (**Figura 3**). Esta técnica requiere de un menor número de etapas que la PCR convencional. Es muy sensible y capaz de detectar seis copias de ADN en la mezcla de reacción (Zhang *et al.,* 2019). Ha sido ampliamente estudiada por numerosos grupos para la detección de mutaciones puntuales (Yamanaka *et al.,* 2018).

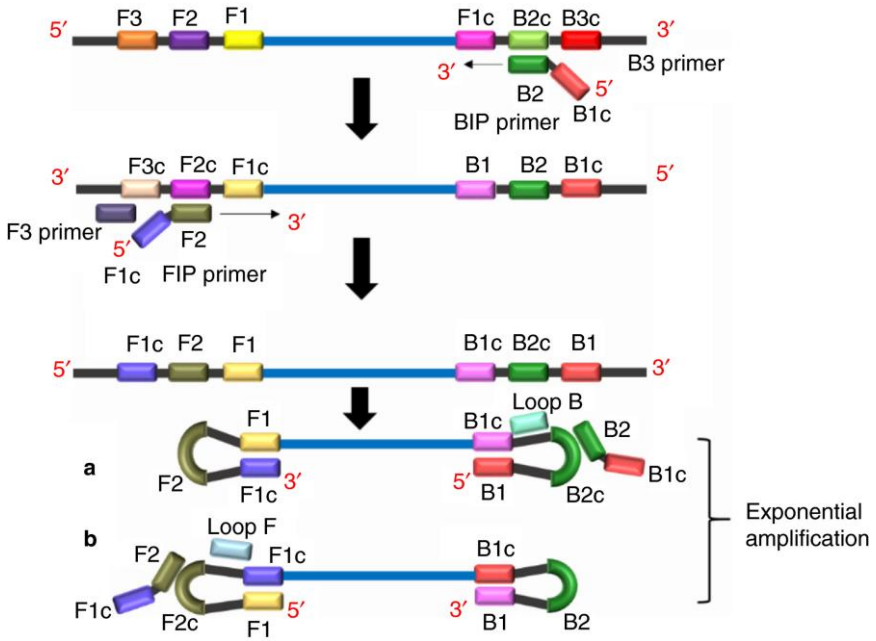

Figura 3. Mecanismo de la amplificación de la LAMP. Figura original de *Wong, 2018*.

NASBA (amplificación basada en secuencia de ácidos nucleicos) es un método de amplificación isotermo basado en transcripción, que se aplica tanto para la detección de ARN como para ADN. Fue desarrollado en 1999 por el grupo de van Deursen (van Deurse

et al., 1999). La reacción de amplificación se lleva a cabo a temperatura constante (41°C) y utiliza tres enzimas, transcriptasa inversa del virus de la mieloblastosis aviar, ARNasa H y ARN polimerasa dependiente del ADN T7 (**Figura 4**). La longitud de la secuencia diana a amplificar está limitada a 100-250 nucleótidos (Teng *et al.,* 2020). Esta tecnología ha sido aplicada recientemente para la detección colorimétrica de genotipos en norovirus (Sun *et al.,* 2020).

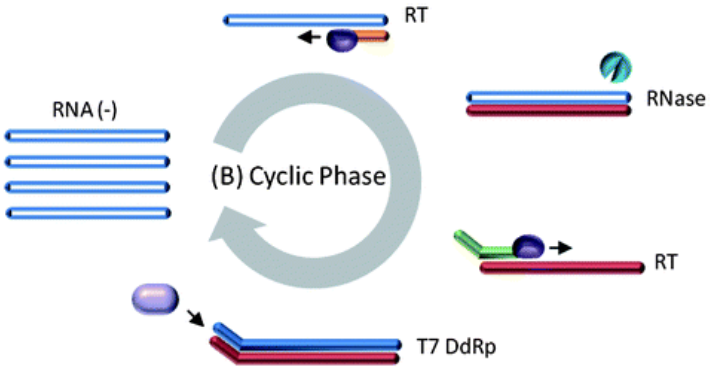

Figura 4. Mecanismo de la amplificación de la NASBA. Figura original de *Asiello, 2011*.

SDA (amplificación con desplazamiento de hebra) es un método de amplificación isotermo (37°C), que utiliza cuatro cebadores diferentes de los cuales uno contiene un sitio de restricción que hibrida con la secuencia de ADN (Zhang *et al.,* 2020). Fue descrito por primera vez en 1992 por el grupo de Walker y Shank (Walker *et al.,* 1992). No requiere de ciclos de desnaturalización, debido a la presencia de enzimas de restricción. El mecanismo se basa en la capacidad de desplazamiento de hebra por parte de la polimerasa modificada e inicio de la replicación del DNA diana. Con esta técnica, las hebras desplazadas sirven como molde para los nuevos ciclos de amplificación (**Figura 5**). Esta técnica ha sido utilizada en un biosensor electroquímico con el objetivo de detectar la mutación *p.H1047R* del oncogén *PIK3CA* ofreciendo resultados prometedores (Wang *et al.,* 2020).

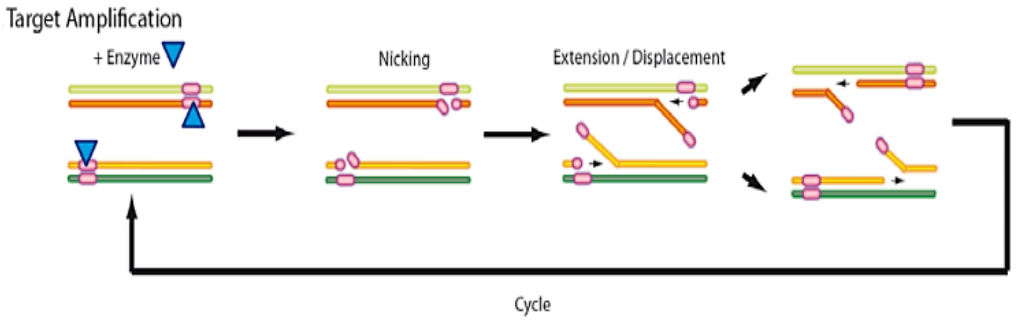

Figura 5. Mecanismo de la amplificación de la SDA. Figura original de *Zhang, 2020*.

RCA (amplificación de círculo rodante) es un método de amplificación de ácidos nucleicos que trabaja a temperatura constante de 61°C. Esta técnica produce una amplificación lineal, ya que la polimerasa (Phi29) va rodando constantemente en cada secuencia circular, de tal modo que los productos complementarios van creciendo a velocidad constante (Ali *et al.,* 2015) (**Figura 6**). La capacidad de la RCA para producir los productos de amplificación unidos a la superficie ofrece ventajas significativas en ensayos de hibridación in situ y de micromatrices. Recientemente, se ha aplicado para la detección del gen *EGFR* sobre soporte de grafeno (Xu *et al.,* 2019), para la detección de *E.coli* sobre superficies dendronizadas plásticas (Jiang *et al.,* 2017), para la detección de polimorfismos (Lapitan *et al.,* 2015) y para la detección de ébola en una plataforma electroquímica (Ciftci *et al.,* 2020).

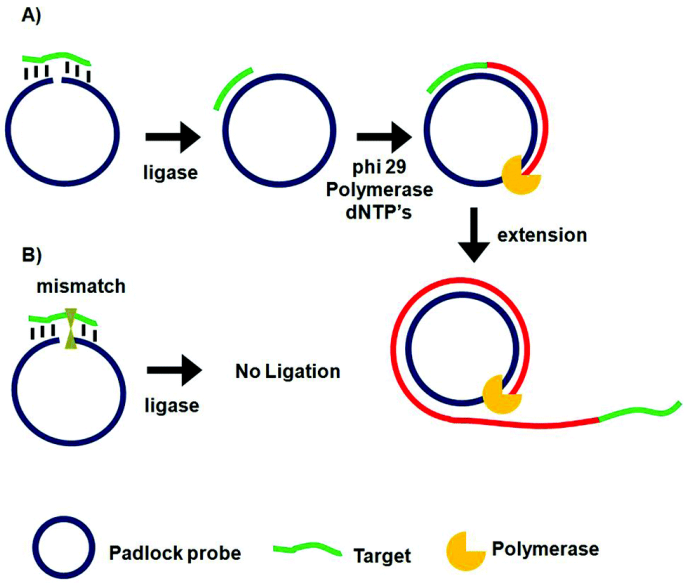

Figura 6. Mecanismo de amplificación de la RCA. Figura original de *Lapitan, 2015.*

HDA (amplificación dependiente de la helicasa) es un método de amplificación isotermo que trabaja a 65°C y fue descrito en 2004 (Vincent y Kong, 2004). El principio básico es la actividad de la enzima helicasa, la cual separa las dos hebras de ADN generando moldes monocatenarios, que son recubiertos por proteínas de unión. Los cebadores específicos se hibridan con el extremo 3 'de cada hebra de ADN (ssDNA) y la ADN polimerasa produce ADN bicatenario (**Figura 7**). Este proceso permite realizar múltiples ciclos de replicación a una sola temperatura de incubación, eliminando por completo la necesidad de termocicladores (Pumford *et al.,* 2020).

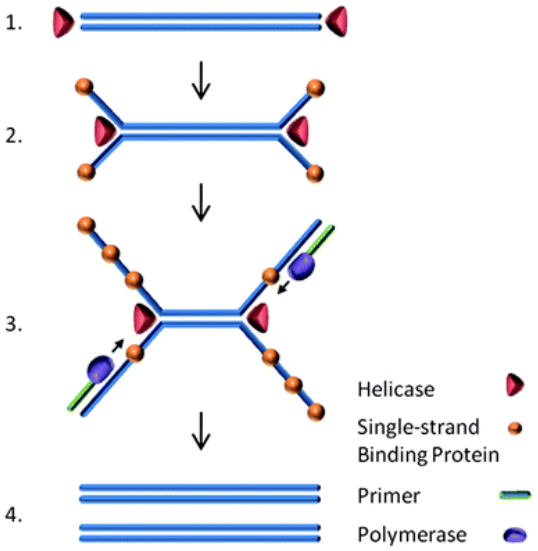

Figura 7. Mecanismo de la amplificación de la HDA. Figura original de *Asiello, 2011*.

Tabla 2. Comparación de diferentes técnicas de amplificación isoterma

Isoterma	Diana	Cebadores	Tª (ºC)	Tiempo (min)	LOD (copias)	Primera publicación
NASBA	ARN	2	41	60-180	1	(Van Deursen, 1999)
SDA	ADN	4	30-55	60-120	10	(Walker, 1992)
RCA	ADN/ARN	1	30-65	60-240	10	(Fire, 1995)
LAMP	ADN	4-6	60-65	60	6	(Notomi, 2000)
HDA	ADN	2	65	30-120	1	(Vicent,2004)
RPA	ADN/ARN	2	37-42	20-40	1	(Piepenburg, 2006)

3.3.2 Amplificación isoterma por recombinasa-polimerasa

La amplificación por recombinasa-polimerasa, **RPA**, (Piepenburg *et al.,* 2006) utiliza tres proteínas principales: una recombinasa, proteínas de unión a ADN de cadena simple y una ADN polimerasa con actividad de desplazamiento de hebras. En este mecanismo, los cebadores son recubiertos por la recombinasa usvX del fago T4 con ayuda de la proteína usvY y el agente entrecruzante Carbowax 20M. Este complejo nucleoproteico es capaz de identificar la región complementaria en el ADN molde, mientras la recombinasa cataliza el intercambio de hebras, formando una estructura loop en forma de D (Lobato y Sullivan, 2018).

La hebra desplazada es estabilizada por proteínas gp32 del fago T4, que son proteínas de unión (SSB) a la hebra simple. Posteriormente, la recombinasa se separa de los cebadores usando una reacción de hidrólisis de ATP, entonces, la ADN polimerasa de Bacillus subtilis (Bsu) puede comenzar a sintetizar usando el extremo 3’ de los cebadores. La actividad de desplazamiento de hebras de Bsu permite continuar la síntesis en ambos sentidos, mientras que la hebra desplazada se estabiliza con las proteínas gp32. Cuando las polimerasas se encuentran, el ADN molde se separa por efecto estérico y se forman dos complejos de amplificación.

Posteriormente, la polimerasa puede terminar la extensión para generar dos copias del ADN original. Tras esta etapa, se siguen formando nuevos complejos nucleoproteicos (cebadores-recombinasa), invadiendo las nuevas copias, para iniciar otro ciclo de amplificación (Li *et al.,* 2018). Todo el proceso se inicia con la presencia de acetato de magnesio, que es el cofactor de la recombinasa y de la ADN polimerasa (**Figura 8**).

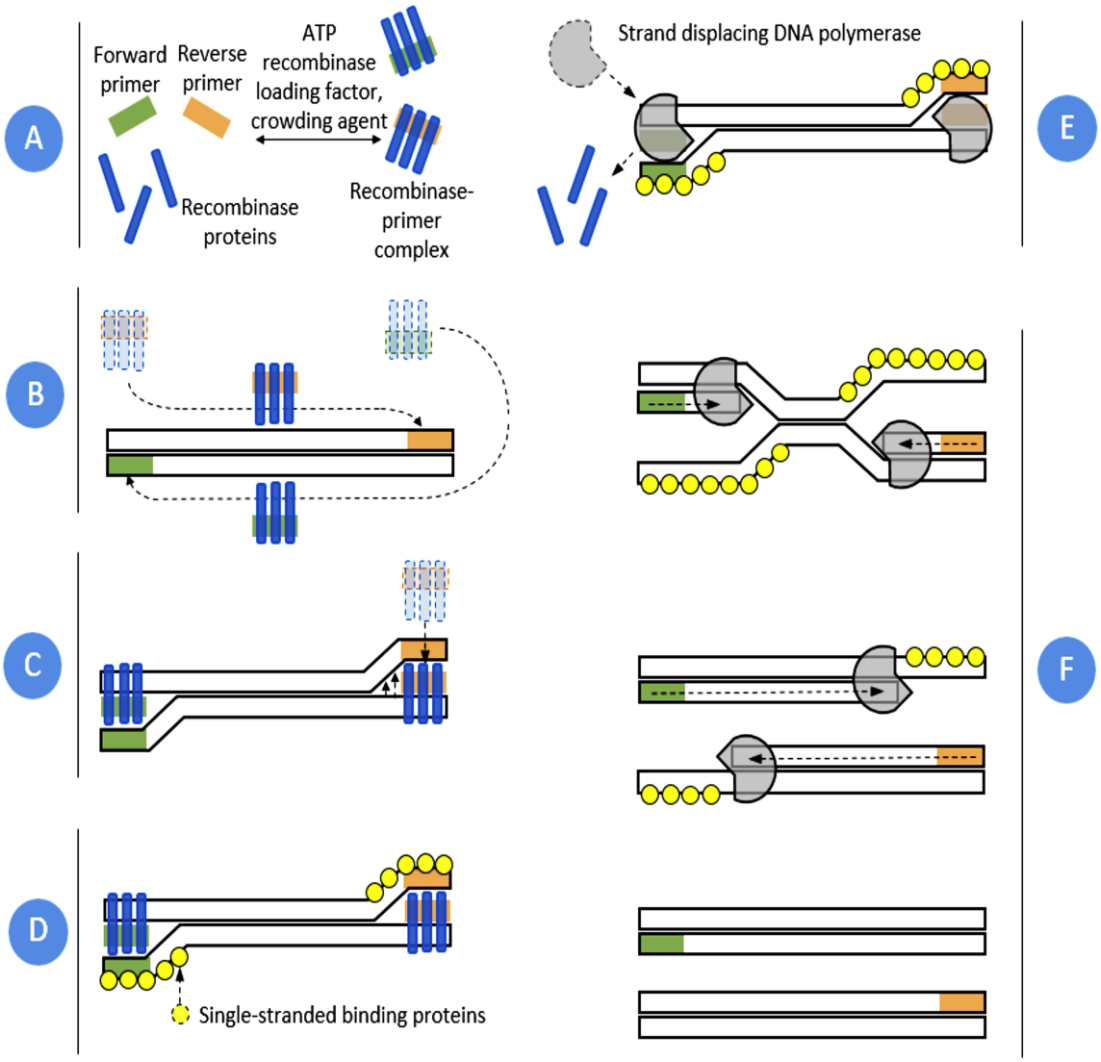

Figura 8. Mecanismo de la amplificación de la RPA. Figura original de *Lobato, 2018*.

Diversos autores han detectado el virus de la fiebre amarilla (Escadafal *et al.,* 2014), el ébola (Magro *et al.,* 2017) o el VIH (Lillis *et al.*, 2014) mediante esta técnica. Recientemente, se ha desarrollado un nuevo mecanismo llamado Sherlock (Gootenberg *et al.,* 2017), (Kellner *et al.*, 2019) que combina la técnica RPA con la novedosa técnica CRISPR/Cas. Sherlock permite la detección multiplexada, portátil y ultrasensible de ARN o ADN de muestras clínicas a partir de una RT-RPA junto con CRISPR/Cas13. Esta técnica, que ha sido aplicada recientemente para la detección de malaria y coronavirus SARS-CoV2 (Lee *et al.,* 2020), está fomentando el desarrollo de dispositivos POCT ópticos y electroquímicos innovadores (Ding *et al.*, 2020).

La RPA destaca por ser una alternativa importante a los métodos de detección que requieren de una elevada infraestructura y de personal cualificado. Se observa una tendencia creciente en las publicaciones científicas y la previsión es que siga en aumento en los próximos años, puesto que presenta claras ventajas frente a otras tecnologías (**Figura 9**).

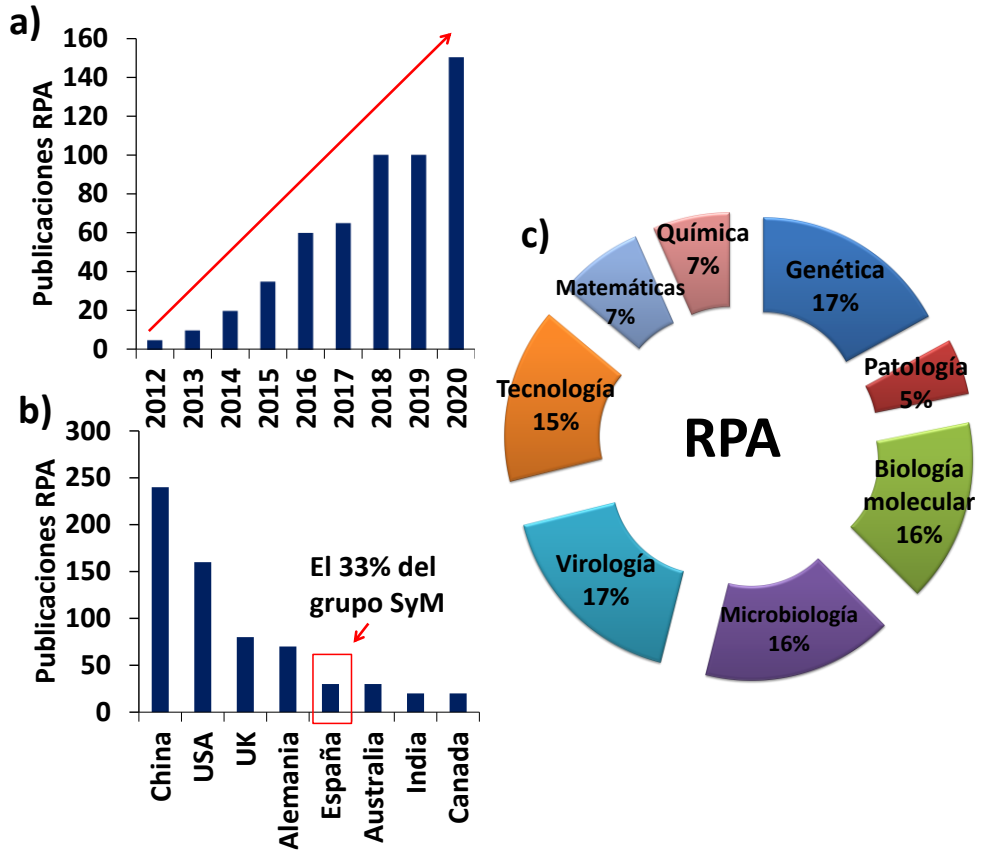

Figura 9. a) Evolución temporal del número de publicaciones sobre la RPA (2012-2020). b) Número de publicaciones por países. c) Áreas de investigación de la RPA. Fuente: Web of Science, 2021.

En la presente tesis doctoral, se ha elegido esta reacción de amplificación para la detección de mutaciones puntuales frente a otras variantes isotermas, puesto que presenta una elevada especificidad y trabaja a temperaturas inferiores (25-40°C) a las otras técnicas citadas, lo cual le confiere una gran versatilidad a la hora de utilizarse en sistemas POCT (Lei *et al.*, 2020). Además, requiere de una menor cantidad de cebadores, es más rápida y no necesita de una etapa previa de desnaturalización, lo que repercute en un menor consumo de energía (**Tabla 2**).

Por otro lado, en la formulación actual se emplea polietilenglicol (PEG) como agente entrecruzante en lugar del Carbowax, este agente le otorga consistencia viscosa, lo cual puede afectar a la reacción (Lobato y Sullivan, 2018), en términos de velocidad de agregación en ensayo de partículas magnéticas, visualización en gel de agarosa o en el incremento de adsorciones inespecíficas en ensayos en fase sólida (Kersting *et al.*, 2014).

La longitud de los cebadores recomendada es de 30 a 35 nucleótidos, sin embargo, varios autores han optimizado la reacción con cebadores cortos (18-25 nucleótidos) (Li *et al.,* 2018). Por el contrario, se ha observado la formación de estructuras secundarias con cebadores largos (>45 nucleótidos). Es recomendable la amplificación de secuencias de entre 100 y 200 pares de bases para alcanzar un mejor rendimiento de reacción (Lobato y Sullivan, 2018). La reacción de amplificación puede operar a temperaturas que varían entre 22-45 °C. Sin embargo, la mayoría de las investigaciones han concluido que la temperatura óptima se encuentra en el rango 37 y 42 °C, mientras que el tiempo necesario para la amplificación de ADN a niveles detectables depende del número de copias de ADN genómico de partida, encontrándose entre los 20 y los 40 minutos (Li *et al.,* 2018). Para controlar la temperatura de reacción se han empleado incubadoras, placas calefactoras, calentadores químicos y calor corporal (Crannel *et al.,* 2014), lo cual ofrece muchas ventajas frente a otras isotermas que trabajan a temperaturas más elevadas, puesto que esta propiedad confiere una gran versatilidad a los sistemas POCT.

La amplificación isoterma RPA presenta ventajas frente a la isoterma más estandarizada LAMP, como es la menor cantidad de cebadores necesarios, así como la reducción de tiempo y temperatura de la reacción, lo cual repercute en un menor consumo de energía (Lei *et al.,* 2020) (**Tabla 2**). Además, esta tecnología se ha aplicado en dispositivos microfluídicos automatizados, puesto que este tipo de sistemas reducen el riesgo de contaminación, minimizando el volumen requerido en el ensayo (Lutz *et al.,* 2010).

Todas estas prestaciones posicionan a la RPA como gran candidata para la explotación y comercialización de kits con soluciones asequibles, sensibles, específicas, fáciles de usar, rápidas, robustas y sin apenas equipos, favoreciendo su uso en prácticamente cualquier entorno (Mondal *et al.,* 2016).

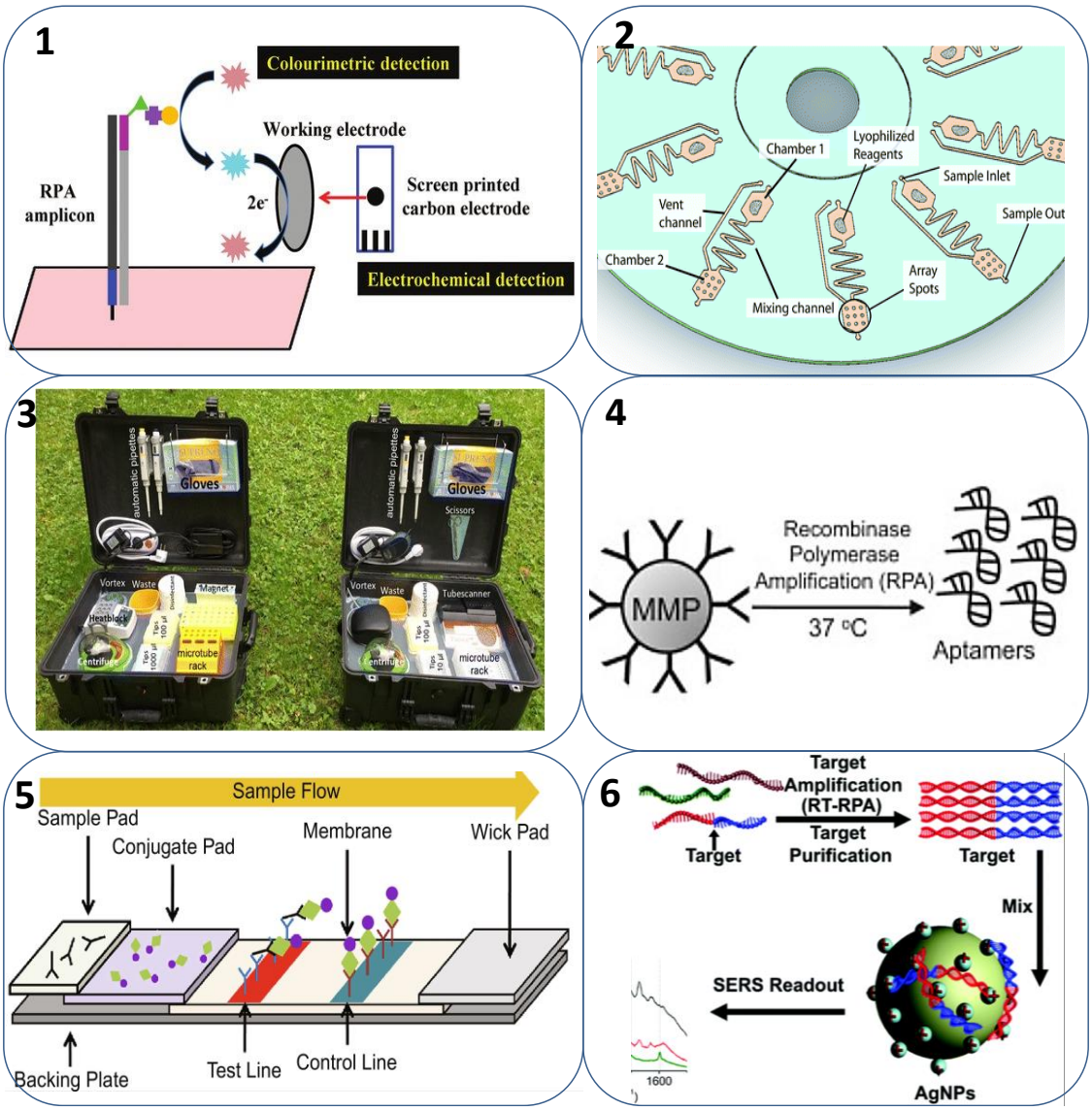

Figura 10. Ejemplos de biosensores basados en RPA: (1) Ensayo electroquímico y colorimétrico (Li, 2018); (2) Ensayo microfluídico en disco DVD (*Tortajada-Genaro et al., 2015*); (3) laboratorio portátil (Mondal *et al.,* 2016); (4) ensayo con partículas magnéticas (Loo *et al.,* 2013); (5) Ensayo de flujo lateral (Ivanov *et al.,* 2020); (6) detección sin marcaje (SERS) (Wang *et al.,* 2017). Figuras tomadas de las publicaciones citadas.

La detección de producto amplificado se puede realizar a tiempo real por medición de fluorescencia o a punto final por electroforesis (Liu *et al.,* 2016), por detección electroquímica (Sánchez Salcedo *et al.,* 2019), quimioluminiscente, dispersión Raman en superficie (SERS) (Wang *et al.,* 2017), siendo la detección de flujo lateral (LFA) una de las más utilizadas (Ivanov *et al.,* 2020). La tecnología de micromatrices también ha sido ampliamente utilizada para la detección en formato multiplexado de productos de RPA post-amplificados, concretamente, en nuestro grupo SyM se ha aplicado para la detección de mutaciones en los genes *CYP2C9* and *VKROC1* combinado con el proceso de ligación (Lázaro *et al.,* 2019) o para la detección de alérgenos alimentarios en discos microfluídicos DVD (*Tortajada-Genaro et al., 2015*).

3.3.3 Detección de mutaciones puntuales con técnicas isotermas

Algunas de estas técnicas de amplificación isoterma se están aplicando para la detección de mutaciones puntuales. En concreto, la isoterma LAMP ha sido la más estudiada para la discriminación de mutaciones en los genes *KRAS, GRIK4, rtV173L, CYP2C19, PIK3CA, BRAF o CARL*, entre otros. Para ello, se han estado desarrollando métodos como PE-LAMP (Ding *et al.,* 2019*)*, AS-LAMP (Yamanaka *et al.,* 2018*)*, USS-sbLAMP (Kalofonou *et al.,* 2020), MB-LAMP (Varona *et al.,* 2020), PA-LAMP (Du *et al.,* 2019), PNA-LAMP (Itonaga *et al.,* 2016) que permiten distinguir entre mutaciones puntuales (**Tabla 3**). La técnica de amplificación por RCA también ha sido estudiada recientemente por varios autores con esta finalidad, utilizando para ello LNAs o ligación entre otros mecanismos para conseguir la selectividad del método (Zhang *et al.,* 2019). Por su parte, la SDA también ha sido estudiada en menor proporción por varios autores para la discriminación de mutaciones del gen *KRAS* (Li *et al.,* 2019). Sin embargo, las técnicas basadas en NASBA y HDA no han sido exploradas en este contexto.

Pese a que se ha demostrado que el mecanismo de la RPA es altamente selectivo (Lobato y Sullivan, 2018), la detección de mutaciones puntuales en muestras heterogéneas complejas, donde la concentración de tejido mutante frente al tejido nativo suele estar en proporciones reducidas, supone un reto importante. En este

contexto, se ha desarrollado un método para detección de mutaciones puntuales de un solo nucleótido para el gen *EGFR*, combinando la amplificación isoterma RPA específica con alelos específicos (ASA), ácidos nucleicos peptídicos (PNA) y detección por SYBR Green, sistema AS-RPA-PNA-SYBR (ARPS) (Liu *et al.,* 2016), mejorando así la especificidad del método. Sin embargo, este requería de una etapa de precalentamiento y enfriamiento (99 y 66°C) para hibridar el ADN genómico con el PNA, con lo cual el proceso deja de ser isotermo. Por otra parte, nuestro grupo ha trabajado en varias aproximaciones para detectar mutaciones de un único nucleótido, en este caso aplicando la técnica AS-RPA alelo-específica (Yamanaka *et al.,* 2017), o mediante ligación (Lázaro *et al.,* 2019) (**Tabla 3**) consiguiendo mejorar la selectividad del método analizando muestras procedentes de frotis bucal.

Por lo tanto, uno de los retos pendientes es mejorar la especificidad de la RPA y conseguir discriminar mutaciones de un único nucleótido a partir de muestras FFPE heterogéneas que presentan una baja proporción de ADN mutante en una matriz de ADN nativa. Una potencial estrategia, investigada en la presente tesis, es el desarrollo de una variante de RPA que permita una amplificación dirigida a las variantes diana, introduciendo un agente bloqueante sintético que se superponga parcialmente a la secuencia complementaria del ADN nativo desde el extremo 5'. La hipótesis es que este oligonucleótido operaría por competitividad, de tal modo que el híbrido ADN/bloqueante, formado durante la amplificación, tendría una mayor estabilidad térmica que el híbrido de ADN/cebador correspondiente. Si el bloqueador también contuviera una modificación química en el extremo 3 ', el oligonucleótido no puede extenderse mediante la polimerasa Bsu. Durante la replicación las secuencias nativas quedarían inhibidas, permitiendo así una amplificación más selectiva enriqueciendo los alelos minoritarios.

Tabla 3. Comparación de los diferentes métodos de detección de mutaciones mediante técnicas de amplificación isoterma.

INNAT	Cebadores	t(min)	v(uL)	plataforma	detección	LOD	Mut	Muestra	Ref
PNA-LAMP	4	50	20	disolución	fluorescencia	1% mut	KRAS G12C	células	Itonaga, 2016
LAMP-PNA	5	40	13	PDMS uF	fluorescencia	1fg/µL	EGFR	FFPE	Liu, 2016
LAMP	4	30	30	PDMS silanizado uF	fluorescencia	11 copias	VRE	células	Ma, 2018
AS-LAMP/ASO-hibridación	4	70-140	13	PC chip	colorimetría	100 copias	GRIK4	bucal	Yamanaka, 2018
USS-sbLAMP	8	50	15	disolución	fluorescencia	50 copias	C580Y,Y493H	suero	Malpartida, 2018
PNA-LNA LAMP	6	60	75	CD uF	colorimetría	10% mut	CARL-1/CARL-2	sangre	Cao, 2018
PE-LAMP	4	80	25	disolución	colorimetría	1000 copias	CYP2C19	bucal	Ding, 2019
PA-LAMP	4	70	30	disolución	fluorescencia	22aM	KRAS G12C	células	Du, 2019
USS-sbLAMP	8	50	15	CMOS con Si3N4	electroquímica/fluorescencia	1000 copias	PIK3CA H1047R	FFPE y células	Kalofonou, 2020
MB-LAMP	6	60	10	disolución	fluorescencia	73.26 Fm	BRAF V600	sangre	Varona, 2020
LAMP	5	40	5	PDMS silanizado uF	fluorescencia	100 copias	EGFR	células	Jia, 2021
LNA-HRCA	2	90	90	PMPs	electroquimioluminiscencia	0.03fM	KRAS G12C	células	Zhang, 2017
PE-RCA	2	325		disolución	fluorescencia	0.05nM	rtV173L	suero	Li, 2019
RCA-ligación	2	190	50	disolución	fluorescencia	0.01%	BRAF V600	células CCR	Zhang, 2019
RCA	2	100	10	electrodo oro	electroquímico	0.28fM	KRAS G12C	suero	Xiao, 2019
PLP-RCA	2	20	40	disolución	colorimetría	3.3pM	H5N1	suero	Hamidi, 2019
RCA	3	50	140	disolución	fluorescencia FRET	60fM	BRAF V600	suero	Dekaliuk, 2019
NESA-RCA	2	40	100	glucosímetro/MNPs	electroquímico	0.36pM	p53	suero	Jia, 2019
RCA	2	120	100	oxido de grafeno		0.3pM	EGFR	células	Xu, 2019
SDA	4	140	25	disolución	sin marcaje/colorimetrico	4pM	KRAS G12C	oligo	Wu, 2017
ISDA(SDA)	4	140	41	disolución	fluorescencia	10pM	KRAS G12C	células	Li, 2019
ISAD-RPA	2	50	10	microanillos de silicona	sin marcaje	50pg/µL	HRAS	células	Shin, 2013
AS-RPA-PNA	3	30	30	disolución	fluorescencia	30%mutante	EGFR	células/FFPE	Liu, 2016
ISAD-RPA	4	30	50	microanillos de silicona	Sin marcaje	1%mutante	KRAS G12C	FFPE	Jin, 2017
RPA	2	30	13	disolución	fluorescencia	1000 copias	Mtb-tuberculosis	células	Ng, 2017
RPA	4	30	6.3	electrodos/PDMS uF	electroquímico	50 copias	TMPRSS2-ERG	ctNA	Koo, 2018
AS-RPA	2	210	4	pocillos PLA/PC chip	colorimetría	5-10%mutante	rs4680,rs1799971	bucal	Yamanaka, 2017
AS-ligación RPA	2	140	6	PC	colorimetría	4ng/µL	CYP2C9, VKROC1	bucal	Lázaro, 2019
RALA(RPA-LAMP)	4	40	50	disolución	fluorescencia	100 copias	BRAF V600	oligo	Chen, 2020

3.4 Micromatrices para biosensado de ADN

El desarrollo de dispositivos biosensores basados en micromatrices de ADN presenta un interés creciente puesto que aportan soluciones de gran utilidad en medicina molecular, expresión génica, detección de mutaciones y genotipado (**Tabla 5**). La capacidad de análisis multiplexado combinado con las altas prestaciones tecnológicas y el bajo coste de los ensayos basados en micromatrices, aportan considerables ventajas para la discriminación de mutaciones puntuales a gran escala (Lu *et al.,* 2020). Durante los últimos años ha crecido exponencialmente la tecnología de micromatrices para el análisis de expresión de todo el genoma humano, junto con herramientas computacionales de *Big Data*. De manera análoga, se han desarrollado tecnologías de micromatrices para genotipado de nucleótidos y detección de mutaciones puntuales, demostrando ser un gran reto debido a la complejidad de la técnica (Gunderson *et al.,* 2005). Estos desarrollos, se han consolidado mostrando ventajas frente a otras tecnologías de análisis de ácidos nucleicos, permitiendo la detección paralela y simultánea de miles de sondas en una misma muestra (He *et al.,* 2020) con distintas técnicas de transducción (**Tabla 4**).

El mercado global de chips genéticos se valoró en 6.8 billones de dólares en 2020, y tiene una previsión de 10.7 billones para 2025, además se prevé una proyección creciente en los años posteriores (**Figura 11**). La capacidad de estos chips genéticos basados en micromatrices de ADN permite un análisis simultáneo completo de miles de genes. Esto, junto a los avances tecnológicos computacionales, robótica y métodos de fabricación han facilitado su rápida asimilación en los laboratorios clínicos de todo el mundo.

Pese a la creciente popularidad de las NGS, los chips genéticos basados en micromatrices no han podido ser reemplazados en el mercado, puesto que presentan claras ventajas en términos portabilidad, multiplexado, capacidades analíticas y coste. Entre las principales compañías posicionadas en el mercado encontramos Thermo Fisher Scientific, Affymetrix, Tecnologías Agilent, Illumina, Perkin Elmer, Arrayit Corporation,

Macrogen, Asper Biotech, CapitalBio Corporation, Greiner Bio-One International GmbH, MYcroarray, Tecnología de Oxford Gene, Toshiba Hokuto electronics corporation, Savyon Diagnostics, Micromatrices aplicadas o bioMérieux SA, entre otras (DNA market chip, 2018).

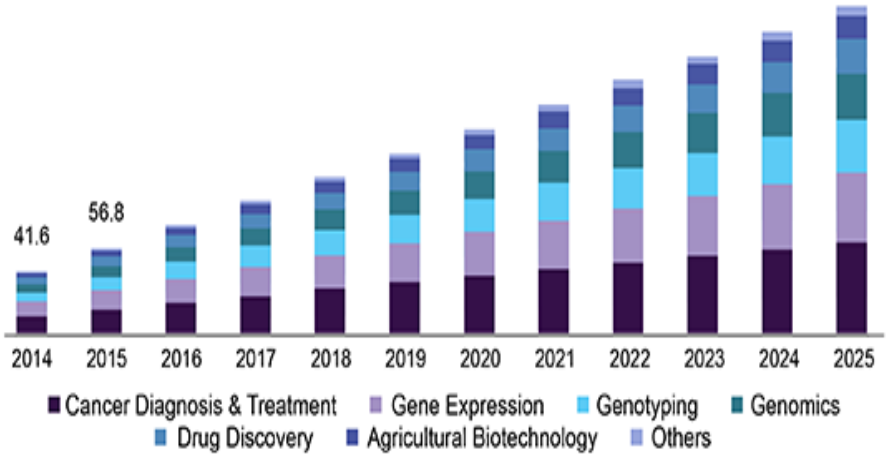

Figura 11. Mercado global de chips genéticos 2014-2025. (Figura original DNA market chip, 2018).

Estos dispositivos son sencillos, portátiles, de bajo coste y utilizan técnicas de microfabricación para la inmovilización altamente selectiva de sus elementos de reconocimiento sobre una superficie sensora orgánica o inorgánica. La exitosa implementación de estos sistemas requiere del desarrollo de métodos de fabricación de matrices de sondas de alta densidad de inmovilización, hibridación selectiva entre secuencias, así como algoritmos para analizar los datos tras la etapa de detección (Sassolas *et al.,* 2008). Esta tecnología interdisciplinar integra conocimientos de biología molecular, tecnologías avanzadas de microfabricación, química de superficies, química analítica, software, robótica y automatización (Johannes *et al.,* 2020).

Entre todos los tipos de biosensores de ADN, los basados en superficies 2D tienen varias ventajas, como alta sensibilidad, selectividad, coste-efectividad, consistencia, versatilidad, precisión, reproducibilidad, reducción de interferencias, robustez y fácil fabricación (Wöhrle *et al.,* 2020). Convencionalmente, las micromatrices de ADN se han fabricado en superficies de vidrio y silicio, sin embargo, se han ido incorporando otros

materiales como los sustratos plásticos, hidrogeles y fibras, entre otros, que están resultando ser muy prometedores por sus prestaciones analíticas. Entre los factores que afectan a la fabricación de micromatrices está el tipo de ácidos nucleicos a inmovilizar, la geometría, la localización, el número, así como la morfología de puntos, la densidad de inmovilización y de hibridación, el formato de ensayo y el modo de detección (Sethi *et al.,* 2008). Las sondas inmovilizadas pueden incluir oligonucleótidos sintéticos o amplicones y éstos a su vez pueden estar unidos covalentemente, electrostáticamente o absorbidos a la superficie sensora (Nimse *et al.,* 2014). La funcionalización del sustrato, así como la longitud y la orientación de la sonda influye notablemente en el rendimiento del ensayo. Idealmente, una matriz biosensora debe ser una superficie organizada molecularmente, que ofrezca una alta densidad de ligandos, accesibilidad adecuada, baja señal inespecífica, unión estable y que no presente estructuras secundarias que puedan generar impedimentos estéricos (Nimse *et al.,* 2014). Por lo tanto, la inmovilización de los bioreceptores a la superficie sensora ha de garantizar la accesibilidad de los sitios activos, puesto que esto afecta a un gran número de parámetros, como son la sensibilidad, estabilidad y reproducibilidad del ensayo, así como tiempo de respuesta, el grado de adsorciones inespecíficas y los tiempos de hibridación con el analito (Prieto-Simón *et al.,* 2008)

Tabla 4. Técnicas de detección, transductor y marcaje empleados en tecnologías de micromatrices de ADN.

Técnicas de detección en micromatrices de ADN

Técnicas	**Transductor**	**Marcaje**
Fluorescencia	Óptico	Fluoróforos
Piezoeléctrico	Piezoeléctrico	Sin marcaje
Impedancia	Electroquímico	Compuestos catiónicos/redox
Capacitancia	Electroquímico	Sin marcaje
Colorimetría	Óptico	Enzimas
SPR	Óptico	Sin marcaje

Tabla 5. Aplicaciones de la tecnología de micromatrices de ácidos nucleicos distribuidas por áreas y tècnicas.

Área	Aplicaciones	Técnicas
Diagnóstico molecular	Detección de patógenos	Detección de secuencias de ADN procedentes de patógenos
Farmacogenética y farmacogenómica	Resistencia a fármacos	Genotipado Análisis de expresión génica
	Diagnóstico y pronóstico oncológico	Genotipado Análisis de expresión génica
	Respuesta a fármacos	Genotipado
	Diagnóstico predictivo	Genotipado
Desarrollo de fármacos	Cribado y ensayos clínicos	Genotipado Análisis de expresión génica

Hay tres formas fundamentales de fabricar una micromatriz de ADN en un soporte sólido: por contacto, por impresión sin contacto y por síntesis in situ. La fabricación de micromatrices mediante impresión sin contacto emplea equipos que están constituidos por un brazo robótico acoplado a un dispensador de líquidos (pL-µL), la cual se desplaza entre las diferentes disoluciones de sonda en función de las coordenadas del software y dispensa la disolución sobre la superficie sensora, creando así una matriz de puntos (Sassolas *et al.,* 2008). A pesar de que la fabricación in situ permite producir matrices de alta densidad, presenta inconvenientes en cuanto a la eficiencia de hibridación y la reproducibilidad del método de inmovilización. Además, requieren de elevada temperatura, así como de procesos más complejos y costosos de fabricación. La temperatura, la humedad, la morfología de los puntos y el modo de inmovilización son otros de los factores clave para optimizar el proceso de fabricación de micromatrices de ADN en pro de conseguir sistemas de biosensado selectivos y sensibles (Bumgarner, 2013).

3.4.1 Inmovilización de sondas de ADN

El mecanismo de inmovilización de los biorreceptores sobre la superficie de un sensor es una de las etapas clave para el proceso posterior de biorreconocimiento, puesto que condiciona su aplicabilidad, correcto funcionamiento, sensibilidad y reproducibilidad del sistema (Sassolas *et al.,* 2012). Para ello, es requisito que el proceso de reconocimiento analito-diana se lleve a cabo de una manera selectiva, para que las propiedades del transductor no se vean alteradas y se genere la máxima respuesta. Algunos de los aspectos críticos de este proceso son la accesibilidad del receptor a la superficie, los procesos de reactividad cruzada, así como las interacciones inespecíficas (Rashid y Yusof, 2017). El proceso de inmovilización se puede definir como la unión de moléculas a una superficie, que tiene como resultante una reducción o pérdida de su movilidad. En concreto, para la fabricación de micromatrices de ADN, la elección de la estrategia de inmovilización está condicionada por las propiedades fisicoquímicas de la superficie y los grupos funcionales de las sondas de ADN (Nimse *et al.,* 2014). Existen diferentes vías de inmovilización de sondas en soportes analíticos, que a continuación se detallan:

Inmovilización por adsorción: Este fenómeno se debe a la adsorción física de biomoléculas sobre la superficie del transductor. Este método de inmovilización es el más simple puesto que no requiere de ninguna modificación química del ligando y es aplicable a una gran variedad de superficies (Rashid y Yusof, 2017). La inmovilización por adsorción puede deberse a procesos de fisisorción o quimisorción, los cuales implican interacciones electrostáticas y fuerzas de Van der Waals, puentes de hidrógeno o interacciones hidrofóbicas (Zouaoui *et al.,* 2020). Este tipo de inmovilización presenta algunas limitaciones puesto que el ADN puede estar orientado aleatoriamente lo cual produciría adsorciones inespecíficas. Además, debido a la debilidad del enlace, cambios en el pH, fuerza iónica o temperatura de trabajo pueden dar lugar a la desorción de los biorreceptores e irregularidad superficial (Sassolas *et al.,* 2008).

Inmovilización por afinidad: Esta técnica se caracteriza por su gran selectividad ya que utiliza un par de moléculas que se reconocen específicamente con gran afinidad. De entre ellos, cabe destacar. La interacción biotina-estreptavidina es una de las más sencillas y aplicadas (Rashid y Yusof, 2017). Estos reactivos han sido ampliamente utilizados en nuestro grupo para la inmovilización indirecta de ssDNA y proteínas en sistemas de detección basados en micromatrices (Santiago-Felipe *et al.,* 2014) sobre superficies de policarbonato, DVD, blu-ray y otros polímeros además de discos (Morais *et al.,* 2016).

Inmovilización por atrapamiento: En este tipo de inmovilización, los receptores se fijan en una matriz polimérica inerte con estructura tridimensional que es capaz de atrapar grandes cantidades de biomoléculas. Dentro de este tipo de matrices poliméricas encontramos la poliacrilamida, el quitosano o el nylon, entre otros. Estas metodologías no necesitan modificaciones covalentes debido a su flexibilidad y el control del tamaño de poro, entre otros. Sin embargo, presenta grandes barreras de difusión, lo cual puede conllevar la pérdida de conformación de la biomolécula debido a su liberación a través de los poros de la matriz y el incremento de las señales inespecíficas derivadas del proceso de atrapamiento no selectivo (Prieto-Simón *et al.,* 2008).

Inmovilización covalente: La unión covalente es el método más estable de inmovilización de ssADN a superficies. Este tipo de inmovilización requiere de la modificación del oligonucleótido en su extremo 5’ y de la superficie transductora, presentando ambas partes grupos reactivos funcionales (Sassolas *et al.,* 2012). Los métodos de inmovilización covalente permiten orientar y posicionar de manera ordenada y controlada las moléculas de ADN de forma que éstas se dispongan de manera mesoespaciada a lo largo de la superficie sensora, manteniendo una posición vertical, lo cual favorece la accesibilidad y la hibridación con su secuencia complementaria.

Entre todas las interacciones covalentes, las interacciones con glutaraldehído, carbodiimida y enlaces tiol son las utilizadas con mayor frecuencia en biosensado. El glutaraldehído o la etilendiamina actúan como agentes entrecruzantes entre el grupo -OH de la superficie y el grupo $–NH_2$ primario de la molécula de ADN, suponiendo esto una ventaja puesto que proporcionan un espaciador físico que puede minimizar los impedimentos estéricos entre la interfaz ADN-superficie (Tjong *et al.,* 2014). En la conjugación de carbodiimida EDC-NHS, el ssDNA se une a la superficie sensora mediante la formación de un enlace amida entre el grupo –COOH del material funcionalizado y el $–NH_2$ del oligonucleótido funcionalizado (Tamarit-López *et al.,* 2011). Esta inmovilización puede realizarse sobre distintas superficies, como por ejemplo soportes inorgánicos, polímeros sintéticos, membranas previamente activadas, nanomateriales como partículas o moléculas dendriméricas (Sassolas *et al.,* 2012).

La silanización es otra técnica ampliamente aplicada para la inmovilización covalente de ADN, por ejemplo, la unión fotoquímica del tiol-eno ha sido estudiada para el anclaje covalente de sondas de ADN tioladas. En concreto, nuestro grupo ha investigado en la funcionalización de vidrio con viniltrietoxi-silano (VTES) (Aragón *et al.,* 2018). También se han usado silanos fluorados como el 1H,1H,2H,2H-perfluorodeciltrietoxi-silano (FFTES) para incrementar la densidad de inmovilización de sondas (Jiménez-Meneses *et al.,* 2018). El 3-aminopropiltrietoxisilano (APTES) también ha sido utilizado ampliamente en el campo de biosensores de ADN (He *et al.,* 2020). En la **Tabla 6** se recogen los modos de inmovilización de sondas de ADN anteriormente citados.

Tabla 6. Modos de inmovilización de sondas de ADN.

Método	Orientación de la sonda	Accesibilidad	Ventajas	Desventajas
Adsorción	Al azar	Baja	Sencillez	Desorción, inespecificidad
Afinidad biotina-estreptavidina	Ordenada	Alta	Sencillez	Tratamiento superficie /o no
Inmovilización por atrapamiento	Al azar	Baja	Gran cantidad de sondas	Tratamiento superficie Adsorción inespecífica
Unión covalente	Ordenada	Alta	Estabilidad Gran cantidad de sondas	Tratamiento superficie
Silanización (covalente)	Ordenada	Alta	Control de la densidad de sonda	Tratamiento superficie Adsorción inespecífica

3.4.2 Hibridación de ADN

La hibridación de ácidos nucleicos es un proceso fundamental en biología. Este proceso se aplica en diversas técnicas, incluyendo la arquitectura molecular, síntesis orgánica mediada por ADN, administración de fármacos y biosensores de ADN (Du *et al.,* 2017).

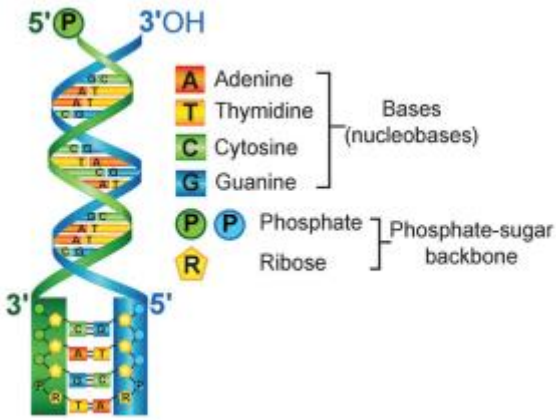

Figura 12. Esquema de la molécula de ADN. Figura original *Tjong, 2014*.

Las fuerzas estabilizadoras entre las bases del duplex (**Figura 12**), cómo son los enlaces por puentes de hidrógeno o fuerzas intermoleculares, pueden romperse fácilmente debido a cambios en el pH, agentes desnaturalizantes, temperatura o fuerza iónica de la disolución de hibridación. Además, sustancias como la urea o la formamida también se emplean para romper los puentes de hidrógeno y para reducir la temperatura de fusión de los ácidos nucleicos, lo cual favorece una hibridación más selectiva (Bielec *et al.,* 2019). La estabilidad de la doble hebra puede cuantificarse definiendo el cambio en la energía libre de reacción de hibridación, ΔG_{hib}, calculada a partir de los enlaces de hidrógeno entre cada par de bases y las interacciones entre las bases adyacentes (Traeger y Schwartz, 2017).

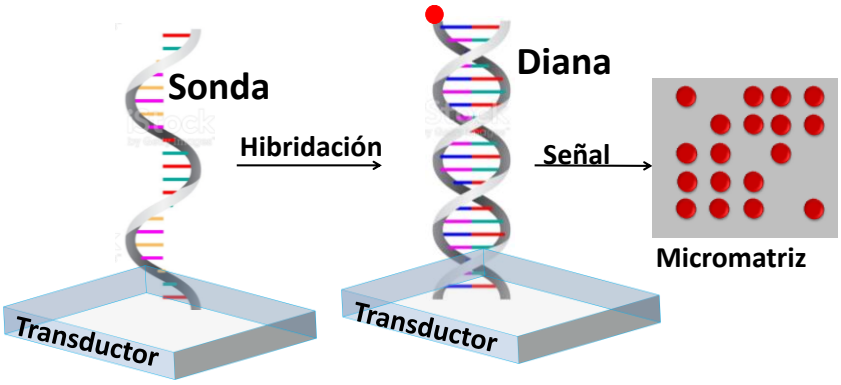

Figura 13. Esquema de hibridación de DNA en tecnología de micromatrices.

El proceso de hibridación constituye el evento de reconocimiento biomolecular intrínseco de la mayoría de los genosensores. En este tipo de sistemas, la cadena de ADN es inmovilizada sobre el biosensor y reconocida por el analito diana durante la hibridación (**Figura 13**). El diseño de sondas resulta clave en este proceso, normalmente, se diseñan oligonucleótidos sintéticos cortos, puesto que no repercuten en cambios conformacionales complejos, impedimentos estéricos o formación de estructuras secundarias que disminuyan la velocidad, la eficiencia o la selectividad de hibridación (Teles y Fonseca, 2008). Además, estos oligonucleótidos pueden introducir funcionalidades y modificaciones útiles para el anclaje en superficie, puesto que la estructura del oligonucleótido proporciona múltiples sitios para modificación **(Figura 14)** (Tjong *et al.,* 2014).

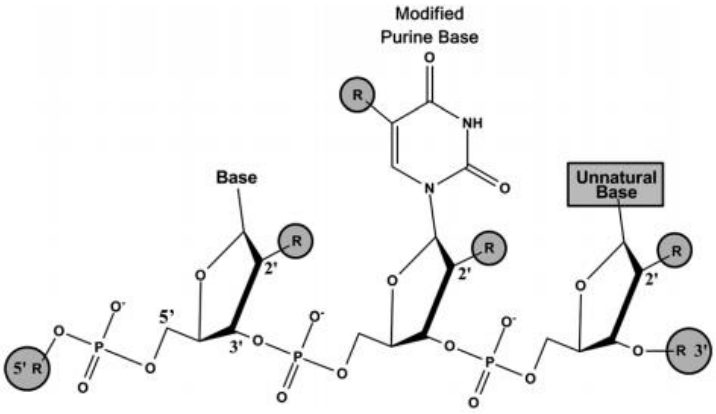

Figura 14. Esquema de la modificación del ADN en sitios específicos. Figura original *Tjong, 2014*

Generalmente, la hibridación de ácidos nucleicos se puede llevar a cabo mediante dos estrategias, que son, la hibridación en fase sólida y en disolución.
Entre los factores que afectan a la hibridación de ácidos nucleicos en una interfaz encontramos, la densidad de sonda y la conformación de la sonda en superficie.

A bajas densidades de inmovilización, es posible que parte de la sonda se adsorba en la superficie, adquiriendo conformaciones plegadas. Una estrategia muy interesante para mejorar la eficiencia de hibridación, es la inserción de un espaciador (enlazador) entre la superficie sólida y la secuencia de reconocimiento de ADN, puesto que promueve el mesoespaciado y una mayor distancia superficie/sonda. Dentro de estos encontramos algunos organosilanos que actúan como brazos espaciadores o moléculas dendriméricas que, además, permiten una mayor densidad de inmovilización por unidad de superficie (Ravan *et. al,* 2014).

La utilización de sondas alelo específicas (ASO) resulta muy interesante para conseguir una hibridación eficiente y específica puesto que permite un reconocimiento altamente selectivo. Este fenómeno se debe a la estabilidad térmica y la complementariedad de bases entre una sonda ASO perfectamente coincidente y el analito diana, lo cual permite distinguir entre los alelos de mutaciones puntuales (Yamanaka *et al.,* 2018).

3.4.3 Formato de ensayo para la detección de ADN

Las reacciones de amplificación e hibridación de ácidos nucleicos y su posterior detección pueden llevarse a cabo en formato homogéneo o heterogéneo. En el primero, el proceso suele desarrollarse en un tubo de ensayo o una plataforma fluídica. Este formato de ensayo resulta muy interesante para el biosensado de ADN, puesto que permite reducir los tiempos de reacción, minimizar etapas y reducir la contaminación por la estanquidad de la muestra (Schrittwieser *et al.,* 2016). Dichos ensayos en disolución suelen beneficiarse de procesos de unión más rápidos que en fase sólida. Además, permiten la simplificación del procedimiento de ensayo, puesto que no

necesitan pasos de separación o lavado, pueden ser monitoreados a tiempo real y son susceptibles de automatización (Demidov*,* 2003). Sin embargo, presentan ciertas desventajas en la especificidad de la detección de muestras biológicas con matrices complejas, dónde se requiere de una detección multianalito combinado con formato multiplexado.

Los ensayos heterogéneos, por su parte, como los ensayos basados en micromatrices (Lázaro *et al.,* 2019) o los ensayos tipo ELISA (Santiago-Felipe *et al.,* 2014), se basan en la difusión de las moléculas de analito en el seno de la disolución hacia la superficie sensora para generar una señal medible. Éstos presentan gran capacidad de multiplexado, especificidad, robustez y elevado rendimiento. En comparación con los ensayos homogéneos, los ensayos en formato heterogéneo pueden utilizar una amplia gama de plataformas de transducción como la óptica, másica o electroquímica. Además, el desarrollo de este tipo de formato, permite la generación de plataformas integradas basadas en superficies inteligentes, que permiten el multiplexado de muestras heterogéneas y la detección múltiple de analitos. Si bien es cierto que éstos requieren pasos de inmovilización, separación y lavado, resultan altamente interesantes para la fabricación de dispositivos POCT sensibles, selectivos y de bajo coste dirigidos al biosensado de ADN (Zhang *et al.,* 2013).

Ambos formatos de ensayo también pueden combinarse e incorporar nanomateriales, presentando cinéticas y eficiencias de hibridación muy interesantes (Ning *et al.,* 2020). En este contexto, surgen los microsistemas de análisis total µTAS (Luka *et al.,* 2015). En dichos sistemas se integran, por ejemplo, amplificaciones isotermas, con nanopartículas en plataformas fluídicas en un único dispositivo miniaturizado que incluyen varias etapas de la reacción como extracción, purificación, amplificación y detección de ADN, reduciendo así la contaminación, el consumo de reactivos y el tiempo de reacción (Moschou y Tserepi*.,* 2017).

3.4.4 Superficies para el biosensado de ADN

Los biosensores de ADN heterogéneos se pueden fabricar sobre una matriz de soporte, que puede estar funcionalizada para unir de manera específica el elemento de biorreconocimiento. La naturaleza del material, el tipo de fabricación, el diseño, la flexibilidad, la permeabilidad al aire, la conductividad eléctrica, la adsorción inespecífica, la compatibilidad biológica y a agentes disolventes, así como la transparencia óptica, influyen en gran medida en la capacidad de detección final, en el tipo de analito a inmovilizar y en el transductor. A continuación, se detallan los principales materiales y tipos de superficies más utilizadas frecuentes en la fabricación de biosensores:

3.4.4.1 Superficies inorgánicas planas

Tanto el **silicio** como el **vidrio,** son materiales muy empleados como soportes biosensores. Su química de inmovilización en superficie aprovecha los grupos silanol nativos (Bañuls *et al.,* 2013). En concreto, el **vidrio** es el soporte utilizado históricamente en la fabricación de biosensores por su gran compatibilidad con muestras biológicas, transparencia y capacidad de generar grupos reactivos para el anclaje de biomoléculas (Escorihuela *et al.,* 2014). Esta superficie sensora presenta baja adsorción inespecífica y fluorescencia. Sin embargo, en el proceso de fabricación de sistemas fluídicos, estas superficies no resultan tan interesantes puesto que poseen un módulo elástico elevado y presentan problemas de mecanizado (Nge *et al.,* 2013).

3.4.4.2 Superficies orgánicas planas

Existe una amplia gama de materiales orgánicos poliméricos que se utilizan como superficies biosensoras, tanto como soportes de inmovilización de ADN como en la fabricación de soportes microfluídicos. El **PDMS** es uno de los materiales más utilizados debido a su elevada transparencia óptica y elasticidad (Jian *et al.,* 2017). La **celulosa** es otro material ampliamente utilizado como superficie sensora puesto que es económico, flexible, biológicamente compatible, puede modificarse químicamente, además su

fondo blanco proporciona un contraste óptimo para los métodos de detección basados en colorimetría (Ivanov *et al.,* 2020). Este material se emplea en los ensayos de flujo lateral (LFA) o μ-PAD, basados en el mecanismo pasivo de acción capilar (Sena-Torralba *et al.,* 2021).

Los **termoplásticos**, por su parte, son polímeros densamente reticulados que se pueden moldear cuando se calientan a su temperatura de transición vítrea, pero conservan su forma cuando se enfrían. Estos materiales son duraderos, susceptibles de micromecanizado, ópticamente transparentes, poseen un bajo porcentaje de absorción de agua y de disolventes orgánicos, además son resistentes a ácidos y bases, son más rígidos que los elastómeros y tienen una buena estabilidad mecánica (Morais *et al.,* 2016). La mayoría de ellos son polímeros sintéticos que poseen propiedades superficiales óptimas para la fabricación de biosensores y en concreto, para aplicaciones microfluídicas (Tsao*,* 2016). Algunos termoplásticos como el polimetilmetacrilato de metilo (PMMA), policarbonato (PC), poliestireno (PS) y la familia de copolímeros de olefinas cíclicas (COC) o polímero de olefina cíclica (COP), se han utilizado ampliamente en la fabricación de biosensores (Prada *et al.,* 2019). Estos materiales poliméricos son relativamente económicos, aptos para producción en masa, de naturaleza hidrófoba, susceptibles de modificación química y funcionalización con grupos reactivos (Tortajada-Genaro *et al.,* 2015).

Los materiales flexibles también son tendencia en la fabricación de biosensores puesto que son adaptables, de bajo coste, alta disponibilidad, ligeros, transparentes, deformables y estirables (Zhang *et al.,* 2018). Dichos sensores pueden ir conectados al cuerpo y mediante una señal eléctrica detectar señales biológicas (Karfa *et al.,* 2020). Los sustratos más utilizados en esta área son el papel y las fibras textiles, aunque mayoritariamente se emplean polímeros termoplásticos (Economou *et al.,* 2018).

3.4.4.3 Partículas

Los nanomateriales particulados son muy útiles en la investigación biomédica de vanguardia. Las nanopartículas metálicas, magnéticas, de sílice, o los nanodots de carbono, entre otros, se están aplicando ampliamente en el desarrollo de genosensores. En concreto, las nanopartículas de oro (AuNPs) funcionalizadas con ADN han sido ampliamente estudiadas en biosensado, tanto en la preparación de conjugados (Liu *et al.,* 2017), como en detección (Wu *et al.,* 2019) y en fabricación de materiales (Jones y Mirkin, 2015). Además, se han utilizado ampliamente en combinación con ensayos de flujo lateral para la detección de ADN y, recientemente, para la detección de productos de amplificación de RPA (Ivanov *et al.,* 2020). Por su parte, los nanodots de carbono (CDs), también resultan especialmente interesantes para el desarrollo de genosensores, recientemente han sido estudiados para detección de patógenos (Martínez-Periñán *et al.,* 2021) y discriminación selectiva de la mutación *BRCA1,* por el grupo de E. Lorenzo (García-Mendiola, *et al.,* 2020) mediante sensado electroquímico.

Las **partículas magnéticas** (MNPs) están constituidas por un núcleo ferroso y pueden estar recubiertas con polímeros, tensoactivos, sílice, carbono o con una matriz químicamente inerte. Este recubrimiento no solo la protege contra la degradación, sino que también se puede usar para funcionalizar la superficie con moléculas específicas (Tang *et al.,* 2020). Dichas MNPs exhiben una elevada especificidad y permiten realizar operaciones de agregación/dispersión magnéticamente controlables, lo cual posibilita la preconcentración, purificación y separación de ácidos nucleicos de manera rápida, sencilla y eficaz (Schrittwieser *et al.,* 2016).

En ausencia de campo magnético, las MNPs se presentan suspendidas y dispersas en disolución, mientras que en el proceso de separación y agregación son retenidas al aplicar un campo magnético usando electroimanes, bobinas o imanes permanentes (Tangchaikeeree *et al.,* 2017). Esta separación magnética de ácidos nucleicos tiene ventajas en comparación con otras técnicas descritas, puesto que permiten aislar, extraer y concentrar ácidos nucleicos en muestras complejas como

sangre, tejidos, cultivo o productos de amplificación (Saiyed *et al.,* 2008), incluso puede aplicarse de forma relativamente fácil a muestras viscosas.

Dichos nanomateriales pueden utilizarse como soporte sólido para la inmovilización de receptores. Esta propiedad resulta muy interesante puesto que ofrece un aumento drástico en la relación superficie-volumen, que se traduce en una mayor respuesta del ensayo, promovida por una mayor densidad de sonda por unidad de superficie (Abi *et al.,* 2019). Además, este tipo de plataformas analíticas se están utilizando para desarrollar nuevos dispositivos integrados (Van Reenen *et al.,* 2014), que reducen los volúmenes de reactivos y el tiempo de ensayo. Estas propiedades resultan muy útiles para la fabricación de sistemas miniaturizados, microfluídicos y automatizados, dónde exista un transporte de materia inducido mediante imanes permanentes externos (Chang *et al.,* 2017*)*.

En concreto, estas partículas magnéticas han sido utilizadas para la discriminación de mutaciones de un único nucleótido a partir de productos de amplificación de PCR (**Tabla 7**). Recientemente el grupo de Lapitan detectó mutaciones del gen *KRAS* mediante un ensayo combinado de MNPS y ligación (Lapitan *et al.,* 2019), mientras que el grupo de Hui también detectó esta mutación a partir de producto de PCR mediante ensayo de LFA (Hui *et al.,* 2016). Mutaciones de este mismo gen también han sido detectadas con este tipo de plataformas mediante procesos de agregación, distinguiendo entre partículas conjugadas con sondas nativas y con sondas mutantes (Sloane *et al.,* 2015), (Sloane *et al.,* 2016). También, el grupo de Chen aplicó la misma estrategia para la detección de esta mutación mediante ligación (Chen *et al.,* 2012). Además, estos sistemas, basados en nanopartículas, se han utilizado para la detección de mutaciones puntuales del gen *BRAF* a partir de productos de PCR (Wang *et al.,* 2017). Previamente, otros grupos ya habían demostrado la utilidad de las MNPS para la detección de mutaciones de único nucleótido a partir de producto de amplificación de PCR (Liong *et al.,* 2013), (Liu *et al.,* 2013) (Liu *et al.,* 2010).

Tabla 7. Discriminación de SNPs con MNPs

Amplificación	LOD	Ref
PCR	1 fM	Lapitan, 2019
PCR	5 nM	Wang, 2017
PCR	5 ng	Hui, 2016
PCR	1nM	Liong, 2013
PCR	0.1 nM	Liu, 2010
PCR	50 ng	Sloane, 2015
PCR-ligación	1 copia	Chen, 2013
RCA	0.1 fM	Hernandez-Neuta, 2018
RCA	0.1 fM	He, 2014
RCA	0.94 pM	Miao, 2020

La aplicación de MNPS en combinación con la amplificación isoterma también ha sido aplicada para la detección de mutaciones puntuales a partir de producto de RCA en formato no fluídico (He *et al.,* 2014) y fluídico (Hernández-Neuta *et al.,* 2018). Sin embargo, el empleo de MNPS con la RPA ha sido abordado por pocos grupos de investigación. Los principales desarrollos incluyen el cribado de fármacos (Loo *et al.,* 2013), la resistencia a antibióticos (Kalsi *et al.,* 2019) y recientemente la detección de patógenos en un sistema POCT microfluídico PDMS/vidrio que combina la extracción, amplificación por RPA y detección (Yin *et al.,* 2020). Sólo el grupo de Dey ha combinado la RPA con MNPs para la detección de mutaciones del oncogen *BRAF* V600 en un sistema integrado con detección electroquímica (Dey *et al.,* 2019).

3.3.4.4 Chips con estructuras tridimensionales

Las matrices bidimensionales se construyen principalmente con capas modificadas a partir de silanos, polianilinas, polilisinas, etc. Dichas capas de interfaz tienen limitaciones para desarrollar una matriz biosensora estable, densa y bien organizada. Por ejemplo, el silano tiende a polimerizar al exponerse al aire / humedad y da como resultado una adherencia defectuosa e irreproducible en el sustrato, presentando bajas eficiencias de inmovilización (Aragón *et al,* 2018). En este contexto, las matrices tipo 3D emergen como alternativa interesante para el desarrollo de chips de alta densidad, por ejemplo, el uso de hidrogeles 3D es una aproximación que se ha

estudiado recientemente (Ramírez *et. al,* 2020) para el biosensado holográfico. Otra aproximación muy interesante se centra en el desarrollo de superficies 3D mediante arquitecturas supramoleculares tridimensionales, tales como sistemas dendriméricos.

Los **dendrímeros** son polímeros fractales de estructura tridimensional, conformados por ramas con grupos funcionales que a su vez son unidades repetidas que crecen desde un núcleo central (Lyu *et al.,* 2019). Varios autores han sintetizado una gran variedad de dendrímeros como de Vögtle, Denkewalter, Tomalia y Newkome (Paez *et al.,* 2012). Algunos de estos polímeros hiperramificados, con diferentes estructuras centrales, grupos terminales, generación y grado de pureza se producen a escala industrial. De ellos, el dendrímero más extendido es la poliamidoamina (PAMAM) (Sánchez *et al.,* 2019).

Los **dendrones**, por su parte, son los monómeros del dendrímero, secciones monodispersas en forma de cono con múltiples grupos terminales y una única función reactiva en el punto focal. Éstos pueden anclarse a la superficie por el ápice o por los grupos periféricos; en el primer caso promueven el mesoespaciado puesto que cada estructura facilita una distancia controlada (Roy y Park, 2015). En el segundo caso los grupos periféricos promueven la unión multipunto en un área concreta, lo cual favorece el incremento de la densidad de inmovilización de sondas por unidad de superficie (Sirianni y Gillies, 2020).

Tanto dendrímeros como dendrones han demostrado ser idóneos en el diseño de bioplataformas mesoespaciadas, ya que su forma globular proporciona un espaciamiento del orden de 18 Å, mientras que una matriz no dendrimérica presenta espaciados de 10 Å, lo cual puede originar impedimentos estéricos en los sitios de unión del analito (Satija *et al.,* 2011). Ambos nanomateriales poseen alto grado de control estructural, autoorganización, elevada densidad y multivalencia (Erdem *et al.,* 2018), además actúan como moduladores de la hidrofilia/hidrofobia de la superficie (Sánchez *et al.,* 2019).

La funcionalización y el número de grupos terminales son algunas de las características más relevantes en el proceso de inmovilización de moléculas dendriméricas, puesto que repercuten tanto en el grado de dendronización como en la química de anclaje (Chandra *et al.,* 2017). Distintos autores han desarrollado superficies 3D a partir de dendrones y dendrímeros funcionalizados con grupos $–NH_2$, -OH, -SH, -COOH para crear micromatrices de ADN de alta densidad sobre superficies de vidrio y oro (Öberg *et al.,* 2013), (Onodera y Toko, 2014). Mientras que otros autores han utilizado portaobjetos comerciales dendronizados (NSB POSTECH, Inc) con diferente funcionalización para incrementar la sensibilidad del ensayo o favorecer el mesoespaciado entre las sondas de ADN ancladas (Kim *et al.,* 2018).

Las matrices de ADN dendronizadas han mostrado mayor capacidad de hibridación y mejor respuesta, puesto que se ha demostrado que la sensibilidad de detección de estas matrices es aproximadamente ocho veces superior a la de las convencionales. Este incremento en el rendimiento se debe a la gran cantidad y disponibilidad de ssDNA por unidad de superficie. Por otra parte, estas estructuras dendriméricas proporcionan una orientación homogénea y una distribución espacial ordenada de los biorreceptores en la matriz sensora, lo cual resulta muy interesante para el desarrollo de biosensores de altas prestaciones (Satija *et al.,* 2011).

Estas estructuras dendríticas han sido aplicadas para la detección de mutaciones a partir de productos de amplificación de PCR (Le Berre *et al.,* 2003), (Caminade *et al.,* 2006) y para la detección de mutaciones de secuencias sintéticas (Jayakumar *et al.,* 2012), (Senel *et al.,* 2019). Sin embargo, no se han aplicado en combinación con amplificaciones isotermas para la detección de mutaciones puntuales. El grupo de Cao es el único que ha combinado la amplificación isoterma RCA con dendrímeros, pero no para la detección de variaciones puntuales de ADN, sino para la detección de células (Jiang *et al.,* 2017).

Por otra parte, existen numerosas publicaciones dónde se han conjugado dendrímeros o dendrones con DNA. Sin embargo, estos híbridos han sido utilizados

como vectores en farmacogenética y terapia génica (Caminade, 2020), (Chis *et al.,* 2020); mientras que una minoría de investigaciones ha conjugado moléculas dendrímericas con ADN previamente a su inmovilización sobre una superficie 2D (Warner *et al.,* 2020), (Liu *et al.,* 2010), lo cual supone un reto interesante para la generación de nuevos biosensores integrados.

Pese a que la inmovilización de dichos polímeros fractales sobre superficies sólidas, planas y convencionales (sílice, oro y mica) ha sido descrita (Caminade *et al.,* 2006), actualmente se están investigando otras superficies novedosas. En concreto, se han desarrollado superficies dendronizadas sobre poliéster (Morshed *et al.,* 2019), celulosa (Vidal *et al.,* 2020), metacrilato (Evans *et al.,* 2021), fibra óptica (Kamil *et al.,* 2019) y polímeros orgánicos como PS o PMMA (Bosnjakovic *et al.,* 2012*),* (Akers *et al.,* 2017). En concreto, el grupo de Cao y colaboradores fue pionero en anclar dendrímeros PAMAM-COOH en superficies termoplásticas híbridas de PDMS y SU-8 (Qin *et al.,* 2015) para la detección de células de *E.Coli* (Jiang *et al.,* 2017), (Hao *et al.,* 2019) y células tumorales CRM-CEM (Qin *et al.,* 2017). Recientemente, el grupo de Habibovic también ha desarrollado un dispositivo microfluídico para el cultivo y detección de células HCT116 tumorales de colon en chips 3D fluídicos (Carvalho *et al.,* 2019) (**Figura 15**).

En la **Tabla 8** se recogen los distintos biosensores basados en superficies planas dendronizadas. La mayoría de estos sensores utiliza detección fluorescente, mientras que una minoría son biosensores colorimétricos de fácil lectura sobre poliestireno y poliéster (Bosnajokovic *et al.,* 2012), (Morshed *et al.,* 2019), no aplicados para la detección de ADN, sino para la detección de glucosa y proteínas.

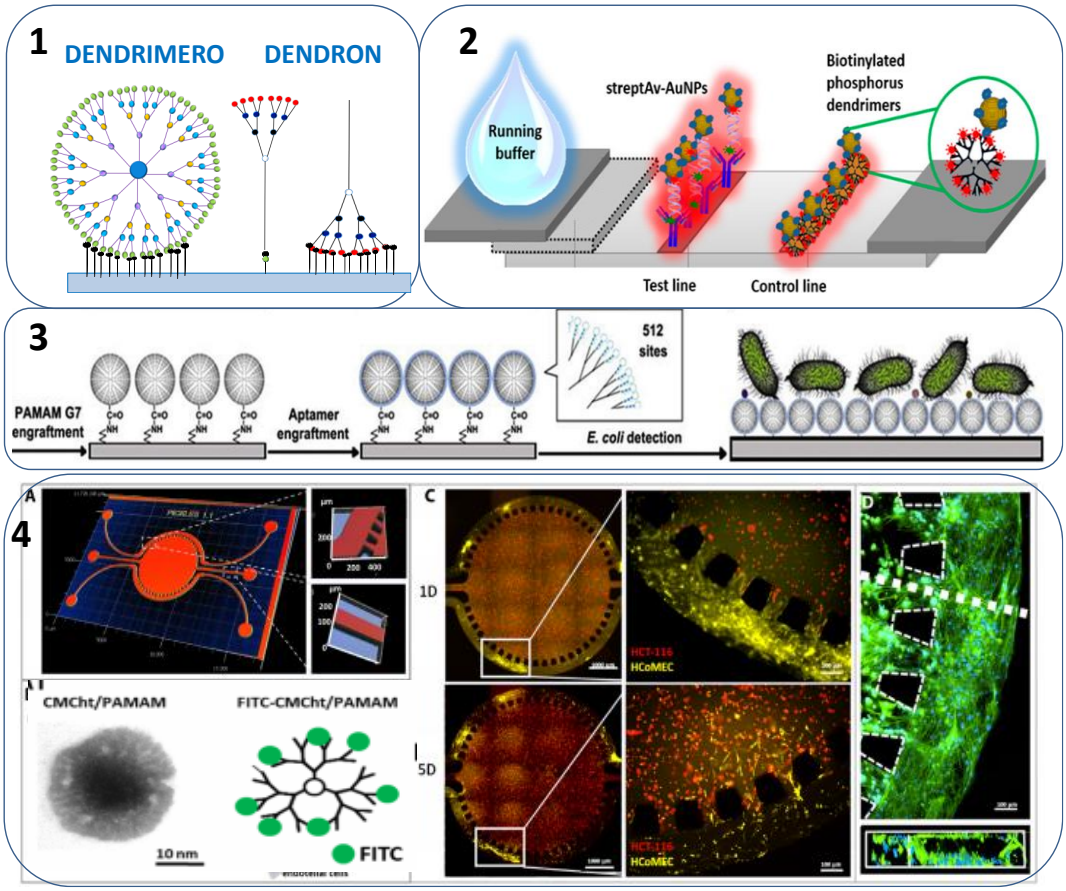

Figura 15. Biosensores basados en superficies dendronizadas: (1) Esquema del anclaje del dendrímero y el dendrón a la superficie 2D; (2) Ensayo en flujo lateral (LFA) (*Vidal, 2020*); (3) Ensayo microfluídico en chip de PDMS (*Hao, 2019*); (4) chip 3d basado en dendrímeros para detección de células HCT 116 (detección cáncer colorectal) (*Carvalho, 2019*). Figuras modificadas de las publicaciones originales citadas.

Tabla 8. Comparación de las características de los biosensores basados en superficies planas dendronizadas

Sustrato	Dendrimero/dendrón	Anclaje	Analito	Biosensor	Referencia
Vidrio/silica	Dendrímeros de propileneimina G1-5	Silano	proteínas		Pathak, 2014
	Dendrímeros carboxílicos	-	proteínas	fluorescencia	Akujimar, 2007
	Dendrímeros de fósforo	APTES silano	Oligos ADN	fluorescencia	Trevisol, 2003
	PAMAM 64-NH_2	APTES/GOPTS silano	PCR HCV virus	fluorescencia	Benters, 2002
	PAMAM -NH_2 G5	-	Oligos ADN		Gogard, 2009
	PAMAM -NH_2 G3	-	Oligos ADN		Lim, 2008
	Dendrímeros de propileneimina G5	trimethoxísililalkilaldehído	Oligos AND/ARN	fluorescencia	Rozkiewicz, 2007
	PAMAM -NH_2 G4, G5, G6			RSL (sin marcaje)	Liu, 2017
	Dendrímeros de fósforo	-	PCR bacteria 16S rDNA,	fluorescencia	Senescau, 2018
	Dendrón-NH_2 ápex	Silano GPDES	Oligos ADN	fluorescencia	Hong, 2005
	Dendrón-NH_2 ápex	TPU silano GPDES	Oligos ADN	AFM	Jung, 2007
	Dendrón-NH_2 ápex	Silane GPDES Aldehído	CCT	fluorescencia	Oh, 2005
	PAMAM -NH_2	APTES, DSG, PDITC silano	Oligos ADN y proteínas	fluorescencia	Benters, 2001
	Dendrímeros de fósforo G4	APTES	PCR producto	fluorescencia	Le Berre, 2003
	Dendrón-NH_2 ápex	GPDES silano	Oligos ADN	fluorescencia	Sunkara, 2006
	Superficies dendrón comerciales	-	Oligos ADN	AFM	Boateng, 2012
	Chips comerciales recubiertos con dendrones-COOH	-	Oligos ADN	SPL/AFM	Lee, 2016
Oro		Aldehído	BSA-anti-BSA	Fluorescencia	Hong, 2003
	Dendrímeros de phofirina	APTES silano	Glucosa	fluorescencoa	Lee, 2009
	PAMAM-Tiol G3	-	Oligos ADN	XPS/SPR	Day, 2011
	Dendrímeros de fósforo G4	-	Oligos ADN	SPR	Yu, 2009
		-	Oligos ADN	SPR	Kwon, 2007
	PAMAM G4	SAM de Hidroxisuccinimidida (NHS-C10)	Avidina-biotina	SPR/fluorescencia	Hong, 2003
	PAMAM -NH_2		-	AFM/XPS	Degenhart, 2004
	Dendrón-NH_2 ápex	DSC activación	Biotina	AFM/XPS	Yang, 2004
			-	IRRAS	Hu, 2014
	PAMAM-NH_2 G2, G3, G4	SAM PEG3-OH y PEG6-NHS	IgG y avidin	SPR	Syahir, 2009
	PAMAM-COOH	SAM	Proteínas	SPR	Matsumoto, 2011
	Dendrímeros de fósforo G4	Amino-funcionalización	Oligos ADN	SPR	Pillet, 2013
	PAMAM-NH_2	-	Dengue	SPR	kamil, 2019
	PAMAM G4-NH_2	-	?	SPR	Satija, 2014
PDMS	COOH-PAMAM G4,G7	SU-8 híbrido	*E.coli*		Qin, 2015
Fibra	PAMAM-COOH	Aptámero	*E. coli*		Hao, 2019

Tabla 8. Continuación

	Dendrinero/ dendron	Anclaje	Analito	Biosensor	Referencia
	PAMAM-COOH G4 y G7	SU-8 híbrido	CCT		Qin, 2017
	PAMAM-COOH	DNA áptameros	*E. coli*		Jiang, 2017
PS	Dendrón –COOH G2,G3	Etilenglicol	proteínas	fluorescencia	Roy, 2008
PMMA	PAMAM-COOH G 1.5- 5.5		IgG	fluorescencia	Akers, 2017
PEI	Dendrímero de porfirina	-	IgG	fluorescencia	Son, 2010
ELISA-placa	PAMAM G4: Bifuncional –OH/SH	PEG	IL-6 y IL-1b	Luminescencia y colorimetría	Han, 2010
	PAMAM-OH G4		(TNF-a)	TMB colorimetría	Bosnjakovic, 2012
	BIS-MPA Dendrón		-	-	Anavi, 2018
	bis-MPA Dendrón-OH		Lectina	QCM	Montañez, 2011
Celulosa	BIS-MPA Dendrón	PEG	IgE	RAST	Tesfaye, 2021
	bis-MPA Dendrón-OH		IgE		Ruiz-Sánchez, 2012
Poliester Híbridos	PAMAM-OH	Plasma	Glucosa	Colorimetría	Morshed, 2019
	PAMAM-MWCNTs-CP	Glutaraldehído	GOx	Electroquímica	Burber, 2017

3.5 Plataformas integradas

El concepto del microsistema de análisis total (µTAS) ha revolucionado las técnnicas analíticas clásicas y las de biosensado, debido a las ventajas que presenta frente a las pruebas de laboratorio convencionales, como es el tiempo de respuesta, la automatización y el coste (Luka *et al.,* 2015). Un µTAS es un dispositivo que integra múltiples funciones bioanalíticas en un instrumento pequeño y portátil, que incorpora funciones de un laboratorio con componentes a microescala o nanoescala (Moschou y Tserep 2017). La combinación de estos biosensores en un chip y pruebas de laboratorio en el lugar de asistencia con sistemas de microfluídos ofrece una alternativa integrada y miniaturizada, puesto que permite una reducción significativa del volumen de muestra y reactivos, así como un consumo menor de energía. Además, permiten mejorar la selectividad y la sensibilidad en comparación con los métodos de detección habituales puesto que facilitan la concentración de la muestra (Gubala *et al.,* 2012).

Un punto importante a la hora de fabricar sistemas tipo POCT es el formato en el que se va a incubar la muestra. En este contexto, las estrategias basadas en microcámaras son más adecuadas para construir dispositivos digitales integrados que las basadas en gotas, ya que la fuerza impulsora suministrada por el sistema de bombeo es suficiente para la dispersión de los ácidos nucleicos en toda la superficie útil de la microcámara. Además, facilitan la concentración de la muestra, la homogeneidad debido a la estanqueidad y el flujo constante del reactivo por la superficie sensora (Li *et al.,* 2020). Dichos sensores permiten automatizar e integrar muchas o todas las etapas del análisis, incluyendo muestreo, extracción, amplificación y detección en un solo chip. Otra propiedad inherente de estos dispositivos es el material estructural con el que están fabricados. En este ámbito, los materiales poliméricos se han posicionado frente a los materiales convencionales, puesto que exhiben excelentes propiedades, como son la alta transparencia, capacidad de prototipado, flexibilidad, química de superficies, coste, versatilidad y biocompatibilidad (Liu *et al.,* 2020). Por otra parte, estos sistemas presentan ventajas como mejorar el rendimiento analítico, detección en tiempo real, mayor velocidad de reacción, portabilidad, miniaturización, automatización y

multiplexado. Además, pueden incorporar ensayos de amplificación isoterma adaptados a aplicaciones tipo POCT.

Las tecnologías emergentes de ácidos nucleicos miniaturizadas, totalmente integradas, disponibles en el punto de atención y de respuesta rápida están avanzando a una velocidad vertiginosa, especialmente para eliminar operaciones complejas y reducir el riesgo de contaminación. Estos dispositivos están evolucionando en cuánto a sus capacidades analíticas tanto a nivel de digitalización de datos, como a nivel cualitativo y cuantitativo con el objetivo de optimizar la sensibilidad y la precisión. Recientemente, con la creciente demanda de pruebas de detección de virus del SARS CoV2, se han desarrollado este tipo de pruebas genéticas y de resistencia a antibióticos, como ID NOW de Abbott, GeneXpert de Cepheid y FilmArray de Biofire (Li *et al.,* 2020*).*

En concreto, se están desarrollando cada vez más sistemas µTAS para detección de ADN, donde la amplificación isoterma es la alternativa a la PCR. Sin necesidad de ciclos térmicos, los microsistemas isotérmicos pueden diseñarse para que sean simples, portátiles, consuman poca energía, y presenten prestaciones analíticas mejoradas (Asiello y Baeumner, 2011). Actualmente, existen numerosos desarrollos de estos biosensores tipo *point-of-care* en combinación con amplificaciones isotermas. Por ejemplo, el grupo de Reboud ha desarrollado un dispositivo analítico microfluídico basado en papel para el análisis multianalito de paludismo en sangre, utilizando la técnica isoterma LAMP, en comunidades rurales de Uganda (Reboud *et al.,* 2019). También se ha desarrollado otro biosensor POCT integrado para la detección colorimétrica del virus Influenza. Este sistema se compone de un dispositivo portátil microfluídico de PDMS combinado con partículas magnéticas para la detección de productos de amplificación isoterma LAMP, acoplado a la interfaz de un teléfono inteligente (Ma *et al.,* 2019).

El grupo de Jung también desarrolló una plataforma POCT de PDMS con canales microfluídicos y matrices de hidrogel 3D para la detección fluorescente de mutaciones puntuales. Este sistema de captura alcanza sensibilidades 1000 veces superiores a las

del del chip plano (Jung *et al.,* 2015). Recientemente, el grupo de Kwon ha diseñado un chip POCT llamado "OPENchip" para análisis de expresión génica y detección de mutaciones oncogénicas de los genes *PIK3CA, KRAS y HER2* a partir de células tumorales circulantes procedentes de biopsia líquida (Lee *et al.,* 2020). El grupo de Trau también ha desarrollado un dispositivo POCT integrado para la detección de mutaciones del oncogén *BRAF* a partir de células tumorales mediante amplificación isoterma mediada por ligación (Dey *et al.,* 2019).

Algunos de estos biosensores POCT integrados se basan en señales colorimétricas observables a simple vista sin instrumentos adicionales, lo cual facilita su detección, además de ser más rentable, sencillo, rápido y directamente medible que otro tipo de biosensores. Recientemente, el grupo de Chen y colaboradores ha desarrollado un biosensor para detección de mutaciones genéticas, basado en el ensayo LFA-LAMP colorimétrico (Chen *et al.,* 2019). Si bien es cierto que con este sistema no existe una detección multiplexada, resulta ser muy rentable puesto que todos los materiales involucrados en la fabricación son asequibles y no se necesitan equipos sofisticados. En nuestro grupo también se han desarrollado sistemas integrados y colorimétricos para la detección de ácidos nucleicos basados en amplificación isoterma LAMP y RPA (Lázaro *et al.,* 2019), (Yamanaka *et al.,* 2017), (Santiago-Felipe *et al.,* 2015). La combinación novedosa de estas tecnologías de biosensores con smartphones se ha convertido en un nuevo campo de POCT conocido como salud digital o salud móvil (mHealth). La unión de estas tecnologías junto con análisis de big data, fomenta el desarrollo de un sistema de salud que transformará el paradigma de la gestión y la clínica de las patologías (Tu *et al.,* 2020).

Todos estos avances ponen de manifiesto la importancia de disponer de nuevos sistemas *point-of-care* integrados (Moschou y Tserepi, 2017) que pueden ser utilizados como herramienta analítica para el desarrollo de pruebas masivas, accesibles y compatibles con un sistema sanitario sostenible (Zhu *et al.,* 2020).

4. Cáncer colorectal

El cáncer se define como el crecimiento celular anormal y descontrolado promovido por una acumulación de defectos genéticos y epigenéticos, tanto de origen ambiental como hereditario, que conllevan la activación de oncogenes y la inactivación de genes supresores de tumores (Sierra, 2020). El cáncer colorrectal (CCR), incluye las neoplasias del colon, recto y apéndice. Durante 2020, este tipo de cáncer ha sid el tercero más diagnosticado en todo el mundo y es uno de los que más fallecimientos causa, junto con el de pulmón y páncreas (Rawla *et. al,* 2019). Para 2021, la Sociedad Española de Oncología Médica (SEOM) prevé que en nuestro país se diagnosticarán 43.581 nuevos casos de cáncer de colon y recto, superando al de próstata (35.764), mama (33.375) y pulmón (29.549). A tenor de estas cifras y teniendo en cuenta que es de vital importancia hacer un correcto diagnóstico, es necesario disponer de sistemas de cribado selectivos para la detección de la enfermedad en sus primeros estadios. En el CCR se trabaja en la detección de mutaciones en los oncogenes *KRAS, BRAF* y *PIK3CA* puesto que son biomarcadores tumorales específicos de esta patología.

4.1 Biomarcadores en los genes *PIK3CA, KRAS y BRAF*

Los receptores del factor de crecimiento se han investigado como posibles biomarcadores de CCR. En concreto, se ha observado que el factor de crecimiento endotelial *EGFR* presenta una elevada incidencia y relación con el proceso de tumorogénesis. Este biomarcador es una glucoproteína transmembrana con actividad tirosina quinasa que juega un papel relevante en la carcinogénesis y sobreexpresión (Noronha *et al.,* 2020).

En los últimos años, los anticuerpos monoclonales (moAbs), con actividad anti-*EGFR* han demostrado ser eficaces en el tratamiento del CCR. Estos moAbs bloquean la señal del *EGFR* inhibiendo la cascada de señalización. El análisis mutacional de los oncogenes implicados en esta ruta de señalización, permite elucidar la respuesta específica de los pacientes ante estos moAbs. Concretamente, la detección de las

mutaciones puntuales en los oncogenes *KRAS, BRAF y PIK3CA* (biomarcadores predictivos en CCR) permiten dar respuesta a las terapias basadas en anticuerpos monoclonales específicos como Cetuximab y Panitumumab (De Roock *et al.,* 2010). La proteína transmembrana *EGFR* interacciona con su receptor, promoviendo la homodimerización, lo cual, a su vez, provoca su activación en los dominios quinasa intracelulares. La cascada de señalización de *RAS* se activa a través de proteínas adaptadoras, promoviendo la fosforilación de las siguientes proteínas participantes, e iniciando la transcripción que interviene en la proliferación celular, apoptosis y muerte celular programada (**Figura 16**) (Tian *et al.,* 2013). La variante nativa del gen *KRAS* presenta respuesta a los moAbs, mientras la variante mutante no responde al tratamiento. Por su parte, las mutaciones de los oncogenes *BRAF y PIK3CA* de la ruta de señalización de EGFR también son responsables de la resistencia a la terapia a anticuerpos monoclonales dirigidos a EGFR. Por lo tanto, es imprescindible conocer el estado de mutación de *KRAS, BRAF y PIK3CA* y determinar con precisión el tipo de terapia a suministrar (Zhao *et al.,* 2017).

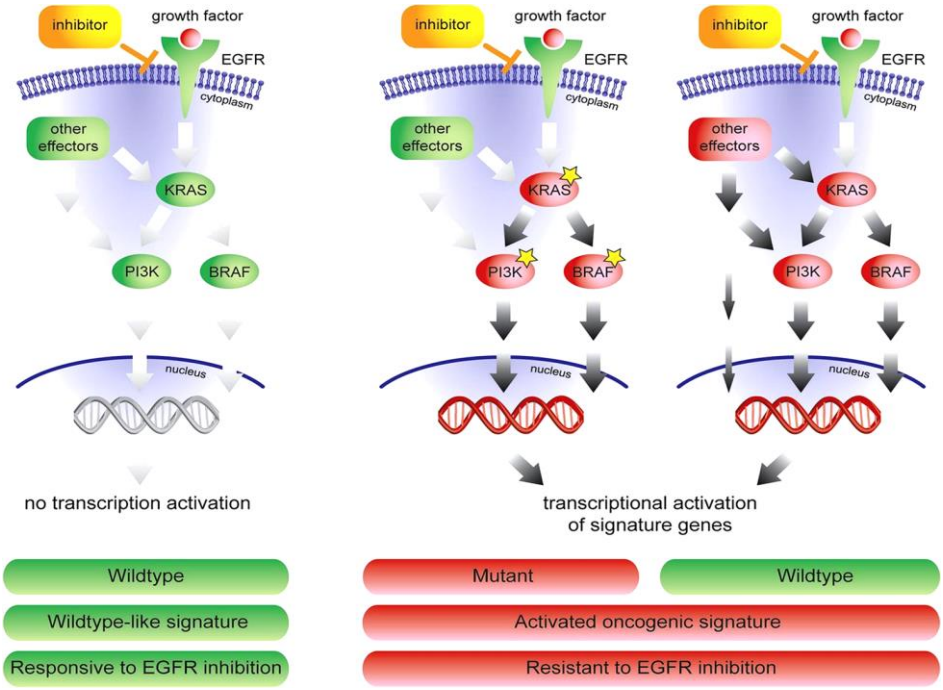

Figura 16. Mecanismo de respuesta a inhibidores anti-EGFR en biomarcadores *PI3K, BRAF Y KRAS*. Figura original de *Tian et al., 2013*.

4.2 Detección de los biomarcadores en oncogenes

Numerosos grupos de investigación han realizado estudios para detectar estos biomarcadores tumorales en los genes *PIK3CA, KRAS, NRAS* y *BRAF* con el fin de predecir la enfermedad de una manera precoz y selectiva. Entre las tecnologías de detección de mutaciones encontramos las citadas en apartados anteriores, como son la secuenciación o las técnicas de amplificación basadas en PCR (Galbiati *et al.,* 2016).

Tal como se ha indicado anteriormente, se han desarrollado métodos basados en la PCR que incluyen el bloqueo del alelo mayoritario (nativo) y/o el enriquecimiento de alelos minoritarios (mutantes). El grupo de Kwon y colaboradores logró discriminar con precisión mutaciones de los genes *PIK3CA, KRAS y BRAF,* mediante péptidos nucleicos (PNA) que actúan como agentes bloqueantes, consiguiendo mayor especificidad que con la técnica de secuenciación masiva (Kwon *et al.,* 2011). El grupo de Song propuso una PCR mediada por PNA para discriminar específicamente la mutación *H1047R* del gen *PIK3CA* (Zeng *et al.,* 2017). El grupo de Koay ensayó la PCR bloqueada para la variante nativa, en este caso para la detección de mutaciones del gen *KRAS* a partir de tejidos biopsiados y células circulantes (Huang *et al.,* 2014).

A lo largo de la última década, y especialmente en los últimos 3 años, se están desarrollando plataformas analíticas de bajo coste tipo POCT que permiten detectar a niveles ultrabajos las mutaciones de los principales oncogenes. La mayoría de estos sistemas integrados utilizan transducción electroquímica empleando electrodos de oro funcionalizados (Xiao *et al.,* 2019), óxido de grafeno (Xu *et al.,* 2019*)* o nanocompuestos metálicos con Si_3N_4 (Kalofanou *et al.,* 2020) entre otros. Estos biosensores también se han aplicado para la detección de productos de amplificación isotermos del gen *PIK3CA* (Wang *et al.,* 2020). Otros autores han desarrollado biosensores para el genotipado de estas variantes de único nucleótido (Wang *et al.,* 2020*)* basados en hidrogeles y detección fluorimétrica (Huang *et al.,* 2015), MNPs *(*Sloane *et al.,* 2015) o sistemas híbridos microfluídicos (Sedighi *et al.,* 2017). Una minoría de estos biosensores se basan

en detección SERS sin marcaje (Lapitan *et al.,* 2019) y en detección colorimétrica (Wang *et al.,* 2017) (**Tabla 9**).

Mientras que la mayoría de contribuciones utilizan PCR, otros investigadores han optado por la amplificación isoterma. En los últimos 3 años, destacan aproximaciones basadas en la RCA (Xiao *et al.,* 2019), LAMP (Kalofonou *et al.,* 2020), SDA (Wang *et al.,* 2020) y RPA (Dey *et al.,* 2019), y detección fluorescente o electroquímica, todos ellos dirigidos a la detección de estas mutaciones. Por su parte, el grupo de Oliveira ha publicado recientemente una extensa revisión sobre la aplicación de dendrímeros como nanoherramientas para aplicaciones en cáncer CCR, concretamente en el área de los nanoteranósticos (Carvalho *et al.,* 2020). El mismo grupo publicó un año antes un artículo en Science sobre el desarrollo de un chip 3D basado en dendrímeros para la detección de células HCT 116 involucradas en el CCR (Carvalho *et al.,* 2019).

A pesar de los avances realizados, todavía existe la demanda de nuevos métodos que apoyen la detección de mutaciones e identificar cual es el cambio de nucleótido presente en muestras de interés oncológico. Desde el punto de vista de la investigación básica-aplicada, para disponer de estas tecnologías integradas, una etapa clave es el desarrollo de nuevas metodologías de ensayo (Tortajada *et al.,* 2016). De acuerdo al estado del arte y la experiencia del grupo de investigación, existen varios avances clave para el desarrollo de genosensores innovadores de tipo ASSURED. Incluyen el estudio del enriquecimiento de los alelos mutantes mediante amplificación isoterma en presencia de un agente bloqueante, el estudio los procesos de biorreconocimiento basados en hibridación alelo específica y el desarrollo de plataformas integradas con termopolímeros y la funcionalización dirigida de su superficie. Esta metodología permitiría, mediante un único ensayo, el pronóstico y clasificación de los pacientes con cáncer colorrectal en el grupo poblacional más adecuado para recibir una terapia personalizada.

Tabla 9. Biosensores integrados para detección de mutaciones en los biomarcadores *KRAS, NRAS y PIK3CA*

Bio marcador	Amplificación	Tipo de biosensor	LOD	Plataforma integrada	uF	Referencia
KRAS	PCR	Electroquímico	0.027ng/uL	Electrodo de carbono	-	Attoye, 2021
	-	electroquímico	0.03fM	Nanocritales de Au/aerogel de grafeno	-	Yuanfeng, 2020
	-	ECL (Electro-Luminiscente)	0.03fM	Electrodo funcionalizado con quitosano	-	Liang, 2020
	-	FRET fluorescencia	6.3 pM	UCNPs/AuNCs	-	Wang, 2020
	EXO III	Electroquímico	20.4fM	Electrodo grafeno	-	Shu, 2020
	RCA	Electroquímico	0.28fM	Electrodo funcionalizado con Au	-	Xiao, 2019
	-	Electroquímico	100pM	Electrodo funcionalizado con Au	-	Zeng, 2019
	RCA	Electroquímico	0.28fM	Electrodo funcionalizado con Au	-	Xiao, 2019
	PCR	SERS	1fM	MNPs	-	Lapitan, 2019
	-	Electroquímico	100 pM	Electrodo funcionalizado con Au	-	Zeng, 2019
	-	SERS	50fM	Nanorods de Au	-	Wu, 2019
	PCR	Bioluminiscencia	5%mut	Digital chip PCB	+	Zou, 2019
	-	Electroquímico	3fM	Nanotubos de carbono	-	Wang, 2018
	RCA	SERS	20atmoles	Nanoshell de Au	-	Chung, 2018
	RCA	Electroquímico	0.03fM	PMPs	-	Zhang, 2017
	LNA-HRCA	ECL (Electro-Luminiscente)	0.03fM	PMPs	-	Zhang, 2017
	HAD	Fluorescencia	1ng	AuNPs Bioarray	-	Sedighi, 2017
	PCR	Fluorescencia	1uM	Vidrio funcionalizado con polímeros	-	Sola, 2016
	PCR	Colorimétrico	0.1fM	LFA AuNPs celulosa	+	Wang, 2016
	PCR	Fluorescencia	25%mut	MNPs	-	Sloane, 2015
	PCR	Electroquímico	10fm/mL	PNA-umatriz-circuito electrónico	-	Das, 2015
	PCR	Fluorescencia	3.1% mut	Hidrogel-partículas-array	-	Huang, 2015
	PCR	Colorimétrico	5%mut	Vidrio silanizado GOPS	+	Steinbach, 2015
	AS-PCR	Fluorescencia	-	Discos PMMA/PDMS	+	Strohmeier, 2014
	PCR	Fluorescencia	300pg	Vidrio/PDMS chip AuNPs	+	Sedighi, 2014
	PCR	Electroquímico	-	Circuito impreso umatriz	-	Moschou, 2013
	PCR-ligación	Colorimétrico	1fM	MNPs	-	Chen, 2012

Tabla 9. Continuación

	Amplificación	Tipo de biosensor	LOD	Plataforma integrada	µF	Referencia
BRAF	PCR	Electroquímico	0.1pmol/L	CGE-PAAM/PA/PDA hidrogel	-	Wei, 2020
	-	Electroquímico	500 pg/µL	Electrodo de Au nano/mesoporoso	-	Ahmed, 2020
	RPA	Electroquímico	10 pg/mL	MNPs	+	Dey, 2019
	-	Electroquímico	10nM	Nanoalambre silicona (SiNW) FET	-	Wu, 2018
	EXPAR	Fluorescencia	0.5%mut	MNPs	-	Wang, 2017
	-	Electroquímico	-	Titanio/SAM oro	-	Huber, 2016
	PCR-ARMS	Electroquímico	-	Fe_3O_4/Au NPs	-	Situ, 2013
	-	Electroquímico	1fM	Nanoalambre silicona (SiNW) FET	-	Wu, 2011
	-	Electroquímico	0.88fM	Nanoalambre silicona (SiNW) FET	-	Wu, 2009
PIK3CA	HCR	Electroquímico	3pM	Electrodo de Au	-	Huang, 2020
	-	Fluorescencia	0.32pM	MNPs-PNA bloqueo	-	Chen, 2020
	USS-sbLAMP	Fluorescencia	1000 copias	CMOS con Si3N4	-	Kalofonou, 2020
	SDA	Electroquímico		Electrodo de Au	-	Wang, 2020
	CRISPR/Cas9	Electroquímico	1.92nM	Electrodo de grafeno	-	Uygun, 2020
	-	Electroquímico	1.2×10^{-17} mol/L	nanocompuesto FMNs/MoS2	-	Zhang, 2020
	-	Electroquímico	1.5×10^{-17} mol/L	nanocompuesto PIn6COOH/MoS_2	-	Yang, 2019
	-	Electroquímico	1.0×10^{-18} M.	polipirrole (PPy)/zinc nanohíbridos	-	Ma, 2019
	-	Electroquímico	-	chip-umatriz ferromagnético MNPs	+	Cho, 2016
KRAS PIK3CA BRAF	-	SPR	50fM	PNA-AuNPs	-	Nguyen, 2015
	-	SERS	10 fM	Au/plata nanorods	+	Wu, 2020
	-	Electroquímico	48.7fM	Electrodo de Au	-	Chen, 2020
	RCA	Fluorescencia	-	Chip canales abiertoS	+	Lee, 2020
	Dpcr	Fluorescencia	2100 copias	Chip-array de silicona	-	Nakagawa, 2020
	PCR-RFLP	Fluorescencia	0.25% mut	droplet-umatriz chip vidrio	-	Feng, 2020
	PCR	SERS	10-11 M	AgNPs	-	Li, 2018
	COLD-PCR	Fluorescencia	0.01%mut	matriz copolímero (DMA-NAS-MAPS)	-	Galbiati, 2014

Referencias bibliográficas

Abi, A., & Safavi, A. (2019). Targeted detection of single-nucleotide variations: progress and promise. ACS sensors, 4(4), 792-807.

Alcaide, M., Cheung, M., Bushell, K., Arthur, S. E., Wong, H. L., Karasinska, J., & Morin, R. D. (2019). A novel multiplex droplet digital PCR assay to identify and quantify KRAS mutations in clinical specimens. The Journal of Molecular Diagnostics, 21(2), 214-227.

Abi, A., & Safavi, A. (2019). Targeted detection of single-nucleotide variations: progress and promise. ACS sensors, 4(4), 792-807.

Ali, M. M., Li, F., Zhang, Z., Zhang, K., Kang, D. K., Ankrum, J. A., & Zhao, W. (2014). Rolling circle amplification: a versatile tool for chemical biology, materials science and medicine. Chemical Society Reviews, 43(10), 3324-3341.

Alzate, D., Cajigas, S., Robledo, S., Muskus, C., & Orozco, J. (2020). Genosensors for differential detection of Zika virus. Talanta, 210, 120648.

Anavi, D., Popowski, Y., Slor, G., Segal, M., Frid, L., Amir, R. J., & Amir, E. (2018). Covalent functionalization of solid cellulose by divergent synthesis of chemically active dendrons. Journal of Polymer Science Part A: Polymer Chemistry, 56(18), 2103-2114.

Aragón, P., Noguera, P., Bañuls, M. J., Puchades, R., Maquieira, Á., & González-Martínez, M. Á. (2018). Modulating receptor-ligand binding in biorecognition by setting surface wettability. Analytical and bioanalytical chemistry, 410(23), 5723-5730.

Asiello, P. J., & Baeumner, A. J. (2011). Miniaturized isothermal nucleic acid amplification, a review. Lab on a Chip, 11(8), 1420-1430.

Attoye, B., Baker, M. J., Thomson, F., Pou, C., & Corrigan, D. K. (2021). Optimisation of an electrochemical DNA sensor for measuring KRAS G12D and G13D point mutations in different tumour types. Biosensors, 11(2), 42.

Ayoib, A., Hashim, U., Gopinath, S. C., Thivina, V., & Arshad, M. M. (2020). Design and fabrication of PDMS microfluidics device for rapid and label-free DNA detection. Applied Physics A, 126(3), 1-8.

Balderston, S., Taulbee, J. J., Celaya, E., Fung, K., Jiao, A., Smith, K., & Aran, K. (2021). Discrimination of single-point mutations in unamplified genomic DNA via Cas9

immobilized on a graphene field-effect transistor. Nature Biomedical Engineering, 1-13

Bañuls, M. J., Puchades, R., & Maquieira, Á. (2013). Chemical surface modifications for the development of silicon-based label-free integrated optical (IO) biosensors: A review. Analytica chimica acta, 777, 1-16.

Batistuti, M. R., Bueno, P. R., & Mulato, M. (2020). The importance of the assembling of DNA strands on the performance of electrochemical genosensors. Microchemical Journal, 159, 105358.

Berensmeier, S. (2006). Magnetic particles for the separation and purification of nucleic acids. Applied microbiology and biotechnology, 73(3), 495-504.

Bielec, K., Sozanski, K., Seynen, M., Dziekan, Z., ten Wolde, P. R., & Holyst, R. (2019). Kinetics and equilibrium constants of oligonucleotides at low concentrations. Hybridization and melting study. Physical Chemistry Chemical Physics, 21(20), 10798-10807.

Bohunicky, B., & Mousa, S. A. (2011). Biosensors: the new wave in cancer diagnosis. Nanotechnology, science and applications, 4, 1.

Bolton, L., Reiman, A., Lucas, K., Timms, J., & Cree, I. A. (2015). KRAS mutation analysis by PCR: a comparison of two methods. PLoS One, 10(1), e0115672.

Bosnjakovic, A., Mishra, M. K., Han, H. J., Romero, R., & Kannan, R. M. (2012). A dendrimer-based immunosensor for improved capture and detection of tumor necrosis factor-α cytokine. Analytica chimica acta, 720, 118-125.

Bruls, D. M., Evers, T. H., Kahlman, J. A. H., Van Lankvelt, P. J. W., Ovsyanko, M., Pelssers, E. G. M., & Prins, M. W. J. (2009). Rapid integrated biosensor for multiplexed immunoassays based on actuated magnetic nanoparticles. Lab on a Chip, 9(24), 3504-3510.

Bumgarner, R. (2013). Overview of DNA microarrays: types, applications, and their future. Current protocols in molecular biology, 101(1), 22-1.

Caminade, A. M. (2020). Phosphorus dendrimers as nanotools against cancers. Molecules, 25(15), 3333.

Caminade, A. M., Padie, C., Laurent, R., Maraval, A., & Majoral, J. P. (2006). Uses of dendrimers for DNA microarrays. Sensors, 6(8), 901-914.

Cao, G., Kong, J., Xing, Z., Tang, Y., Zhang, X., Xu, X. & Guan, M. (2018). Rapid detection of CALR type 1 and type 2 mutations using PNA-LNA clamping loop-mediated isothermal amplification on a CD-like microfluidic chip. Analytica chimica acta, 1024, 123-135.

Cao, G., Kong, J., Xing, Z., Tang, Y., Zhang, X., Xu, X., & Guan, M. (2018). Rapid detection of CALR type 1 and type 2 mutations using PNA-LNA clamping loop-mediated isothermal amplification on a CD-like microfluidic chip. Analytica chimica acta, 1024, 123-135.

Carvalho, M. R., Barata, D., Teixeira, L. M., Giselbrecht, S., Reis, R. L., Oliveira, J. M., & Habibovic, P. (2019). Colorectal tumor-on-a-chip system: A 3D tool for precision onco-nanomedicine. Science advances, 5(5), eaaw1317.

Carvalho, M. R., Reis, R. L., & Oliveira, J. M. (2020). Dendrimer nanoparticles for colorectal cancer applications. Journal of Materials Chemistry B, 8(6), 1128-1138.

Cha, W., Fan, R., Miao, Y., Zhou, Y., Qin, C., Shan, X., & Li, J. (2017). Mesoporous silica nanoparticles as carriers for intracellular delivery of nucleic acids and subsequent therapeutic applications. Molecules, 22(5), 782.

Chandra, S., Mayer, M., & Baeumner, A. J. (2017). PAMAM dendrimers: A multifunctional nanomaterial for ECL biosensors. Talanta, 168, 126-129.

Chang, Y. M., Ding, S. T., Lin, E. C., Wang, L. A., & Lu, Y. W. (2017). A microfluidic chip for rapid single nucleotide polymorphism (SNP) genotyping using primer extension on microbeads. Sensors and Actuators B: Chemical, 246, 215-224.

Chen, C., & Wang, J. (2020). Optical biosensors: an exhaustive and comprehensive review. Analyst, 145(5), 1605-1628.

Chen, G., Chen, R., Ding, S., Li, M., Wang, J., Zou, J., & Tang, Z. (2020). Recombinase assisted loop-mediated isothermal DNA amplification. Analyst, 145(2), 440-444.

Chen, P., Chen, C., Liu, Y., Du, W., Feng, X., & Liu, B. F. (2019). Fully integrated nucleic acid pretreatment, amplification, and detection on a paper chip for identifying EGFR mutations in lung cancer cells. Sensors and Actuators B: Chemical, 283, 472-477.

Chen, S., & Shamsi, M. H. (2017). Biosensors-on-chip: a topical review. Journal of Micromechanics and Microengineering, 27(8), 083001.

Chen, W., Fang, X., Li, H., Cao, H., & Kong, J. (2017). DNA-mediated inhibition of peroxidase-like activities on platinum nanoparticles for simple and rapid colorimetric detection of nucleic acids. Biosensors and Bioelectronics, 94, 169-175.

Chen, X., Ying, A., & Gao, Z. (2012). Highly sensitive and selective colorimetric genotyping of single-nucleotide polymorphisms based on enzyme-amplified ligation on magnetic beads. Biosensors and Bioelectronics, 36(1), 89-94.

Chen, Y. T., Lee, Y. C., Lai, Y. H., Lim, J. C., Huang, N. T., Lin, C. T., & Huang, J. J. (2020). Review of Integrated Optical Biosensors for Point-Of-Care Applications. Biosensors, 10(12), 209.

Chircov, C., Bîrcă, A. C., Grumezescu, A. M., & Andronescu, E. (2020). Biosensors-On-Chip: An Up-to-Date Review. Molecules, 25(24), 6013.

Chis, A. A., Dobrea, C., Morgovan, C., Arseniu, A. M., Rus, L. L., Butuca, A.,& Frum, A. (2020). Applications and Limitations of Dendrimers in Biomedicine. Molecules, 25(17), 3982.

Ciftci, S., Cánovas, R., Neumann, F., Paulraj, T., Nilsson, M., Crespo, G. A., & Madaboosi, N. (2020). The sweet detection of rolling circle amplification: Glucose-based electrochemical genosensor for the detection of viral nucleic acid. Biosensors and Bioelectronics, 151, 112002.

Crannell, Z. A., Rohrman, B., & Richards-Kortum, R. (2014). Equipment-free incubation of recombinase polymerase amplification reactions using body heat. PloS one, 9(11), e112146.

Craw, P., & Balachandran, W. (2012). Isothermal nucleic acid amplification technologies for point-of-care diagnostics: a critical review. Lab on a Chip, 12(14), 2469-2486.

Cutler, J. I., Auyeung, E., & Mirkin, C. A. (2012). Spherical nucleic acids. Journal of the American Chemical Society, 134(3), 1376-1391

De Roock, W., Claes, B., Bernasconi, D., De Schutter, J., Biesmans, B., Fountzilas, G., & Tejpar, S. (2010). Effects of KRAS, BRAF, NRAS, and PIK3CA mutations on the efficacy of cetuximab plus chemotherapy in chemotherapy-refractory metastatic colorectal cancer: a retrospective consortium analysis. The lancet oncology, 11(8), 753-762.

Dekaliuk, M., Qiu, X., Troalen, F., Busson, P., & Hildebrandt, N. (2019). Discrimination of the V600E mutation in BRAF by rolling circle amplification and Forster resonance energy transfer. ACS sensors, 4(10), 2786-2793.

Demidov, V. V. (2003). PNA and LNA throw light on DNA. Trends in Biotechnology, 21(1), 4-7.

Dey, S., Koo, K. M., Wang, Z., Sina, A. A., Wuethrich, A., & Trau, M. (2019). An integrated multi-molecular sensor for simultaneous BRAF V600E protein and DNA single point mutation detection in circulating tumour cells. Lab on a Chip, 19(5), 738-748.

Díaz-Fernández, A., Lorenzo-Gómez, R., Miranda-Castro, R., de-Los-Santos-Álvarez, N., & Lobo-Castañón, M. J. (2020). Electrochemical aptasensors for cancer diagnosis in biological fluids–a review. Analytica Chimica Acta.

Ding, S., Chen, R., Chen, G., Li, M., Wang, J., Zou, J., & Tang, Z. (2019). One-step colorimetric genotyping of single nucleotide polymorphism using probe-enhanced loop-mediated isothermal amplification (PE-LAMP). Theranostics, 9(13), 3723.

Ding, S., Chen, R., Chen, G., Li, M., Wang, J., Zou, J., & Tang, Z. (2019). One-step colorimetric genotyping of single nucleotide polymorphism using probe-enhanced loop-mediated isothermal amplification (PE-LAMP). Theranostics, 9(13), 3723.

Ding, X., Yin, K., Li, Z., & Liu, C. (2020). All-in-One dual CRISPR-cas12a (AIOD-CRISPR) assay: a case for rapid, ultrasensitive and visual detection of novel coronavirus SARS-CoV-2 and HIV virus. bioRxiv.

DNA & Gene Chip Market Size, Share & Trends Analysis Report By Product (Consumables, Instrumentation), By Application (Cancer Diagnosis & Treatment, Drug Delivery, Genomics), By End Use, And Segment Forecasts, 2018 – 2025.

Du, W. F., Ge, J. H., Li, J. J., Tang, L. J., Yu, R. Q., & Jiang, J. H. (2019). Single-step, high-specificity detection of single nucleotide mutation by primer-activatable loop-mediated isothermal amplification (PA-LAMP). Analytica chimica acta, 1050, 132-138.

Du, W. F., Ge, J. H., Li, J. J., Tang, L. J., Yu, R. Q., & Jiang, J. H. (2019). Single-step, high-specificity detection of single nucleotide mutation by primer-activatable loop-mediated isothermal amplification (PA-LAMP). Analytica chimica acta, 1050, 132-138.

Du, Y., & Dong, S. (2017). Nucleic acid biosensors: recent advances and perspectives. Analytical chemistry, 89(1), 189-215.

DuVall, J. A., Cabaniss, S. T., Angotti, M. L., Moore, J. H., Abhyankar, M., Shukla, N., & Landers, J. P. (2016). Rapid detection of Clostridium difficile via magnetic bead aggregation in cost-effective polyester microdevices with cell phone image analysis. Analyst, 141(19), 5637-5645.

Economou, A., Kokkinos, C., & Prodromidis, M. (2018). Flexible plastic, paper and textile lab-on-a chip platforms for electrochemical biosensing. Lab on a Chip, 18(13), 1812-1830.

Erdem, A., Eksin, E., Kesici, E., & Yaralı, E. (2018). Dendrimers Integrated Biosensors for Healthcare Applications. In Nanotechnology and Biosensors (pp. 307-317). Elsevier

Escadafal, C., Faye, O., Faye, O., Weidmann, M., Strohmeier, O., von Stetten, F., & Patel, P. (2014). Rapid molecular assays for the detection of yellow fever virus in low-resource settings. PLoS negl trop dis, 8(3), e2730.

Escorihuela, J., Bañuls, M. J., Puchades, R., & Maquieira, A. (2012). DNA microarrays on silicon surfaces through thiol-ene chemistry. Chemical Communications, 48(15), 2116-2118.

Evans, C. W., Ho, D., Lee, P. K., Martin, A. D., Chin, I. L., Wei, Z., & Iyer, K. S. (2021). A dendronised polymer architecture breaks the conventional inverse relationship between porosity and mechanical properties of hydrogels. Chemical Communications, 57(6), 773-776.

Fan, X., White, I. M., Shopova, S. I., Zhu, H., Suter, J. D., & Sun, Y. (2008). Sensitive optical biosensors for unlabeled targets: A review. Analytica chimica acta, 620(1-2), 8-26.

Fixe, F., Dufva, M., Telleman, P., & Christensen, C. B. V. (2004). Functionalization of poly (methyl methacrylate)(PMMA) as a substrate for DNA microarrays. Nucleic acids research, 32(1), e9-e9.

Fouz, M. F., & Appella, D. H. (2020). PNA clamping in nucleic acid amplification protocols to detect single nucleotide mutations related to cancer. Molecules, 25(4), 786.

Fu, Y., Duan, X., Huang, J., Huang, L., Zhang, L., Cheng, W., & Min, X. (2019). Detection of KRAS mutation via ligation-initiated LAMP reaction. Scientific reports, 9(1), 1-7.

Galbiati, S., Monguzzi, A., Damin, F., Soriani, N., Passiu, M., Castellani, C., & Cremonesi, L. (2016). COLD-PCR and microarray: two independent highly sensitive approaches allowing the identification of fetal paternally inherited mutations in maternal plasma. Journal of medical genetics, 53(7), 481-487.

García-Mendiola, T., Requena-Sanz, S., Martínez-Periñán, E., Bravo, I., Pariente, F., & Lorenzo, E. (2020). Influence of carbon nanodots on DNA-Thionine interaction. Application to breast cancer diagnosis. Electrochimica Acta, 353, 136522

Gao, Y., Wolf, L. K., & Georgiadis, R. M. (2006). Secondary structure effects on DNA hybridization kinetics: a solution versus surface comparison. Nucleic acids research, 34(11), 3370-3377.

Gilson, P., Franczak, C., Dubouis, L., Husson, M., Rouyer, M., Demange, J., & Harlé, A. (2019). Evaluation of KRAS, NRAS and BRAF hotspot mutations detection for patients with metastatic colorectal cancer using direct DNA pipetting in a fully-automated platform and next-generation sequencing for laboratory workflow optimisation. PloS one, 14(7), e0219204

Giuffrida, M. C., & Spoto, G. (2017). Integration of isothermal amplification methods in microfluidic devices: Recent advances. Biosensors and Bioelectronics, 90, 174-186.

Gootenberg, J. S., Abudayyeh, O. O., Lee, J. W., Essletzbichler, P., Dy, A. J., Joung, J., & Myhrvold, C. (2017). Nucleic acid detection with CRISPR-Cas13a/C2c2. Science, 356(6336), 438-442.

Grant, B. D., Anderson, C. E., Williford, J. R., Alonzo, L. F., Glukhova, V. A., Boyle, D. S., ... & Nichols, K. P. (2020). SARS-CoV-2 coronavirus nucleocapsid antigen-detecting half-strip lateral flow assay toward the development of point of care tests using commercially available reagents. Analytical chemistry, 92(16), 11305-11309.

Gubala, V., Harris, L. F., Ricco, A. J., Tan, M. X., & Williams, D. E. (2012). Point of care diagnostics: status and future. Analytical chemistry, 84(2), 487-515.

Gunderson, K. L., Steemers, F. J., Lee, G., Mendoza, L. G., & Chee, M. S. (2005). A genome-wide scalable SNP genotyping assay using microarray technology. Nature genetics, 37(5), 549-554.

Hamidi, S. V., & Perreault, J. (2019). Simple rolling circle amplification colorimetric assay based on pH for target DNA detection. Talanta, 201, 419-425.

Han, H. J., Kannan, R. M., Wang, S., Mao, G., Kusanovic, J. P., & Romero, R. (2010). Multifunctional dendrimer-templated antibody presentation on biosensor surfaces for improved biomarker detection. Advanced functional materials, 20(3), 409-421.

He, Q., Chen, M., Lin, X., & Chen, Z. (2020). Allele-specific PCR with a novel data processing method based on difference value for single nucleotide polymorphism genotyping of ALDH2 gene. Talanta, 220, 121432

He, Y., Chen, D., Li, M., Fang, L., Yang, W., Xu, L., & Fu, F. (2014). Rolling circle amplification combined with gold nanoparticles-tag for ultra sensitive and specific quantification of DNA by inductively coupled plasma mass spectrometry. Biosensors and Bioelectronics, 58, 209-213.

Hernández-Neuta, I., Pereiro, I., Ahlford, A., Ferraro, D., Zhang, Q., Viovy, J. L., & Nilsson, M. (2018). Microfluidic magnetic fluidized bed for DNA analysis in continuous flow mode. Biosensors and Bioelectronics, 102, 531-539.

Hong, B. J., Sunkara, V., & Park, J. W. (2005). DNA microarrays on nanoscale-controlled surface. Nucleic acids research, 33(12), e106-e106.

Horne, M. T., Fish, D. J., & Benight, A. S. (2006). Statistical thermodynamics and kinetics of DNA multiplex hybridization reactions. Biophysical journal, 91(11), 4133-4153.

Huang, L., Xia, Q., Zhang, Y., Bai, H., Luo, N., Xiang, L., & Cheng, W. (2019). Allele specific DNAzyme assembly for fast and convenient SNP colorimetric genotyping directly from noninvasive crude samples. Analytical Methods, 11(5), 596-603.

Huang, M. M. C., Leong, S. M., Chua, H. W., Tucker, S., Cheong, W. C., Chiu, L., & Koay, E. S. C. (2014). Highly sensitive KRAS mutation detection from formalin-fixed paraffin-embedded biopsies and circulating tumour cells using wild-type blocking polymerase chain reaction and Sanger sequencing. Molecular diagnosis & therapy, 18(4), 459-468.

Huertas, C. S., Soler, M., Estevez, M. C., & Lechuga, L. M. (2020). One-Step Immobilization of Antibodies and DNA on Gold Sensor Surfaces via a Poly-Adenine Oligonucleotide Approach. Analytical Chemistry, 92(18), 12596-12604.

Hui, W., Zhang, S., Zhang, C., Wan, Y., Zhu, J., Zhao, G., & Cui, Y. (2016). A novel lateral flow assay based on GoldMag nanoparticles and its clinical applications for genotyping of MTHFR C677T polymorphisms. Nanoscale, 8(6), 3579-3587.

Isothermal nucleic acid amplification technology (INAAT) market analysis by product, by technology (NASBA, HDA, LAMP, SDA, SPIA, NEAR, TMA, RCA, RPA, SMAP2), and segment forecasts, 2018–2025, Report GVR-1-68038-588-5, Grand View Research, 2017

Itonaga, M., Matsuzaki, I., Warigaya, K., Tamura, T., Shimizu, Y., Fujimoto, M., & Murata, S. I. (2016). Novel methodology for rapid detection of KRAS mutation using PNA-LNA mediated loop-mediated isothermal amplification. PLoS One, 11(3), e0151654.

Ivanov, A. V., Safenkova, I. V., Zherdev, A. V., & Dzantiev, B. B. (2020). Nucleic acid lateral flow assay with recombinase polymerase amplification: Solutions for highly sensitive detection of RNA virus. Talanta, 210, 120616.

Jayakumar, K., Rajesh, R., Dharuman, V., Venkatasan, R., Hahn, J. H., & Pandian, S. K. (2012). Gold nano particle decorated graphene core first generation PAMAM dendrimer for label free electrochemical DNA hybridization sensing. Biosensors and Bioelectronics, 31(1), 406-412.

Jayanthi, V. S. A., Das, A. B., & Saxena, U. (2017). Recent advances in biosensor development for the detection of cancer biomarkers. Biosensors and Bioelectronics, 91, 15-23.

Jia, Y., Sanchez, J. A., & Wangh, L. J. (2014). Kinetic hairpin oligonucleotide blockers for selective amplification of rare mutations. Scientific reports, 4(1), 1-8.

Jia, Y., Sun, F., Na, N., & Ouyang, J. (2019). Detection of p53 DNA using commercially available personal glucose meters based on rolling circle amplification coupled with nicking enzyme signal amplification. Analytica chimica acta, 1060, 64-70.

Jia, Z., Yuan, H., Zhao, X., Yin, J., Cong, H., Gao, W., & Zhao, J. (2021). Single-cell genetic analysis of lung tumor cells based on self-driving micro-cavity array chip. Talanta, 122172.

Jiang, Y., Zou, S., & Cao, X. (2017). A simple dendrimer-aptamer based microfluidic platform for E. coli O157: H7 detection and signal intensification by rolling circle amplification. Sensors and Actuators B: Chemical, 251, 976-984. (incluido en el artículo dendrimeros)

Jiménez-Meneses, P., Bañuls, M. J., Puchades, R., & Maquieira, A. (2018). Fluor-thiol photocoupling reaction for developing high performance nucleic acid (NA) microarrays. Analytical chemistry, 90(19), 11224-11231.

Jin, C. E., Yeom, S. S., Koo, B., Lee, T. Y., Lee, J. H., Shin, Y., & Lim, S. B. (2017). Rapid and accurate detection of KRAS mutations in colorectal cancers using the isothermal-based optical sensor for companion diagnostics. Oncotarget, 8(48), 83860.

Jo, P., König, A., Schirmer, M., Kitz, J., Conradi, L. C., Azizian, A., & Ströbel, P. (2016). Heterogeneity of KRAS mutation status in rectal cancer. PloS one, 11(4), e0153278.

Johannes, W., Krämer, S. D., Meyer, P. A., Christin, R., Matthias, H., Urban, G. A., & Roth, G. (2020). Digital DNA microarray generation on glass substrates. Scientific Reports (Nature Publisher Group), 10(1).

Jones, M. R., Seeman, N. C., & Mirkin, C. A. (2015). Programmable materials and the nature of the DNA bond. Science, 347(6224).

Juárez, M. J., Morais, S., & Maquieira, A. Digitized microimmunoassays with nuclear antigens for multiplex quantification of human specific IgE to β-lactam antibiotics. Sensors and Actuators B: Chemical, 328, 129060.

Jung, Y. K., Kim, J., & Mathies, R. A. (2015). Microfluidic linear hydrogel array for multiplexed single nucleotide polymorphism (SNP) detection. Analytical chemistry, 87(6), 3165-3170.

Kalofonou, M., Malpartida-Cardenas, K., Alexandrou, G., Rodriguez-Manzano, J., Yu, L. S., Miscourides, N., & Toumazou, C. (2020). A novel hotspot specific isothermal amplification method for detection of the common PIK3CA p. H1047R breast cancer mutation. Scientific reports, 10(1), 1-10.

Kamil, Y. M., Al-Rekabi, S. H., Yaacob, M. H., Syahir, A., Chee, H. Y., Mahdi, M. A., & Bakar, M. H. A. (2019). Detection of dengue using PAMAM dendrimer integrated tapered optical fiber sensor. Scientific reports, 9(1), 1-10.

Karfa, P., Majhi, K. C., & Madhuri, R. (2020). Flexible Substrate-Based Sensors in Health Care and Biosensing Applications. Nanosensor Technologies for Environmental Monitoring, 431-454.

Kellner, M. J., Koob, J. G., Gootenberg, J. S., Abudayyeh, O. O., & Zhang, F. (2019). SHERLOCK: nucleic acid detection with CRISPR nucleases. Nature protocols, 14(10), 2986-3012.

Kersting, S., Rausch, V., Bier, F. F., & von Nickisch-Rosenegk, M. (2014). Multiplex isothermal solid-phase recombinase polymerase amplification for the specific and fast DNA-based detection of three bacterial pathogens. Microchimica Acta, 181(13-14), 1715-1723.

Khaliliazar, S., Ouyang, L., Piper, A., Chondrogiannis, G., Hanze, M., Herland, A., & Hamedi, M. M. (2020). Electrochemical Detection of Genomic DNA Utilizing Recombinase Polymerase Amplification and Stem-Loop Probe. ACS omega, 5(21), 12103-12109.

Khan, M. Z. H., Hasan, M. R., Hossain, S. I., Ahommed, M. S., & Daizy, M. (2020). Ultrasensitive detection of pathogenic viruses with electrochemical biosensor: state of the art. Biosensors and Bioelectronics, 112431.

Kim, D. H., Kang, H. S., Hur, S. S., Sim, S., Ahn, S. H., Park, Y. K., & Lee, J. H. (2018). Direct detection of drug-resistant hepatitis B virus in serum using a Dendron-modified microarray. Gut and liver, 12(3), 331.

Kim, H. R., Lee, S. Y., Hyun, D. S., Lee, M. K., Lee, H. K., Choi, C. M., & Lee, K. Y. (2013). Detection of EGFR mutations in circulating free DNA by PNA-mediated PCR clamping. Journal of Experimental & Clinical Cancer Research, 32(1), 50.

Kim, Y. T., Kim, J. W., Kim, S. K., Joe, G. H., & Hong, I. S. (2015). Simultaneous genotyping of multiple somatic mutations by using a clamping PNA and PNA detection probes. Chembiochem, 16(2), 209-213.

Kirsch, J., Siltanen, C., Zhou, Q., Revzin, A., & Simonian, A. (2013). Biosensor technology: recent advances in threat agent detection and medicine. Chemical Society Reviews, 42(22), 8733-8768.

Koo, K. M., Dey, S., & Trau, M. (2018). A sample-to-targeted gene analysis biochip for nanofluidic manipulation of solid-phase circulating tumor nucleic acid amplification in liquid biopsies. ACS sensors, 3(12), 2597-2603.

Kwon, M. J., Lee, S. E., Kang, S. Y., & Choi, Y. L. (2011). Frequency of KRAS, BRAF, and PIK3CA mutations in advanced colorectal cancers: Comparison of peptide nucleic

acid-mediated PCR clamping and direct sequencing in formalin-fixed, paraffin-embedded tissue. Pathology-Research and Practice, 207(12), 762-768.

Lapitan Jr, L. D., Guo, Y., & Zhou, D. (2015). Nano-enabled bioanalytical approaches to ultrasensitive detection of low abundance single nucleotide polymorphisms. Analyst, 140(12), 3872-3887.

Lapitan, L. D., Xu, Y., Guo, Y., & Zhou, D. (2019). Combining magnetic nanoparticle capture and poly-enzyme nanobead amplification for ultrasensitive detection and discrimination of DNA single nucleotide polymorphisms. Nanoscale, 11(3), 1195-1204.

Lázaro, A., Yamanaka, E. S., Maquieira, A., & Tortajada-Genaro, L. A. (2019). Allele-specific ligation and recombinase polymerase amplification for the detection of single nucleotide polymorphisms. Sensors and Actuators B: Chemical, 298, 126877.

Le Berre, V., Trévisiol, E., Dagkessamanskaia, A., Sokol, S., Caminade, A. M., Majoral, J. P., & François, J. (2003). Dendrimeric coating of glass slides for sensitive DNA microarrays analysis. Nucleic Acids Research, 31(16), e88-e88.

Lee, A. C., Svedlund, J., Darai, E., Lee, Y., Lee, D., Lee, H. B., & Kwon, S. (2020). OPENchip: an on-chip in situ molecular profiling platform for gene expression analysis and oncogenic mutation detection in single circulating tumour cells. Lab on a Chip, 20(5), 912-922.

Lee, R. A., De Puig, H., Nguyen, P. Q., Angenent-Mari, N. M., Donghia, N. M., McGee, J. P., & Collins, J. J. (2020). Ultrasensitive CRISPR-based diagnostic for field-applicable detection of Plasmodium species in symptomatic and asymptomatic malaria. Proceedings of the National Academy of Sciences, 117(41), 25722-25731.

Lee, S., Brophy, V. H., Cao, J., Velez, M., Hoeppner, C., Soviero, S., & Lawrence, H. J. (2012). Analytical performance of a PCR assay for the detection of KRAS mutations (codons 12/13 and 61) in formalin-fixed paraffin-embedded tissue samples of colorectal carcinoma. Virchows Archiv, 460(2), 141-149.

Lei, R., Wang, X., Zhang, D., Liu, Y., Chen, Q., & Jiang, N. (2020). Rapid isothermal duplex real-time recombinase polymerase amplification (RPA) assay for the diagnosis of equine piroplasmosis. Scientific reports, 10(1), 1-11

Li, G., Li, X., Wan, J., & Zhang, S. (2009). Dendrimers-based DNA biosensors for highly sensitive electrochemical detection of DNA hybridization using reporter probe DNA modified with Au nanoparticles. Biosensors and Bioelectronics, 24(11), 3281-3287.

Li, H., Tang, Y., Zhao, W., Wu, Z., Wang, S., & Yu, R. (2019). Palindromic molecular beacon-based intramolecular strand-displacement amplification strategy for ultrasensitive detection of K-ras gene. Analytica chimica acta, 1065, 98-106.

Li, J., Macdonald, J., & von Stetten, F. (2018). A comprehensive summary of a decade development of the recombinase polymerase amplification. Analyst, 144(1), 31-67

Li, X. H., Zhang, X. L., Wu, J., Lin, N., Sun, W. M., Chen, M., & Lin, Z. Y. (2019). Hyperbranched rolling circle amplification (HRCA)-based fluorescence biosensor for ultrasensitive and specific detection of single-nucleotide polymorphism genotyping associated with the therapy of chronic hepatitis B virus infection. Talanta, 191, 277-282.

Li, Z., Bai, Y., You, M., Hu, J., Yao, C., Cao, L., & Xu, F. (2020). Fully integrated microfluidic devices for qualitative, quantitative and digital nucleic acids testing at point of care. Biosensors and Bioelectronics, 112952.

Lillis, L., Lehman, D., Singhal, M. C., Cantera, J., Singleton, J., Labarre, P., & Overbaugh, J. (2014). Non-instrumented incubation of a recombinase polymerase amplification assay for the rapid and sensitive detection of proviral HIV-1 DNA. PloS one, 9(9), e108189.

Lin, C., Zhang, Y., Zhou, X., Yao, B., & Fang, Q. (2013). Naked-eye detection of nucleic acids through rolling circle amplification and magnetic particle mediated aggregation. Biosensors and Bioelectronics, 47, 515-519.

Lin, M. T., Mosier, S. L., Thiess, M., Beierl, K. F., Debeljak, M., Tseng, L. H., & Wheelan, S. J. (2014). Clinical validation of KRAS, BRAF, and EGFR mutation detection using next-generation sequencing. American journal of clinical pathology, 141(6), 856-866.

Liong, M., Hoang, A. N., Chung, J., Gural, N., Ford, C. B., Min, C., & Weissleder, R. (2013). Magnetic barcode assay for genetic detection of pathogens. Nature communications, 4(1), 1-9.

Liu, B., & Liu, J. (2017). Methods for preparing DNA-functionalized gold nanoparticles, a key reagent of bioanalytical chemistry. Analytical Methods, 9(18), 2633-2643.

Liu, B., Jia, Y., Ma, M., Li, Z., Liu, H., Li, S., & He, N. (2013). High throughput SNP detection system based on magnetic nanoparticles separation. Journal of biomedical nanotechnology, 9(2), 247-256.

Liu, D., Wang, J., Wu, L., Huang, Y., Zhang, Y., Zhu, M., & Yang, C. (2020). Trends in miniaturized biosensors for point-of-care testing. TrAC Trends in Analytical Chemistry, 122, 115701.

Liu, H., Li, S., Liu, L., Tian, L., & He, N. (2010). An integrated and sensitive detection platform for biosensing application based on Fe@ Au magnetic nanoparticles as bead array carries. Biosensors and Bioelectronics, 26(4), 1442-1448.

Liu, H., Tørring, T., Dong, M., Rosen, C. B., Besenbacher, F., & Gothelf, K. V. (2010). DNA-templated covalent coupling of G4 PAMAM dendrimers. Journal of the American Chemical Society, 132(51), 18054-18056.

Liu, Y. H., Deng, H. H., Li, H. N., Shi, T. F., Peng, H. P., Liu, A. L., & Hong, G. L. (2018). A DNA electrochemical biosensor based on homogeneous hybridization for the determination of Cryptococcus neoformans. Journal of Electroanalytical Chemistry, 827, 27-33.

Liu, Y., Lei, T., Liu, Z., Kuang, Y., Lyu, J., & Wang, Q. (2016). A novel technique to detect EGFR mutations in lung cancer. International journal of molecular sciences, 17(5), 792.

Liu, Y., Zhao, Y., Qin, Y., Du, X., Wang, Q., & Lyu, J. (2016). A novel microfluidic device that integrates nucleic acid extraction, amplification, and detection to identify an EGFR mutation in lung cancer tissues. RSC advances, 6(16), 13399-13406.

Lobato, I. M., & O'Sullivan, C. K. (2018). Recombinase polymerase amplification: basics, applications and recent advances. Trac Trends in analytical chemistry, 98, 19-35.

Lobo-Castañón, M. J. (2016). Isothermal nucleic acid amplification in bioanalysis.

Loo, J. F., Lau, P. M., Ho, H. P., & Kong, S. K. (2013). An aptamer-based bio-barcode assay with isothermal recombinase polymerase amplification for cytochrome-c detection and anti-cancer drug screening. Talanta, 115, 159-165.

López-Ríos, F., de Castro, J., Concha, Á., Garrido, P., Gómez-Román, J., Isla, D., & Felip, E. (2015). Actualización de las recomendaciones para la determinación de biomarcadores en el carcinoma de pulmón avanzado de célula no pequeña.

Consenso Nacional de la Sociedad Española de Anatomía Patológica y de la Sociedad Española de Oncología Médica. Revista Española de Patología, 48(2), 80-89.

Lu, X., Cui, M., & Yi, Q. (2020). Detection of mutant genes with different types of biosensor methods. TrAC Trends in Analytical Chemistry, 126, 115860.

Lu, X., Cui, M., & Yi, Q. (2020). Detection of mutant genes with different types of biosensor methods. TrAC Trends in Analytical Chemistry, 115860.

Luka, G., Ahmadi, A., Najjaran, H., Alocilja, E., DeRosa, M., Wolthers, K., & Hoorfar, M. (2015). Microfluidics integrated biosensors: A leading technology towards lab-on-a-chip and sensing applications. Sensors, 15(12), 30011-30031.

Luo, J. D., Chan, E. C., Shih, C. L., Chen, T. L., Liang, Y., Hwang, T. L., & Chiou, C. C. (2006). Detection of rare mutant K-ras DNA in a single-tube reaction using peptide nucleic acid as both PCR clamp and sensor probe. Nucleic acids research, 34(2), e12-e12.

Lutz, S., Weber, P., Focke, M., Faltin, B., Hoffmann, J., Müller, C., & Piepenburg, O. (2010). Microfluidic lab-on-a-foil for nucleic acid analysis based on isothermal recombinase polymerase amplification (RPA). Lab on a Chip, 10(7), 887-893.

Lyu, Z., Ding, L., Huang, A. T., Kao, C. L., & Peng, L. (2019). Poly (amidoamine) dendrimers: Covalent and supramolecular synthesis. Materials Today Chemistry, 13, 34-48.

Ma, Y. D., Chang, W. H., Luo, K., Wang, C. H., Liu, S. Y., Yen, W. H., & Lee, G. B. (2018). Digital quantification of DNA via isothermal amplification on a self-driven microfluidic chip featuring hydrophilic film-coated polydimethylsiloxane. Biosensors and Bioelectronics, 99, 547-554.

Ma, Y. D., Li, K. H., Chen, Y. H., Lee, Y. M., Chou, S. T., Lai, Y. Y., ... & Lee, G. B. (2019). A sample-to-answer, portable platform for rapid detection of pathogens with a smartphone interface. Lab on a Chip, 19(22), 3804-3814.

Magro, L., Jacquelin, B., Escadafal, C., Garneret, P., Kwasiborski, A., Manuguerra, J. C., & Tabeling, P. (2017). Based RNA detection and multiplexed analysis for Ebola virus diagnostics. Scientific reports, 7(1), 1-9.

Mahato, K., & Chandra, P. (2019). Based miniaturized immunosensor for naked eye ALP detection based on digital image colorimetry integrated with smartphone. Biosensors and Bioelectronics, 128, 9-16.

Mahmoudi, T., de la Guardia, M., & Baradaran, B. (2020). Lateral flow assays towards point-of-care cancer detection: A review of current progress and future trends. TrAC Trends in Analytical Chemistry, 125, 115842.

Malpartida-Cardenas, K., Rodriguez-Manzano, J., Yu, L. S., Delves, M. J., Nguon, C., Chotivanich, K., & Georgiou, P. (2018). Allele-specific isothermal amplification method using unmodified self-stabilizing competitive primers. Analytical chemistry, 90(20), 11972-11980.

Malpartida-Cardenas, K., Rodriguez-Manzano, J., Yu, L. S., Delves, M. J., Nguon, C., Chotivanich, K., & Georgiou, P. (2018). Allele-specific isothermal amplification method using unmodified self-stabilizing competitive primers. Analytical chemistry, 90(20), 11972-11980.

Manmana, Y., Kubo, T., & Otsuka, K. (2020). Recent Developments of Point-of-Care (POC) Testing Platform for Biomolecules. TrAC Trends in Analytical Chemistry, 116160.

Martínez-Periñán, E., García-Mendiola, T., Enebral-Romero, E., Del Caño, R., Vera-Hidalgo, M., Sulleiro, M. V., ... & Lorenzo, E. (2021). A MoS2 platform and thionine-carbon nanodots for sensitive and selective detection of pathogens. Biosensors and Bioelectronics, 113375.

Matharu, Z., Bandodkar, A. J., Gupta, V., & Malhotra, B. D. (2012). Fundamentals and application of ordered molecular assemblies to affinity biosensing. Chemical Society Reviews, 41(3), 1363-1402.

Matsuda, K. (2017). PCR-based detection methods for single-nucleotide polymorphism or mutation: Real-time PCR and its substantial contribution toward technological refinement. Advances in clinical chemistry, 80, 45-72.

Mayboroda, O., Katakis, I., & O'Sullivan, C. K. (2018). Multiplexed isothermal nucleic acid amplification. Analytical biochemistry, 545, 20-30.

Miao, X., Zhu, Z., Jia, H., Lu, C., Liu, X., Mao, D., & Chen, G. (2020). Colorimetric detection of cancer biomarker based on enzyme enrichment and pH sensing. Sensors and Actuators B: Chemical, 320, 128435.

Milbury, C. A., Li, J., & Makrigiorgos, G. M. (2009). PCR-based methods for the enrichment of minority alleles and mutations. Clinical chemistry, 55(4), 632-640.

Milbury, C. A., Zhong, Q., Lin, J., Williams, M., Olson, J., Link, D. R., & Hutchison, B. (2014). Determining lower limits of detection of digital PCR assays for cancer-related gene mutations. Biomolecular detection and quantification, 1(1), 8-22.

Mondal, D., Ghosh, P., Khan, M. A. A., Hossain, F., Böhlken-Fascher, S., Matlashewski, G., & Abd El Wahed, A. (2016). Mobile suitcase laboratory for rapid detection of Leishmania donovani using recombinase polymerase amplification assay. Parasites & vectors, 9(1), 281.

Montanez, M. I., Hed, Y., Utsel, S., Ropponen, J., Malmstrom, E., Wagberg, L., & Malkoch, M. (2011). Bifunctional dendronized cellulose surfaces as biosensors. Biomacromolecules, 12(6), 2114-2125

Morais, S., Puchades, R., & Maquieira, Á. (2016). Disc-based microarrays: principles and analytical applications. Analytical and bioanalytical chemistry, 408(17), 4523-4534.

Morais, S., Tortajada-Genaro, L. A., Maquieira, A., & Martinez, M. A. G. (2020). Biosensors for food allergy detection according to specific IgE levels in serum. TrAC Trends in Analytical Chemistry, 115904.

Morandi, L., De Biase, D., Visani, M., Cesari, V., De Maglio, G., Pizzolitto, S., & Tallini, G. (2012). Allele specific locked nucleic acid quantitative PCR (ASLNAqPCR): an accurate and cost-effective assay to diagnose and quantify KRAS and BRAF mutation. PloS one, 7(4), e36084

Morin, T. J., Shropshire, T., Liu, X., Briggs, K., Huynh, C., Tabard-Cossa, V., & Dunbar, W. B. (2016). Nanopore-based target sequence detection. PloS one, 11(5), e0154426.

Morshed, M. N., Behary, N., Bouazizi, N., Guan, J., Chen, G., & Nierstrasz, V. (2019). Surface modification of polyester fabric using plasma-dendrimer for robust immobilization of glucose oxidase enzyme. Scientific reports, 9(1), 1-16.

Moschou, D., & Tserepi, A. (2017). The lab-on-PCB approach: tackling the μTAS commercial upscaling bottleneck. Lab on a Chip, 17(8), 1388-1405.

Navarro, E., Serrano-Heras, G., Castaño, M. J., & Solera, J. J. C. C. A. (2015). Real-time PCR detection chemistry. Clinica chimica acta, 439, 231-250.

Ng, B. Y., Wee, E. J., Woods, K., Anderson, W., Antaw, F., Tsang, H. Z., & Trau, M. (2017). Isothermal point mutation detection: toward a first-pass screening strategy for multidrug-resistant tuberculosis. Analytical chemistry, 89(17), 9017-9022.

Nge, P. N., Rogers, C. I., & Woolley, A. T. (2013). Advances in microfluidic materials, functions, integration, and applications. Chemical reviews, 113(4), 2550-2583.

Nguyen, H. H., Lee, S. H., Lee, U. J., Fermin, C. D., & Kim, M. (2019). Immobilized enzymes in biosensor applications. Materials, 12(1), 121.

Nimse, S. B., Song, K., Sonawane, M. D., Sayyed, D. R., & Kim, T. (2014). Immobilization techniques for microarray: challenges and applications. Sensors, 14(12), 22208-22229.

Ning, T., Liao, F., Cui, H., Yin, Z., Ma, G., Cheng, L., & Fan, H. (2020). A homogeneous electrochemical DNA sensor on the basis of a self-assembled thiol layer on a gold support and by using tetraferrocene for signal amplification. Microchimica Acta, 187(6).

Noronha, V., Patil, V. M., Joshi, A., Menon, N., Chougule, A., Mahajan, A., & Prabhash, K. (2020). Gefitinib versus gefitinib plus pemetrexed and carboplatin chemotherapy in EGFR-mutated lung cancer. Journal of Clinical Oncology, 38(2), 124-136

Notomi, T., Okayama, H., Masubuchi, H., Yonekawa, T., Watanabe, K., Amino, N., & Hase, T. (2000). Loop-mediated isothermal amplification of DNA. Nucleic acids research, 28(12), e63-e63.

Oberg, K., Ropponen, J., Kelly, J., Löwenhielm, P., Berglin, M., & Malkoch, M. (2013). Templating gold surfaces with function: A self-assembled dendritic monolayer methodology based on monodisperse polyester scaffolds. Langmuir, 29(1), 456-465

Onodera, T., & Toko, K. (2014). Towards an electronic dog nose: Surface plasmon resonance immunosensor for security and safety. Sensors, 14(9), 16586-16616.

Ørum, H. (2000). PCR clamping. Curr. Issues Mol. Biol, 2(1), 27-30.

P.W. Akers, N.C.H. Le, A.R. Nelson, M. McKenna, C. O'Mahony, D.J. McGillivray, D.E. Williams, Surface engineering of poly (methylmethacrylate): Effects on fluorescence immunoassay. Biointerphases. 12 (2017) 02C415.

Paez, J. I., Martinelli, M., Brunetti, V., & Strumia, M. C. (2012). Dendronization: A useful synthetic strategy to prepare multifunctional materials. Polymers, 4(1), 355-395.

Park, S. H., Yin, P., Liu, Y., Reif, J. H., LaBean, T. H., & Yan, H. (2005). Programmable DNA self-assemblies for nanoscale organization of ligands and proteins. Nano Letters, 5(4), 729-733

Pascual, L., Baroja, I., Aznar, E., Sancenón, F., Marcos, M. D., Murguía, J. R., & Martínez-Máñez, R. (2015). Oligonucleotide-capped mesoporous silica nanoparticles as DNA-responsive dye delivery systems for genomic DNA detection. Chemical Communications, 51(8), 1414-1416.

Pei, H., Li, F., Wan, Y., Wei, M., Liu, H., Su, Y., & Fan, C. (2012). Designed diblock oligonucleotide for the synthesis of spatially isolated and highly hybridizable functionalization of DNA–gold nanoparticle nanoconjugates. Journal of the American Chemical Society, 134(29), 11876-11879.

Perumal, V., & Hashim, U. (2014). Advances in biosensors: Principle, architecture and applications. Journal of applied biomedicine, 12(1), 1-15.

Piepenburg, O., Williams, C. H., Stemple, D. L., & Armes, N. A. (2006). DNA detection using recombination proteins. PLoS Biol, 4(7), e204.

Pinchon, E., Leon, F., Temurok, N., Morvan, F., Vasseur, J. J., Clot, M., & Molès, J. P. (2020). Rapid and specific DNA detection by magnetic field-enhanced agglutination assay. Talanta, 219, 121344.

Pirker, R., Herth, F. J., Kerr, K. M., Filipits, M., Taron, M., Gandara, D. & Stahel, R. (2010). Consensus for EGFR mutation testing in non-small cell lung cancer: results from a European workshop. Journal of Thoracic Oncology, 5(10), 1706-1713.

Prada, J., Cordes, C., Harms, C., & Lang, W. (2019). Design and Manufacturing of a Disposable, Cyclo-Olefin Copolymer, Microfluidic Device for a Biosensor. Sensors, 19(5), 1178.

Prieto-Simon, B., Campas, M., & Marty, J. L. (2008). Biomolecule immobilization in biosensor development: tailored strategies based on affinity interactions. Protein and peptide letters, 15(8), 757-763.

Pumford, E. A., Lu, J., Spaczai, I., Prasetyo, M. E., Zheng, E. M., Zhang, H., & Kamei, D. T. (2020). Developments in integrating nucleic acid isothermal amplification and detection systems for point-of-care diagnostics. Biosensors and Bioelectronics, 112674.

Purohit, B., Vernekar, P. R., Shetti, N. P., & Chandra, P. (2020). Biosensor nanoengineering: design, operation, and implementation for biomolecular analysis. Sensors International, 100040.

Qin, Y., Yang, X., Zhang, J., & Cao, X. (2017). Developing a non-fouling hybrid microfluidic device for applications in circulating tumour cell detections. Colloids and Surfaces B: Biointerfaces, 151, 39-46.

Rasheed, P. A., & Sandhyarani, N. (2017). Electrochemical DNA sensors based on the use of gold nanoparticles: a review on recent developments. Microchimica Acta, 184(4), 981-1000.

Rashid, J. I. A., & Yusof, N. A. (2017). The strategies of DNA immobilization and hybridization detection mechanism in the construction of electrochemical DNA sensor: A review. Sensing and bio-sensing research, 16, 19-31.

Ravan, H Kashanian, Sanadgol, Badoei-Dalfard, Z (2014). Strategies for optimizing DNA hybridization on surfaces. Anal. Biochem. 444 41-46.

Reboud, J., Xu, G., Garrett, A., Adriko, M., Yang, Z., Tukahebwa, E. M., & Cooper, J. M. (2019). Based microfluidics for DNA diagnostics of malaria in low resource underserved rural communities. Proceedings of the National Academy of Sciences, 116(11), 4834-4842.

Rees, H. A., & Liu, D. R. (2018). Base editing: precision chemistry on the genome and transcriptome of living cells. Nature reviews genetics, 19(12), 770-788.

Ribes, À., Santiago-Felipe, S., Aviñó, A., Candela-Noguera, V., Eritja, R., Sancenon, F., & Aznar, E. (2018). Design of oligonucleotide-capped mesoporous silica nanoparticles for the detection of miRNA-145 by duplex and triplex formation. Sensors and Actuators B: Chemical, 277, 598-603.

Rodrigues, D., Barbosa, A. I., Rebelo, R., Kwon, I. K., Reis, R. L., & Correlo, V. M. (2020). Skin-Integrated wearable systems and implantable biosensors: a comprehensive review. Biosensors, 10(7), 79.

Roy, D., & Park, J. W. (2015). Spatially nanoscale-controlled functional surfaces toward efficient bioactive platforms. Journal of Materials Chemistry B, 3(26), 5135-5149.

Roy, D., Kwak, J. W., Maeng, W. J., Kim, H., & Park, J. W. (2008). Dendron-modified polystyrene microtiter plate: surface characterization with picoforce AFM and influence of spacing between immobilized amyloid beta proteins. Langmuir, 24(24), 14296-14305.

Saiyed, Z. M., Ramchand, C. N., & Telang, S. D. (2008). Isolation of genomic DNA using magnetic nanoparticles as a solid-phase support. Journal of Physics: Condensed Matter, 20(20), 204153.

Sánchez, A., Villalonga, A., Martínez-García, G., Parrado, C., & Villalonga, R. (2019). Dendrimers as Soft Nanomaterials for Electrochemical Immunosensors. Nanomaterials, 9(12), 1745.

Sánchez Salcedo, R., Miranda Castro, R., Santos Álvarez, N. D. L., & Lobo Castañón, M. J. (2019). On-gold Recombinase Polymerase Primer elongation for electrochemical detection of bacterial genome: mechanism insights and influencing factors. ChemElectroChem, 6.

Sandoval-Yañez, C., & Castro Rodriguez, C. (2020). Dendrimers: amazing platforms for bioactive molecule delivery systems. Materials, 13(3), 570.

Santiago-Felipe, S., Tortajada-Genaro, L. A., Puchades, R., & Maquieira, A. (2014). Recombinase polymerase and enzyme-linked immunosorbent assay as a DNA amplification-detection strategy for food analysis. Analytica Chimica Acta, 811, 81-87.

Santiago-Felipe, S., Tortajada-Genaro, L. A., Puchades, R., & Maquieira, A. (2014). Recombinase polymerase and enzyme-linked immunosorbent assay as a DNA amplification-detection strategy for food analysis. Analytica Chimica Acta, 811, 81-87.

Sassolas, A., Blum, L. J., & Leca-Bouvier, B. D. (2012). Immobilization strategies to develop enzymatic biosensors. Biotechnology advances, 30(3), 489-511.

Sassolas, A., Leca-Bouvier, B. D., & Blum, L. J. (2008). DNA biosensors and microarrays. Chemical reviews, 108(1), 109-139.

Satija, J., Sai, V. V. R., & Mukherji, S. (2011). Dendrimers in biosensors: Concept and applications. Journal of Materials Chemistry, 21(38), 14367-14386.

Schermer, B., Fabretti, F., Damagnez, M., Di Cristanziano, V., Heger, E., Arjune, S., & Joung, J. (2020). Rapid SARS-CoV-2 testing in primary material based on a novel multiplex RT-LAMP assay. PloS one, 15(11), e0238612.

Schrittwieser, S., Pelaz, B., Parak, W. J., Lentijo-Mozo, S., Soulantica, K., Dieckhoff, J., & Schotter, J. (2016). Homogeneous biosensing based on magnetic particle labels. Sensors, 16(6), 828.

Schrittwieser, S., Pelaz, B., Parak, W. J., Lentijo-Mozo, S., Soulantica, K., Dieckhoff, J., & Schotter, J. (2016). Homogeneous biosensing based on magnetic particle labels. Sensors, 16(6), 828.

Schuster, S. C. (2008). Next-generation sequencing transforms today's biology. Nature methods, 5(1), 16-18.

Sena-Torralba, A., Pallás-Tamarit, Y., Morais, S., & Maquieira, Á. (2020). Recent advances and challenges in food-borne allergen detection. TrAC Trends in Analytical Chemistry, 116050.

Senel, M., Dervisevic, M., & Kokkokoğlu, F. (2019). Electrochemical DNA biosensors for label-free breast cancer gene marker detection. Analytical and bioanalytical chemistry, 411(13), 2925-2935.

Sethi, D., Kumar, A., Gupta, K. C., & Kumar, P. (2008). A facile method for the construction of oligonucleotide microarrays. Bioconjugate chemistry, 19(11), 2136-2143.

Shen, C., Shen, B., Mo, F., Zhou, X., Duan, X., Wei, X., & Ding, S. (2018). High-sensitive colorimetric biosensing of PIK3CA gene mutation based on mismatched ligation-triggered cascade strand displacement amplification. Sensors and Actuators B: Chemical, 273, 377-383.

Shen, C., Shen, B., Mo, F., Zhou, X., Duan, X., Wei, X., & Ding, S. (2018). High-sensitive colorimetric biosensing of PIK3CA gene mutation based on mismatched ligation-triggered cascade strand displacement amplification. Sensors and Actuators B: Chemical, 273, 377-383.

Shin, Y., Perera, A. P., Kim, K. W., & Park, M. K. (2013). Real-time, label-free isothermal solid-phase amplification/detection (ISAD) device for rapid detection of genetic alteration in cancers. Lab on a Chip, 13(11), 2106-2114.

Shu, Q., Liao, F., Hong, N., Cheng, L., Lin, Y., Cui, H., & Fan, H. (2020). A novel DNA sensor of homogeneous electrochemical signal amplification strategy. Microchemical Journal, 104777.

Siegel, R. L., Miller, K. D., Goding Sauer, A., Fedewa, S. A., Butterly, L. F., Anderson, J. C., & Jemal, A. (2020). Colorectal cancer statistics, 2020. CA: a cancer journal for clinicians.

Sierra, J., Marrugo-Ramírez, J., Rodriguez-Trujillo, R., Mir, M., & Samitier, J. (2020). Sensor-Integrated Microfluidic Approaches for Liquid Biopsies Applications in Early Detection of Cancer. Sensors, 20(5), 1317.

Sirianni, Q. E., & Gillies, E. R. (2020). The architectural evolution of self-immolative polymers. Polymer, 122638.

Slatko, B. E., Gardner, A. F., & Ausubel, F. M. (2018). Overview of next-generation sequencing technologies. Current protocols in molecular biology, 122(1), e59.

Sloane, H. S., Kelly, K. A., & Landers, J. P. (2015). Rapid KRAS mutation detection via hybridization-induced aggregation of microbeads. Analytical chemistry, 87(20), 10275-10282.

Sloane, H. S., Landers, J. P., & Kelly, K. A. (2016). Hybridization-Induced Aggregation Technology for Practical Clinical Testing: KRAS Mutation Detection in Lung and Colorectal Tumors. The Journal of Molecular Diagnostics, 18(4), 546-553.

Smith, S., Mager, D., Perebikovsky, A., Shamloo, E., Kinahan, D., Mishra, R., & Madou, M. (2016). CD-based microfluidics for primary care in extreme point-of-care settings. Micromachines, 7(2), 22.

Solassol, J., Vendrell, J., Märkl, B., Haas, C., Bellosillo, B., Montagut, C., & Sillekens, P. (2016). Multi-center evaluation of the fully automated PCR-based Idylla™ KRAS mutation assay for rapid KRAS mutation status determination on formalin-fixed paraffin-embedded tissue of human colorectal cancer. PLoS One, 11(9), e0163444.

Sun, Q., Cao, M., Zhang, X., Wang, M., Ma, Y., & Wang, J. (2020). A simple and low-cost paper-based colorimetric method for detecting and distinguishing the GII. 4 and GII. 17 genotypes of norovirus. Talanta, 121978

Syvänen, A. C. (2005). Toward genome-wide SNP genotyping. Nature genetics, 37(6), S5-S10.

Tamarit-López, J., Morais, S., Puchades, R., & Maquieira, A. (2011). Oxygen plasma treated interactive polycarbonate DNA microarraying platform. Bioconjugate chemistry, 22(12), 2573-2580.

Tang, C., He, Z., Liu, H., Xu, Y., Huang, H., Yang, G. & Chen, Z. (2020). Application of magnetic nanoparticles in nucleic acid detection. Journal of Nanobiotechnology, 18, 1-19.

Tangchaikeeree, T., Polpanich, D., Elaissari, A., & Jangpatarapongsa, K. (2017). Magnetic particles for in vitro molecular diagnosis: From sample preparation to integration into microsystems. Colloids and Surfaces B: Biointerfaces, 158, 1-8.

Teles, F. R. R., & Fonseca, L. P. (2008). Trends in DNA biosensors. Talanta, 77(2), 606-623.

Teng, F., Wu, X., Hong, T., Munk, G. B., & Libera, M. (2020). Integrating nucleic acid sequence-based amplification and microlensing for high-sensitivity self-reporting detection. Analyst.

Thaxton, C. S., Georganopoulou, D. G., & Mirkin, C. A. (2006). Gold nanoparticle probes for the detection of nucleic acid targets. Clinica Chimica Acta, 363(1-2), 120-126.

Tian, S., Simon, I., Moreno, V., Roepman, P., Tabernero, J., Snel, M., & Capella, G. (2013). A combined oncogenic pathway signature of BRAF, KRAS and PI3KCA mutation improves colorectal cancer classification and cetuximab treatment prediction. Gut, 62(4), 540-549.

Tjong, V., Tang, L., Zauscher, S., & Chilkoti, A. (2014). “Smart” DNA interfaces. Chemical Society Reviews, 43(5), 1612-1626.

Tjong, V., Tang, L., Zauscher, S., & Chilkoti, A. (2014). “Smart” DNA interfaces. Chemical Society Reviews, 43(5), 1612-1626.

Tortajada-Genaro, L. A., Mena, S., Niñoles, R., Puigmule, M., Viladevall, L., & Maquieira, Á. (2016). Genotyping of single nucleotide polymorphisms related to attention-deficit hyperactivity disorder. Analytical and bioanalytical chemistry, 408(9), 2339-2345.

Tortajada-Genaro, L. A., Santiago-Felipe, S., Amasia, M., Russom, A., & Maquieira, Á. (2015). Isothermal solid-phase recombinase polymerase amplification on microfluidic digital versatile discs (DVDs). RSC Advances, 5(38), 29987-29995.

Tortajada-Genaro, L. A., Yamanaka, E. S., & Maquieira, Á. (2019). Consumer electronics devices for DNA genotyping based on loop-mediated isothermal amplification and array hybridisation. Talanta, 198, 424-431.

Traeger, J. C., & Schwartz, D. K. (2017). Surface-mediated DNA hybridization: effects of DNA conformation, surface chemistry, and electrostatics. Langmuir, 33(44), 12651-12659.

Trinh, K. T. L., Trinh, T. N. D., & Lee, N. Y. (2019). Fully integrated and slidable paper-embedded plastic microdevice for point-of-care testing of multiple foodborne pathogens. Biosensors and Bioelectronics, 135, 120-128.

Tsao, C. W. (2016). Polymer microfluidics: Simple, low-cost fabrication process bridging academic lab research to commercialized production. Micromachines, 7(12), 225.

Tu, J., Torrente-Rodríguez, R. M., Wang, M., & Gao, W. (2020). The era of digital health: A review of portable and wearable affinity biosensors. Advanced Functional Materials, 30(29), 1906713.

Turner, A. P. (2013). Biosensors: sense and sensibility. Chemical Society Reviews, 42(8), 3184-3196.

Valiadi, M., Kalsi, S., Jones, I. G., Turner, C., Sutton, J. M., & Morgan, H. (2016). Simple and rapid sample preparation system for the molecular detection of antibiotic resistant pathogens in human urine. Biomedical microdevices, 18(1), 18.

van Deursen, P. B., Gunther, A. W., Spaargaren-van Riel, C. C., van den Eijnden, M. M., Vos, H. L., van Gemen, B., & Bertina, R. M. (1999). A novel quantitative multiplex NASBA method: application to measuring tissue factor and CD14 mRNA levels in human monocytes. Nucleic acids research, 27(17), e15-i

Van Reenen, A., de Jong, A. M., den Toonder, J. M., & Prins, M. W. (2014). Integrated lab-on-chip biosensing systems based on magnetic particle actuation–a comprehensive review. Lab on a Chip, 14(12), 1966-1986.

Varona, M., Eitzmann, D. R., Pagariya, D., Anand, R. K., & Anderson, J. L. (2020). Solid-Phase Microextraction Enables Isolation of BRAF V600E Circulating Tumor DNA from Human Plasma for Detection with a Molecular Beacon Loop-Mediated Isothermal Amplification Assay. Analytical chemistry, 92(4), 3346-3353.

Vidal, L., Ben Aissa, A., Salabert, J., Jara, J. J., Vallribera, A., Pividori, M. I., & Sebastián, R. M. (2020). Biotinylated Phosphorus Dendrimers as Control Line in Nucleic Acid Lateral Flow Tests. Biomacromolecules, 21(3), 1315-1323

Vincent, M., Xu, Y., & Kong, H. (2004). Helicase-dependent isothermal DNA amplification. EMBO reports, 5(8), 795-800

Walker, G. T., Little, M. C., Nadeau, J. G., & Shank, D. D. (1992). Isothermal in vitro amplification of DNA by a restriction enzyme/DNA polymerase system. Proceedings of the National Academy of Sciences, 89(1), 392-396.

Wang, H. B., Ma, L. H., Zhang, T., Huang, K. C., Zhao, Y. D., & Liu, T. C. (2020). Simple and accurate visual detection of single nucleotide polymorphism based on colloidal gold nucleic acid strip biosensor and primer-specific PCR. Analytica chimica acta, 1093, 106-114.

Wang, H., Jiang, J., Mostert, B., Sieuwerts, A., Martens, J. W., Sleijfer, S., & Wang, Y. (2013). Allele-specific, non-extendable primer blocker PCR (AS-NEPB-PCR) for DNA mutation detection in cancer. The Journal of Molecular Diagnostics, 15(1), 62-69.

Wang, J., Xiong, G., Ma, L., Wang, S., Zhou, X., Wang, L., & Yu, C. (2017). A dynamic sandwich assay on magnetic beads for selective detection of single-nucleotide mutations at room temperature. Biosensors and Bioelectronics, 94, 305-311.

Wang, T., Peng, Q., Guo, B., Zhang, D., Zhao, M., Que, H., & Yan, Y. (2020). An integrated electrochemical biosensor based on target-triggered strand displacement amplification and “four-way” DNA junction towards ultrasensitive detection of PIK3CA gene mutation. Biosensors and Bioelectronics, 150, 111954.

Warner, C. N., Hunter, Z. D., Carte, D. D., Skidmore, T. J., Vint, E. S., & Day, B. S. (2020). Structure and Function Analysis of DNA Monolayers Created from Self-Assembling DNA–Dendron Conjugates. Langmuir, 36(19), 5428-5434.

Wen, T., Huang, C., Shi, F. J., Zeng, X. Y., Lu, T., Ding, S. N., & Jiao, Y. J. (2020). Development of a lateral flow immunoassay strip for rapid detection of IgG antibody against SARS-CoV-2 virus. Analyst, 145(15), 5345-5352.

Wöhrle, J., Krämer, S. D., Meyer, P. A., Rath, C., Hügle, M., Urban, G. A., & Roth, G. (2020). Digital DNA microarray generation on glass substrates. Scientific reports, 10(1), 1-9.

Won, B. Y., Shin, S. C., Chung, W. Y., Shin, S., Cho, D. Y., & Park, H. G. (2009). Mismatch DNA-specific enzymatic cleavage employed in a new method for the electrochemical detection of genetic mutations. Chemical communications, (28), 4230-4232.

Wong, Y. P., Othman, S., Lau, Y. L., Radu, S., & Chee, H. Y. (2018). Loop-mediated isothermal amplification (LAMP): a versatile technique for detection of micro-organisms. Journal of applied microbiology, 124(3), 626-643.

Wu, D., Xu, H., Shi, H., Li, W., Sun, M., & Wu, Z. S. (2017). A label-free colorimetric isothermal cascade amplification for the detection of disease-related nucleic acids based on double-hairpin molecular beacon. Analytica chimica acta, 957, 55-62.

Wu, R., Jiang, L. P., Zhu, J. J., & Liu, J. (2019). Effects of small molecules on DNA adsorption by gold nanoparticles and a case study of tris (2-carboxyethyl) phosphine (TCEP). Langmuir, 35(41), 13461-13468.

X. Hao, P. Yeh, Y. Qin, Y. Jiang, Z. Qiu, S. Li, X. Cao, Aptamer surface functionalization of microfluidic devices using dendrimers as multi-handled templates and its application in sensitive detections of foodborne pathogenic bacteria. Anal. Chim. Acta. 1056 (2019) 96-107

Xiao, Q., Feng, J., Li, J., Liu, Y., Wang, D., & Huang, S. (2019). A ratiometric electrochemical biosensor for ultrasensitive and highly selective detection of the K-ras gene via exonuclease III-assisted target recycling and rolling circle amplification strategies. Analytical Methods, 11(32), 4146-4156.

Xu, H., Wu, D., Jiang, Y., Zhang, R., Wu, Q., Liu, Y., & Wu, Z. S. (2017). Loopback rolling circle amplification for ultrasensitive detection of Kras gene. Talanta, 164, 511-517.

Xu, X., Xing, S., Xu, M., Fu, P., Gao, T., Zhang, X., & Zhao, C. (2019). Highly sensitive and specific screening of EGFR mutation using a PNA microarray-based fluorometric assay based on rolling circle amplification and graphene oxide. RSC Advances, 9(66), 38298-38308.

Xu, X., Xing, S., Xu, M., Fu, P., Gao, T., Zhang, X., & Zhao, C. (2019). Highly sensitive and specific screening of EGFR mutation using a PNA microarray-based fluorometric assay based on rolling circle amplification and graphene oxide. RSC Advances, 9(66), 38298-38308

Yamanaka, E. S., Tortajada-Genaro, L. A., & Maquieira, Á. (2017). Low-cost genotyping method based on allele-specific recombinase polymerase amplification and colorimetric microarray detection. Microchimica Acta, 184(5), 1453-1462.

Yamanaka, E. S., Tortajada-Genaro, L. A., Pastor, N., & Maquieira, Á. (2018). Polymorphism genotyping based on loop-mediated isothermal amplification and smartphone detection. Biosensors and Bioelectronics, 109, 177-183.

Yin, J., Zou, Z., Hu, Z., Zhang, S., Zhang, F., Wang, B., & Mu, Y. (2020). A "sample-in-multiplex-digital-answer-out" chip for fast detection of pathogens. Lab on a Chip, 20(5), 979-986.

Yoo, W. S., Han, H. S., Kim, J. G., Kang, K., Jeon, H. S., Moon, J. Y., & Park, H. (2020). Development of a tablet PC-based portable device for colorimetric determination of assays including COVID-19 and other pathogenic microorganisms. RSC Advances, 10(54), 32946-32952.

Yoon, J., Cho, H. Y., Shin, M., Choi, H. K., Lee, T., & Choi, J. W. (2020). Flexible electrochemical biosensors for healthcare monitoring. Journal of Materials Chemistry B, 8(33), 7303-7318.

Zeng, N., & Xiang, J. (2019). Detection of KRAS G12D point mutation level by anchor-like DNA electrochemical biosensor. Talanta, 198, 111-117.

Zeng, Q., Xie, L., Zhou, N., Liu, M., & Song, X. (2017). Detection of PIK3CA mutations in plasma DNA of colorectal cancer patients by an ultra-sensitive PNA-mediated PCR. Molecular Diagnosis & Therapy, 21(4), 443-451.

Zhang, H., Li, F., Dever, B., Li, X. F., & Le, X. C. (2013). DNA-mediated homogeneous binding assays for nucleic acids and proteins. Chemical reviews, 113(4), 2812-2841.

Zhang, H., Li, F., Dever, B., Li, X. F., & Le, X. C. (2013). DNA-mediated homogeneous binding assays for nucleic acids and proteins. Chemical reviews, 113(4), 2812-2841.

Zhang, H., Xu, Y., Fohlerova, Z., Chang, H., Iliescu, C., & Neuzil, P. (2019). LAMP-on-a-chip: Revising microfluidic platforms for loop-mediated DNA amplification. TrAC Trends in Analytical Chemistry, 113, 44-53.

Zhang, J. X., Fang, J. Z., Duan, W., Wu, L. R., Zhang, A. W., Dalchau, N., ... & Zhang, D. Y. (2018). Predicting DNA hybridization kinetics from sequence. Nature chemistry, 10(1), 91-98.

Zhang, J. X., Fang, J. Z., Duan, W., Wu, L. R., Zhang, A. W., Dalchau, N., ... & Zhang, D. Y. (2018). Predicting DNA hybridization kinetics from sequence. Nature chemistry, 10(1), 91-98.

Zhang, L., Zhang, Y., Huang, L., Zhang, Y., Li, Y., Ding, S., & Cheng, W. (2019). Ultrasensitive biosensing of low abundance BRAF V600E mutation in real samples by coupling dual padlock-gap-ligase chain reaction with hyperbranched rolling circle amplification. Sensors and Actuators B: Chemical, 287, 111-117.

Zhang, Y., Li, S., Tian, J., Li, K., Du, Z., & Xu, W. (2020). Universal linker Polymerase Chain Reaction-triggered Strand Displacement Amplification visual biosensor for ultra-sensitive detection of Salmonella. Talanta, 222, 121575.

Zhang, Y., Wang, L., Luo, F., Qiu, B., Guo, L., Weng, Z., & Chen, G. (2017). An electrochemiluminescence biosensor for Kras mutations based on locked nucleic acid functionalized DNA walkers and hyperbranched rolling circle amplification. Chemical communications, 53(20), 2910-2913.

Zhao, B., Wang, L., Qiu, H., Zhang, M., Sun, L., Peng, P., & Yuan, X. (2017). Mechanisms of resistance to anti-EGFR therapy in colorectal cancer. Oncotarget, 8(3), 3980

Zhao, Z., Bao, Y., Chu, L. T., Ho, J. K. L., Chieng, C. C., & Chen, T. H. (2017). Microfluidic bead trap as a visual bar for quantitative detection of oligonucleotides. Lab on a Chip, 17(19), 3240-3245.

Zhou, Q. Y., Zhong, X. Y., Zhao, L. L., Wang, L. J., Zhou, Y. L., & Zhang, X. X. (2020). High-throughput ultra-sensitive discrimination of single nucleotide polymorphism via click chemical ligation. Analyst, 145(1), 172-176.

Zhu, H., Fohlerová, Z., Pekárek, J., Basova, E., & Neužil, P. (2020). Recent advances in lab-on-a-chip technologies for viral diagnosis. Biosensors and Bioelectronics, 153, 112041.

Zouaoui, F., Bourouina-Bacha, S., Bourouina, M., Jaffrezic-Renault, N., Zine, N., & Errachid, A. (2020). Electrochemical sensors based on molecularly imprinted chitosan: A review. TrAC Trends in Analytical Chemistry, 115982.

Zuo, P., Li, X., Dominguez, D. C., & Ye, B. C. (2013). A PDMS/paper/glass hybrid microfluidic biochip integrated with aptamer-functionalized graphene oxide nano-biosensors for one-step multiplexed pathogen detection. Lab on a Chip, 13(19), 3921-3928.

Objetivos

El objetivo principal de la presente tesis doctoral es el desarrollo de metodologías innovadoras con altas prestaciones para la identificación y cuantificación de biomarcadores oncológicos asociados a cáncer colorectal. Estas aproximaciones se materializan como sistemas bioanalíticos capaces de detectar mutaciones puntuales en el genoma de los tejidos tumorales sólidos, integrando avances en el campo de los biosensores, amplificación isoterma, soportes poliméricos funcionalizados y moléculas dendriméricas.

Los objetivos específicos son los siguientes:

1. Puesta a punto de amplificación isoterma por recombinasa-polimerasa mediante la adición de agentes bloqueantes, para el enriquecimiento de alelos minoritarios.
2. Estudio de estrategias de miniaturización y automatización de ensayos en formato de micromatriz y mediante partículas magnéticas.
3. Funcionalización de superficies mediante anclaje covalente de moléculas lineales y dendriméricas con el fin de incrementar la densidad de inmovilización de sondas de ADN.
4. Detección de mutaciones puntuales en los oncogenes *PIK3CA, KRAS y BRAF* presentes en tejidos biopsiados obtenidos de pacientes con cáncer colorectal.
5. Desarrollo de demostradores que integren los logros de los hitos previos para contar con sistemas sensibles, específicos, fáciles de usar, rápidos, robustos y sin dependencia de infraestructuras centralizadas (ASSURED).

Capítulo 1

Amplificación por recombinasa-polimerasa bloqueada para el análisis de mutaciones del gen *PIK3CA*

Resumen

El presente capítulo se centra en la puesta a punto y demostración del procedimiento de amplificación bloqueada isoterma por recombinasa-polimerasa y posterior detección en un chip termoplástico. La amplificación isoterma RPA se llevó a cabo utilizando dos tipos de agentes bloqueantes, con modificación dideoxicitidina (ddC) y sin modificación. La adición de dicho oligonucleótido complementario a la secuencia nativa formó un complejo más estable que con la variante mutante, activando selectivamente la elongación mediante la recombinasa-polimerasa. Se confirmó que el agente bloqueante no actuaba como cebador en el mecanismo de amplificación isoterma y se optimizó la concentración de agente bloqueante, factor que resultó ser determinante en el proceso. Esta reacción se aplicó para la detección de mutaciones en los exones 9 y 20 del gen *PIK3CA* presente en muestras de pacientes con cáncer colorectal.

El diseño y desarrollo de chips termoplásticos para el anclaje covalente de sondas alelo-específicas, en combinación con la hibridación en formato heterogéneo del producto post-amplificación de la RPA-bloqueada, permitió disponer de una plataforma portátil y multiplexada para el genotipado de líneas celulares y tejidos tumorales. Con este formato se consiguió el enriquecimiento de alelos minoritarios a partir de muestras heterogéneas de tejido tumoral, superando el reto de detectar mutaciones puntuales a partir de muestras reales complejas. Los datos obtenidos se compararon con PCR bloqueada y con el método de referencia NGS, obteniendo selectividades del 95% de modo tecnológicamente sencillo y efectivo, trabajando a temperatura constante de 37ºC, reduciendo los tiempos de reacción y el consumo energético.

ELSEVIER

Analytical Biochemistry
Volume 544, 1 March 2018, Pages 49-56

Blocked recombinase polymerase amplification for mutation analysis of *PIK3CA* gene

Sara Martorell [a], Sarai Palanca [b], Ángel Maquieira [a, c, d], Luis A. Tortajada-Genaro [a, c, d]

Abstract

A blocked recombinase polymerase amplification (blocked-RPA) approach has been developed for the enrichment of mutated templates in heterogeneous specimens as tumor tissues. This isothermal amplification technique opens alternative solutions for meeting the technological demand of physician office laboratories. Herein, the detection of mutations in PIK3CA gene, such as p.E545K, and p.H1047L, is presented. The main element was an oligonucleotide (dideoxycytidine functionalized at 3'-end) which matched with wild-type sequence in the target locus. The amplification was performed operating at 37 ºC during 40 min. The results demonstrated that the competition between the upstream primer and the blocker reduced the percentage of amplified wild-type allele, making the detection of the present mutation easier.

For mutation discrimination, a fast hybridization assay was performed in microarray format on plastic chip and colorimetric detection. This approach enabled the reliable discrimination of specific mutations against a background of up to 95% wild-type DNA. The applicability of the method, based on the combination of blocked-RPA and low-cost chip hybridization, was successfully proven for the genotyping of various cancer cell lines as well as tumor tissues. The assignations agreed with those provided by next-

generation sequencing. Therefore, these investigations would support a personalized approach to patient care based on the molecular signature of human cancers.

Keywords: recombinase polymerase amplification; blocking agent; mutations in *PIK3CA* oncogene; gel electrophoresis; colorimetric assay.

Introduction

Neoplastic diseases are currently the leading cause of morbidity and mortality in developed countries, making cancer a public health problem of the first magnitude. The success of anticancer therapies depends on the correct assignation of disease subtype. Therefore, the detection of tumour biomarkers is important for the application of a personalized medicine [1,2]. Somatic mutations on oncogenes are excellent predictive biomarkers since the response to a particular line of treatment can be anticipated, reducing the adverse effects and improving efficiency [3]. They also can be prognostic biomarkers enabling the prediction of disease progression.

Several molecular techniques can be applied for knowing the mutational status of oncogene hotspots. In a DNA extract from patient sample (solid tissues and body fluids), the mutant variant is found in a low proportion compared to wild-type variant. This scenario presents an analytical challenge because wild-type variant can exhaust essential reagents and/or mask the mutant signal during detection assays [4]. Next-generation sequencing instruments holds great promise for point mutation detection, but currently, this technology is available in few health centers and clinics. The alternative solutions are based on introducing an enrichment method combined to more simple detection techniques. Particularly interesting are PCR-based methods proposed for a selective (or quasi-selective) amplification of minority alleles and mutations. These include the use of allele-specific primers to selectively initiate the amplification of the mutated genotype [5,6]; addition of oligonucleotide clamps to preferentially inhibit primer extension on wild type targets [7-9]; and control of temperature thermocycling to favor the preferential denaturation of mutant targets [10]. The differential behavior between wild-type and mutant variants was obtained using real-time or end-point

amplification, fluorescence being the main detection principle. Most of described methods are able to detect the presence of mutation in the selected hotspot, but they do not provide information about their identification.

Herein, we developed an *in vitro* method based on a blocked isothermal amplification as enrichment technique for analyzing point mutations in *PIK3CA* gene (phosphatidylinositol-4,5-bisphosphate 3-kinase, catalytic subunit alpha) as oncogene model. This gene codifies important cell membrane element and second messenger involved in cell signaling. The mutation has been located in human cancer as colorectal, breast, glioblastoma, gastric, ovary, lung, and skin [11,12]. There is an important basic and clinical research for understanding the impact of mutation on cancer cell growth, survival, motility, and metabolism [13]. Additionally, novel inhibitor drugs are targeting this mutant protein [14].

Isothermal amplifications are revolutionizing the development of point-of-care testing due to their capability for the integration in portable, inexpensive instruments or devices [15,16]. Loop-mediated isothermal amplification (LAMP) is the most cited alternative to PCR. Their allele-specific option has displayed excellent results in the detection of a specific point mutation in *EGFR* gene [17], *BRAF* gene [18] and *KRAS* gene [19]. Rolling circle amplification (RCA) and recombinase polymerase amplification (RPA) have been used for the detection of point mutation [20, 21]. In our previous research, the genotyping of a single-point polymorphism was achieved using allele-specific primers for discriminating perfect-match and mismatch allele. In the current study, a new strategy is addressed for improving sensitivity, based on the addition of a blocking oligonucleotide to reduce the amplification of wild-type variant. Then, the presence of mutated variants can be established. Furthermore, an allele-selective hybridization is proposed in order to discriminate between different nucleotide changes. As proof of concept, the selected format involves a plastic chip as analytical platform and colorimetric imagining as detection approach. Microarrays represent an accurate tool for parallel identification of multiple markers, suitable for routine analysis in medical diagnostics [22].

Experimental

Material and reagents

Oligonucleotide sets were designed for the analysis of two important hotspots in *PIK3CA* gene (Table S1.1). In the helicase domain of exon 9, the most frequent mutations are in codon 542 (p.E542K) and codon 545 (p.E545K, p.E545A, and p.E545G). In the kinase domain of exon 20, they are in codon 1047 (p.H1047R and p.H1047L). Thermodynamic parameters were calculated for inducing the selective recognition of target regions [23]. The list of used oligonucleotides, supplied by Eurofins, is included as Supplementary Material (Table S1.2).

The reagents used for genomic DNA amplification were TwistAmp Basic RPA kit (TwistDx, UK). For microarray detection, the printing buffer composition was (2-(N-morpholino) ethanesulfonic acid at 0.1 M, 1-ethyl-3-(3-dimethylaminopropyl) carbodiimide at 20 mM, glycerol 10% (pH 5.5). The hybridization buffer was saline-sodium citrate (SSC) 2×: sodium chloride at 150 mM, sodium citrate at 15 mM, formamide 20% (pH 7.0). Hybridization washing buffer was a solution with NaCl 15 mmol L^{-1}, trisodium citrate 1.5 mmol L^{-1}. Developing buffer was a phosphate buffered saline solution (PBS-T) containing 137 mM NaCl, 12 mM phosphate, 2.7 mM KCl, 0.05% Tween 20 (pH 7.4).

The hybridization chips were prepared by immobilizing the allele-specific probes on rectangular slides (25 mm × 75 mm). For covalent anchoring of probes, polycarbonate surface was activated by UV-ozone incubation (model FHR.Clean.150-Lab, FHR, Germany) using UV lamps (50 mW cm^{-1}) at 254 nm. After, the chips were immersed in a solution of NaOH 1M at 60 °C, washed with distilled water and dried. The dispensation of amine-DNA probes in printing buffer on the modified surface was performed by non-contact array printer equipment (AD1500, Biodot). The printing volume drop was 40 nL. Six arrays were printed per chip, including 4 replicates per target probe and controls. The chips were incubated for 1 hour, washed with PBS-T and water, dried and stored at 4 °C until use.

Samples and DNA extraction

Patients and several volunteers were recruited for the present study according to ethics and with informed consents. Genomic DNA was extracted from three 5-µm thick FFPE sections using Deparaffinization Solution and the GeneRead DNA FFPE Kit (Qiagen, Hilden, Germany) according to manufacturer's protocol. This isolation kit contains uracil-DNA glycosylase (UDG) that leads to the reduction of C>T sequence artefacts. Buccal cells were collected by rolling the swab (Catch-All sample collection swab, Epicenter) on the inside of the cheek. DNA extraction was performed using the PureLink Genomic DNA Mini Kit (Invitrogen). Briefly, the swab was incubated with Proteinase K, RNAse and lysate buffer. The purification was performed by using a spin column-based centrifugation procedure. Human cell lines SK-N-AS (ATCC CRL-2137) and HCT 116 (ATCC CCL-247) were used as native (wild type) and heterozygous (p.H1047R/c.3140A>G) controls, respectively. In these cases, DNA extraction was performed using PureLink kits (Invitrogen).

In addition, the assay included a negative control (DNA from *Salmonella Typhimurium*). The concentration of the DNA extracts (ng μL^{-1}) was obtained by spectrophotometry using NanoDrop 2000c, and by fluorimetry using Qubit dsDNA HS Assay Kit (ThermoFisher Scientific).

PCR amplification

PCR amplification in single format was performed for each target hotspot in *PIK3CA* gene (exon 9 or exon 20). Each reaction mixture contained 1 × DNA polymerase buffer, 3 mM of $MgCl_2$, 200 µM of each deoxynucleotide triphosphate, 200 nM of upstream primer and downstream digoxigenin-labeled primer, 4 ng of genomic DNA, and 1 unit of DNA polymerase (Biotools, Madrid, Spain). In certain experiments, a blocking oligonucleotide complementary to wild-type variant was added to each mixture (10 nM – 400 nM). The reaction was performed in thermocycler (United

Nations, VWR) under the following conditions: initial denaturation cycle of 95 °C for 5 min, 35 cycles of denaturation at 95 °C for 30 s, annealing 57 °C for 30 s and elongation at 72 °C for 60 s, finally one cycle extension at the end for 5 min.

RPA amplification

RPA amplification in single format was performed for each target hotspot in *PIK3CA* gene (exon 9 or exon 20). The reaction mixtures (12.5 µL) were prepared with rehydrated buffer, 14 mM of magnesium acetate, 480 nM of upstream primer and downstream digoxigenin-labeled primer, 50 nM of blocking agent, 4 ng of genomic DNA, and the enzyme pellet. The reaction mixtures for conventional RPA did not contained the oligonucleotide complementary to wild-type variant. The heating system used was a thermocycler (United Nations, VWR) at 37 ºC for 40 min.

Gel electrophoretic detection

The RPA amplicons were cleaned for being visualized using agarose gel electrophoresis. Two methods were compared, the first being based on silica-gel membrane adsorption (PCR purification kit, Jena Bioscience, Germany). The RPA products, mixed with binding buffer and isopropanol, was transferred to the activated column and centrifuged at 10.000g for 30 s. After washing the column twice, the elution fraction was collected in distilled water. The second method was based on denaturation protocol. The RPA products were incubated at 65 °C in dry bath (model FB 15103, Fisher Scientific) for 10 min. After centrifugation at 10.000g for 20 s, the supernatant fraction was collected.

The electrophoretic separation was conducted in agarose gel 3 %. Amplification solutions were mixed with loading buffer and transferred to gel wells. After separation at 110 V, fluorescent dye (Realsafe Nucleic acid Staining Solution 2x, Real Lab.) was incubated for 30 min. Gel images were captured using a smartphone Iphone 7 and analyzed using ImageJ software.

Colorimetric chip detection

The RPA products were detected and identified by a hybridization assay using allele selective probes immobilized on polycarbonate chips. Amplified products (5 μL) were mixed with 45 μL of hybridization buffer, heated (95 °C, 5 min) and dispensed onto sensing arrays to perform the simultaneous analysis of 6 samples (four probe replicates). After incubation (37 °C, 60 min), the arrays were rinsed with progressive dilutions of hybridization washing buffer. To develop the probe-product duplex, an immunoreaction was used. PBST solution with 1:2500 monoclonal anti-Dig antibody (Abcam) and 1:400 monoclonal antisheep-HRP antibody in PBST, was dispensed (room temperature, 30 min). As HRP-substrate, 3,3',5,5'-tetramethylbenzidine solution (ep(HS)TMB-mA, SDT Reagents) was selected, generating a solid deposit.

Chips were directly scanned (Epson Perfection 1640SU office scanner), producing gray-scale images (Tagged Image File Format, color depth 16 bit, scale 0-65535). The optical intensity signals of each spot were quantified using in-home software. Image processing (feature gridding, addressing, segmentation and quality assurance) was automatically performed in less than 5 min.

Reference method

Several methods for detecting somatic mutations are currently available. NGS, considered to be an optimum method for mutation detection, was conducted employing the Ion Torrent PGM technology (ThermoFisher Scientific). The *Oncomine Solid Tumor DNA kit* was used for DNA analysis (ThermoFisher Scientific). This assay simultaneously screens hotspots mutations in 22 genes (included PIK3CA). For generating the DNA barcoded libraries, a multiplex PCR amplification of 10 ng of genomic DNA was performed. Sequencing was performed on the Ion Torrent PGM system on a 318v2 Ion Chip using Ion PGM Sequencing Hi-Q kit (Thermo Fisher Scientific). Data from sequencing runs were transferred to the Torrent Server, alignment to the hg19 human

reference genome and variant calling was performed by the Ion Torrent Suite Software 5.4 (Thermo Fisher Scientific). In addition, all identified variants, such as PIK3CA mutations in exon 9 and 20 (p.E545K and p.H1047L), were visually checked using the Integrative Genomics Viewer (IGV) software

Results

Assay design

A flow diagram showing the main steps in our assay for the detection of point mutations is illustrated in Fig.1.1 From total genomic DNA extracted from human tissues, the target sequence is amplified following a clamp blocked RPA reaction. Compared to conventional RPA method, the reaction solution also contained an oligonucleotide complementary to wild-type DNA (blocker), the target nucleotide being in the central position of oligonucleotide. The upstream primer is in the vicinity of blocking oligonucleotide, and partially overlaps its 5'-end. The blocker oligonucleotide is designed for producing more stable complexes than upstream primer. The method operates by a competition for a common target site.

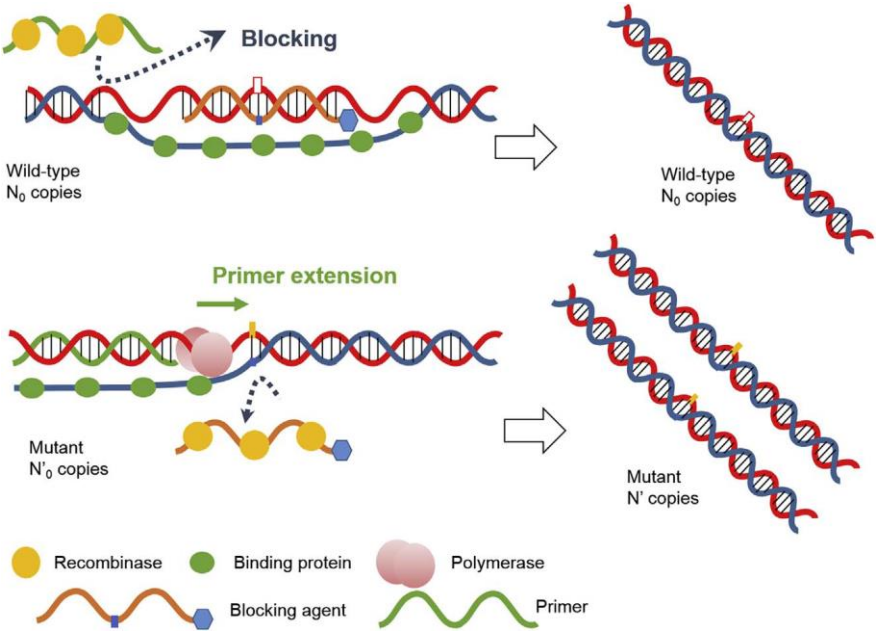

Fig.1.1 Schematic illustration of the RPA reaction for minority allele enrichment based on the addition of blocking agent. (Up) Wild-type blocked amplification. (Bottom) Mutant amplification.

The amplification mechanism of mutant variants is based on the action of recombinases (T4 uvsX and loading factor T4 uvsY), which form complexes with primers and bind them with their homologous sequences in duplex DNA [24]. A single-stranded DNA binding (SSB) protein binds to the displaced DNA strand and stabilizes the resulting D loop. Bsu polymerase (large fragment of *Bacillus subtilis* Pol1) produces the primer extension from the 3'-end, replicating mutant allele. The amplification of wild-type variants is impaired due to the presence of the blocking oligonucleotide. In this case, the blocking oligonucleotide dominates the binding to the template over the primer. Since the blocker also contains a chemical modification at the 3'-end, the oligonucleotide cannot be extended by Bsu polymerase. Then, the addition of this blocking agent during amplification of the target region induces the competition for the binding site in DNA template, leading to a preferential amplification of minority mutations. This clamping effect has been previously described for PCR-based methods [12,13], but this is the first time for RPA.

RPA amplification

The proposed assay was tested for the genotyping of the main hotspots in *PIK3CA* gene (codon 542/545 and codon 1047). An *in-silico* design was applied for the selection of the sequence-specific primers based on the requirements established for the product properties and method performances. Compared to the conventional RPA methods, short primers (< 30 nucleotides) were selected to facilitate the subsequent allele-specific assay. Even though they had little recombinase-mediated strand-invasion activity, short primers can still function via hybridization recognition [25]. An additional design restriction was taken into account. The length of products was limited to short amplification products (lower than 100 bp). As the conservation of biopsied tissues as formalin-fixed and paraffin-embedded can lead to an important degradation of nucleic acids, this selection criteria can minimize false-negative results.

Using the selected oligonucleotide sets (upstream and downstream primers), the first experiments were focused on the optimization of reaction conditions for the

amplification of both hotpots in single format. Regarding kinetic behavior, the amplification process reached a stationary phase after 40 min. A similar product formation was obtained when the RPA reaction was produced within the 37-42 ºC range, showing high tolerance to temperature fluctuations. Therefore, the selected conditions were similar to previous studies for human cancer tissues [26].

RPA specificity was checked on the basis on the detection of target regions from human and non-human genomic DNA. Negative results were reported for the non-target genes or samples, demonstrating the absence of false-positive results. The matrix effect was also examined, analyzing different samples (cell culture, buccal swap, colon tissue) and storage conditions (fresh tissues and formaldehyde fixed-paraffin embedded tissues). Under the selected extraction and amplification conditions, excellent end-point amplification yields were obtained. A detectable signal was measured for $5 \cdot 10^2$ DNA copies. The results were comparable to those obtained with the PCR-based method, independently on sample source (paired t-test, p-value <0.05).

Selection of blocking oligonucleotides

A preferential RPA-based amplification of minority mutations was studied based on the addition of a blocking oligonucleotide to the reaction solution. Following the modalities described for blocked PCR amplification, two kinds of oligonucleotide sets were assayed. The first approach, both oligonucleotides (upstream primer and blocking agent) are complementary to different template regions, preventing the amplification in the elongation step. In the second approach, also called clamp strategy, the blocker partially overlaps with the upstream primer, reducing the amplification in the primer annealing step.

As the number of possible oligonucleotides can achieve hundreds, the thermodynamic stability of DNA duplexes was examined. The parameters were the variation of free energy associated to the formation of DNA duplexes (ΔG) and melting temperature (T_m), or temperature at which half of the blocking oligonucleotides are

single-stranded state (0.1 M NaCl, 25 ºC at pH=7). Firstly, the formation of upstream primer duplexes was studied in both hotspots of *PIK3CA* gene. The ΔG-values for the selected primers ranged between -19.8 kcal mol^{-1} and -20.5 kcal mol^{-1}, corresponding to T_m = 58.6-60.9 ºC. Secondly, the effect of design parameters on the blocking oligonucleotide/template hybrids was estimated. Blocking agents with length higher than 22 nucleotides produced DNA complexes more stable than the selected primers (T_m>62°C). The differential variation of free energy associated to the formation of DNA duplexes (wild-type vs. mutant variants) was calculated in function of clamp-region length and mutation position. The nucleotide number that overlapped with the primer produced a slight effect on the discrimination recognition for perfect match complex (wild-type template) respect to the mismatched complexes (mutant templates). However, the position of mutation on blocking agent sequence varied drastically the stability of the mismatched hybrids. In fact, the maximum difference between blockers and wild-type/mutant complexes was achieved when the mutations was located in a central position.

On the basis on these experiments, several design requirements of blocking oligonucleotide were defined for blocked RPA assay (Table 1.1). Applying *in silico* calculations, two primers and a blocking oligonucleotide compose the selected set per studied mutation. The estimated ΔG-values for wild-type complex were -23.6 kcal mol^{-1} for exon 9 and -21.9 kcal mol^{-1} for exon 20, corresponding to T_m = 64.5 ºC and T_m = 63.3 ºC, respectively. The selected blocking oligonucleotides should form a more stable complex with wild-type than with the mutated variant (about 4 kcal mol^{-1}). Regarding the clamp effect, the common nucleotides (3'-end of primer and 5'-end of blocking agent) were 2 in both targeted hotspots. Under these conditions, the expected reduction of upstream primer annealing was about ΔG = 1.9-2.0 kcal mol^{-1} for wild-type hybrid. Although RPA mechanism is based on the action of several enzymes, a differential behavior was expected. The blocker would preferentially hybridize onto the wild type template strand and the upstream primer would bind to the mutant template.

Table 1.1: (a) Design criteria of blocking oligonucleotide. (b) Optimized variables for blocked RPA.

(a)

Criteria	Restriction
Sequence[a]	Complementary to the wild-type variant
Mutation position	Central position of oligonucleotide
Melting temperature[b]	Higher to both primers (upstream and downstream primers)
Secondary structures	Low stability
Self-complementarity	None
Modification	3'-end to inhibit the extension
Upstream primer position	Overlap in order to induce the competition for the binding site in DNA template

(b)

Variable	Studied range	Selected
Magnesium acetate concentration (nM)	14–30	14
Primer concentration (nM)	42–420	420
Blocker concentration (nM)	0–600	50
DNA (ng)	0–40	4
Temperature(°C)	25–45	37
Time (min)	0–60	40

Set-up of blocked amplification

The following step was the study of experimental conditions for blocked RPA, using DNA extracts from control/mutant cell lines and the selected olignucleotides. In a first set of RPA experiments, reaction mixtures contained the downstream primer and the unmodified blocker (without upstream primer). Positive responses were observed, indicating that the blocking oligonucleotide acted as upstream primer (Fig.1.2a). Later, the same RPA reactions were performed, including modifications at the 3'-end of the blocker (capped extension). The studied modifications were dideoxycytidine (ddC) and non-sense 3-mer tail (not complementary to template molecule), leading a signal reduction (t-test: p-value<0.002). Both chain terminator avoided the 3'-extension, yielding similar responses to negative controls, even for high concentrations of blockers (t-test: p-value>0.95). For further assays, ddC modified blocker was selected.

Human genomic DNA was added in PCR and RPA reactions containing three oligonucleotides (primers and blocker) for non-clamp and clamp approaches (Fig.1.2b). In case of PCR, the addition of the blocker reduced the amplification of wild-type variant, the effect being higher for clamp approach. These results agreed with those previously described for PCR-based methods, where the overlapping region between primer and blocker provided better assay performances [7,8]. In case of isothermal method, using a primer complementary to a different region than blocker, the primer elongation of wild-type DNA was produced (t-test: p-value = 0.89). The amplification of wild-type DNA only was reduced for clamp option (t-test: p-value = 0.01). This differential blocking effect compared to PCR agreed with the expected features of RPA mechanism. In the first approach, recombinase mediated in the formation of both complexes (primer/template and blocker/template). However, polymerase used in RPA (Bsu polymerase) has strand-displacing activity that means the ability to displace downstream DNA encountered during synthesis. Although the blocking oligonucleotide was initially bound, the primer elongation was possible, replicating wild-type templates. In case of second strategy, the observed behavior fitted with a physico-chemical competition for the same template region. The blocker operates a competitor of the upstream primer for the common target site. As the stability of blocker was higher, the primer annealing in RPA process was interfered. As the non-clamp option was incompatible with RPA biochemistry, further experiments were performed using the oligonucleotide set based on clamp effect.

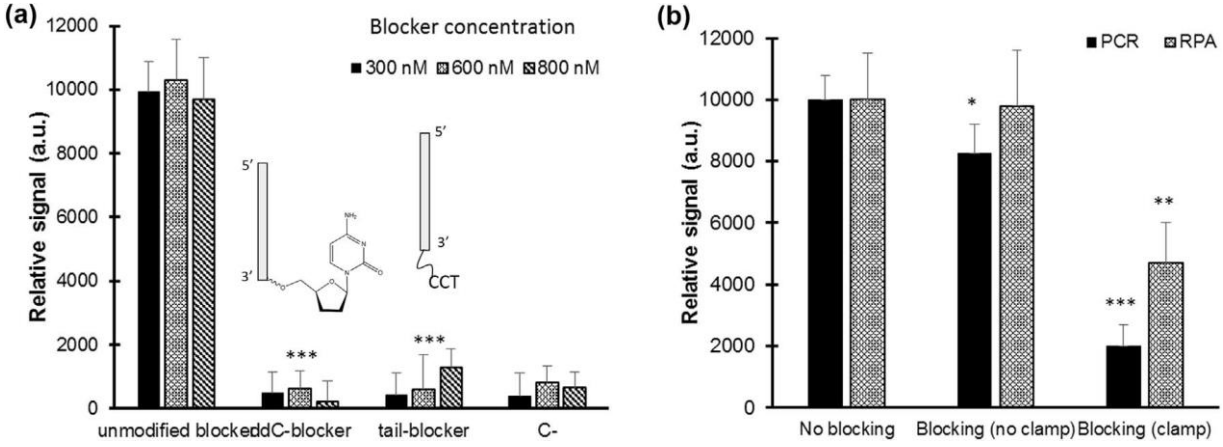

Fig.1.2: (a) Modification of blocker oligonucleotide for the prevention of Bsu extension in a RPA mixture without upstream primer. Blocker concentration: 300, 600 and 800 nM. (b) Amplifications (PCR and RPA) performed in conventional and blocked formats

(blocker concentration 200 nM). T-test: * p-value<0.05, ** p-value<0.01, *** p-value<0.001. Wild-type genomic DNA: 1300 copies.

Agarose gel electrophoresis was used for confirming the blocking effect on PCR and RPA reaction for PIK3CA (Fig. S1.1). In case of PCR, the expected bands were detected (83 pb for exon 9 and 79 pb for exon 20). However, RPA products yielded smear bands due to mixture components (i.e. DNA binding proteins, detergents). Therefore, two post-amplification treatments were assayed (column purification and protein denaturation). The first method involved that silica-membrane columns retained short DNA molecules under high-salt conditions and eluted them using a low-salt buffer. The second method consisted in the denaturation of proteins at high temperature. Although both treatments provided a single band located at the estimated position, the separation obtained after heating strategy led to band intensities comparable to the PCR results. Further experiments showed that the band intensity decreased in the presence of blocking nucleotide in RPA reactions, being undetectable for high concentrations. Finally, the kinetic profile in the presence of blocker was compared to the conventional profile. Although amplification yield was lower than conventional value (about 50 %), the maximum signal was achieved after 40 min of reaction in both cases. Therefore, gel electrophoresis results proved the variation of replication activity as the consequence of blocker binding to the template.

For the selection of blocker concentration, genomic DNA extracted from human cell cultures (wild-type and mutant) were amplified, varying up to 400 nM (stoichiometric ratio of 1.33 compared to the upstream primer). End-point responses decreased as the concentration of blocking oligonucleotide increased for both kind of templates (Fig.1.3). As the amplification variation was also observed in mutated variants, an unspecific interaction of blocker was produced in the mismatched templates. Nevertheless, certain reaction mixtures produced a nearly null signal for native variant and perfectly detectable signal for mutant variant. Experimental data fitted to a typical four-parameter logistic curve with a suitable model goodness (R^2=0.94 and 0.98, exon 9 and 20, respectively). The equation of this nonlinear regression was

Signal = *d* + (*a*-*d*)/(1+([*bloq*]/*c*)^{b}), where [*bloq*] is the concentration of blocking agent, *d* is the background signal, *a* is the signal for the absence of blocking oligonucleotide, *c* is related to the concentration at the inflection point and *d* is related to the curve steepness. Table 1 displays the estimated values for both hotspots of *PIK3CA* gene. Significative differences were found in the value of *c*-parameter that is related to half maximal effective concentration (EC50) or blocking concentration that reduced the signal to half. The EC50 values for wild-type templates were about 2 times lower than the values calculated for mutant templates for both target regions. The observed differential behavior confirmed that the addition of blocking agent produced a higher reduction of RPA reaction on perfect-match template (native) than a mismatched template (mutant). A concentration of 50 nM was selected for further experiments.

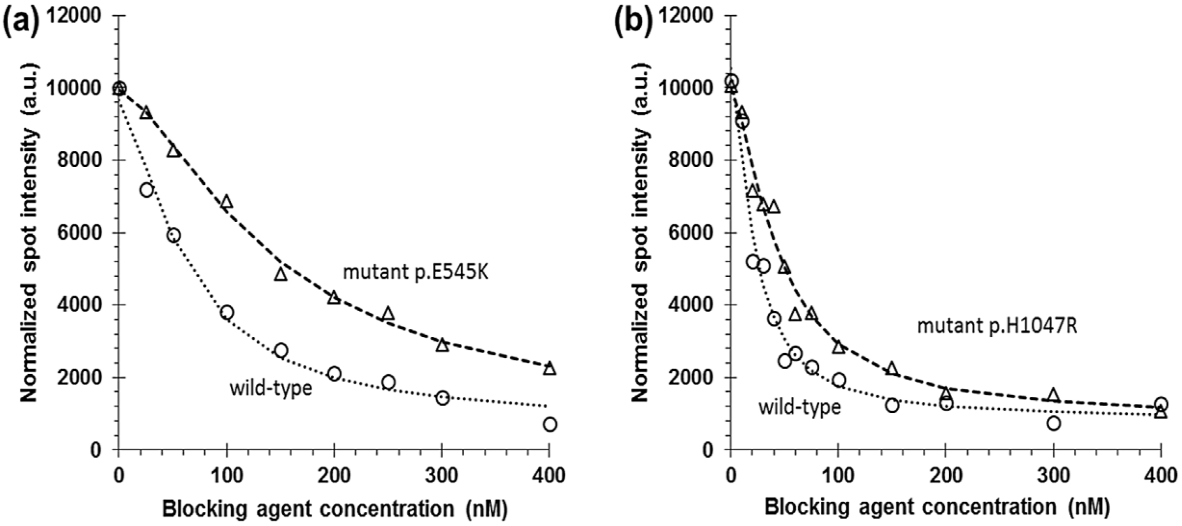

Fig.1.3: Effect of blocking concentration on the end-point response of RPA-based methods: Reactions for exon 9 (a) and exon 20 (b). Discontinue lines correspond to the regression curve applying four-parameter logistic model.

Table 1.2: Regression parameters obtained applying four-parameter logistic model to experimental data: blocking concentration vs. end-point response of RPA-based methods.

		a	b	c	d	R^2
exon 9	wild-type	10000 ± 300	1.5 ± 0.3	62 ± 8	700 ± 300	0.990
	mutant p.E545K	10000 ± 200	1.5 ± 0.2	140 ± 14	600 ± 400	0.995
exon 20	wild-type	10500 ± 400	1.5 ± 0.2	22 ± 2	800 ± 400	0.980
	mutant p.H1047R	10000 ± 300	1.5 ± 0.2	44 ± 5	800 ± 300	0.982

Identification of mutations

The presence of a mutation was established from the results (electrophoresis or fluorescence) for blocked RPA reactions (single format). Then, the detection of a band indicated that a mutated variant was amplified, achieving a selectivity of 100 %.

The determination of the specific genetic variant needed an additional end-point method (i.e. chip hybridization, bead hybridization, among others). In the present study, a simple colorimetric microarray assay based on using allele specific probes was developed for discriminating each specific mutation for a particular hotspot (Fig.S1.2). The resulting RPA amplicons were hybridized to the chip which carried probes complementary to the targeted sequence. The use of microarray detection of RPA products has been previously described in previous studies [21,27]. Nevertheless, the method was further improved to serve the purpose of integrated mutational analysis.

Pursing the goal of a point-of-care test, a low-cost DNA chip combined with consumer electronic device for the readout of results, was developed. Firstly, specific probes were designed to maximize the selective recognition process, considering thermodynamic calculations (Table S1.3). The estimated free energy variation for the complexes between the specific probes to its fully complementary target sequence varied from -21.4 to -22.4 kcal mol^{-1} for exon 9 and from -21.7 to -22.4 kcal mol^{-1} for exon 20. The values calculated for mismatched complexes ranged between -14.0 to -20.0 kcal mol^{-1}. Then, the estimated differences were large enough for a discriminatory assay. Secondly, the probe immobilization on polycarbonate chips was examined via photochemical surface activation [28,29]. Under selected conditions, the conjugation of amine-functionalized probes to carboxylate groups on chip surface produced an amide bond. The calculated immobilization probe density was 3.5 pmol cm^{-2}. A stable and strong bound was not affected by pH, temperature or microfluidic flows (losses < 5%).

Latterly, the hybridization experiments were performed by incubating the RPA products on chips with allele specific probes immobilized in microarray format. So, the discriminating elements were spatially separated, but integrated in a single assay. The

optimization criteria were a high response signal for perfect-match probe and minimal response for the mismatched probes. Therefore, the mutation can be identified due to the formation of a perfect-match hybrid between the RPA product and one specific probe. The composition of hybridization solution (formamide 20 %, low ionic strength) was critical for the restrictive recognition. Another important factor was the volume of RPA product dispensed on chip. A beneficial effect of assay performed in a microarray format is the reduced distance that molecules need to travel from the bulk solution to the solid-liquid interface. Selected volume (45 μL) minimized the time required to obtain high spots signal, associated to shortened diffusion times. Compared to PCR chip, higher background signals were registered for RPA products. However, the signal-to-noise ratio (S/N), calculated as the ratio of the signal and the standard deviation of the background noise, was between 12 and 22.

Under the selected conditions, unblocked RPA products from human cell cultures were hybridized on the chip. Given the presence of the biorecognition product, a variation of the reflection properties of chip surface was measured (Fig.1.4). If there was no reaction product, the maximum intensity of the reflected beam was collected (background signal). If target gene-probe recognition and subsequent solid deposit formation occurred, the light would strike the product, modifying the optical response. Wild-type products yielded a high response for their specific probes (S/N>15), and were low or null for the remaining ones (S/N<6). Mutant products of exon 9 (p.E545K) were specifically recognized for the corresponding probe (S/N = 12), since the spot signals were significantly higher than controls (t-test: p-value = 0,005). Mutant products of exon 20 (p.H1074R) hybridized to two probes (wild-type and p.H1074R probe), giving detectable signals (S/N>15) with similar intensities (t-test: p-value = 0,07). These values agreed with a genomic DNA coming from a human cell culture that is heterozygote for this locus. Therefore, a sensitive and selective hybridization assay was achieved. The results obtained using a planar polycarbonate chip and a simple optical detection also demonstrated that the assay is compatible with a typical mass produced material and a sensing technology of DNA devices [16,22,30].

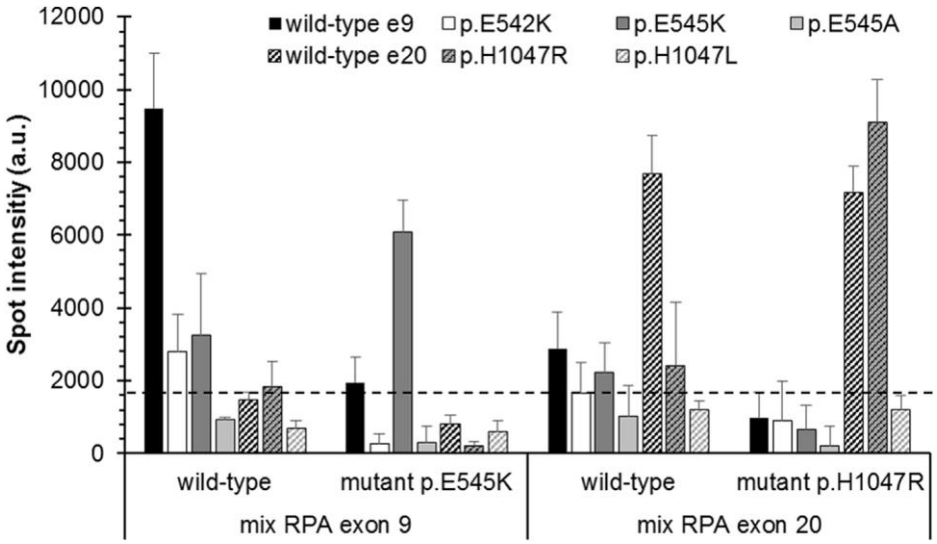

Fig.1.4: Probe Selectivity: spot intensity of array probes obtained from different unblocked RPA reactions and samples. Dashed line indicates control negative response.

Patient analysis

There were important analytical challenges associated to the mutation detection and identification related to solid cancer screening. DNA from FFPET used to determine mutation status was highly degraded due to fixation. In fact, the nature of clinical sample and the conservation mode led to low amount/poor-quality of DNA in same samples. Intact double strand DNA ranged from 10 to 270 ng μL^{-1}, with a purity 260/280nm ranged from 1.7 to 2.1. In addition, the small proportion of mutated DNA can limit the success of the assay. So, assay sensitivity was determined by preparing heterozygous mixtures with increasing percentages of mutant DNA compared to the wild-type type (Fig.S1.3). These experiments emulated the wide range of clinical scenarios regarding the variable proportion of tumor cells (mutant DNA) respect to non-tumor cells (native DNA) in a biopsied sample. Experimental data was adjusted to a linear regression with an excellent model goodness (R^2=0.994), indicating that blocked RPA produced a proportional amount of mutated sequences to the initial concentration of mutant genomic DNA. Mismatched DNA was detected up to 5 %, which indicated that the system was capable of detecting the mutant variant, even in low concentrations. In absence of blocker, the mutant variants were only detected when the percentage was 2-8 times higher. These results confirmed the formation of a stable duplex between

blocker and wild-type template, limiting the primer hybridization and consequently producing the mutant enrichment.

Intra and inter-day reproducibility, expressed as the relative standard deviation of spot intensities for the replicated assays (five replicates), were 13 % and 17 %, respectively. The ANOVA test showed that the end-point responses were comparable for the four studied genes (p-value > 0.05).

The next experiments were focused on the analysis of blind samples collected from oncological patients (formalin fixed and paraffin embedded tissues). For each sample, a blocked RPA reaction per exon was performed. The arrangement of the microarray matrixes on the chip was designed in such a way that 6 samples (4 spot replicates) would be analyzed in parallel. The incorporation of quality controls (positive and negative) helped to ensure reliable results considering the possible variation of analytical process. Examples of the obtained microarray images are shown in Fig.1.5. Despite of the blocked amplification, positive responses for both wild-type probes were observed in all chips (S/N 6±2). Nevertheless, a clear assignation was achieved based on the spot signals for mutant probes. Most of samples were assigned as wild-type for both studied locus (exon 9 and exon 20) because the mutant probe intensities were comparable to negative controls. The exceptions were two chips that showed a detectable response for one of the mutant probes. The S/N were 10±2 for p.E545K mutant and 17±2 for p.H1047R mutant. Therefore, patients were classified as mutant in exon 9 and mutant in exon 20, respectively. The assignations agreed with those obtained using next-generation sequencing technology in all cases. However, sequencing analysis required higher amount of DNA, labor-intensive sample preparation and took longer to generate data compared with our method. The results highlighted that blocked RPA was an adequate approach since the copy number of mutated regions was high enough to be detected and discriminated in a hybridization assay. Furthermore, the proposed method fulfilled the requirements for a mutational analysis in a simple health system framework (i.e. short analysis time, low cost, and simple).

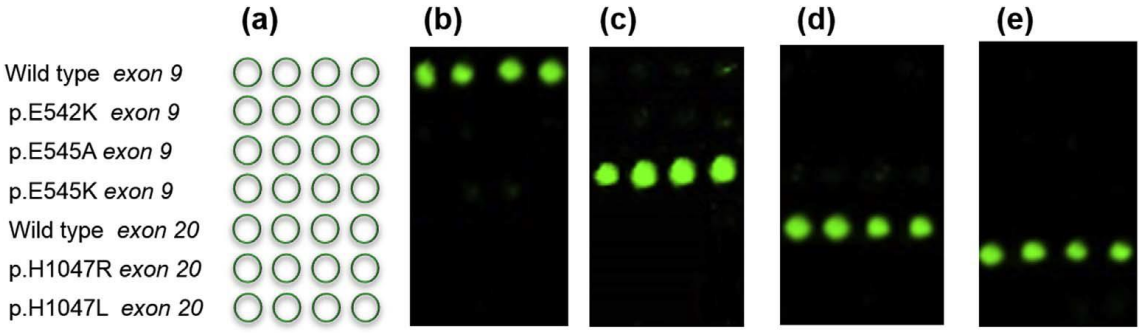

Fig.1.5: On-chip hybridization results for oncological patient samples: (a) Microarray layout, (b) Blocked RPA for exon 9, sample: wild-type, (c) Blocked RPA for exon 9, sample: mutant p.E545K, (d) Blocked RPA for exon 20, sample: wild-type, and (e) Blocked RPA for exon 20, sample: mutant p.H1074R.

CONCLUSIONS

Increasing knowledge on genetic variants and availability of specific therapeutic agents is enabling the development of a more personalized oncogenic medicine (e.g. specific monoclonal antibodies). However, a parallel technological development is required for translating them to clinic routine. Real-time PCR, droplet digital PCR and DNA sequencing are the most widely used method for mutational analysis. Although this objective has been effectively addressed, they involve a labor-intensive expensive solution or a limited capability in multiplex analysis. This study is aligned with the research line of developing alternative solutions.

RPA-based methods are a successful approach for supporting portable diagnostic DNA assays due to their performances. However, this study is the first in demonstrating that blocked RPA is an adequate mutant enrichment technique. The results have shown that this blocking behavior is a less effective process compared to other approaches, but the achieved sensitivity (about 5 %) and reproducibility (about 15 %) are enough for their application to biopsied samples in solid tumors.

The other relevant issue approached in this study is the discrimination of point mutations. In large hospitals, several methods are applied for determining the presence

of a mutation in certain locus, without identifying the specific variant. Others perform a reaction per each mutation. The consequences are a lack of information limiting the possibilities of modern oncology or an increase of laboratory efforts, reducing the sustainability of the health system. Chip-based detection approaches, such as we have introduced, show the advantage of multiplexing. All investigated variants can be implemented on the same microarray. In addition, the inclusion of controls guarantees the assay reliability. Indeed, the optimized protocol is faster (performed in less than 2.5 h) and easier to handle than sequencing.

According to the amplitude of described applications based on blocked PCR, the expectations of the blocked RPA are high. Furthermore, the method can potentially support the detection/discrimination of mutations in more health scenarios (e.g. small hospital or clinics). Demonstrated for *PIK3CA* mutational analysis, the next experimental activities are addressed to expand to other mutations. Then, a better stratification of patients, or division of patients into subgroups based on the molecular characteristics, can be achieved and a subsequent individualized treatment can be assigned.

Conflict of Interest Statement

The authors declare that the research was conducted in the absence of any commercial or financial relationships that could be construed as a potential conflict of interest.

Acknowledgments

PROJECT ONCOMARKER (MINECO RTC-2015-3625-1), CTQ 2013-45875-R, FEDER and GVA PROMETEO 2014/40

References

[1] M. Pajic, C.J. Scarlett, D.K. Chang, R.L. Sutherland, A.V. Biankin, Preclinical strategies to define predictive biomarkers for therapeutically relevant cancer subtypes, Hum. Genet. 130 (2011) 93–101.

[2] A. Ziegler, A. Koch, K. Krockenberger, A. Großhennig, (2012). Personalized medicine using DNA biomarkers: a review, Hum. Genet. 131 (2012) 1627-1638.

[3] R.E. Shackelford, N.A. Whitling, P. McNab, S. Japa, D. Coppola, D. KRAS Testing a Tool for the Implementation of Personalized Medicine, Gene Cancer, 3 (2012) 459-466.

[4] C.A. Milbury, J. Li, G.M. Makrigiorgos, PCR-based methods for the enrichment of minority alleles and mutations, Clin. Chem. 55 (2009) 632-640.

[5] R.E. Board, N.J. Thelwell, P.F. Ravetto, S. Little, M. Ranson, C. Dive, A. Hughes, D. Whitcombe, Multiplexed assays for detection of mutations in PIK3CA, Clin. Chem. 54 (2008), 757-760.

[6] J. Morlan, J. Baker, D. Sinicropi, Mutation detection by real-time PCR: a simple, robust and highly selective method, PLoS One, 4 (2009), e4584.

[7] J.D. Luo, E.C. Chan, C.L. Shih, T.L. Chen, Y. Liang, T.L. Hwang, C.C. Chiou, Detection of rare mutant K-ras DNA in a single-tube reaction using peptide nucleic acid as both PCR clamp and sensor probe, Nucleic Acids Res. 34 (2006) e12-e12.

[8] H. Wang, J. Jiang, B. Mostert, A. Sieuwerts, J.W. Martens, S. Sleijfer, J.A. Foekens, Y. Wang, Allele-specific, non-extendable primer blocker PCR (AS-NEPB-PCR) for DNA mutation detection in cancer, J. Mol. Diagn. 15 (2013) 62-69.

[9] Y. Jia, J.A. Sanchez, L.J. Wangh,. Kinetic hairpin oligonucleotide blockers for selective amplification of rare mutations, Sci. Rep. 4 (2014) 5921.

[10] I. Mancini, C. Santucci, R. Sestini, L. Simi, N. Pratesi, F. Cianchi, R. Valanzano, P. Pinzani, C. Orlando, The use of COLD-PCR and high-resolution melting analysis improves the limit of detection of KRAS and BRAF mutations in colorectal cancer, J. Mol. Diagn. 12 (2010) 705-711.

[11] Y. Samuels, T. Waldman, Oncogenic mutations of PIK3CA in human cancers, Curr. Top Microbiol Immunol. 347 (2010) 21–41

[12] G. Cathomas, PIK3CA in colorectal cancer, Front. Onco., 4 (2014) 35

[13] K.D. Courtney, R.B. Corcoran, J.A. Engelman, The PI3K pathway as drug target in human cancer, J. Clin. Oncol. 28 (2010) 1075-1083.

[14] C. O'Brien, J.J. Wallin, D. Sampath, D. GuhaThakurta, H. Savage, E.A. Punnoose, P. Guan, L. Berry, W.W. Prior, L.C. Amler, M. Belvin, L. Friedman, M. Lackner, Predictive biomarkers of sensitivity to the phosphatidylinositol 3' kinase inhibitor GDC-0941 in breast cancer preclinical models, Clin. Cancer Res. 16 (2010) 3670-3683.

[15] Y. Zhao, F. Chen, Q. Li, L. Wang, C. Fan, Isothermal amplification of nucleic acids, Chem. Rev, 115 (2015) 12491-12545.

[16] C.D. Ahrberg, A. Manz, B.G. Chung, Polymerase chain reaction in microfluidic devices, Lab Chip, 16 (2016), 3866-3884.

[17] S. Ikeda, K. Takabe, M. Inagaki, N. Funakoshi, K. Suzuki, Detection of gene point mutation in paraffin sections using in situ loop-mediated isothermal amplification, Pathol. Int. 57 (2007) 594-599.

[18] Y.S. Jiang, S. Bhadra, B. Li, Y.R. Wu, J.N. Milligan, A.D. Ellington, Robust strand exchange reactions for the sequence-specific, real-time detection of nucleic acid amplicons, Anal. Chem. 87 (2015) 3314-3320.

[19] M. Itonaga, I. Matsuzaki, K. Warigaya, T. Tamura, Y. Shimizu, M. Fujimoto, F. Kojima, M. Ichinose, S.I. Murata, Novel Methodology for Rapid Detection of KRAS Mutation Using PNA-LNA Mediated Loop-Mediated Isothermal Amplification, PloS one, 11 (2016) e0151654.

[20] Q. Su, D. Xing, X. Zhou, Magnetic beads based rolling circle amplification–electrochemiluminescence assay for highly sensitive detection of point mutation, Biosens. Bioelectron. 25 (2010) 1615-1621.

[21] E.S. Yamanaka, L.A. Tortajada-Genaro, A. Maquieira, Low-cost genotyping method based on allele-specific recombinase polymerase amplification and colorimetric microarray detection, Microchim. Acta, 184 (2017) 1453-1462.

[22] S. Galbiati, F. Damin, P. Pinzani, I. Mancini, S. Vinci, M. Chiari, C. Orlando, L. Cremonesi, M. Ferrari, A new microarray substrate for ultra-sensitive

genotyping of KRAS and BRAF gene variants in colorectal cancer, PLoS one, 8 (2013) e59939.

[23] L.A. Tortajada-Genaro, R. Puchades, A. Maquieira, Primer design for SNP genotyping based on allele-specific amplification—Application to organ transplantation pharmacogenomics, J. Pharm. Biomed. Anal. 136 (2017) 14-21.

[24] O. Piepenburg, C.H. Williams, D.L. Stemple, N.A. Armes, DNA detection using recombination proteins, PLoS Biol. 4 (2006) e204.

[25] Santiago-Felipe, S., Tortajada-Genaro, L. A., Morais, S., Puchades, R., & Maquieira, Á. Isothermal DNA amplification strategies for duplex microorganism detection. Food Chem. 174 (2015) 509-515.

[26] Y. Liu, T. Lei, Z. Liu, Y. Kuang, J. Lyu, Q. Wang, A Novel Technique to Detect EGFR Mutations in Lung Cancer, Int. J. Mol. Sci. 17 (2016) 792.

[27] S. Santiago-Felipe, L.A. Tortajada-Genaro, S. Morais, R. Puchades, A. Maquieira, One-pot isothermal DNA amplification–Hybridisation and detection by a disc-based method, Sens. Actuators B Chem. 204 (2014) 273-281.

[28] A. Bhattacharyya, C.M. Klapperich, Mechanical and chemical analysis of plasma and ultraviolet–ozone surface treatments for thermal bonding of polymeric microfluidic devices, Lab Chip, 7 (2007) 876-882.

[29] Y. Li, Z. Wang, L.M. Ou, H.Z. Yu, DNA detection on plastic: surface activation protocol to convert polycarbonate substrates to biochip platforms, Anal. Chem. 79 (2007) 426-433.

[30] R. Patel, A. Tsan, R. Tam, R. Desai, J. Spoerke, N. Schoenbrunner, T.W. Myers, K. Bauer, E. Smith, R. Raja, Correction: Mutation Scanning Using MUT-MAP, a High-Throughput, Microfluidic Chip-Based, Multi-Analyte Panel, PLoS one, 8 (2013) 10-1371.

Supplementary information

Recombinase polymerase amplification for mutation analysis of *PIK3CA* gene

Sara Martorell, Sarai Palanca, Ángel Maquieira, Luis A. Tortajada-Genaro

Table S1.1: Summary about mutational information of PIK3CA gene: exon 9 and 20.

Exón	Mutation (Nucleotide)	Mutation (Amino Acid)	Mutation ID (COSMIC)	Count	Mutation Type	Rs
9	c.1624G>A	p.E542K	COSM760	960	Substitution	121913273
	c.1624G>C	p.E542Q	COSM17442	12	Substitution	
	c.1633G>A	p.E545K	COSM763	1524	Substitution	104886003
	c.1633G>C	p.E545Q	COSM27133	41	Substitution	
	c.1634A>C	p.E545A	COSM12458	188	Substitution	121913274
	c.1634A>G	p.E545G	COSM764	107	Substitution	
	c.1634A>T	p.E545V	COSM27155	5	Substitution	
	c.1635G>A	p.E545E	COSM1716554	1	Substitution	121913275
	c.1635G>C	p.E545D	COSM27374	16	Substitution	
	c.1635G>T	p.E545D	COSM765	15	Substitution	
20	c.3139C>A	p.H1047N	COSM5029129	1	Substitution	121913281
	c.3139C>T	p.H1047Y	COSM774	75	Substitution	
	c.3140A>C	p.H1047P	COSM249874	2	Substitution	121913279
	c.3140A>G	p.H1047R	COSM775	2115	Substitution	
	c.3140A>T	p.H1047L	COSM776	307	Substitution	
	c.3141T>A	p.H1047Q	COSM1041525	5	Substitution	-
	c.3141T>G	p.H1047Q	COSM24714	7	Substitution	

Gene: http://www.ncbi.nlm.nih.gov/gene/5290

Table S1.2: List of tested oligonucleotides.

Exon	codon	Use	Sequence 5'-3'
9	542-545	FP	AGCTCAAAGCAATTTCTACACG
		FP-clam	ATTTCTACACGAGATCCTCTCT
		RP	DIG-CTCCATTTTAGCACTTACCTGT
		B	TCTCTGAAATCACTGAGCAGGAGA-23ddC
		Wild-type	NH_2-C6-TTTTT-CTCTCTGAAATCACTGAGCAGGA
		p.E542K	NH_2-C6-TTTTT-CTCTCTCTAAAATCACTGAGCAG
		p.E545K	NH_2-C6-TTTTT-CTCTCTGAAATCACTAAGCAGGA
		p.E545A	NH_2-C6-TTTTT-TCTCTGAAATCACTGCGCAGGA
		p.E545G	NH_2-C6-TTTTT-TGAAATCACTGGGCAGGAGAAA
20	1047	FP	CTGAGCAAGAGGCTTTGGAG
		FP-c	TTTGGAGTATTTCATGAAACAAATG
		RP	DIG-TGTGTGGAAGATCCAATCCATT
		B	TGAATGATGCACATCATGGTGGCT-23ddC
		Wild-type	NH_2-C6-TTTTTTTTTT-AATGATGCACATCATGGTGGCT
		p.H1047R	NH_2-C6-TTTTTTTTTT-ATGATGCACGTCATGGTGGC
		p.H1047L	NH_2-C6-TTTTTTTTTT-AATGATGCACTTCATGGTGGCT
		p.H1047P	NH_2-C6-TTTTTTTTTT-ATGATGCACCTCATGGTGGC
		RP	FAM-TGTGTGGAAGATCCAATCCATT

FP: upstream or forward primer; FP-c: clamp forward primer; RP: downstream or reverse primer; B: blocker; p: probe; DIG: digoxigenin; 23ddC: 2',3'-dideoxyC functionalization.

Table S1.3: Estimated free energy variation (kcal mol^{-1}) for the formation of DNA complexes between probes and templates. The bold numbers correspond to perfect-match complexes.

		Templates				
	Probes	**Wild-type**	**p.E542K**	**p.E545K**	**p.E545A**	**p.E545G**
Exon 9	Wild-type	**-22.1**	-18.7	-18.6	-19.7	-17.9
	p.E542K	-17.5	**-21.3**	-14.0	-15.0	-14.1
	p.E545K	-17.6	-14.0	**-21.4**	-16.8	-16.6
	p.E545A	-16.7	-15.1	-13.8	**-22.1**	-16.2
	p.E545G	-17.9	-16.3	-15.4	-18.9	**-21.4**

		Templates			
	Probes	**Wild-type**	**p.H1047R**	**p.H1047L**	**p.H1047P**
Exon 20	Wild-type	**-22.4**	-18.5	-19.0	-20.0
	p.H1047R	-19.0	**-22.2**	-18.3	-18.8
	p.H1047L	-19.5	-19.0	**-22.3**	-19.7
	p.H1047P	-17.2	-16.6	-16.9	**-21.7**

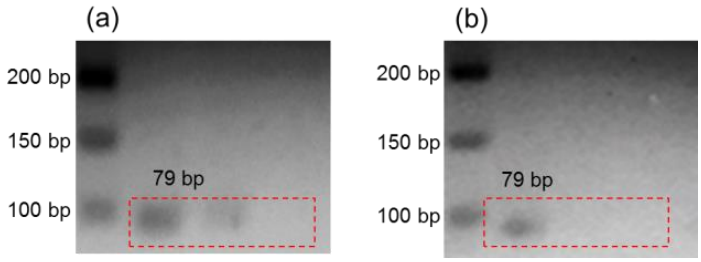

Fig.S1.1: Images of agarose gel electrophoresis after amplifying *PIK3CA* gene exon 20: (a) PCR products and (b) RPA products after centrifugation-based purification. 1: Ladder, 2: Without blocking agent, 3: Blocker at 50 nM, 4: Blocker at 300 nM. Sample: Wild-type template (human cell line).

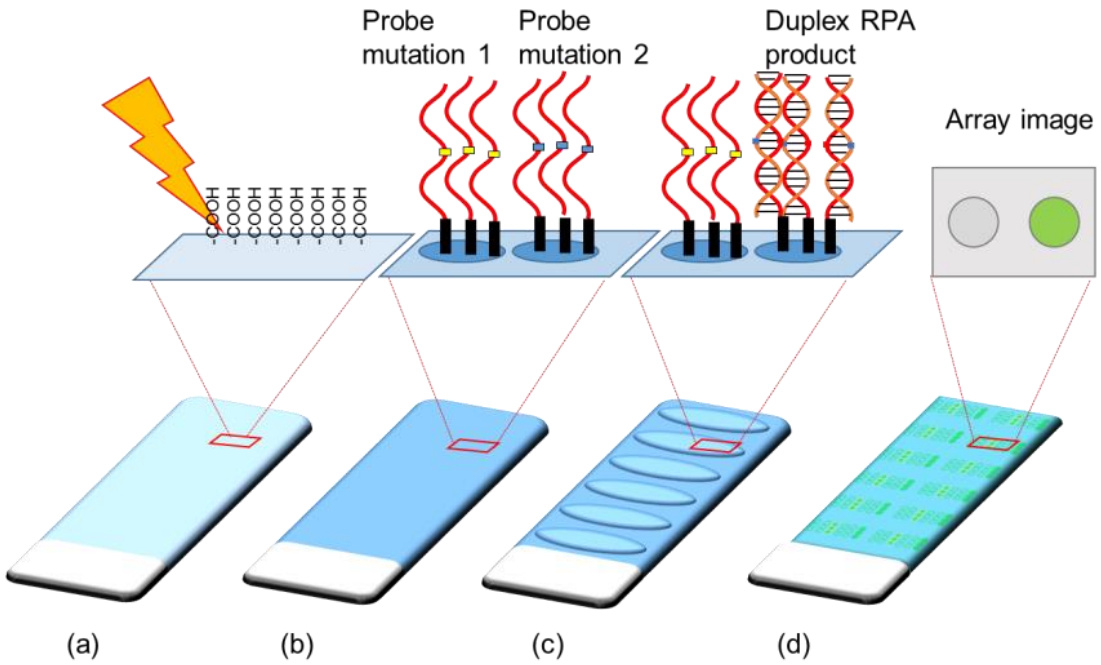

Fig.S1.2: Identification of mutation based on chip hybridization assay: (a) Surface activation (photochemical treatment), (b) immobilization of probes (amide bond formation), (c) incubation with RPA products, (d) image developing.

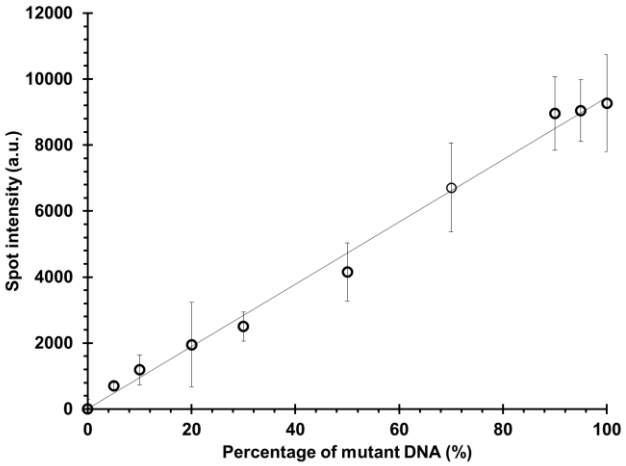

Fig. S1.3: Spot intensity of array probe for mutation p.H1047R obtained from different concentrations of mutant DNA. Target region: exon 20. Sample: cell culture HCT 116. Linear model: y = (94±3) x + (10±160), R^2 = 0.994. Limit of detection: 5.1

Capítulo 2

Concentración magnética de productos alelo-específicos obtenidos mediante amplificación por recombinasa-polimerasa

Resumen

El capítulo 2 se centró en la integración del ensayo de hibridación del producto de la RPA-bloqueada con sondas alelo-específicas conjugadas a partículas magnéticas en un chip termoplástico de canales microfluídicos, diseñado para el ensayo simultáneo. Para ello, se conjugaron sondas alelo específicas a partículas magnéticas funcionalizadas covalentemente. Esto permitió avanzar en la miniaturización y automatización del proceso de hibridación en chips de cicloolefina (COP). El sistema incorpora imanes permanentes para controlar la agregación de dsDNA y partículas magnéticas.

Con el desarrollo de este genosensor portátil, se consiguieron reducir los tiempos de hibridación a 20 minutos, así como los volúmenes de reacción de amplificación y de la mezcla de hibridación un 50%, en comparación con el ensayo en formato heterogéneo. Dado que cada chip dispone de 8 microcanales fluídicos paralelos, se pudo hacer un diagnóstico múltiple en formato test-line de pacientes sanos y mutantes que presentaban mutación en el codón 12 del gen *KRAS*, a partir de muestras complejas procedentes de tejidos incluidos en parafina. Los resultados fueron comparados con productos de PCR bloqueada consiguiendo resultados equiparables. Sin embargo, la plataforma basada en amplificación bloqueada isoterma no necesitó de ciclos térmicos, lo que es una ventaja al reducir tiempos de reacción y consumo energético.

Analytica Chimica Acta 1092 (2019) 49–56

Contents lists available at ScienceDirect

Analytica Chimica Acta

journal homepage: www.elsevier.com/locate/aca

Magnetic concentration of allele-specific products from recombinase polymerase amplification

Sara Martorell [a, b], Luis A. Tortajada-Genaro [a, b, c, *], Ángel Maquieira [a, b, c, **]

Abstract

The studied challenge is the specific detection of low-abundant genomic variants that differ by a single nucleotide from the wild type. The combination of blocked recombinase polymerase amplification (RPA) and selective capture by probes immobilised on magnetic-core particles integrated into a flow system is presented. The sensing principle was demonstrated as the effective concentration-detection of the specific generated products was achieved. The analytical performance of resulting assay was successfully compared to PCR-based methods or array formats, providing faster effective detection of the selective products. As proof of concept, the single-nucleotide substitutions of the *KRAS* gene at codon 12 were studied in chip with parallel microchambers and permanent magnets. The blocked RPA products (generated at 37 °C) from tumour biopsies (extracted DNA 4 ng) provided a specific fluorescent bead-line that depends on the present mutation. The results agree with those reported by next-generation sequencing and provide new opportunities for *in vitro* diagnostic and personalised medicine.

Keywords: isothermal amplification; magnetic beads; in-chip hybridization; DNA genotyping; optical biosensing

Introduction

Molecular technologies has advanced the identification of the genomic diversity and their role in human diseases [1]. Implementing a personalised approach into patient care needs fast-response methods that are cost-effective and compatible with low-resource settings to solve the limitations of technically skilled personnel and specialized infrastructures. Early diagnostics reduces disease effects and health-care expenses. A conventional methodology relies on the selective recognition of the sequence-specific oligonucleotides on active electrodes or passive planar chip surfaces, and subsequent signal transduction in integrated microsystems [2]. Another successful approach is based on oligonucleotide-coated particles, which involves fewer technical requirements, a bigger surface area, easy chemical modification and effective mixing with samples [3,4]. Micro-sized magnetic beads have been the most extensively applied in diagnostic chips as the external magnetic field (electro-magnets, coils or permanent magnets) controls their movement [4,5]. The selective magnet-induced isolation of the molecules captured to particles improves the assay selectivity and sensitivity [6]. Furthermore, these assays reduce both volumes of reagents and samples and cuts the time required for target molecules to diffuse to the interrogating probes [7]. Their use has enabled well-established protocols for the simplified extraction, amplification and detection of nucleic acids. Thus the microfluidic systems yield a platform that facilitates the rapid and automated DNA analyses [8,9].

One common limitation of these methods is that the need for a DNA amplification step to achieve a copy number big enough to be detected. The consequences are complex platforms for DNA-based diagnostic tools with a high demand for the auxiliary instrumentation. To overcome some of these drawbacks, several isothermal techniques have been developed, and their integration into microsystems or portable devices has improved nucleic acid-based on-site assays [10]. Probe-conjugated magnetic beads have recognised specific templates from clinical sample lysates and are later amplified by either loop-mediated isothermal amplification (LAMP) [11] or rolling circle amplification (RCA) [12]. Regarding to detection, promising

assays combine a linear RCA-type amplification and later particle aggregation [13]. However, other enzymatic methods can potentially perform better (e.g. high yield, exponential reaction kinetics, lower temperature). Recombinase polymerase amplification (RPA) is an unexplored candidate, despite being one of most sensitive and selective isothermal techniques, with excellent operational conditions for integrated devices [14].

We herein firstly report research that focused on the selective capture of RPA products onto probe-conjugated microbeads confined within a microfluidic channel and using a permanent magnet. This challenge spans from the impact on the hybridisation kinetics and to the assay integration, and includes the dynamics during magnetic-concentration. Due to the amplification mechanism, the nature of the RPA mixture is complex and an influence on the detection of the generated products compared to PCR or other isothermal techniques was expected, as reported previously [15].

The aim of the presented approach is the concentration of allele-specific products from RPA using magnetic beads for the sensitive identification of single-point mutations. The detection of these variations in the genome is important because they have been associated with disease progression and treatment efficiency [16]. Although some examples describe the discrimination of single-nucleotide mismatches based on allele-specific hybridisation to probes anchored on magnetic beads [8,17,18], they all are restricted by the PCR amplification technique. For achieving the challenge of specific discrimination, an affordable fast-response method was developed, based on blocked isothermal amplification, bead-based hybridization, magnetic concentration and optical detection. Our empirical goal was to establish the principles and experimental conditions for the differential capture and detection of the RPA products in a microfluidic system. In case of a correct discrimination of single-base variants, patients could be classified in the adequate group and the suitable treatment could be applied as personalised medicine.

Experimental

Chip assembly

The micro-system was composed of a supporting platform and microfluidic chips that enable the simultaneous analysis of eight samples. The 3D-printted platform, designed using the CAD-3D Autodesk inventor (Autodesk, USA), was manufactured in polylactic acid (PLA, RS Components, UK). The printing technology was fused filament fabrication (The Ultimaker Cura 2, Ultimaker, Netherlands). The printing parameters were: nozzle 0.4 mm; layer height 0.1 mm; infill density 100%; print speed 60 mm/s; travel speed 120 mm/s; print temperature 210 °C and bed temperature 60 °C. Eight neodymium magnets (dimensions 2.2×0.5×5 mm, vertical force 0.1 kg, slip resistance 0.02 kg) were integrated. The microfluidic chip, manufactured in cyclic olefin polymer, contained eight 20 µL-rhombic chamber reactors (ChipShop, Germany). The dimensions of each chamber were 4 mm×13.8 mm×0.35 mm. The chip was aligned to the platform by placing the magnets below the middle of the chip.

Target

As proof of concept, the method was developed to analyse hotspots in the *KRAS* gene. Single-base substitutions of this oncogene are extensively investigated as genetic markers in human cancer pathogenesis and therapies [19]. We specifically identified the most frequent mutations (codon 12), which were p.G12C (c.34G>T, rs121913530), p.G12S (c.34G>A, rs121913530) and p.G12V (c.35G>T, rs121913529). Primer and probes were designed by considering the thermodynamic parameters of recognition process. Bioinformatic tools (OligoCalc software, Northwestern University, USA) reported that the selected sequences were unlikely to form internal hairpin structures, self-dimers or heterodimers. The used oligonucleotides were supplied by Eurofins (Germany).

Conjugation of particles

A set of magnetic-core particles coated with probes (wild-type and mutants p.G12C, p.G12S and p.G12V) were prepared. The selected particles were Dynabeads MyOne carboxylic acid (Invitrogen, NY, USA). Beads (7.12×10^8) were washed with 2-(N-morpholino)-ethanesulfonic acid buffer (MES, 100 mM, pH 4.8) (Sigma-Aldrich) for 30 min (2 times) and resuspended. A total of 0.6 nmol amino-modified probe (NH_2-C_6-T_5-AGTTGGAGCTNGTGGCGTAGG, N = A, C, T or G) in MES buffer with ethyl carbodiimide hydrochloride (1.25 M) was added and incubated (overnight, room temperature). Then beads were washed 3 times with Tris-Tween buffer (1 M of Tris 1 M, 10 % of Tween 20, pH 8) and suspended in Tris-EDTA buffer (1 M of Tris, 100 mM of EDTA, pH 8). Functionalisation efficiency was quantified by determining the probe excess in relation to its initial concentration (absorbance at λ=260 nm).

DNA extraction and amplification

For the optimisation assays, two cell cultures were used, cell line SK-N-AS (ATCC, wild-type for *KRAS* codon 12) and cell line HCT 116 (ATCC, c.38G>A), from a primary carcinoma tissue. For method validation, healthy and oncological patients were recruited for the present study according to ethics regulations. QIAcube robotic workstation (Qiagen, Germany) extracted genomic DNA from 5-µm thick formalin-fixed paraffin-embedded tissue sections. The used reagents were mini kit FFPE Qiagen. The concentration of the DNA extracts (ng μL^{-1}) was obtained by spectrophotometry using NanoDrop 2000c (ThermoFisher Sci., USA), and by fluorimetry using Qubit dsDNA HS Assay Kit (ThermoFisher Sci.).

The reagents used for the genomic DNA amplification came in the TwistAmp Basic RPA kit (TwistDx, UK). The mixtures (50 µL) for the blocked isothermal amplification were prepared with the enzyme pellet in rehydrated buffer, 480 nM of magnesium acetate, 480 nM of upstream primer and downstream primer, 70 nM of blocking agent, 4 ng of genomic DNA, 0.01 mM aminoally-dUTP-Cy5. The employed

heating system was an Eppendorf Thermomixer with MTP adapter (300 rpm, Eppendorf), operating at 37 °C for 40 min. Also, real time thermocycler (TS2, Qiagen) was used for the optimisation assay. The reaction mechanism is described in Fig. S2.1.

In-chip assay

The amplification products (2 μL) were mixed with 18 μL of hybridisation buffer (1x saline sodium citrate buffer, 30% formamide), containing beads conjugated with each specific probe (final concentration 7.12×10^5 beads μL^{-1}). Solutions were loaded to chip by a pressure-driven flow (20 μL, < 3 s) (Fig. S2.2). Incubations were run at 95 °C for 10 min (denaturation) and at 37 °C for 30 min (hybridisation). Then, the magnets retained the magnetic particles inside each reaction chamber to enable the total removal of the supernatant. The reactor was washed with 20 μL of 0.01% SSC buffer (SSC 1×: 150 mM sodium chloride-15 mM trisodium citrate pH 7.3).

A surface fluorescence reader imaged the bead-line in each reactor. This detector was equipped with a high sensitivity charge coupled device camera (Retiga EXi, Qimaging Inc., Canada), with light emitting diodes (Toshiba TLOH157P, Japan) and filters (λ_{ex} 635 nm, λ_{em} 670 nm). Intensities were also compared to those obtained by fluorescence microscopy (Leica DCF 3000G, Germany). Image processing (segmentation and quality assurance) was performed by reporting the bead-line and background intensities (mean and standard deviation).

A discrimination factor was calculated to assign each patient to a genetic population (wild-type, p.G12C, p.G12S or p.G12V). Specifically, the factor for a given population was the relative response of the corresponding probe-conjugated bead in relation to all the beads. The patient was assigned to the group with the highest discrimination factor.

Reference methods

Hybridisation on chip (colorimetric chip detection). The RPA products were detected and identified by a hybridisation assay on rectangular slides (25 mm×75 mm). The protocol is described in a previous paper [20]. Briefly, amine-DNA probes were immobilised on a modified plastic chip. The format was four arrays per chip and four replicates per target.

The amplified products (5 µL) were mixed with 45 µL of hybridisation buffer, heated (95 °C, 5 min) and dispensed onto sensing arrays. After incubation (37 °C, 60 min), the arrays were rinsed with progressive dilutions of hybridisation washing buffer. After performing the colorimetric staining chip, the results were read.

Sequencing. Somatic mutations detection was performed by the Ion Torrent PGM technology (ThermoFisher Scientific). The Oncomine Solid Tumor DNA kit enabled the simultaneously analysis of hotspots mutations in 22 genes (included *KRAS* gene). A multiplex PCR amplification of 10 ng of genomic DNA generated the DNA barcoded libraries. The data from the sequencing runs were aligned to the hg19 human reference genome and variant calling.

Results and discussion

Bead capture and concentration of RPA products

After an isothermal DNA amplification, the specific isolation of the products was studied, based on the selective hybridisation onto beads and their magnetic concentration. A relevant variable was the probe amount immobilised onto the magnetic-core particles. Conjugation was performed to obtain optimal surface-probe density to maximise hybridisation efficiency (probe density about 10^{12} molecules cm^{-2}). The selected relationship between the 5'-amino-labelled probes and the carboxylic-functionalized particles (1 µm diameter) was 8.4×10^{-19} moles per particle. Thus, an

important of probe excess was needed compared to the particle surface area (3.14×10^{-8} cm^2).

The number of probe-conjugated particles and the washing protocol are relevant parameters for the hybridisation of DNA to the bead-immobilised probes confined within a microfluidic channel [6,7,9]. Specific experiments were performed to establish the best assay conditions. Fig. 2.1 shows that by increasing the bead number, the signal and the area occupied by the magnetic particles in the reaction chamber were, respectively, more intensive and bigger until saturation. The selected amount was 14.2×10^6 of probe-conjugated beads for a rhombic chamber chip of 20 μL. A stringent hybridisation buffer (low ionic strength buffer, high formamide content) favoured the perfect-match bonds and reduced non-specific interactions. By increasing the number of wash cycles, the percentage of the captured beads was lower. Also, the linear decreases in the bead-line signal were observed for both single-strand DNA and RPA product, being higher for the double-strand DNA. The results revealed a loss of particles despite of magnet action and a major denaturation for the amplification products, respectively. Thus, the method succeeded in controlling the hybridisation and washing conditions and yielded a final concentration factor that ranged between 1:8 and 1:10.

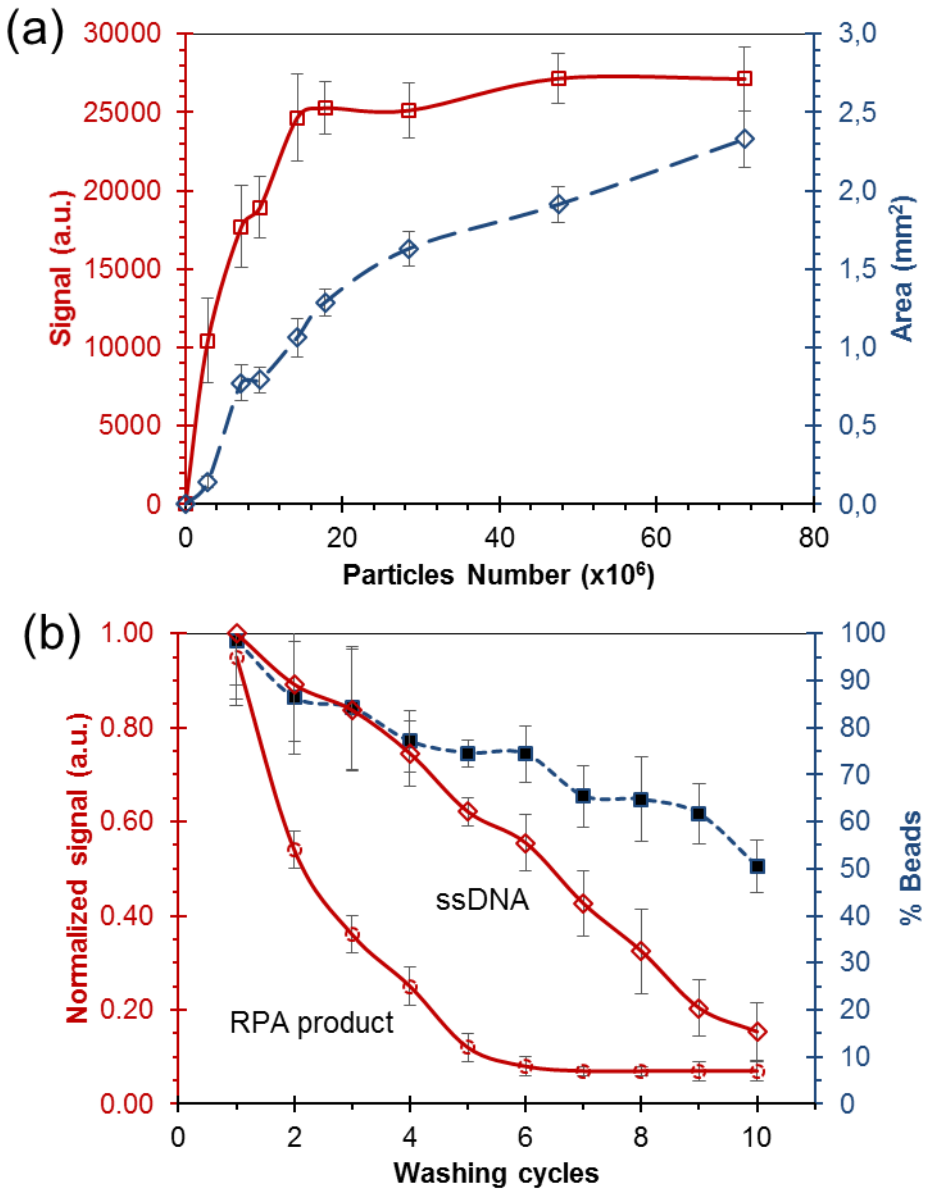

Fig. 2.1 (a) Effect of the number of particles on the hybridisation reaction. (b) Effect of wash cycle on the hybridisation reaction. Replicates = 3.

Under those experimental conditions, the hybrids RPA product/probe were formed at low temperature (37 °C, about 20°C lower than the melting temperatures) for a short period (30 min). After applying the magnetic field and washing, the particle aggregation was induced and a packed bead-line was observed with a width of about 0.8 mm (Fig. S2.3). Null and low responses, comparable to those obtained for an empty microchamber, were observed for the probe-free particles and the non-complementary probe-conjugated particles, respectively. Thus, the method was reliable because

significant fluorescent responses were recorded only in the microchambers with the particles conjugated with the complementary probes. Replicate experiments also confirmed that the method was reproducible, obtaining a relative standard deviation of 15-20 %. Regarding the sensitivity, the estimated detection limit was 250 copies of genomic DNA from biopsy tissue.

Comparison with PCR-based method

The proposed assay demonstrated a relevant potential for detecting DNA templates and for being integrated onto point-of-care genetic platforms. The following experiments were focused on the performances of the isothermal and the PCR-based approach [5,7,9]. The results showed that the capture yields (>90 %) were similar between RPA products and PCR products, but the magnetic-induced concentration differed depending on the employed amplification technique (Fig. 2.2). The movement of beads with PCR products to the magnet zone was effective at 15 s, while the beads with RPA products needed 60 s and external flushing. This behaviour was related to the differences of reaction composition of both enzymatic DNA amplifications. The RPA formulation contained a high-molecular-weight polyethylene glycol (PEG) and crowing agents, used to facilitate isothermal amplification and to reduce the mixing effects of thermal convection during the reaction run at low temperatures [14]. However, these components negatively affected the bead-based assay. In high-viscosity fluids like RPA media, the balance between the drag (viscous resistance) and magnetic force leaded to a lower particle velocity. Some groups of beads were aggregated through the microfluidic channel, slowing down the bead-concentration towards the magnet. Nevertheless, the magnetic-field-induced concentration of the RPA products was robust and effective in terms of the final amount of beads over the magnet.

Other analytical performances, such as reproducibility, sensitivity and hybridization selectivity were also similar. As expected, the main advantages of RPA derived from their isothermal nature, such faster response (i.e. amplification 30 min RPA vs. 90 min PCR) and minimal auxiliary instruments (i.e. unnecessary thermal cycler).

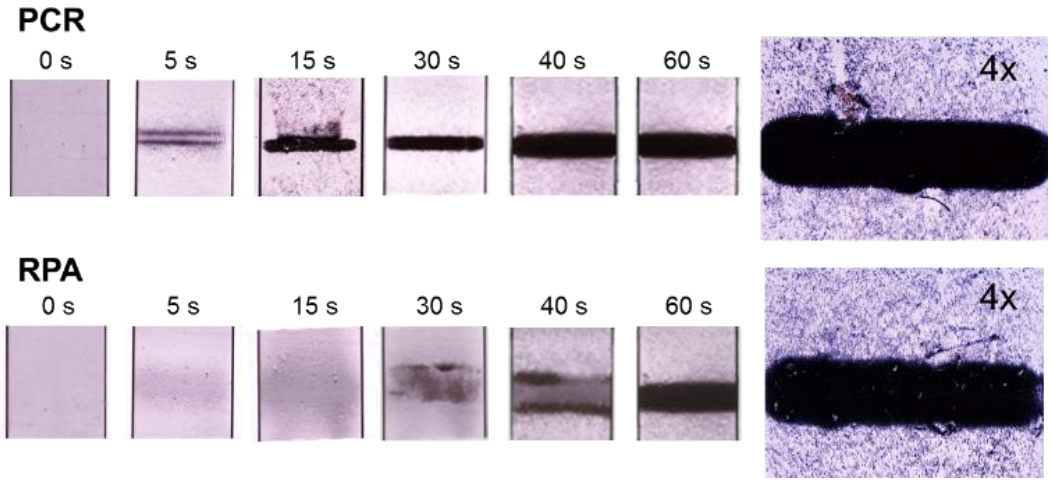

Fig. 2.2 Sequential micrography of the magnetic-field-induced bead concentration into the microfluidic chip, depending on the used amplification technique. Magnification factor: 10×. Target: wild-type variants of KRAS gene.

Comparison with the planar chip format

The performances of homogeneous hybridisation on the magnetic particles in the microfluidic chamber chip was also compared against a conventional approach based on a heterogeneous format (array in chip) [2,20].

The hybridisation kinetics of RPA products at 37 °C were examined (Fig. 2.3a). A saturation-type curve was obtained at the 30-minutes incubation time for the assay based on magnetic beads in the microfluidic device, with 50 min for planar chip assays. The observed behaviours matched to the Lagmuir model for DNA hybridisation [21], described by the following equation:

$$x(t) = x_{eq}[1 - \exp\left(-\frac{t}{\tau}\right)]$$

where x(t) is the time dependent hybridisation fraction, x_{eq} the equilibrium hybridisation fraction and τ is related to the hybridisation rate constant (including the denaturation correction).

The estimated half-life times (τ-values) were 48.2 min for the planar chip format and 14.8 min for the bead-based format with regression coefficients of 0.960 and 0.997, respectively. Thus, the hybridisation process of the RPA amplification products was faster with the probes immobilised on beads than on chip. The cause of these differences were examined. The estimated immobilization densities of specific probes were similar, being 1-5 pmol cm^{-2} for magnetic beads and 2-6 pmol cm^{-2} for plastic chip. Also, the number of binding sites, calculated from the active areas in both approaches, was comparable. However, there are important differences in the reaction nature. In a planar chip, the transportation process of target molecule for the bulky solution to the surface must be considered, delaying the time required until the saturation. A homogeneous format (i.e. solid-liquid interface) would need much longer time compared to the heterogeneous format (i.e. liquid) [22].

For DNA-based diagnostic or prognostic, tests need to display high sensitivity because numerous applications involve the detection of the target sequence present in small copy numbers. To explore this detection capability, dilution experiments were performed, using the amplification products obtained from genomic DNA. Fig. 3b shows that the data fitted to a logistic response curve (regression coefficients 0.990-0.993). The limits of detection, defined as the target amount and statistically differed from the negative controls, were a dilution factor of RPA products about 1:200. These results agreed with the lower hybridisation yields expected for the amplification products by considering the competiveness between the probe and the complementary strand for the same target strand [5,7,15]. Assay reproducibility, obtained from replicate experiments and expressed as relative standard deviation, ranged between 5% and 15%. The calibration curves were similar for the homogeneous and heterogeneous formats (equation parameters, t-test p-value >0.05, F-test p-value >0.05), which confirmed the feasibility of the developed analytical approach.

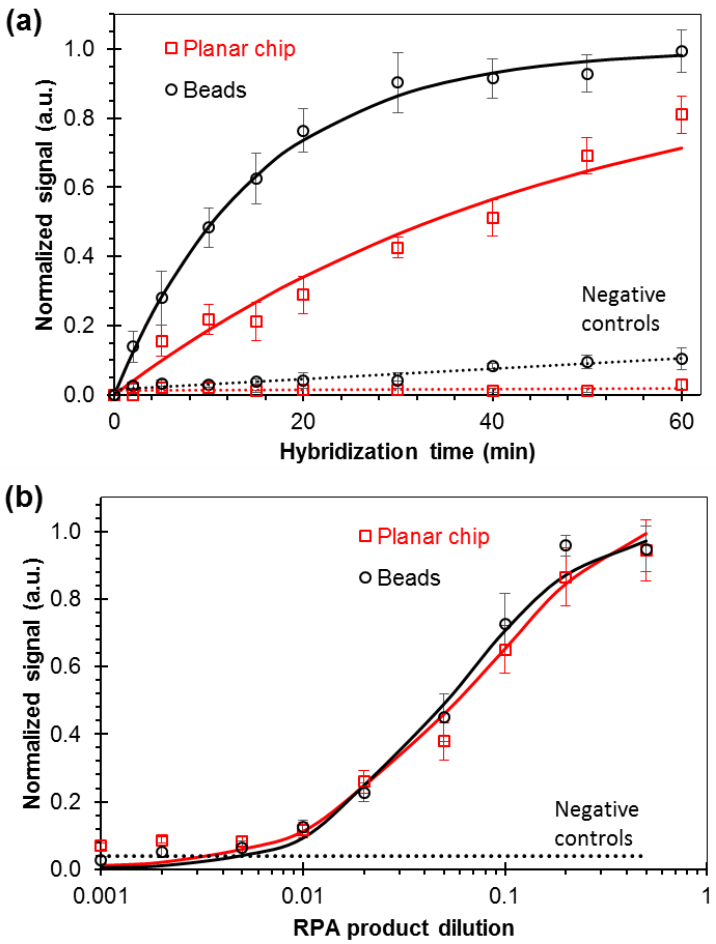

Fig. 2.3 Comparison of planar chip and bead formats. a) Effect of hybridisation time on fluorescence signal. Fitting curve: $y = a \cdot (1-e^{-x/b})$. b) Influence of the number of copies on fluorescence intensity. Incubation time: 60 min for the planar chip and 30 min for beads. Fitting curve: $y = L/(1 + a \cdot e^{-b*x})$.

Enrichment of mutant variants

As proof of concept, the RPA-particle concentration method was applied in the challenging filed of the detection of sequence changes. In case of single nucleotide variations, a high-selective amplification approach prior to the detection was required because the mutant variants must be identified in a wild-type genomic DNA background. A novel method for the preferential amplification of minority mutations before the magnetic-based concentration was studied, called blocked RPA [20]. The hypothesis was that the enrichment of these variants against the wild-type strand could induced, based

on the addition of a blocking oligonucleotide to the RPA reaction solution, improving the latter on-bead hybridization.

The first stage was to select a wild-type blocker following a design criteria based on an RPA mechanism and from the calculated thermodynamic properties. In order to reduce the amplification in the primer annealing step, one restriction was for the blocker candidates to partially overlap the upstream primer (clamp effect). This design avoids the strand-displacing activity of the polymerase used in RPA (Bsu polymerase) if the primer was bond to the template.

Moreover, the position of the hotspot in the blocking agent sequence drastically varied the estimated stability of the mismatched hybrids. A central position allowed a variation in free energy to lower between 1.5 and 1.7 $\times$ 10^5 J mol^{-1} for the single-nucleotide mutations (Fig. 2.4). According to these values, the blocker would compete with the upstream primer for the same site in the wild-type strand. The DNA extracts from control/mutant cell lines were amplified in the presence of the blocker (0-400 nm) by the PCR and RPA approaches in solution format. If the blocking agent was absent, there were no differences between the yield amplification of the wild-type and the mutant templates (10^7-10^8, test t: p=1.0). By increasing the concentration, the end-point responses decreased in both mixtures. The experimental data were fitted to a four-parameter logistic equation:

$$Signal = d + \frac{a - d}{1 + \left(\frac{[bloq]}{c}\right)^b}$$

where [bloq] is the blocking agent concentration, d is the background signal, a is the signal for the lack of the blocking oligonucleotide, c is related to the concentration at the inflection point and b is related to curve steepness. The c-parameter was related to the effective blocking concentration that reduced the signal to half. The values were 46±7 and 160±30 for the wild-type and mutant templates, respectively. Thus adding the blocker led to a selective reduction in amplification, and showed that the blocker was preferentially hybridised onto the wild-type strand than onto the mutant. The selected concentration was 70 nm (stoichiometric ratio of 1:7 compared to the upstream primer)

because the biggest differences were observed at this concentration. The experiments also confirmed that the chain terminator, dideoxycytidine included in the 3'-end blocker, avoided its undesired extension by polymerase action.

These results were confirmed from the kinetics measurements in vials (Fig. 2.4). When the blocking agent was absent, a similar behaviour was observed for the wild-type and mutant solutions. Positive signals were observed after 5-10 min, and the maximum difference was achieved after 40 min of amplification. The addition of the oligonucleotide blocker preferentially inhibited the primer extension on the wild-type strands (a 40 % reduction) compared to the mutant variants (a 7% reduction).

(a)

	ΔG (J mol^{-1})
Wild-type	-1.08×10^5
p.G12C	-0.91×10^5
p.G12S	-0.94×10^5
p.G12R	-0.93×10^5

(b)

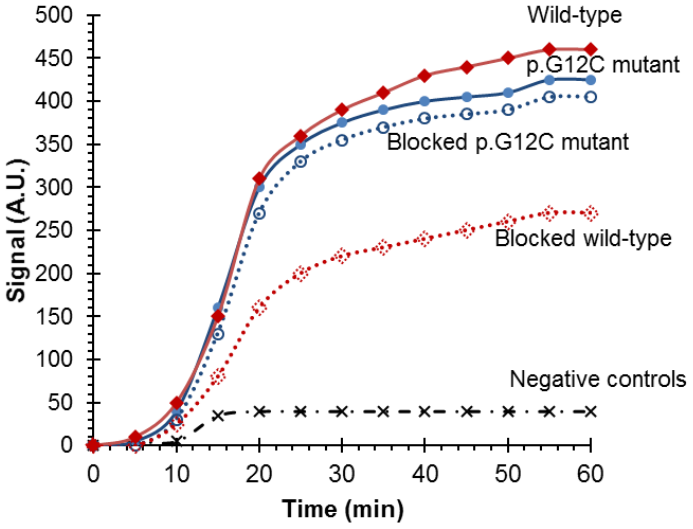

Fig. 2.4 Blocked RPA of *KRAS* hotspot: (a) Variation of the free energy associated with the formation of DNA duplexes (blocker-template) at 37ºC. (b) Real-time RPA amplification in the solution format using DNA extracts from the wild-type (◊), mutant (O) and negative control (×) samples in the presence of blocking agent at 0 nM (continuous line) and 70 nM (discontinuous line).

The versatility of method was examined, performing the enrichment of the mutant variants in three hotspots. The method was applied for the allele discrimination of *KRAS* (codon 12), *PIK3CA* (exon 9) and *PIK3CA* (exon 20). The reported data (gel electrophoresis, real-time fluorescence and solid-phase hybridization) confirmed that

blocked RPA is a reliable enrichment method, because wild-type DNA amplification was minimized while mutant DNA would be promoted to be amplified (Fig. S2.4 and 5). The products from blocked RPA were effectively isolated using magnetic-core particles coated with specific probes. A selective detection was achieved (Fig. S2.6), because the mutant variants provided a fluorescent bead-line with a higher signal-to-noise ratio than the wild-type variant (t-test, p-value <0.05).

The detection capability was quantified by mixing products from the mutant and wild-type genomic DNA incubated with both types of magnetic beads. To better evaluate cross-reactivity, a double labelling experiment was performed. The labelling fluorophores of dUTPs were 5-FAM and Cy5 for the wild-type and mutant RPA mixtures, respectively. Significant fluorescent responses were obtained only in the assay when the bead was conjugated to the complementary allele specific probe (Fig. 2.5). A relationship between the responses and mutation percentage was clearly established (Fig. S2.7), and demonstrated that it was possible to detect a small amount of mutant strands even in the presence of large amounts of the wild-type gene.

Bead-based identification of the mutant variants

The discrimination among several variants that only differ in a single nucleotide requires a selective recognition and isolation. Thus, the ability of selectively identifying each specific mutation for a particular hotspot was investigated (*KRAS* targets: wild-type, p.G12C, p.G12S, p.G12R). Blocked RPA products were aliquoted to different reactors of the microfluidic chip that contained specific probe-conjugated particles. So, the discriminating elements were spatially separated, but integrated into a single chip (parallel assay). Under the selected conditions, each variant provided a high response in the bead-line of the corresponding probe, whereas the responses associated with the other probes were significantly low (t-test, p<0.005). The comparison made with the heterogeneous assay confirmed the correct formation of a perfect-match hybrid between the RPA product and one specific probe (Fig. 2.6a). Therefore, these results

demonstrated a selective capture, an effective concentration and, consequently, an unequivocal identification (Fig. 2.6b).

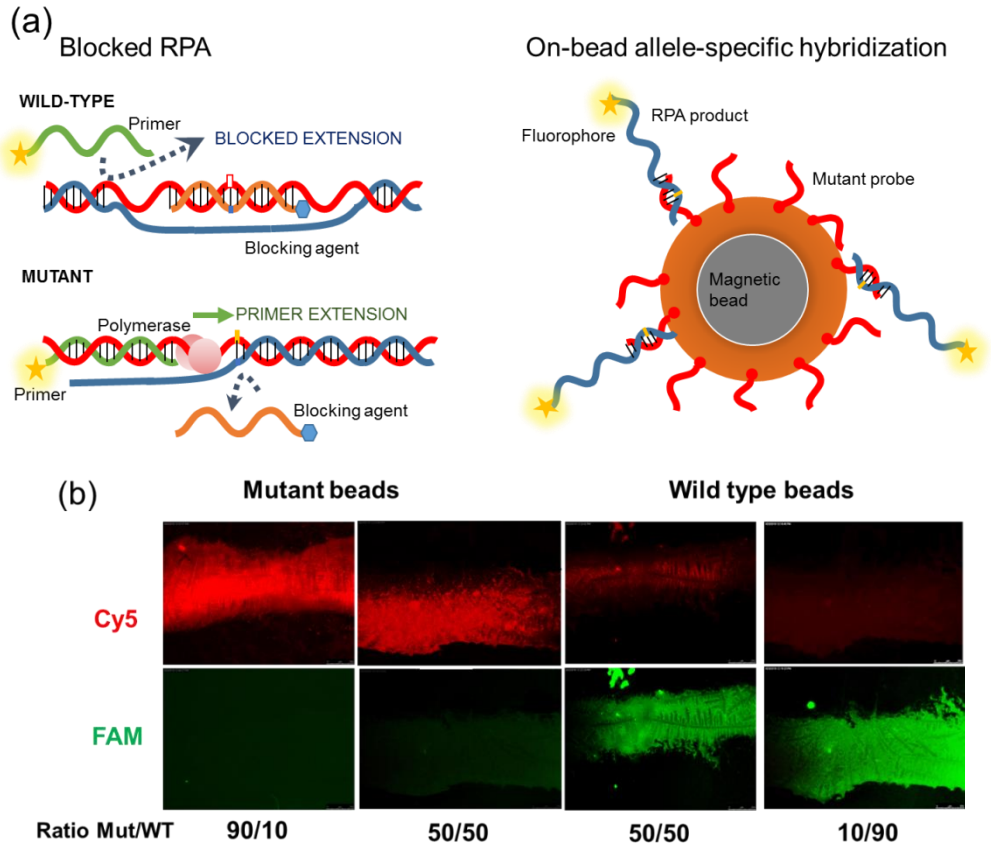

Fig. 2.5. Mutation discrimination based on the blocked isothermal amplification and the allele-specific capture and concentration to the probe-conjugated magnetic particles. (a) Reaction schemes. (b) Fluorescence images for Cy5 and FAM channels obtained by a three-variable experimental design: KRAS gene p.G12C mutant/wild-type ratio (M/WT), labelling method (Cy5-dUTPs: mutant RPA and FAM-dUTPs: wild-type RPA) and probe-conjugated bead nature. Magnification factor: 10×. Genomic DNA: 1,333 copies.

In a blind-assay, the developed method was applied to analyse the samples from the tumour biopsies (genomic DNA from formalin-fixed paraffin-embedded tissues). On-chip assay was parallelised for mutation detection and identification in a simple assembly (Fig. S2.8). Compared to the results obtained using the cell cultures, the inter-assay reproducibility for the tissue samples was about 2-folds worse (relative standard deviation: 20-25%) and non-specific responses were higher (30 %). Nevertheless, the population assignation was achieved by calculating of a discrimination factor based on

the relative responses for all the probe-conjugated beads (Fig. 2.6c). Four samples were classified as wild-type and six samples as p.G12C mutant. These genetic variant assignations agreed with the results reported by the reference method (next-generation sequencing). Therefore, the hybridisation of the RPA products from complex biological samples onto probe-conjugated microbeads confined within a microfluidic channel was satisfactorily demonstrated.

Several advantages have been identified compared to similar approaches for determining the mutational status of clinically relevant hotspots [6,23–25]. First, the amplification at a low constant temperature (37 °C, 60 min) allowed the analysis time and material resources to be reduced. Second, magnetic-induced formats are most useful for developing miniaturised sensors with enhanced assay sensitivity and exceptional selectivity (e.g. low-amount of DNA template, high concentration factor for detection, exhaustive washing). Third, there are several compatible detection principles for the cost-effective measurement of biosensing responses by enabling point-of-care genetic analyses. The developed system is aimed to fulfil the ASSURED requirements described by the World Health Organization: Affordable, Sensitive, Specific, User-friendly, Rapid & robust, Equipment-free, and Delivered.

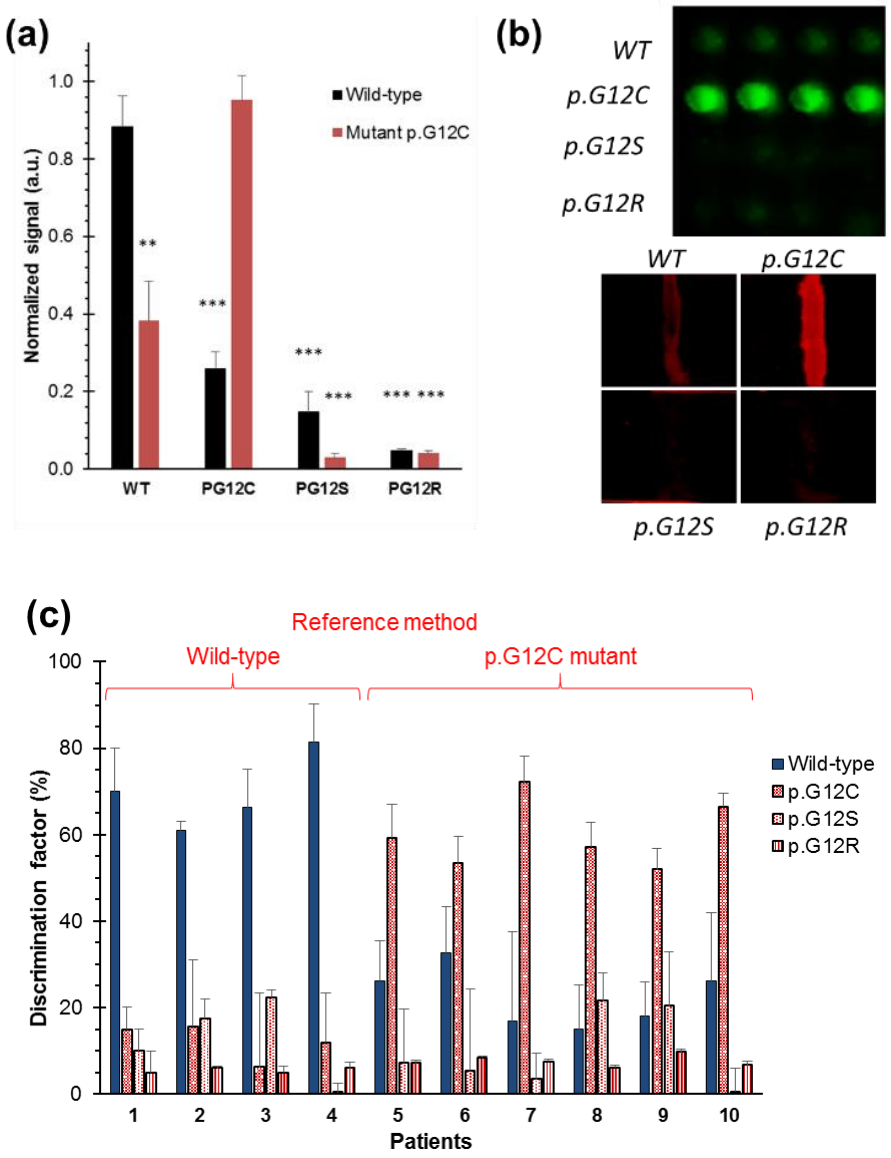

Fig.2.6. a) Normalised signal obtained for the probe-conjugated beads for a wild-type sample and a mutant sample (p.G12C). **: p-value < 0.005, ***: p-value < 0.0005. b) Image obtained for a mutant sample (p.G12C). Top: Planar chip format. Bottom: Bead format. c) Analysis of patient samples. Discrimination factor for each genetic variant was calculated from the bead-line responses. Samples were grouped based on next-generation-sequencing results.

Conclusions

In the last few decades, major progresses has been made in the DNA-based diagnosis field by applying probe-coated magnetic particles in microfluidic chips. One important pending challenge is to improve analytical performances for widespread exploitation, such as portability, fast-response and selectivity. The presented research addresses the problem by integrating an isothermal amplification technique. Our study shows that RPA fulfils the demanded requirements with excellent capabilities. The assay is performed at constant temperature, with fewer needs for auxiliary instruments and by keeping the concentration yields of the conventional PCR-based approach or other isothermal techniques.

Most of the similar published techniques have been applied to detect large regions (tens of nucleotides) or variants in synthetic templates. Collected evidence has endorsed that the presented approach is able to recognise low-abundant variants of single-nucleotide mutations in DNA from tumour tissues to support the clinical treatment.

As our results have been generated using a simple prototype, more efforts are required to achieve a fully-integrated device. Nevertheless, the study has demonstrated its efficiency, reliability and sensitivity, as well as it has provided insights into the development of innovative DNA diagnostic platforms.

Acknowledgements

The authors acknowledge the financial support received from the Spanish Ministry of Economy and Competitiveness (MINECO project CTQ2016-75749-R and Technical Support Personnel PTA- 2016).

References

[1] L.E. MacConaill, Existing and emerging technologies for tumor genomic profiling, J. Clin. Oncol. 31 (2013) 1815–1824. doi:10.1200/JCO.2012.46.5948.

[2] O.Y.F. Henry, C.K. O'Sullivan, Rapid DNA hybridization in microfluidics, TrAC - Trends Anal. Chem. 33 (2012) 9–22. doi:10.1016/j.trac.2011.09.014.

[3] J.P. Lafleur, A. Jönsson, S. Senkbeil, J.P. Kutter, Recent advances in lab-on-a-chip for biosensing applications, Biosens. Bioelectron. 76 (2016) 213–233. doi:10.1016/j.bios.2015.08.003.

[4] T. Jamshaid, E.T.T. Neto, M.M. Eissa, N. Zine, M.H. Kunita, A.E. El-Salhi, A. Elaissari, Magnetic particles: From preparation to lab-on-a-chip, biosensors, microsystems and microfluidics applications, TrAC - Trends Anal. Chem. 79 (2016) 344–362. doi:10.1016/j.trac.2015.10.022.

[5] S. Rödiger, C. Liebsch, C. Schmidt, W. Lehmann, U. Resch-Genger, U. Schedler, P. Schierack, Nucleic acid detection based on the use of microbeads: A review, Microchim. Acta. 181 (2014) 1151–1168. doi:10.1007/s00604-014-1243-4.

[6] T. Tangchaikeeree, D. Polpanich, A. Elaissari, K. Jangpatarapongsa, Magnetic particles for in vitro molecular diagnosis: From sample preparation to integration into microsystems, Colloids Surfaces B Biointerfaces. 158 (2017) 1–8. doi:10.1016/j.colsurfb.2017.06.024.

[7] A. Van Reenen, A.M. De Jong, J.M.J. Den Toonder, M.W.J. Prins, Integrated lab-on-chip biosensing systems based on magnetic particle actuation-a comprehensive review, Lab Chip. 14 (2014) 1966–1986. doi:10.1039/c3lc51454d.

[8] S. Wang, Y. Sun, W. Gan, Y. Liu, G. Xiang, D. Wang, L. Wang, J. Cheng, P. Liu, An automated microfluidic system for single-stranded DNA preparation and magnetic bead-based microarray analysis, Biomicrofluidics. 9 (2015) 1–17. doi:10.1063/1.4914024.

[9] V.F. Cardoso, A. Francesko, C. Ribeiro, M. Bañobre-López, P. Martins, S. Lanceros-Mendez, Advances in Magnetic Nanoparticles for Biomedical Applications, Adv. Healthc. Mater. 7 (2017) 1700845. doi:10.1002/adhm.201700845.

[10] Y. Zhao, F. Chen, Q. Li, L. Wang, C. Fan, Isothermal Amplification of Nucleic Acids, Chem. Rev. 115 (2015) 12491–12545. doi:10.1021/acs.chemrev.5b00428.

[11] C.H. Wang, K.Y. Lien, J.J. Wu, G. Bin Lee, A magnetic bead-based assay for the rapid detection of methicillin- resistant Staphylococcus aureus by using a microfluidic system with integrated loop-mediated isothermal amplification, Lab Chip. 11 (2011) 1521–1531. doi:10.1039/c0lc00430h.

[12] M. Kühnemund, D. Witters, M. Nilsson, J. Lammertyn, Circle-to-circle amplification on a digital microfluidic chip for amplified single molecule detection, Lab Chip. 14 (2014) 2983–2992. doi:10.1039/c4lc00348a.

[13] C. Lin, Y. Zhang, X. Zhou, B. Yao, Q. Fang, Naked-eye detection of nucleic acids through rolling circle amplification and magnetic particle mediated aggregation, Biosens. Bioelectron. 47 (2013) 515–519. doi:10.1016/j.bios.2013.03.056.

[14] I.M. Lobato, C.K. O'Sullivan, Recombinase polymerase amplification: Basics, applications and recent advances, TrAC - Trends Anal. Chem. 98 (2018) 19–35. doi:10.1016/j.trac.2017.10.015.

[15] S. Santiago-Felipe, L.A. Tortajada-Genaro, R. Puchades, Á. Maquieira, Parallel solid-phase isothermal amplification and detection of multiple DNA targets in microliter-sized wells of a digital versatile disc, Microchim. Acta. 183 (2016) 1195–1202. doi:10.1007/s00604-016-1745-3.

[16] N. Dey, C. Williams, B. Leyland-Jones, P. De, Mutation matters in precision medicine: A future to believe in, Cancer Treat. Rev. 55 (2017) 136–149. doi:10.1016/J.CTRV.2017.03.002.

[17] H.S. Sloane, K.A. Kelly, J.P. Landers, Rapid KRAS Mutation Detection via Hybridization-Induced Aggregation of Microbeads, Anal. Chem. 87 (2015) 10275–10282. doi:10.1021/acs.analchem.5b01876.

[18] Y.M. Chang, S.T. Ding, E.C. Lin, L.A. Wang, Y.W. Lu, A microfluidic chip for rapid single nucleotide polymorphism (SNP) genotyping using primer extension on microbeads, Sensors Actuators, B Chem. 246 (2017) 215–224. doi:10.1016/j.snb.2017.01.160.

[19] A.I. Phipps, D.D. Buchanan, K.W. Makar, A.K. Win, J.A. Baron, N.M. Lindor, J.D. Potter, P.A. Newcomb, KRAS-mutation status in relation to colorectal cancer survival: The joint impact of correlated tumour markers, Br. J. Cancer. 108 (2013) 1757–1764. doi:10.1038/bjc.2013.118.

[20] S. Martorell, S. Palanca, Á. Maquieira, L.A. Tortajada-Genaro, Blocked recombinase polymerase amplification for mutation analysis of PIK3CA gene, Anal. Biochem. 544 (2018) 49–56. doi:10.1016/j.ab.2017.12.013.

[21] A. Halperin, A. Buhot, E.B. Zhulina, Hybridization isotherms of DNA microarrays and the quantification of mutation studies, Clin. Chem. 50 (2004) 2254–2262. doi:10.1373/clinchem.2004.037226.

[22] Y. Gao, L.K. Wolf, R.M. Georgiadis, Secondary structure effects on DNA hybridization kinetics: A solution versus surface comparison, Nucleic Acids Res. 34 (2006) 3370–3377. doi:10.1093/nar/gkl422.

[23] W. Shen, Y. Tian, T. Ran, Z. Gao, Genotyping and quantification techniques for single-nucleotide polymorphisms, TrAC - Trends Anal. Chem. 69 (2015) 1–13. doi:10.1016/j.trac.2015.03.008.

[24] E.S. Yamanaka, L.A. Tortajada-Genaro, N. Pastor, Á. Maquieira, Polymorphism genotyping based on loop-mediated isothermal amplification and smartphone detection, Biosens. Bioelectron. 109 (2018) 177–183. doi:10.1016/j.bios.2018.03.008.

[25] I. Hernández-Neuta, I. Pereiro, A. Ahlford, D. Ferraro, Q. Zhang, J.L. Viovy, S. Descroix, M. Nilsson, Microfluidic magnetic fluidized bed for DNA analysis in continuous flow mode, Biosens. Bioelectron. 102 (2018) 531–539. doi:10.1016/j.bios.2017.11.064.

SUPLEMENTARY INFORMATION

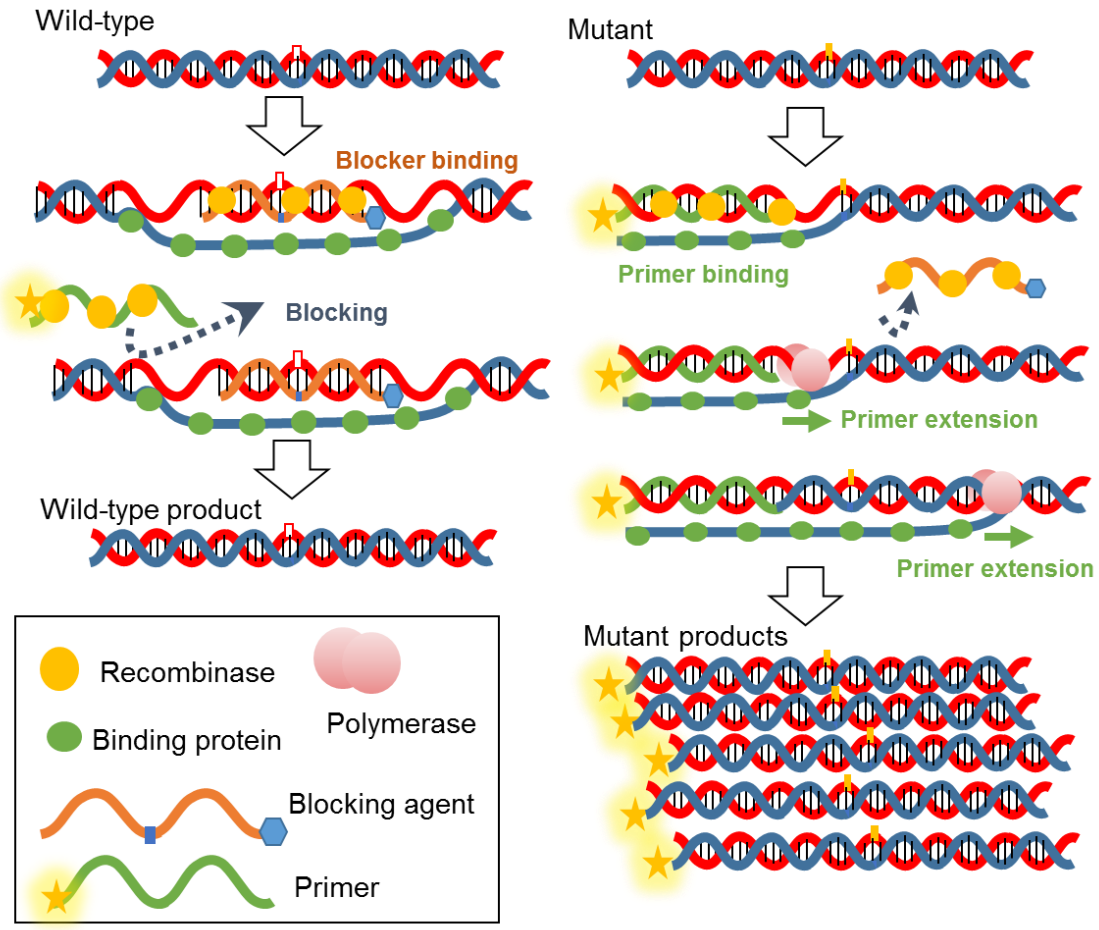

Fig. S2.1. Blocked RPA mechanism for mutant enrichment. (Left) Blocking of wild-type variant. The amplification is impaired due to the presence of the blocking oligonucleotide that is perfect-match to this variant. Since the blocker also contains a chemical modification at the 3'-end, the oligonucleotide cannot be extended by Bsu polymerase. (Right) Amplification of mutant variant. The action of recombinases forms complexes with primers and bind them with their homologous sequences in duplex DNA. Binding protein supports the displaced DNA strand and stabilizes the resulting D loop. Bsu polymerase (large fragment of Bacillus subtilis Pol1) produces the primer extension from the 3'-end, replicating mutant allele.

(a)

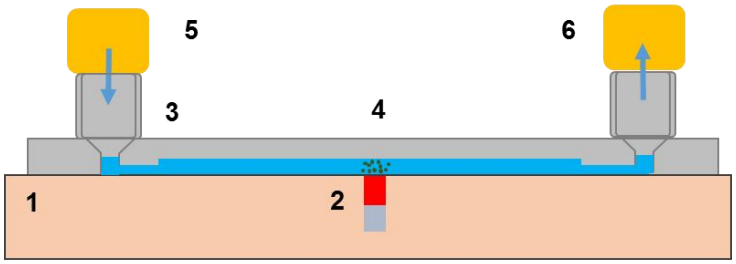

(b)

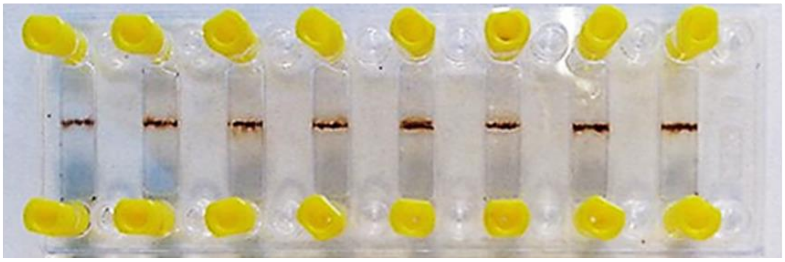

Fig. S2.2. Chip description. (a) Scheme of chip assembly: 1. polylactic acid holder; 2. Nd magnet; 3. chamber chip; 4. magnetic beads conjugated to oligonucleotide probes; 5. input connector; 6. output connector. (b) Image of chip for performing 8 assays simultaneously. Magnetic polymeric platform: height 2.15 mm, width 85 mm, length 60 mm. Chip: height 1.5 mm, width 75.5 mm, length 25.5 mm, material: Zeonor. Chamber: length 18 mm, chamber width 4 mm, lid thickness 188 μm, reaction volume 20 μL.

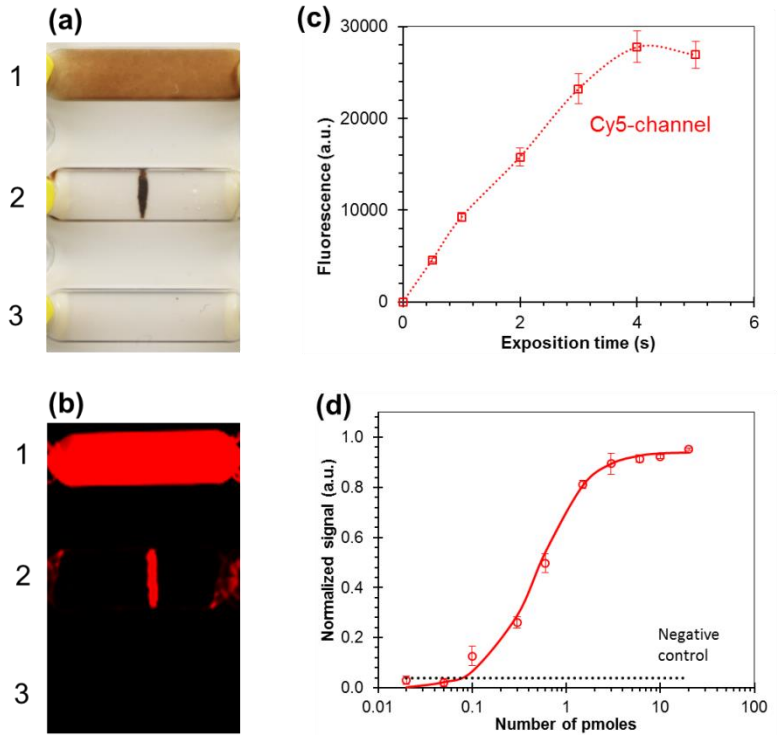

Fig. S2.3. Formation of bead-line. (a) Photograph of microchambers. 1: Initial hybridisation mixture, 2: Final bead-line after the magnetic concentration and washing, 3: Reference microchamber. (b) Image from the fluorescence reader (Cy5 channel, λ_{ex} 635 nm, λ_{em} 670 nm, exposure time: 1 s, gain: 1). (c) Effect of exposure time on the signal intensity of the bead-line. RPA product: p.G12C mutant template (1,300 copies of genomic DNA). (d) Effect of single-strand DNA concentration. Probe-conjugated particles: 7.12×10^7 (p.G12C probe).

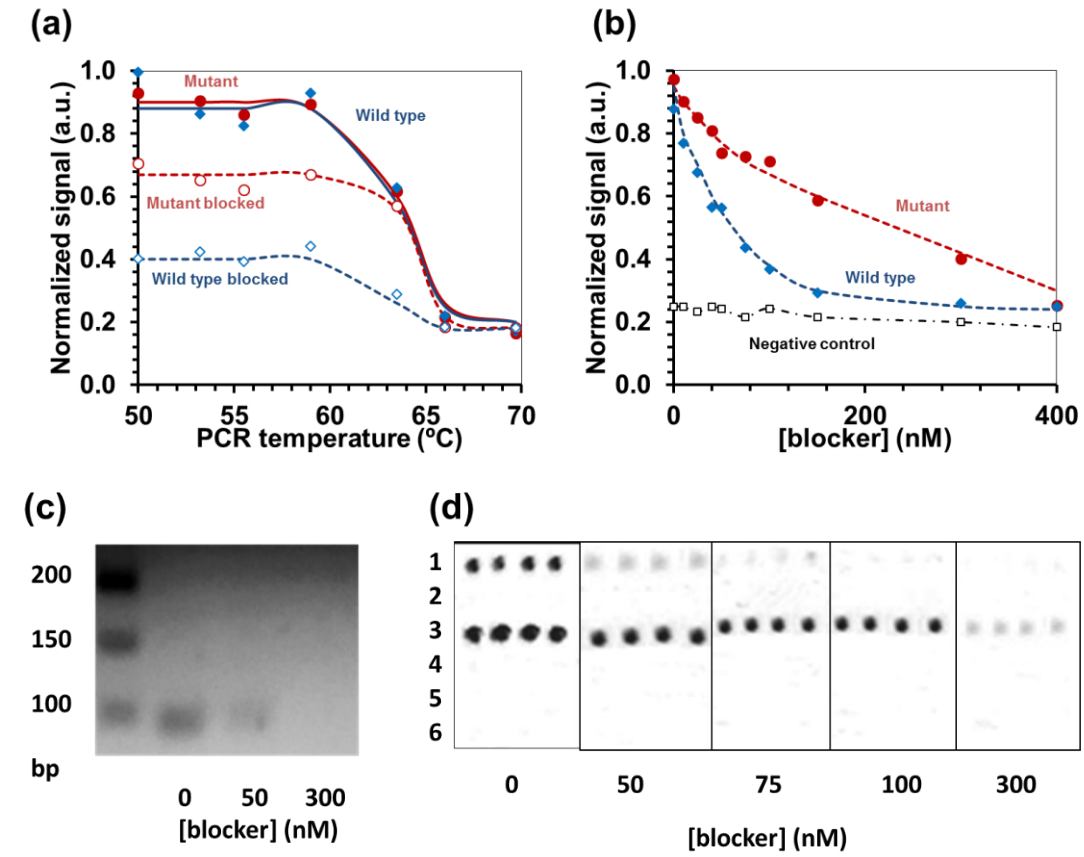

Fig. S2.4. Optimization of blocked RPA of *PIK3CA* gene (exon 20). Forward primer 5'-TTTGGAGTATTTCATGAAACAAATG, reverse primer 5'-TGTGTGGA AGATCCAATCCATT and blocker 5'-TGAATGATGCACATCATGGTGGCT-23ddC. (a) Effect of annealing PCR temperature in fluorescence measurements (Sybr Safe intercalant dyer). (b) Effect of blocker concentration in fluorescence measurements (Sybr Safe intercalant dyer). (c) Effect of blocker concentration in agarose gel measurements (wild-type sample = 1,300 copies). (d) Effect of blocker concentration in solid-phase hybridization assay (polycarbonate chip, mixture of 50% wild-type and 50% mutant = 1,300 copies). Amine-probes: 1. Wild-type probe: AATGATGCACATCATGGTGGCT; 2. Negative control; 3. Probe of p.H1047R: ATGATGCACGTCATGGTGGC; 4. Probe of p.H1047L: AATGATGCACTTCATGGTGGCT; 5. Probe of p.H1047P: ATGATGCACCT CATGGTGGC; 6. Negative control.

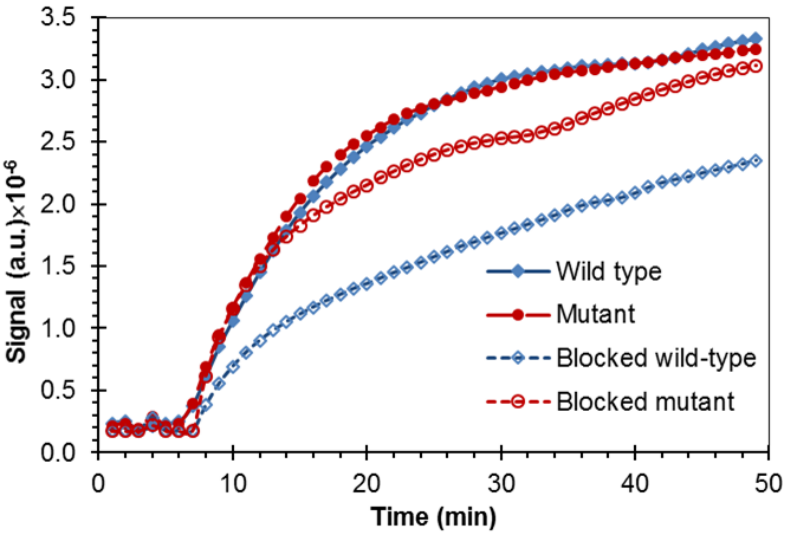

Fig. S2.5. Optimization of blocked RPA of *PIK3CA* gene (exon 9). Real-time amplification using DNA extracts from wild type and mutant sample in presence of blocking agent at 0 nM (continuous line) and 50 nM (discontinuous line). Forward primer 5'-ATTTCTACACGAGATCCTCTCT, reverse primer 5'- CTCCATTTTAGCACTTACC TGT and blocker 5'- TCTCTGAAATCACTGAGCAGGAGA-23ddC.

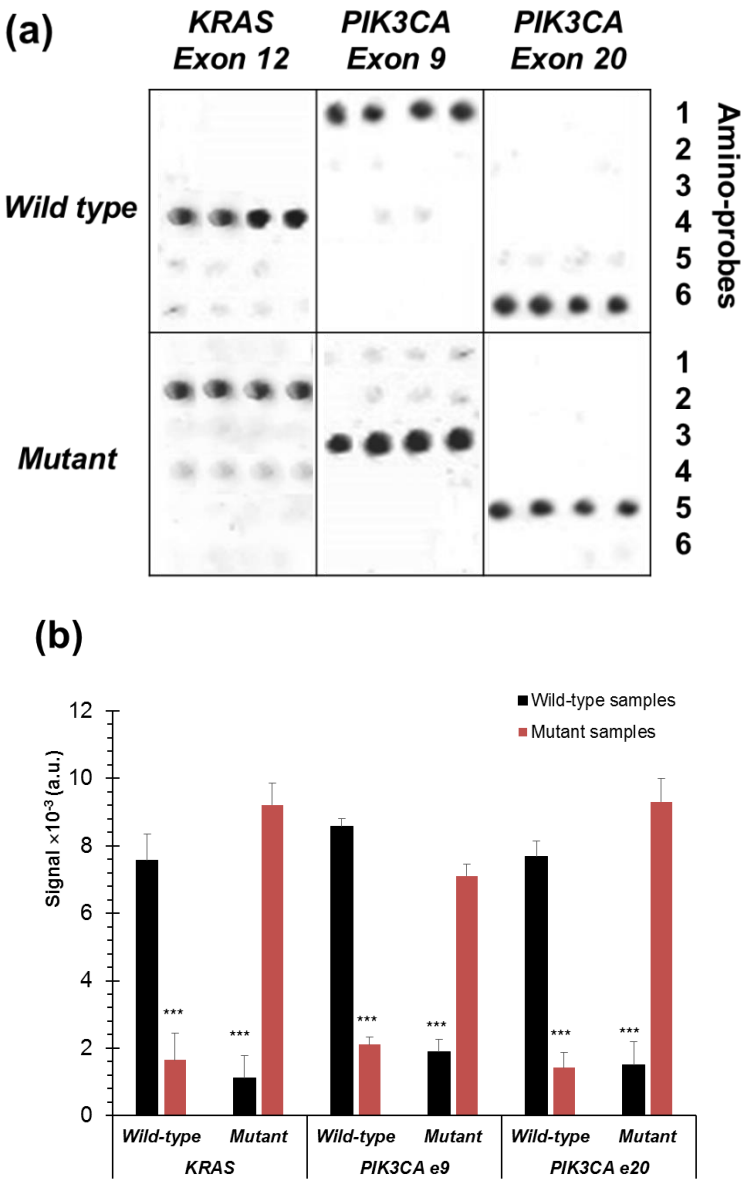

Fig. S2.6. Allele specific hybridization of blocked RPA products. a) Images of polycarbonate chip with probes immobilized in array format: 1. Wild type *PIK3CA* exon 9; 2. Mutant *KRAS* pG12C; 3. Mutant *PIK3CA* p.E545K; 4. Wild type *KRAS*; 5. Wild type *PIK3CA* exon 20; 6. Mutant *PIK3CA* p.H1047R. b) Mean intensities from replicate samples (n = 3). ***: p-value of t-test <0.01. Genomic DNA: 1,300 copies.

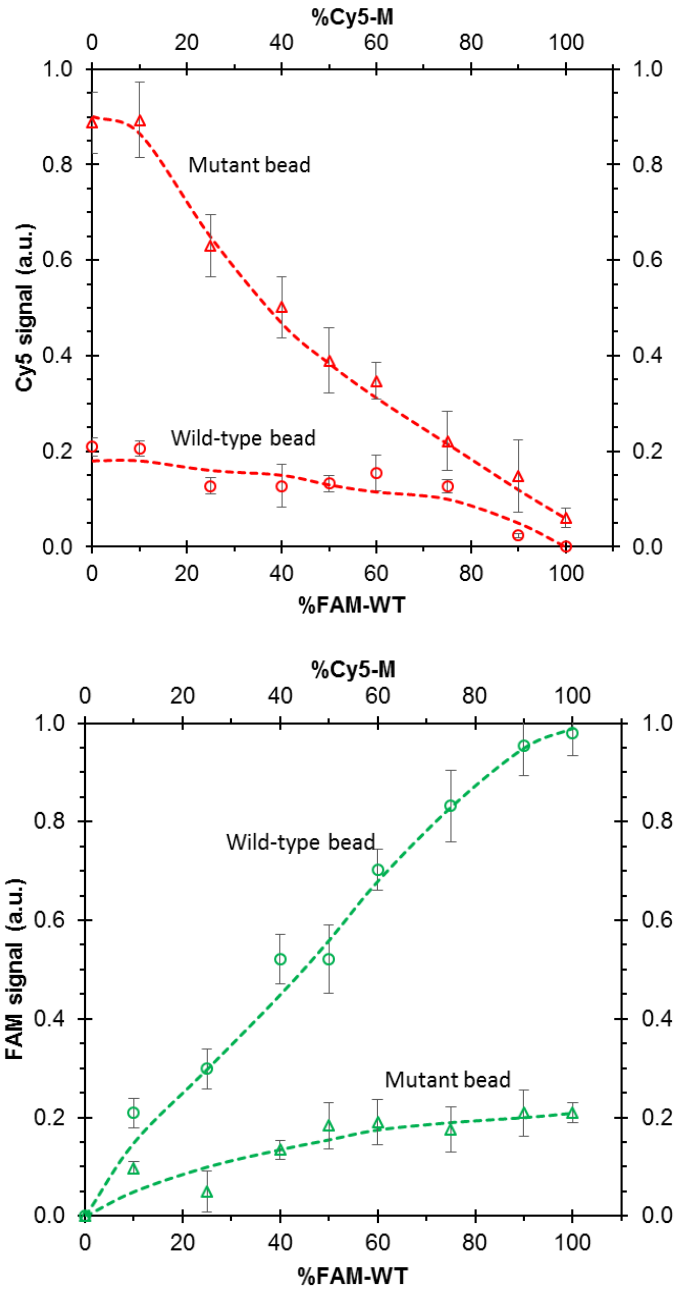

Fig. S2.7. Optical detection. Fluorescence signal recorded for the corresponding bead-line (wild-type or p.G12C mutant) according to template composition. (Top) Cy5 channel. (Bottom) FAM channel. Labelling: FAM-dUTPs in the wild-type RPA mixture and Cy5-dUTPs in the mutant RPA mixture. (1,333 copies of genomic DNA). Replicates: 12 measurements per bead-line.

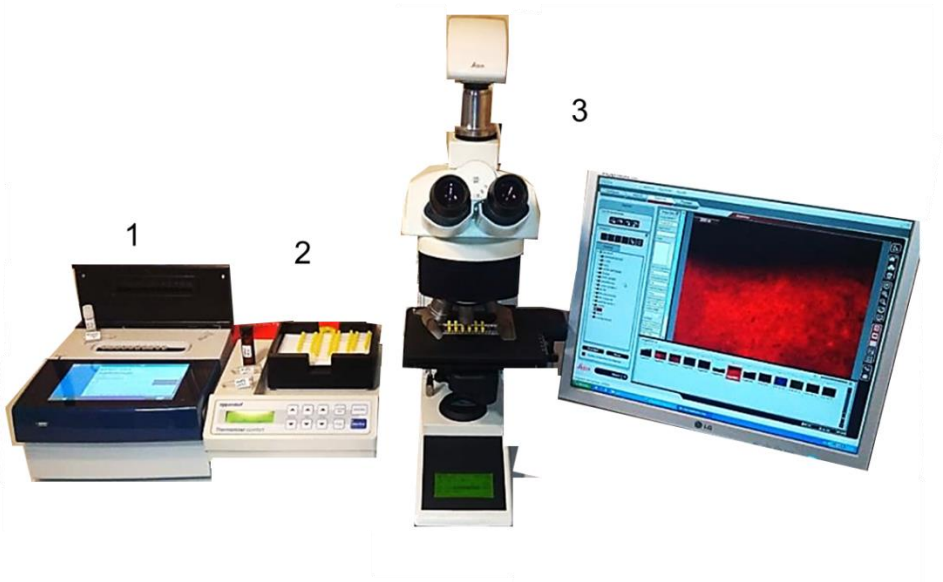

Fig. S2.8. Assay equipment. 1. Isothermal amplification, 2. Hybridisation and magnetic concentration, 3. Fluorescence detection.

Capítulo 3

Anclaje de dendrímeros oligo-funcionalizados a superficies termoplásticas para la detección de mutaciones por amplificación por recombinasa-polimerasa bloqueada.

Resumen

Una vez alcanzados los objetivos 1 y 2 de la presente tesis referentes a selectividad, miniaturización y reducción de los tiempos de hibridación, el capítulo 3, se centra en la funcionalización de superficies poliméricas mediante anclaje covalente de moléculas lineales y dendriméricas con el fin de incrementar la densidad de inmovilización de sondas de ADN. Concretamente, en este estudio, se presenta una estrategia útil de bioconjugación de sondas a dendrímeros para el desarrollo de chips versátiles de alto rendimiento para la biodetección de productos procedentes de la RPA-bloqueada.

Para ello, se anclaron híbridos de dendrímeros-DNA (dendrímeros carboxílicos covalentemente anclados a sondas alelo-específicas) a las superficies activadas de policarbonato y cicloolefina. Las técnicas de caracterización de superficies y los ensayos de hibridación demostraron que los múltiples grupos funcionales del dendrímero promovieron la inmovilización eficiente de las sondas ASO y la captura sensible de las dianas de ADN. El rendimiento de la matriz desarrollada fue mejor que el de las superficies funcionalizadas con organosilanos lineales. Dichos genosensores se aplicaron en la detección de mutaciones puntuales de productos de RPA bloqueada del gen *BRAF V600* a partir de muestras representativas procedentes de tejido biopsiado de pacientes oncológicos. Los resultados fueron muy satisfactorios, presentado alta selectividad y sensibilidad.

Microchemical Journal
Available online 18 June 2021, 106546
In Press, Journal Pre-proof

Surface coupling of oligo-functionalized dendrimers to detect DNA mutations after blocked isothermal amplification

Sara Martorell [a], Luis Antonio Tortajada-Genaro [a, b, c] ✉, Miguel Angel González-Martínez [b, c], Angel Maquieira [a, b, c]

Abstract

This study presents a useful strategy for the bioconjugation of probes for developing high-performance versatile chips applied to fast-response, low-cost DNA biosensing. We herein demonstrate that the high-density immobilization of dendrimer-oligonucleotide hybrids promotes the reliable sensitive sensing of single-nucleotide variants despite their low concentration.

Carboxyl-terminated poly(amidoamine) dendrimers directly coupled to amine-derivatized oligonucleotides were anchored to the activated surfaces of thermoplastics (polycarbonate and cycloolefin polymer). Surface characterization techniques and hybridization assays reported that the multiple functional sites of the oligo-functionalized dendrimer facilitated the efficient immobilization of probes and the sensitive capture of DNA targets (5 pM detection limit). Array performance was better than that of the surfaces functionalized with linear crosslinkers, such as vinyltriethoxysilane or 3-(triethoxysilyl) propyl isocyanate, as well films with unconjugated dendrimer molecules.

Based on oligo-dendrimers hybrids, disposable DNA-based biosensing platforms were developed for point-of-care diagnostics. A selective high-sensitive hybridization assay was performed that included amplification products of blocked PCR and

recombinase polymerase amplification (RPA) as an isothermal reaction. The chip results indicated that the single-nucleotide mutant variant of the BRAF oncogene was correctly discriminated in colorectal tissues from cancer patients.

Keywords: conjugated dendrimers; DNA biosensing; biochips; isothermal amplification; mutation detection

Introduction

Scientific advances have allowed biosensors to play an important role for in vitro diagnostic purposes based on nucleic acids. The integration of novel sensing components has promoted the development of reliable devices to fulfill the smart, simple and inexpensive detection goal of clinical targets [1]. Of these, hybridization-based sensors occupy a relevant position because they enable the high-throughput identification of specific sequences associated with disease diagnostics and prognostics [2]. They generally involve the hybridization of the target sequence to an immobilized probe on the sensor substrate.

The most widely used substrates are mainly solid inorganic materials, such as glass slides, metal electrodes, silica chips/fibers and plastic substrates [3]. Several strategies to modify the physico-chemical properties of surfaces for immobilizing specific probes have been reported [4]. Nevertheless, these reactions are single-site systems or linear approaches for oligonucleotide coupling (i.e. 2D immobilization).

Nanotechnology offers novel issues for the biosensing of nucleic acids, such as smart materials [5]. For instance, three-dimensional supramolecular architectures based on highly branched macromolecules have been successfully proposed [6]. In particular, poly(amidoamine) dendrimers (PAMAM) show a well-defined 3D-globular backbone, as well as higher versatile moieties to be further modified [7]. Different end-group functionalized dendrimers are available like thiol, phosphate, aldehyde, amino and carboxylic acid, among others. They are an excellent entity to link oligonucleotide

probes with a solid surface in electrochemical [8] and optical sensors [9]. As a result, the larger active area of dendrimers provides more sensitive devices than those based on linear molecules [10].

The general approach is a dendrimer-mediated immobilization method, i.e. the oligonucleotide is coupled to the surface coated with a dendrimer film. Thus several surface modification techniques for inorganic materials have been reported, including both covalent and non covalent binding [7,10-13]. Some examples are the attachment of DNA probes to dendrimer-modified thermoplastics, such as SU-8 and PDMS for E. coli adsorption in a microfluidic chip [14-16] and PMMA for immunoassays on conventional plates [17]. However, the aggregation of dendrimer molecules has been described during the functionalization of surfaces [18]. This cluster formation reduces the later immobilization of DNA probes and hybridization assays, but worsens sensing performance results. Our proposal is to directly anchor oligo-functionalized dendrimers to planar chips to minimize chain interactions and to improve chip fabrication and assay sensitivity. We hypothesized that dendrimers conjugated with oligonucleotides in solution would provide flexible orientation and higher reaction yields compared to other surface modification chemistries, including dendrimer-mediated approaches.

In this work, we study the potential biosensing properties of DNA-dendrimer-functionalized surfaces based on plastic polymer substrates, such as polycarbonate (PC) and cycloolefin polymer (COP). Both substrates have the potential of being integrated into disposable chips, miniaturized biosensors or wearable devices for personalized health monitoring purposes [1,3,19]. As proof-of-concept for clinical diagnostics, this research was addressed to discriminate the amplification products obtained by polymerase chain reaction (PCR) and a novel variant of recombinase polymerase amplification (RPA) called blocked RPA, which was recently developed by our research group [20]. The former was the commonest DNA amplification reaction and the latter was a relevant isothermal alternative with a high potential for accessible sensitive nucleic acid detection outside laboratories, and even for self-testing [21,22]. The approach is based on the selective blocking of reactions to detect single nucleotide

variations under isothermal conditions (37 ºC for 40 min). The reaction mixture contains a blocker oligonucleotide that matches the wild-type sequence in the target locus by inhibiting its amplification. Here the studied application of the oligo-functionalized dendrimer-based chips was the sensitive identification of single-point mutations for genotyping in tumor tissues required for the correct selection of therapies, such as lung cancer or colorectal cancer [23].

Materials and Methods

Materials

Unmodified slides of COP (cycloolefin polymer, Zeonor® 1060R) and PC (polycarbonate, Makrolon®) were used as substrates (dimensions 75 mm × 25 mm). Carboxyl terminated PAMAM dendrimers (generation 3.5), ethylendiamine (EDA), N-hydroxysuccinimide (NHS), bovine serum albumin (BSA), 2-(N-morpholino)ethanesulfonic acid (MES) and 1-ethyl-3-(3-dimethylaminopropyl) carbodiimide (EDC) were purchased from Sigma-Aldrich (St. Louis, MO, USA). The reagents used for genomic DNA extraction formed part of the MagMax Cell-free DNA Isolation Kit (Applied Biosystems, Austin, TX). The DNA amplification kits for PCR and RPA were the DNA Amplitool kit (Biotools, Madrid, Spain) and the TwistAmp Basic RPA kit (TwistDx, Cambridge, UK), respectively. The array printing solution was EDC at 50 mM and NHS 50 mM in MES 0.1 M. The hybridization buffer was saline-sodium citrate (SSC) 1×: sodium chloride at 150 mM, sodium citrate at 15 mM, formamide 25% (pH 7.0). The hybridization washing solution contained NaCl 15 mM and trisodium citrate 1.5 mM. The developing buffer (pH 7.4) was a Tween 20 (0.05%) solution in phosphate-buffered saline (PBS) containing 137 mM NaCl, 12 mM phosphate and 2.7 mM KCl. Abcam (Cambridge, UK) supplied the sheep monoclonal anti-digoxigenin and monoclonal antisheep-HRP antibodies. The HRP-substrate was 3,3',5,5'-tetramethylbenzidine solution (ep(HS) TMB-mA, SDT Reagents, Baesweiler, Germany). DNA oligomers were purchased from Eurofins genomics (Ebersberg, Germany) (Table S3.1).

Chip fabrication

Activation of substrates PC and COP was achieved by UV/ozone oxidation as previously described [20]. Amine functionalization was performed by incubating in crosslinker solution (1% EDA, 50 mM EDC) for 30 min at room temperature with gentle stirring. Later chips were immersed in 70% ethanol solution and air-dried. The mixtures of dendrimer (10 nM), NH2-oligonucleotide probes (100 nM) and EDC (50 mM) were incubated in printing solution at room temperature for 30 min with end-over rotation. After DNA-dendrimer coupling, solutions were arrayed on EDA-functionalized surfaces by a non contact spotter (AD 1500 BioDot Inc., Irvine, CA, USA) at room temperature, 40 nL drop volume and 70% humidity. The end-NH2 groups were coupled with the free COOH of the oligo-functionalized dendrimer by a carbodiimide reaction. After incubation at room temperature for 1 h, excess dendrimer was removed by washing the chip twice with PBST, followed by air drying. Finally, BSA (30 mg mL-1) was dispensed for surface blocking. DNA biochips were stored at 4 ºC.

Hybridization assay and detection

Chips enabled DNA products to be detected by selective hybridization assays. Briefly, amplification products (5 µL) were mixed with hybridization buffer (45 µL) and heated (95 ºC, 5 min) to unwind the double strand in a laboratory heater (VWR, Leuven, Belgium). Solutions were dispensed over sensing areas and incubated at 37 ºC for 60 min in an oven (Memmert, Schwabach, Germany). Arrays were rinsed with progressive dilutions of hybridization washing buffer. An immunoreaction was performed for chip staining. For digoxigenin labeling, the reagents were the anti-digoxigenin antibody (1:2500) and the HRP-labeled secondary antibody (1:400) in developing buffer. After substrate dispensation, a dark blue solid deposit formed on positive spots. Plastic-dendrichips were directly scanned (Epson Perfection 1640SU office scanner, Los Alamitos, CA, USA) to give monochromatic images (Tagged Image File Format, color depth 16-bit, scale 0-65535). The optical intensities of each spot and the local background were quantified.

Application 1: Generic detection of oncogenes based on PCR and RPA

The KRAS (codon 12), NRAS (codon 61) and BRAF (codon 600) genes were the target regions. The genomic DNA from both the human cell line SK-N-AS (ATCC CRL-2137) and patient tumor tissues was isolated as described in [20]. Six arrays of specific probes were printed per chip for the simultaneous analysis of six samples, including six replicates per probe.

PCR-based method. Each amplification mixture (50 µL) contained 1×DNA polymerase buffer, 3 mM of MgCl2, 200 µM of deoxynucleotide triphosphate, 300 nM of upstream primer, 300 nM of downstream digoxigenin-labeled primer, 4 ng of genomic DNA and 1 unit of DNA polymerase. The reaction was performed by an initial denaturation cycle of 95 ºC for 5 min, 35 cycles of denaturation at 95 ºC for 30 s, annealing at 59 ºC for 30 s and elongation at 72 ºC for 60 s. The thermal cycler was a Mastercycler Gradient (Eppendorf, Westbury, NY, USA).

RPA-based method. Each reaction mixture (50 µL) was prepared by mixing rehydrated buffer, 14 mM of magnesium acetate, 480 nM of upstream primer, 480 nM of downstream digoxigenin-labeled primer, 4 ng of genomic DNA and the enzyme pellet. Vials were incubated at 37 ºC for 40 min in a block heater (VWR, Leuven, Belgium). Measurements were taken by ESEquant TS2 for optimization purposes (Qiagen, Stockach, Germany).

The hybridization-detection assays were performed on the chip as described above. Application 2: Detection of a single-nucleotide mutation based on blocked RPA
The studied hotspot was the V600E mutation located in the BRAF gene, in which thiamine (T) was substituted for adenine (A) at nucleotide 1799. The genomic DNA from patients' tumor tissues was isolated as described in [20]. Six arrays of allele-specific probes were printed per chip, including three replicates per target probe and controls (the chip layout was 3×3).

Each reaction mixture (50 µL) was prepared by mixing rehydrated buffer, 14 mM of magnesium acetate, 480 nM of upstream primer, 480 nM of downstream digoxigenin-labeled primer, 50 nM of blocker, 4 ng of genomic DNA and the enzyme pellet. The blocking oligonucleotide was complementary to the wild-type variant, designed as previously described [24]. Solutions were incubated at 3 ºC for 40 min. The hybridization-detection assays were performed on the chip as described above.

Results and Discussion

Surface activation and immobilization based on an amine-end crosslinker.In the present study, the dendrimers of generation 3.5 were selected because these polymers have enough terminal groups (64 end-groups) for effective multi-point coupling to nucleic acids [11, 17]. The initial experiments were performed using the hybrids between the COOH-functionalized dendrimers (COOH-PAMAM) and amino-end oligonucleotides, prepared following the carbodiimide reaction. As the initial challenge was high-yield immobilization, stoichiometric relation 1:34 was chosen to ensure that enough free COOH-groups were available (at least 50%).

The coupling chemistry of these oligo-functionalized dendrimers on chips was explored (Fig. S3.1). In all the studied approaches, the first step was the activation of thermoplastics (PC and COP) based on plasma UV/ozone oxidation by generating carboxylic-activated surfaces. Water contact angle measurements (WCA) showed that the activation method yielded a high coverage of oxygenated groups (WCA 20º-50º) compared to the raw material (WCA 80º-90º).

The second step involved attaching the amine-end crosslinkers for generating amine-functionalized chips. APTES as a crosslinker was evaluated in the presence of FPTS as a horizontal spacer molecule (Fig. S3.2). By controlling the silanization conditions (APTES 1%, PFTS 0.1%), the surface was quite hydrophobic (WCA 90±0.5º) and the spot shape was regular. Residual non-specific binding was associated with excess free amino

groups on the active surface, which induced electrostatic interactions. EDA-mediated coupling was studied. The spot signal showed a linear dependence from its concentration and immobilization yield of the DNA-dendrimer hybrid (Fig. 3.1). This short-length crosslinker at the 1% concentration provided low background signals, short reaction times and very sensitive responses.

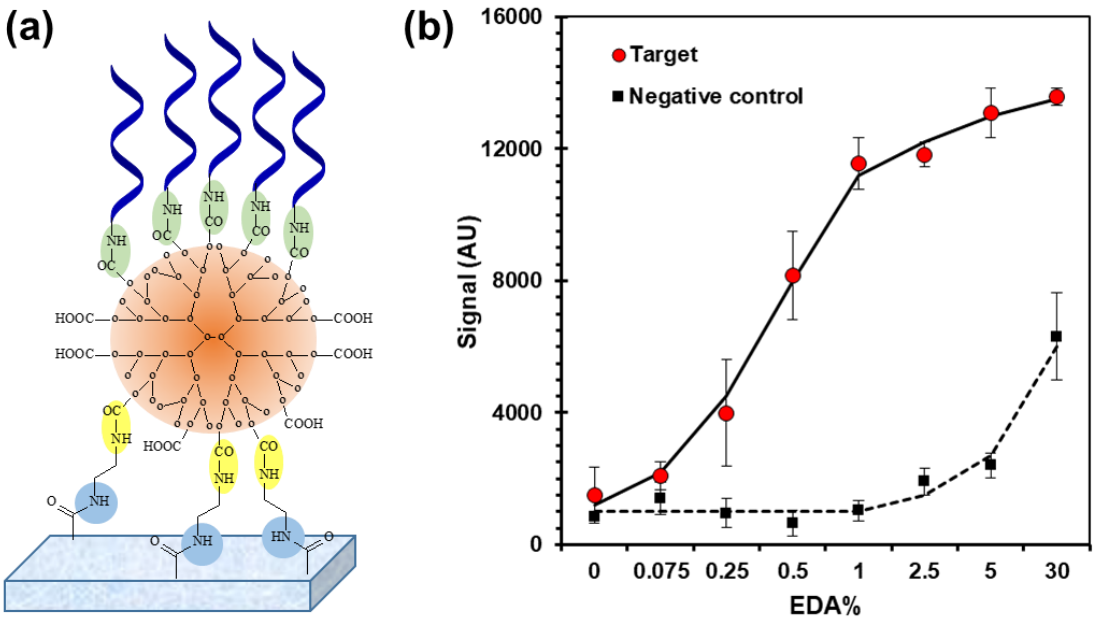

Fig.3.1. Immobilization of oligo-functionalized dendrimers on thermoplastic substrates: (a) Scheme of EDA-mediated reaction. (b)Spot signal of the hybridization assay at different EDA crosslinker concentrations (0.0075-30%). Substrate: PC.

The following experiments focused on the binding specificity of oligo-functionalized dendrimer by running simple recognition assays on the control chips that lacked one anchoring procedure step (or more), as reported in Fig. 3.2a. The direct immobilization of the DNA probes in raw substrates (no activation, no dendrimer) led to low signals associated with residual unspecific binding. In the chips without photo-activation, positive responses were found, and were slightly higher in the APTES than in the EDA approach. These results showed the formation of an adsorption film of the crosslinker on the raw plastic chip (hydrophilic interactions). With no crosslinker, the recorded signals were also comparable to the background of activated chips because

the electrostatic repulsion of carboxylic groups on the surface totally prevented the non-specific retention of the carboxylic terminated-dendrimers. In the absence of a dendrimer, a residual signal was measured, and was associated with non-covalent binding between free carboxylic reactive groups on the surface and amino probes (electrostatic forces). As expected, the experiment performed with no probe confirmed the null signal contribution of the immobilization reagents. Finally, the chips fabricated with all the reagents gave the highest responses, which demonstrated the multi-site covalent bonding of oligo-functionalized dendrimers. Also, the flexible structure of multi-branched dendrimers allowed a correct coupling to surface despite of its partial oligo-functionalization.

An evaluation of biosensing capabilities was assessed by performing multiplexed hybridization assays in an array format (Fig. 3.2b). Selective responses were found for the dendrimer-mediated platforms because positive spots were detected only for the perfect-match probe. The recorded spot intensities showed a quantitative response against different concentrations of the targets (Table S3.2). In short, these results confirmed the adequate oligo-functionalized dendrimer immobilization on both amino-modified plastic surfaces, maintaining probe activity and enabling hybridization assays. Nevertheless, the chips prepared using EDA as the crosslinker provided higher spot intensities and low backgrounds than those functionalized by APTES.

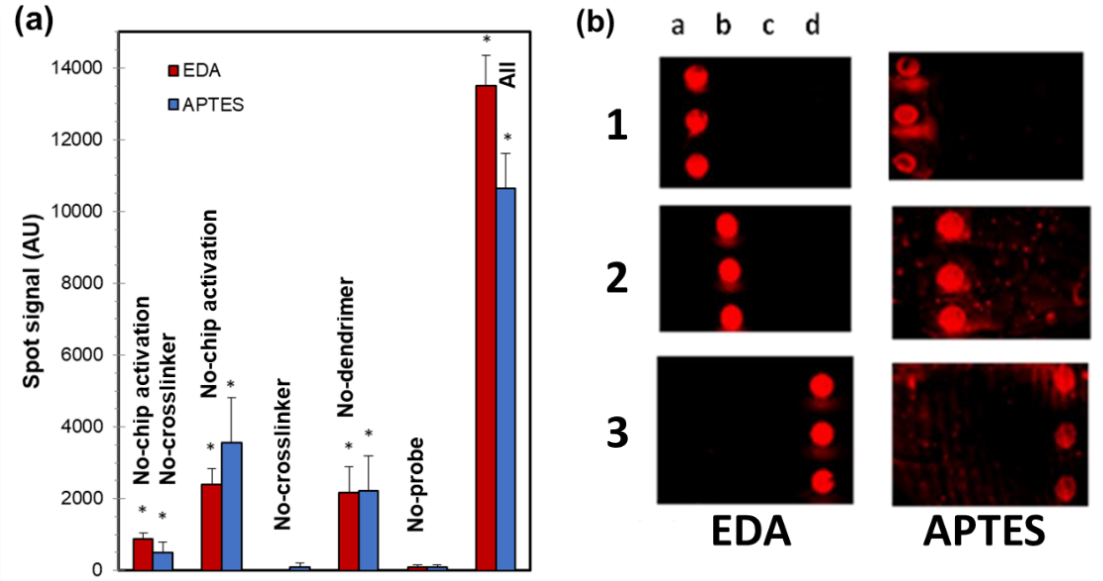

Fig. 3.2. (a) Spot signals recorded for the manufactured dendrimer chips compared to the control chips built with some preparation step missing. Assay: Recognition of perfect-match oligonucleotide. (b) Capture array image for the EDA and APTES dendrimer-plastic chips for the discrimination of targets. Assay: Multiplex hybridization; samples (1-3) are perfect-match oligonucleotides to probe a-b-d, respectively (c is a negative control).

Nature of the dendrimer

Demonstrated the principle, the following challenge was to improve the oligo-immobilization, modifying the dendrimer properties. The carboxyl-end (COOH-PAMAM) and amino-end (NH_2-PAMAM) dendrimers were examined because those nanomaterials have demonstrated to provide excellent performances for DNA biosensing [4,10]. For NH_2-PAMAM dendrimers, the coupling chemistry also involved glutaraldehyde as secondary crosslinker (bi-aldehyde molecule).

After coupling to oligonucleotide probes, NH_2-PAMAM/probe and COOH-PAMAM/probe hybrids were coupled to EDA-functionalized surface by a carbodiimide reaction. The concentration of oligonucleotide and dendrimer was examined for generating PAMAM/probe hybrids. The adequate signals were obtained for dendrimer at 10^{-8} moles and probe at 10^{-7} - 10^{-6} moles, equivalent a stochiometric ratio of 1:10 – 1:100 (Fig. S3.3). Also, AFM measurements reported two well-defined surface regions, which were respectively associated with quite densely packed spots (350 µm diameter) and a background surface. Higher concentrations of hybrids lead to signal saturation and irregular spots.

Biosensing performances of both hybrids (NH_2-PAMAM/probe and COOH-PAMAM/probe) were compared (Fig. S3.4). Amine dendrimers yielded a better spot morphology and homogeneity (positive), but a lower response (about 40%) and a higher (2-fold) degree of non-specific adsorption (negative). These results agree with those reported by a previous study based on the DNA immobilization on dendrimer-activated

surfaces that compared carboxylic and amine dendrimers on glass slides [13]. In their study, the researchers observed lower background signals of up to 100-fold. Therefore, the COOH-PAMAM/probe hybrids were chosen for further experiments on thermoplastic chips.

Thermoplastic substrate selection

The studied thermoplastic materials were PC and COP given their high resistance, transparency and flexibility for biochips fabrication. In order to test dendrimer binding, parallel experiments were performed for physicochemical characterizations. The AFM measurements showed a homogeneous surface structure of EDA-active chips (Table 3.1). Compared to the raw materials, marked variations in wettability features, measured by contact angles, were observed, which confirmed correct surface modification in each functionalization step (Table S3.3). As expected, the WCA values varied according to the surface group; i.e., lowering for polar groups. The results concluded that both functionalized surfaces enabled the solutions to be correctly confined at the anchored probe site.

Table 3.1. Comparison of PC chip and COP chip based on the physico-chemical data. Immobilization chemistry: the EDA/COOH-dendrimer/NH_2-probe.

	PC	COP
Formula	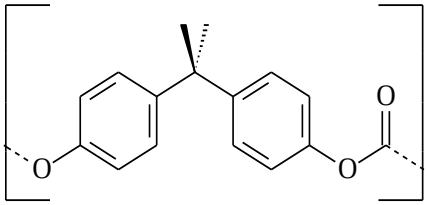	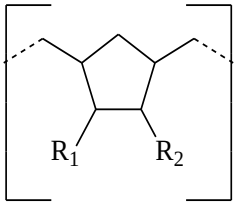
Raw material AFM image	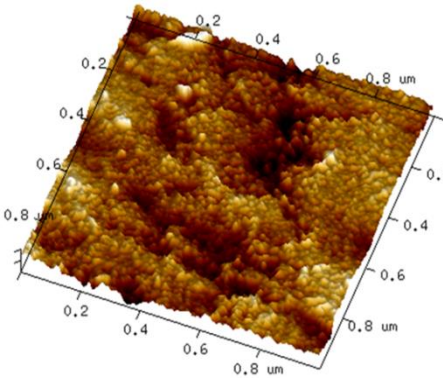	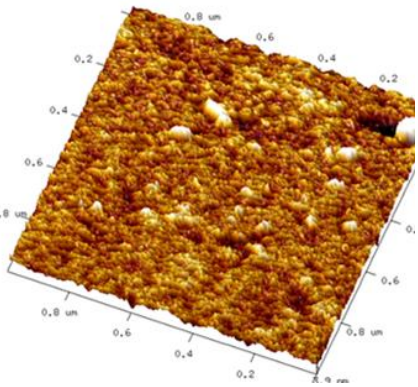
	Rq =0.66	Rq = 0.93
EDA-Functionalized chip AFM image	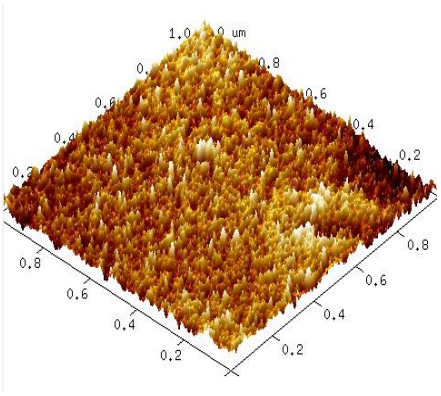	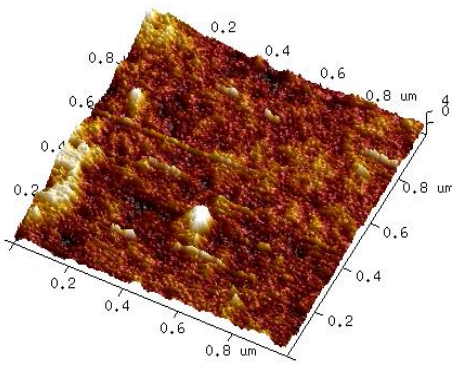
	Rq = 1.17	Rq = 0.98
Spot	Contact angle 68±2º Diameter 300±10 μm Background 10300±900	Contact angle 74±2 º Diameter 210±20 μm Background 10600±1900
Array image	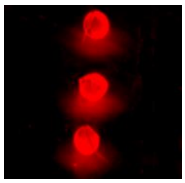	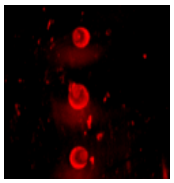

Regarding the DNA biosensing features, immobilization capability was examined by varying the amount of probe to be immobilized (Fig. 3). The observed behavior matched the Langmuir model and the standard base-to-base pairing in the solid-phase format [27,28]. However, the saturation signal was lower for COP (8,000 AU) than for PC (13,000 AU), which indicates fewer immobilized probes. The maximum immobilization density was around 13 pmol cm^{-2} for PC according to the measurements taken of the double functionalized probes (amine and Cy5-fluorophore). The estimated immobilization yield was 55-60% at the 100 nM probe concentration. Compared to previous studies, these values are adequate for DNA chips in several applications [10, 11].

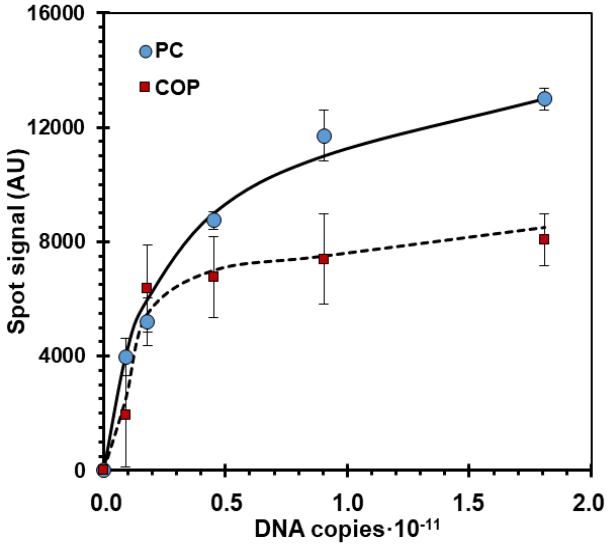

Fig. 3.3. Comparison of the PC chip and COP chip based on the DNA hybridization assay. Immobilization chemistry: the DNA/COOH-dendrimer/NH_2-probe.

The optical response after a recognition assay was also evaluated (Table 1). On both platforms, the proposed reaction succeeded to chemically modify these low-reactivity materials, which led to site-specific immobilization. High response ratios were observed at the spots for the fully complementary probes compared to those for the non-complementary probes, which proved the multiplexing capabilities. Nevertheless, homogeneity, spot intensities and the standard deviation of background signals were better for PC than for COP (around 2-fold).

In conclusion, both substrates showed specific oligo-dendrimer binding, excellent compatibility with the hybridization assays and recognition selectivity. Nevertheless, the PC substrate was selected because it exhibited low non-specific absorption and higher responses and, thus, better biosensing capabilities were expected.

Comparison to other coupling chemistries

The performances of the developed coupling reaction were examined and compared to other described surface reactions to engraft the DNA probe to plastic or glass substrates. These chips (layout 6×3×4) were fabricated as reported in the Supplementary Material.

The first immobilization reaction was the dendrimer-mediated approach [14-19]. This method is based on a two-step sequence, including the film formation of non-conjugated dendrimers, followed by the binding of oligonucleotide probes (Table S3.4). A controlled film formation of COOH-PAMAM dendrimers was achieved by spin coating, particularly for low concentrations (Table S3.5). The AFM images and roughness data suggested that surfaces were quite homogeneous, without the formation of cluster. In addition, the mean depth variation agreed well with the EDA-dendrimer dimensions (approx. 5 nm). Also, amino-ended oligonucleotides were attached to the dendrimer film by a carbodiimide reaction in heterogenous format.

However, dendrimer-mediated approach yielded several drawbacks for biosensing proposes compared to our method (Table S3.4). High background signals were recorded (12,000±1,000 au), accompanied by low reproducibility and no uniformity of spot profiles, which all suggest incomplete oligonucleotide probes coupling, which would render free COOH groups and the consequent physisorption of non-specific molecules. Indeed, this reaction sequence should be discarded because homogeneity and reproducibility are crucial for reliable quantitative assays [2]. Likewise, probe attachment based on our approach was faster (40 min less) and reagent

consumption was lower (2500-fold, calculated from the volume ratio). Other identified advantages included the fact that part of the synthesis procedure was performed in the solution phase [15].

Three non-dendrimer-mediated systems were also analyzed, including the non-crosslinker, ICPTS and VTES functionalized chips (Fig. S3.5). The first approach involved amino-end probes directly coupled to the carboxyl groups (-COOH) of the activate substrates. In the second approach, the ICPTS reagent acted as an organosilane crosslinker. Then the surface was covered by isocyanate groups (-C=N=O) capable of binding amino-end probes. The third chemistry also required the silanization of platforms by VTES, an organosilane reagent that contains a terminal vinyl group (-$CH=CH_2$), and the attachment of thiol-end probes was easily achieved via the photoclick-chemistry mechanism.

Regarding the required resources, dendrimer-plastic functionalization offered advantages over other linear crosslinkers or previously published immobilization chemistries for plastics [4, 5]. The activation procedure based on photo-oxidation by UV-ozone was feasible in of complexity, cost-effectiveness and required instrumentation terms if alternative techniques are considered, such as physical vapor deposition, chemical vapor deposition, physical laser deposition or sputtering [4,5]. For instance, the time was 45 min for the novel strategy, 90 min for the silane-based approaches and several hours for the other techniques. For the covalent binding of amino probes, our method was also fast (1 h), and was overcame only by thiol-ene click reactions like VTES-based chemistry. All the platforms were stable considering the conventional requirements for DNA biosensing platforms [3,21]. Based on the cost and amount of reagents, our immobilization scheme was considerably cheaper.

Wettability features were also estimated from the spot diameter measurements (Fig. 3.4a). As expected, the smallest spots were obtained for the VTES-functionalized chips (80 μm), with the highest spots for the dendrimer-mediated chips (350 μm). These

results indicated that silane modification exhibited a more hydrophobic nature due to the terminal vinyl groups (-CH=CH_2) than the other active surfaces, including the novel approach. Likewise, all the chips displayed sharp spots with excellent signal distribution. Intraspot homogeneity was slightly better for the novel method, with a 15±5% relative standard deviation for direct activation, 9±7% for ICTPS, 15±5% for VTES and 7±3% for EDA-dendrimer-chip.

The multiplexed hybridization assay in the array format was studied. First, no relevant surface effect was observed because the recognition kinetics of the DNA target and probe on the sensing surface was comparable to other coupling chemistries (Fig. S6). Second, an excellent recognition process between the probe and the target DNA was achieved, as all the array images show (Fig. 3.4a). Assay selectivity, expressed as the signal percentage for the complementary probe compared to other probes, was 94% for the dendrimer-based coupling and 92-96% for the other bindings. Reproducibility, expressed as the relative standard variation of replicated experiments, was 4% and 4-7%, respectively.

a)

	Sample 1				Sample2				Sample3				WCA	Ø	SNR
	1	2	3	4	1	2	3	4	1	2	3	4			
Direct	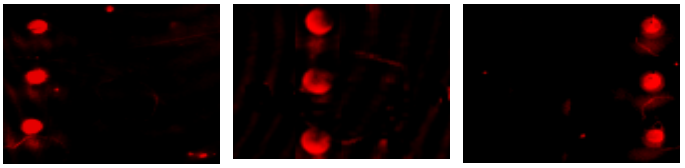												80±2	240±40	10.2
ICPTS	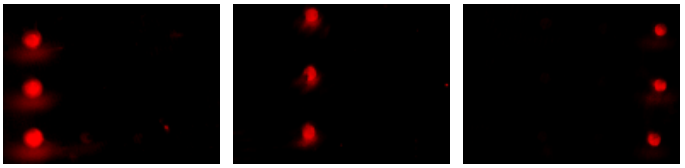												69±4	180±20	9.4
VTES	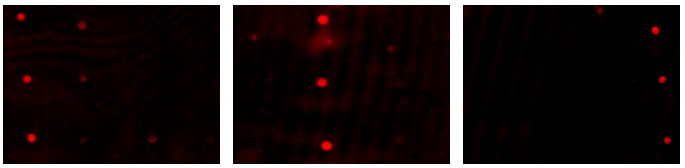												89±3	80±20	14.6
Dendrimer													65±5	350±20	19.9

WCA: water contact angle (º); Ø: spot diameter (μm); SNR: mean signal-to-noise ratio

b)

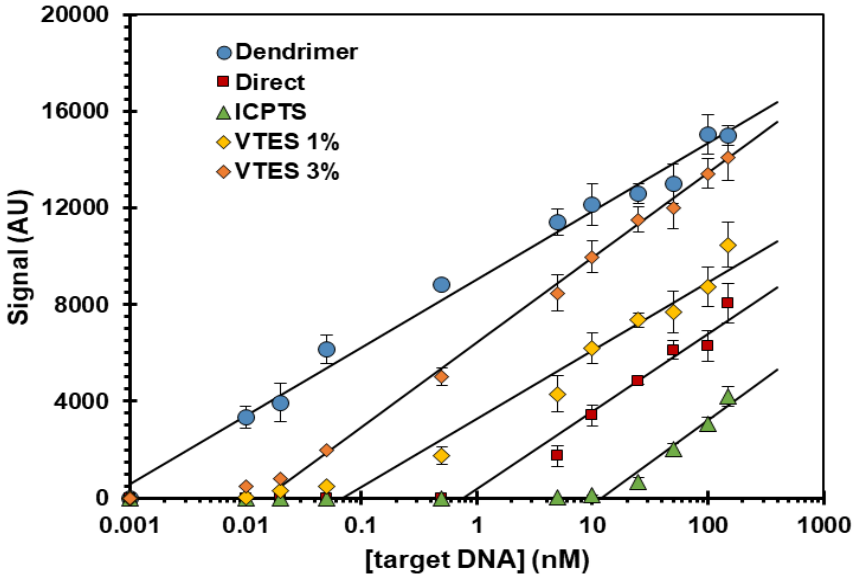

Fig. 3.4. Comparison of dendrimer-based immobilization to other coupling chemistries. (a) Array features. (b) Spot signal according to the target concentration. Array layout: 4 probes × 3 replicates. Probes: target 1 (1); target 2 (2); negative control (3); target 3 (4). Targets: Perfectly matched oligonucleotides at 100 nM.

The most relevant difference for DNA biosensing was assay sensitivity (Fig. 4b). The spot intensities in the dendrimer chips went from 2- to 100-fold higher. Specially, the dynamic range for dendrimer coupling significantly improved compared to direct functionalization [22]. These better results can be mainly explained by the structure of the highly branched macromolecules (3D immobilization) compared to brush-like structure of single-site attachment (2D immobilization). The flexible probe configuration should facilitate the displacement of the target molecule from the solution to the surface (interface movement) and further binding. These hyperbranched molecules reduce the interaction between adjacent probe molecules, compared to the typical vertical alignment of a linear functionalization [27]. Hybridization event to the template is promoted reaching better detection limits. The values were 0.005 nM, 0.05 nM, 0.5 nM, 5 nM and 50 nM for dendrimer, VTES 3%, VTES 1%, direct and ICTPS approaches. In conclusion, the excellent analytical performances displayed a clear advantage for our

dendrimer-based chips (multipoint attachment) over all the other systems for oligonucleotide immobilization.

Generic detection of oncogenes based on PCR and RPA

One important application of DNA-based chips and biosensors is the multiplexed detection of amplification products [1,2]. This study examined two amplification reactions, standard PCR and an isothermal alternative.

Experiments were addressed to test the platform capabilities for the specific detection of clinically relevant DNA regions. As proof of concept, the hotspots in oncogenes *KRAS, NRAS* and *BRAF* were amplified from cell line cultures and human samples (biopsied tissues). The PCR and RPA products were hybridized in the PC/EDA/COOH-PAMAM/probe chips. However, the RPA products led to high background signals. These results were interpreted as the non-specific binding of certain RPA mix components, such as high-molecular-weight polyethylene glycol and crowding agents. They facilitate isothermal amplification and reduce the mixing effects of thermal convection when the reaction is run at low temperature [23]. After including a BSA blocking treatment of chip surfaces, background signals were comparable to the PCR products (test t, p-value 0.27).

Table 3.2 provides examples of the recorded array images. Selective and sensitive responses were found for both amplification techniques, proven that the amplicons hybridized with gene-specific probes, while no responses were obtained for the others. The same human tissues were analyzed by the chips with probes directly immobilized on photo-activated plastics, as described in [22]. The signals recorded for the dendrimer-based coupling increased 40% vs. the direct coupling between amino-end probes and carboxyl groups of the activate chips.

These results demonstrated that our immobilization method can attach specific probes with performance for DNA assays independently of the amplification reaction.

Nevertheless, RPA was faster and had better operational conditions to develop integrated devices [24].

Table 3.2. Comparison of the oncogene detection using the oligo-functionalized dendrimer chips after PCR and RPA amplification.

		Patient 1	Patient 2	Patient 3
	Target	*KRAS* gene	*NRAS* gene	*BRAF* gene
PCR	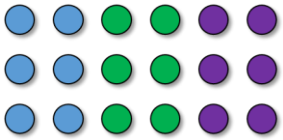	- - + 	+ - - 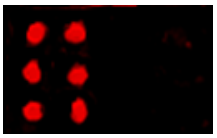	- + - 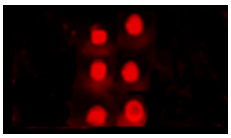
RPA	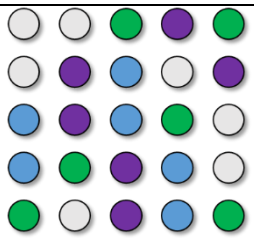	KRAS + 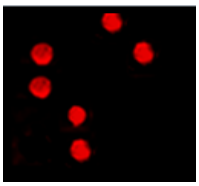	NRAS + 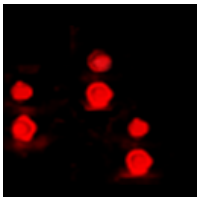	BRAF + 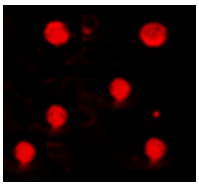
	Reference method	KRAS: T>G	NRAS: C>A	BRAF: T>A

Probes: *KRAS* (purple), *NRAS* (blue) and *BRAF* (green).

Specific detection of the mutations based on blocked RPA

The performance of the dendrimer-based DNA microarrays in the point-mutation discrimination was investigated for their clinical relevance [29]. As proof of concept, the variant p.V600E in *BRAF* gene (c.1799T>A) was identified from human samples (biopsied tissues). The analytical challenge was the discrimination between A-mutant and the wild-type (T) because the probability of a human genome with cytosine (C) or guanidine (G) in that locus is extremely low.

The suppression of wild-type variant was studied by blocked RPA operating at 37 ºC a simple heater system [21]. In this isothermal technique, the addition of blocking agent, complementary to wild-type template, decreases the polymerase action (Fig. 5a).

To enhance this effect, the blocker was designed in order to partially overlap to the upstream primer, because the primer annealing step is also modified (Fig. S3.7). Firstly, the designed oligonucleotides (primers and blocker) were confirmed using conventional blocked PCR approach and thermocycler (Fig. S3.8). Then, the blocked RPA combined to array hybridization assay was optimized, varying the reaction time, blocker concentration, relative concentrations of primers (Fig. S3.9). The responses associated to the wild-type variant decreased significantly in the presence of 50 nM of blocker, a ratio between forward and reverse primers of 1:1 and reaction time of 40 min.

The following experiments were focused on the detection of mutant variant (c.1799T>A) in clinical sample (biopsied tissues). An effective reduction of wild-type variant was obtained by blocked PCR and blocked RPA, although detectable signals were observed associated to wild-type probe (Fig. 3.5). The remaining signal was related to non-specific recognition during hybridization because the difference between the wild-type and mutant variants is a single nucleotide. To improve performances, a restrictive hybridization buffer (2×SSC, 25% formamide) was tested. The results confirmed the hypothesis and a clear spot pattern, depending on the patient genotype, was achieved (Fig. S3.10).

For quantitative analysis, discrimination ratios were determined, as the ratio between the mutant and the wild-type signals. The values were 0.4-0.5 for the wild-type samples (genotype: T) and 3.8-12.4 for the mutant samples (genotype: A). These values were similar with those obtained with blocked RPA approach and restrictive hybridization assay for *KRAS* gene [25]. For this mutation, high spot signals were registered associated to perfect-match probes, being the discrimination ratios higher than 1 (Fig. S3.11). The ratios were lower than 1 for wild-type and other mutants in the same locus (single-nucleotide change). Thus, the experiments proved the discrimination capability applied to real clinical samples and endorsed that this method can be an important tool for supporting the correlation of genetic variations and individual phenotypes [29,30].

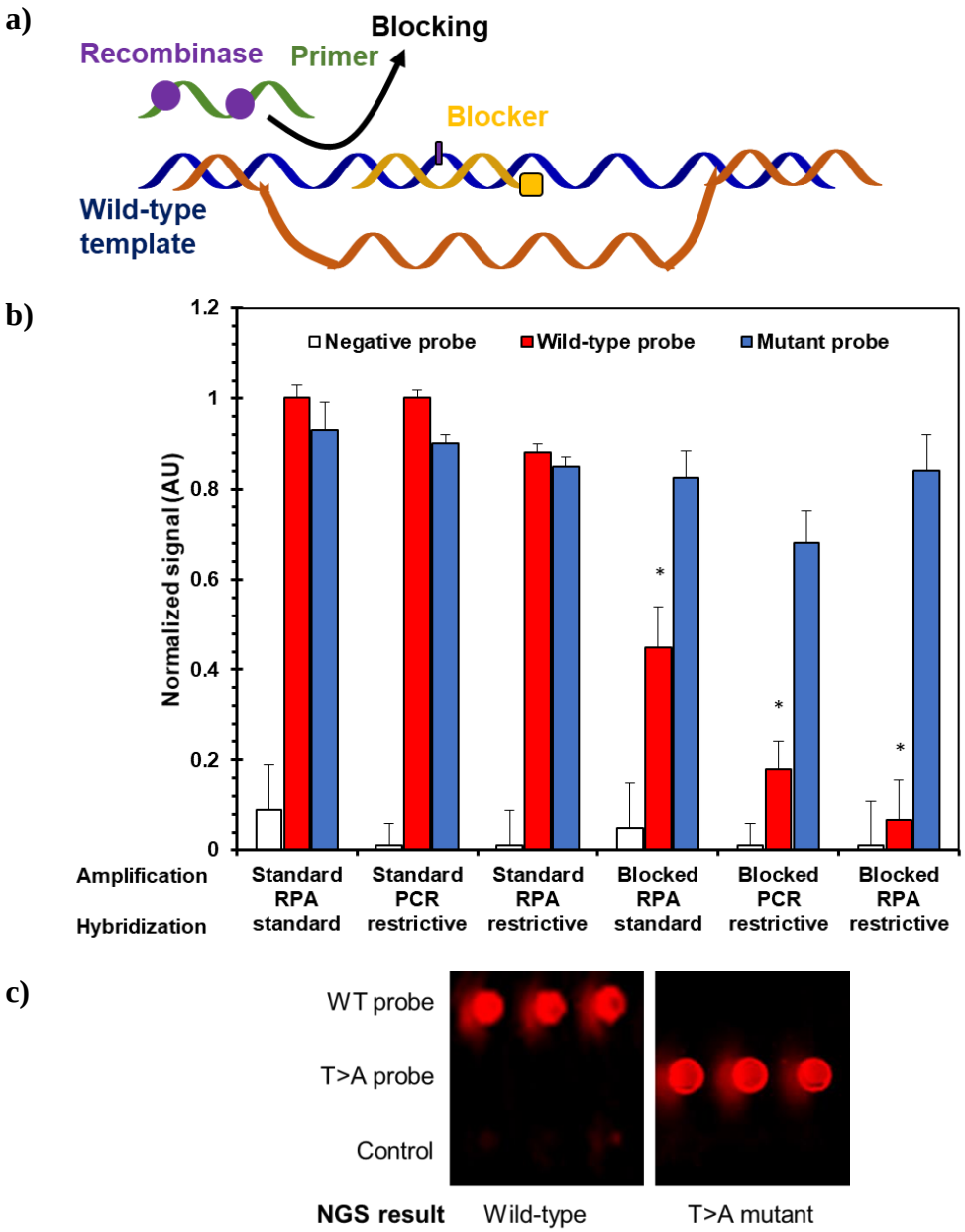

Fig. 3.5. (a) Scheme of blocked RPA, inhibiting the wild-type amplification. (b) Mutant detection capability on dendrimer-mediated chips depending on the amplification method and the hybridization conditions (standard or restrictive). * p-value < 0.01 (t test). (c) Array image for developed method based on blocked RPA and sequencing result (reference method) from tumor tissue from the oncology patients (wild-type and *V600E BRAF* mutant).

Conclusions

We demonstrate that the multipoint attachment of oligonucleotide probes based on dendrimers is an excellent approach for the functionalization of polycarbonate and cycloolefin thermoplastics, which are widely used materials in commercial microfluidic chips. Our novel approach comprises the formation of dendrimer-probe hybrids and their later effective immobilization, which are precise at the surface site and robust in surface wettability or roughness terms. The branched flexible structure nature of hybrids should particularly favor higher recognition of DNA target yields by providing up to 100-fold lower detection limits. These values are better than those achieved with surfaces functionalized with either linear crosslinkers or other dendrimer-based approaches.

Apart from these chips being able to detect several PCR products, we herein report for the first time the selective hybridization of RPA products on dendrimer-mediated probes. This isothermal amplification combines constant low reaction temperature with high sensitivity, specificity, fast reaction speed, portability and capability for clinical diagnostics outside laboratories. The dendronized-thermoplastic chip enhancement of sensitivity allowed us to address a challenging need: the discrimination of low-frequent specific DNA biomarkers, such as single-nucleotide mutations in clinical samples. Having been proved for the selective rapid detection of oncogene mutations in human tissues, the results will contribute to better diagnose diseases and toward reliable prognoses based on the use of disposable devices.

Author information

The authors declare no competing financial interest.

Acknowledgments

Authors acknowledge the financial support received from EU FEDER, the Spanish Ministry of Economy and Competitiveness (MINECO project CTQ2016-75749-R and Technical Support Personnel PTA- 2016).

References

[1] M. Zarei M. Portable biosensing devices for point-of-care diagnostics: Recent developments and applications. Trends Anal. Chem. 91 (2017) 26-41.

[2] Y. Du, S. Dong, Nucleic acid biosensors: recent advances and perspectives. Anal. Chem. 89 (2017) 189-215.

[3] L. Syedmoradi, M. Daneshpour, M. Alvandipour, F.A. Gomez, H. Hajghassem, K. Omidfar, Point of care testing: The impact of nanotechnology. Biosens. Bioelectron. 87 (2017) 373-387.

[4] J.I.A. Rashid, N.A. Yusof, The strategies of DNA immobilization and hybridization detection mechanism in the construction of electrochemical DNA sensor: A review. Sens. Biosensing Res., 16 (2017) 19-31.

[5] Z. Wang, Y. Li, P. Cui, L. Qiu, B. Jiang, C. Zhang, Integration of nanomaterials with nucleic acid amplification approaches for biosensing. Trends Anal. Chem. 129 (2020) 115959.

[6] J. Satija, V.V.R. Sai, S. Mukherji, Dendrimers in biosensors: Concept and applications. J. Mater. Chem. 21 (2011) 14367-14386.

[7] A. Erdem, E. Eksin, E. Kesici, E. Yaralı, Dendrimers integrated biosensors for healthcare applications. Nanotech. and Biosens. (2018). 307-317.

[8] G. Congur, A. Erdem, PAMAM dendrimer modified screen printed electrodes for impedimetric detection of miRNA-34a. Microchem. J. 148 (2019) 748-758.

[9] E. Soršak, J.V. Valh, S.K. Urek, A. Lobnik, Application of PAMAM dendrimers in optical sensing. Analyst. 140 (2015) 976-989.

[10] J.I. Paez, M. Martinelli, V. Brunetti, M.C. Strumia, Dendronization: A useful synthetic strategy to prepare multifunctional materials. Polymers. 4 (2012) 355-395.

[11] P.K. Ajikumar, J.K. Ng, Y.C. Tang, J.Y. Lee, Stephanopoulos G, Too H. P. Carboxyl-terminated dendrimer-coated bioactive interface for protein microarray: High-sensitivity detection of antigen in complex biological samples. Langmuir. 23 (2007) 5670-5677.

[12] C. Warner, Z. Hunter, D. Carte, T. Skidmore, E. Vint, B. Day, Structure and Function Analysis of DNA Monolayers Created from Self-Assembling DNA–Dendron Conjugates. Langmuir, 36 (2020) 5428-5434.

[13] Y.M. Kamil, S.H. Al-Rekabi, M.H. Yaacob, A. Syahir, H.Y. Chee, M.A. Mahdi, M.H.A. Bakar, Detection of dengue using PAMAM dendrimer integrated tapered optical fiber sensor. Sci. Rep. 9 (2019) 1-10

[14] Y. Qin, X. Yang, J. Zhang, X. Cao, Developing a non-fouling hybrid microfluidic device for applications in circulating tumour cell detections. Colloids Surf B Biointerfaces. 151 (2017) 39-46.

[15] Y. Jiang, S. Zou, X. Cao, A simple dendrimer-aptamer based microfluidic platform for E. coli O157: H7 detection and signal intensification by rolling circle amplification. Sens. Actuators B Chem. 251 (2017) 976-984.

[16] X. Hao, P. Yeh, Y. Qin, Y. Jiang, Z. Qiu, S. Li, X. Cao, Aptamer surface functionalization of microfluidic devices using dendrimers as multi-handled templates and its application in sensitive detections of foodborne pathogenic bacteria. Anal. Chim. Acta. 1056 (2019) 96-107.

[17] P.W. Akers, N.C.H. Le, A.R. Nelson, M. McKenna, C. O'Mahony, D.J. McGillivray, D.E. Williams, Surface engineering of poly(methylmethacrylate): Effects on fluorescence immunoassay. Biointerphases. 12 (2017) 02C415.

[18] H. Zhang, K. Müllen, S. De Feyter, Pulsed-force-mode AFM studies of polyphenylene dendrimers on self-assembled monolayers. J. Phys. Chem. C. 111 (2007) 8142-8144.

[19] S. Wang, T. Chinnasamy, M.A. Lifson, F. Inci, U. Demirci, Flexible substrate-based devices for point-of-care diagnostics. Trends Biotechnol. 34 (2016) 909-921.

[20] S. Martorell, S. Palanca, A. Maquieira, L.A. Tortajada-Genaro, Blocked recombinase polymerase amplification for mutation analysis of PIK3CA gene. Anal Biochem. 544 (2018) 49-56.

[21] I.M. Lobato, C.K. O'Sullivan, Recombinase polymerase amplification: Basics, applications and recent advances. Trends Anal. Chem. 98 (2018) 19-35.

[22] J. Li, J. Macdonald, F. von Stetten, A comprehensive summary of a decade development of the recombinase polymerase amplification. Analyst. 144 (2018) 31-67.

[23] N. Dey, C. Williams, B. Leyland-Jones B, P. De, Mutation matters in precision medicine: A future to believe in. Cancer Treat. Rev. 55 (2017) 136-149.

[24] S. Martorell, L.A. Tortajada-Genaro, A. Maquieira, Magnetic concentration of allele-specific products from recombinase polymerase amplification. Anal. Chim. Acta. 1092 (2019) 49-56.

[25] H. Ravan, S. Kashanian, N. Sanadgol, A. Badoei-Dalfard, Z. Karami, Strategies for optimizing DNA hybridization on surfaces. Anal. Biochem. 444 (2014) 41-46.

[26] H. Willems, A. Jacobs, W.W. Hadiwikarta, T. Venken, D. Valkenborg, N. Van Roy, J. Hooyberghs, Thermodynamic framework to assess low abundance DNA mutation detection by hybridization. PloS one. 12 (2017) 0177384.

[27] R. Ranjan, E.N. Esimbekova, V.A. Kratasyuk, Rapid biosensing tools for cancer biomarkers. Biosens. Bioelectron. 87 (2017) 918-930.

[28] A. Lázaro, L.A. Tortajada-Genaro, A. Maquieira, Enhanced asymmetric blocked qPCR method for affordable detection of point mutations in KRAS oncogene. Anal. Bioanal. Chem. 413 (2021) 2961-2969.

SUPPLEMENTARY INFORMATION

Experiment protocol. Surface characterization

Water contact angle measurements. Contact angle measurements were performed using the sessile drop method. After deposition of 1 µL drops of MilliQ water on chips, images were taken by a contact angle measuring system (One Attension equipment, Biolin Scientific). Droplet profiles were fitted using different mathematical functions and the mean contact angle was reported.

Atomic force microscopy (AFM). Surface measurements were obtained using Multimode 8 microscope (Bruker-Nano Inc.) equipped with a heater-cooler stage, FESPA and TAP 150 cantilevers and NanoscopeV controller. Images (1 μm^2) were analyzed, calculating the root mean square roughness (Rq).

Experiment protocol. Estimation of probe immobilization density

The immobilization density ($d_{immbolization}$) was calculated by determining the amount of immobilized oligo expressed in moles per unit area. Conjugates of COOH-dendrimer with dual labelled probe (5'-NH_2-T_{12}TGATTACAGCCGGTGTACGACCCT-Cy5-3'), at concentration between 10 nM and 2 µM, were dispensed onto PC surface (volume = 40 nL). Considering the surface area of spot (diameter = 300 µm), fluorescence signals were registered and a linear regression was estimated. The equation was *Signal = 2800 + 830* $d_{immobilization}$, $r^2 = 0.993$, being the immobilization density expressed as pmol cm^{-2}. Washing steps removed excess probe and chips were scanned. The registered fluorescence was interpolated on the calibration curve and the calculated immobilization density was 13 pmol cm^{-2}.

Experiment protocol. Fabrication of alternative chips

For optimization and comparison purposes, additional chips were fabricated. In all cases, the initial step was substrate activation by plasma UV/ozone oxidation.

EDA/COOH-PAMAM chips (two-steps protocol). A solution composed by non-conjugated dendrimer (0.65 mM) and EDC (50 mM) was prepared and dispensed on the activated chip based on spin coating technique. Film was formed by spin-coater equipment (WS-650Mz-23 NPPB, Laurell Technologies) at 3000 rpm for 60 s. Later, each NH_2-oligonucleotide probe (100 nM) in printing solution was spotted in array format by non-contact printer equipment (1500 CE, Biodot). The conditions were drop volume 40 nL, room temperature and 70 % humidity. The chips were incubated for 1 h, washed with PBS-T and water, dried and stored at 4 °C until use.

*APTES/COOH-PAMAM chips***.** Alternative amination chemistry was performed on the basis of the silanization with (3-aminopropyl)-triethoxysilane (APTES, Sigma Aldrich). Also, 1H,1H,2H, perfluorodecyltriethoxysilane (PFTS, Alfa Aesar) was added in order to increase the hydrophobic nature of surface. Briefly, the activated chips were immersed in functionalization solution (APTES 1%, PFTS0.1% in isopropanol) for 1 h, room temperature and stirring. Chips were washed several times with isopropanol, air-dried and heated at 110 °C for 1 h. Then, surface amino groups were coupling with carboxyl groups of dendrimers by EDC/NHS reaction, after nano-dispensation (40 nL). The chips were incubated for 1 h, washed with PBS-T and water, dried and stored at 4 °C until use.

EDA/NH_2-PAMAM chips. Amine functionalized dendrimers (NH_2-PAMAM dendrimer, generation 3.0, Sigma Aldrich) were immobilized in active-amino-plastic chip using glutaraldehyde crosslinking. The treatment of activated chips consisted in incubation of cross-linker solution (EDA 1%, EDC 50 mM) and followed by glutaraldehyde (0.2%) in PBS buffer. Non-contact printing of NH_2-dendrimer conjugated with NH_2-probe via glutaraldehyde (0.2%) yielded the probe immobilization after 1 h at room temperature.

Non-cross linker chips. Direct immobilization of oligonucleotides was also performed. Amine-DNA probes in printing solution (MES buffer 0.1 M and EDC 50 mM) were nano-dispensed on the activated surface (40 nL). After 1 h at room temperature, the reagent excess was removed washing with PBS-T and water.

ICPTS chips. These non-dendrimer plastic biochips were fabricated using 3-(triethoxysilyl)propyl isocyanate (ICPTS, Sigma Aldrich) as silanization reagent. After photo-activation, a solution of ICPTS (1%) in isopropanol was incubated for 1 h at room temperature. Chips were washed several times with isopropanol, air-dried and heated at 110 °C for 1 h. Amine-DNA probes in printing solution (MES buffer 0.1 M and EDC 20 mM) were nano-dispensed on the activated surface (40 nL). After 1 h at room temperature, the reagent excess was removed washing with PBS-T and water.

VTES chips. Thiol-probes were grafted on activated plastic chips by thiol-ene click chemistry reaction. After photo-activation, a solution of vinyltriethoxysilane (VTES, Sigmal-Aldrich) at 1% and isopropanol at 3 % was incubated for 1 h at room temperature. Chips were washed several times with isopropanol, air-dried and heated at 110 °C for 1 h. Thiol-DNA probes in PBS buffer were nano-dispensed on the activated surface (40 nL). Finally, chips were irradiated during 30 s by UV-ozone at 254 nm, washed and dried.

Experiment protocol. Optimization of blocked RPA

Reaction time of blocked RPA. Blocked amplification wild type products at variable concentration of ddC blocker (0-600 nM) were amplified at 37ºC at different times (0-50 minutes). RPA amplicons were separated by gel electrophoresis (2 % agarose) and band intensities were registered. The results were confirmed performing amplification with TS2 Qiagen equipment at different reaction times.

Concentration of blocking agent and primers Different amounts (0-150 nM) of ddC blocker oligonucleotide were mixed with 4 ng of wild type, FFPE mutant genomic samples and negative control with a premix of 480 nM upstream primer and downstream digoxigenin-labeled primer, 280 mM of magnesium acetate and 29.5 µL of rehydrated pellet, which contains a recombinase polymerase enzyme in a total volume of 50 µL. Different ratios of upstream and downstream digoxigenin-labeled primer (ratios between 1:1 to 10:1 for FP/RP and RP/FP) were mixed with 4 ng of wild type and FFPE mutant genomic samples, 50 nM of blocking agent, 280mM of magnesium acetate and 29.5 µL of rehydrated pellet in a total volume of 50 µL. The used heating system was a simple laboratory heater (Memmert) at 37°C for 40 min for both experiments.

Detection of blocked products and single-nucleotide mutation based on blocked RPA hybridization. Five arrays of allele-specific probes (wild type, mutant and negative control) were printed per chip, including four replicates per target probe and controls (chip layout was 4×3). Blocked amplification products of RPA and PCR aproach at different concentrations were hybridized onto chip. Five arrays of allele-specific probes (wild type, G>T, G>A, G>C) were printed per chip, including four replicates per target probe (chip layout was 4×4) Blocked RPA *KRAS* gene product was hybridize onto chip. Restrictive conditions of hybridization (2xSSC, 25% formamide) were applied for 1 hour at 37ºC.

Table S3.1. List of used oligonucleotides. (a) Optimization assay. (b) Mutational analysis of human samples

(a)

Target	Use	Sequence 5'-3'
A	Thiol-probe	TTGCTGATTTTCAACATCAGTCTGATAAGCTA-T_{10}-SH
	Amine-probe	GATTTTCAACATCAGTCTGATAAGCTATTTTT-NH_2
	Target	TAGCTTATCAGACTGATGTTGAAAATCAGCAA-DIG
B	Thiol-probe	TTGCTGATTTCAGCTGCTTTTGGGATTCCGTTG-T_{10}-SH
	Amine-probe	GATTTCAGCTGCTTTTGGGATTCCGTTGTTTTT-NH_2
	Target	CAACGGAATCCCAAAAGCAGCTGAAATCAGCAA-DIG
C	Thiol-probe	TTGCTGATTTACCCCTATCACGATTAGCATTAA-T_{10}-SH
	Amine-probe	GATTTACCCCTATCACGATTAGCATTAATTTTT-NH_2
	Target	TTAATGCTAATCGTGATAGGGGTAAATCAGCAA-DIG

(b)

Use	Gene	*Sequence 5'-3'*
FP	*KRAS*	CTGAATATAAACTTGTGGTAGTTG
	NRAS	CCTGTTTGTTGGACATACTGGATA
	BRAF	TGATGGGACCCACTCCATC
RP	*KRAS*	CTCTATTGTTGGATCATATTCGT-DIG
	NRAS	DIG-TTCGCCTGTCCTCATGTATTG
	BRAF	TTTCTTCATGAAGACCTCACAG-DIG
Probe	*KRAS*	NH_2-C_6-T_5-TTTTTGTTGGAGCTGGTGGCGTAGG
	NRAS	NH_2-C_6-T_5-ATACAGCTGGACAAGAAGAGTACA
	BRAF	NH_2-C_6-T_5-CCATCGAGATTTCACTGTAGCTAGA

(c)

Gene	Use	*Sequence 5'-3'*
BRAF	FP	TGATGGGACCCACTCCATC
	RP	TTTCTTCATGAAGACCTCACAG-DIG
	Blocker	CCATCGAGATTTC**A**CTGTAGCTAGA-TTCC-23ddC
	p.Wild-type	NH_2-C_6-T_5-CCATCGAGATTTC**A**CTGTAGCTAGA

p.*BRAF V600E*	NH_2-C_6-T_5-CCATCGAGATTTC**T**CTGTAGCTAGACC

FP: upstream or forward primer; RP: downstream or reverse primer; p: probe; DIG: digoxigenin; 23ddC: 2',3'-dideoxyC functionalization.

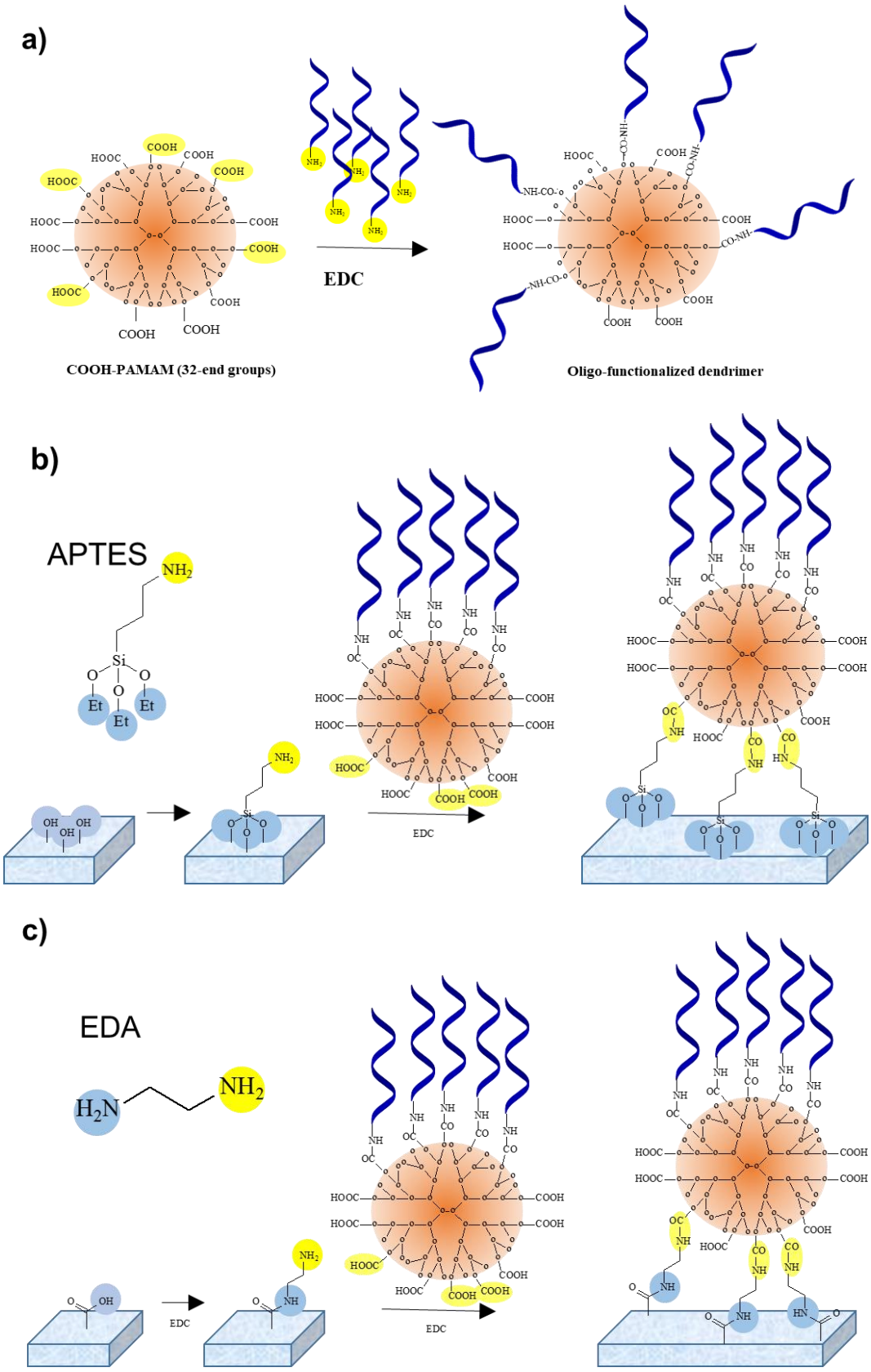

Fig. S3.1. Reaction schemes: (a) Synthesis of carboxylic oligo-functionalized dendrimers. (b) APTES-mediated immobilization. (c) EDA-mediated immobilization.

a)

APTES	0% PFTS	0.1% PFTS
1%		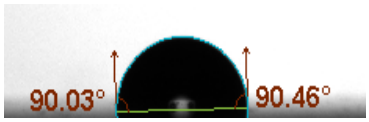
2%	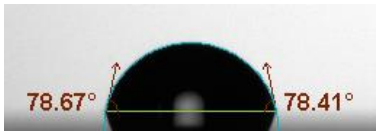	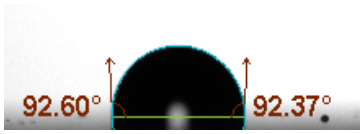
3%	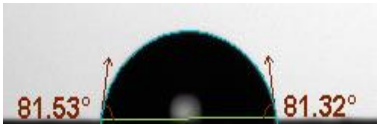	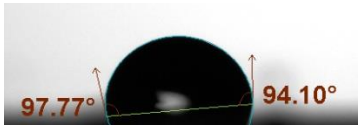

b)

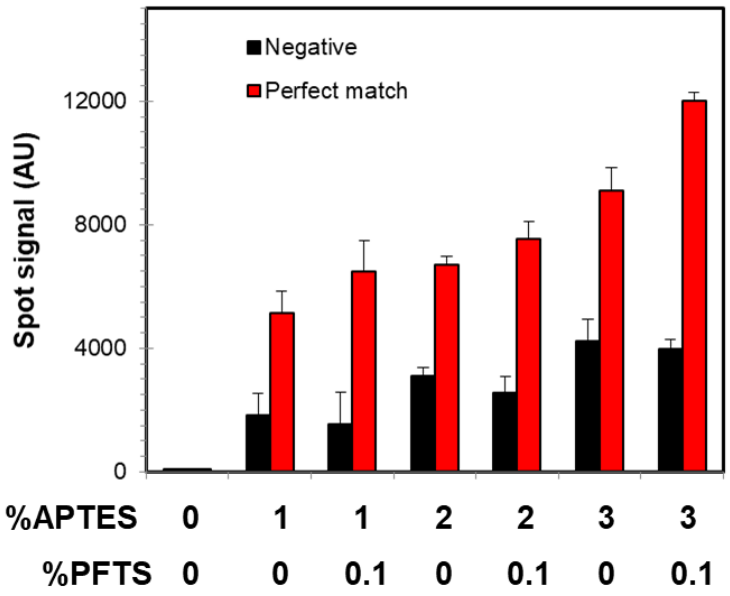

Fig. S3.2. Binding of carboxylic oligo-functionalized dendrimers to thermoplastics via APTES sylanization. Images of contact angle (a) and spot signals (b), at different APTES/PFTS concentrations.

Table S3.2. Registered optical responses of APTES functionalized chips after hybridization assay. Chip: polycarbonate. Probe: carboxylic DNA-dendrimer.

	Mix A	Mix B	Mix C	Mix D	Mix E	Mix F	Mix G
Target 1	100	80	60	50	40	20	0
Target 2	0	20	40	50	60	80	100
Image	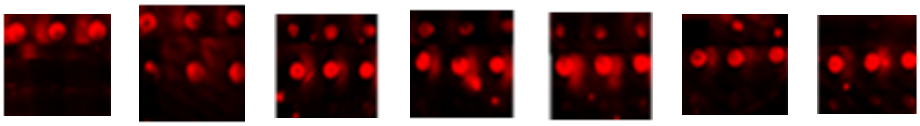						
Signal 1	1.00	0.96	0.95	0.94	0.73	0.35	0.00
Signal 2	0.00	0.52	0.55	0.60	0.63	0.64	1.00
Signal C	0.12	0.11	0.16	0.14	0.14	0.15	0.16

Row 1: target 1, Row 2: target 2. Row 3: negative control,

a)

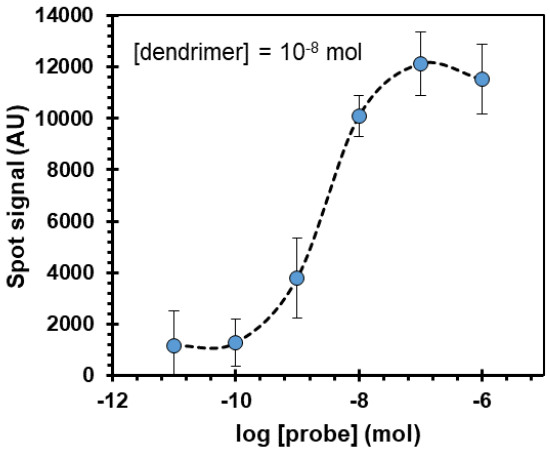

b)

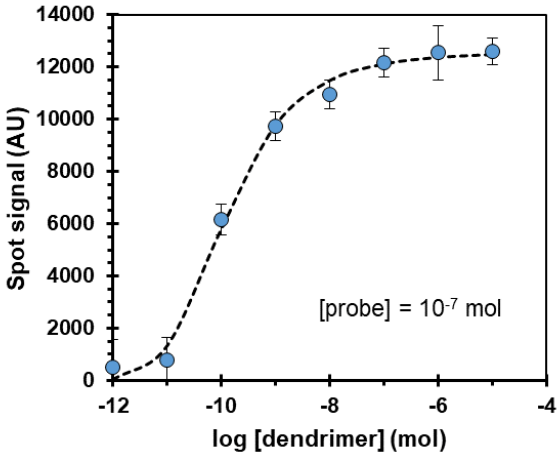

c)

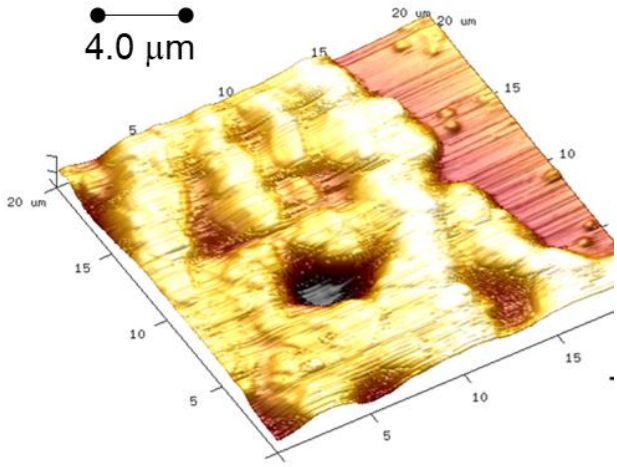

Fig. S3.3 (a) Effect of probe amount on the registered signal. (b) Effect of dendrimer amount on the registered signal. (c) AFM image of array spot after deposition of oligo-conjugated dendrimer at 10 nM. The image shows the spot edge (area 400 μm^2, height scale 1 µm). Material: PC.

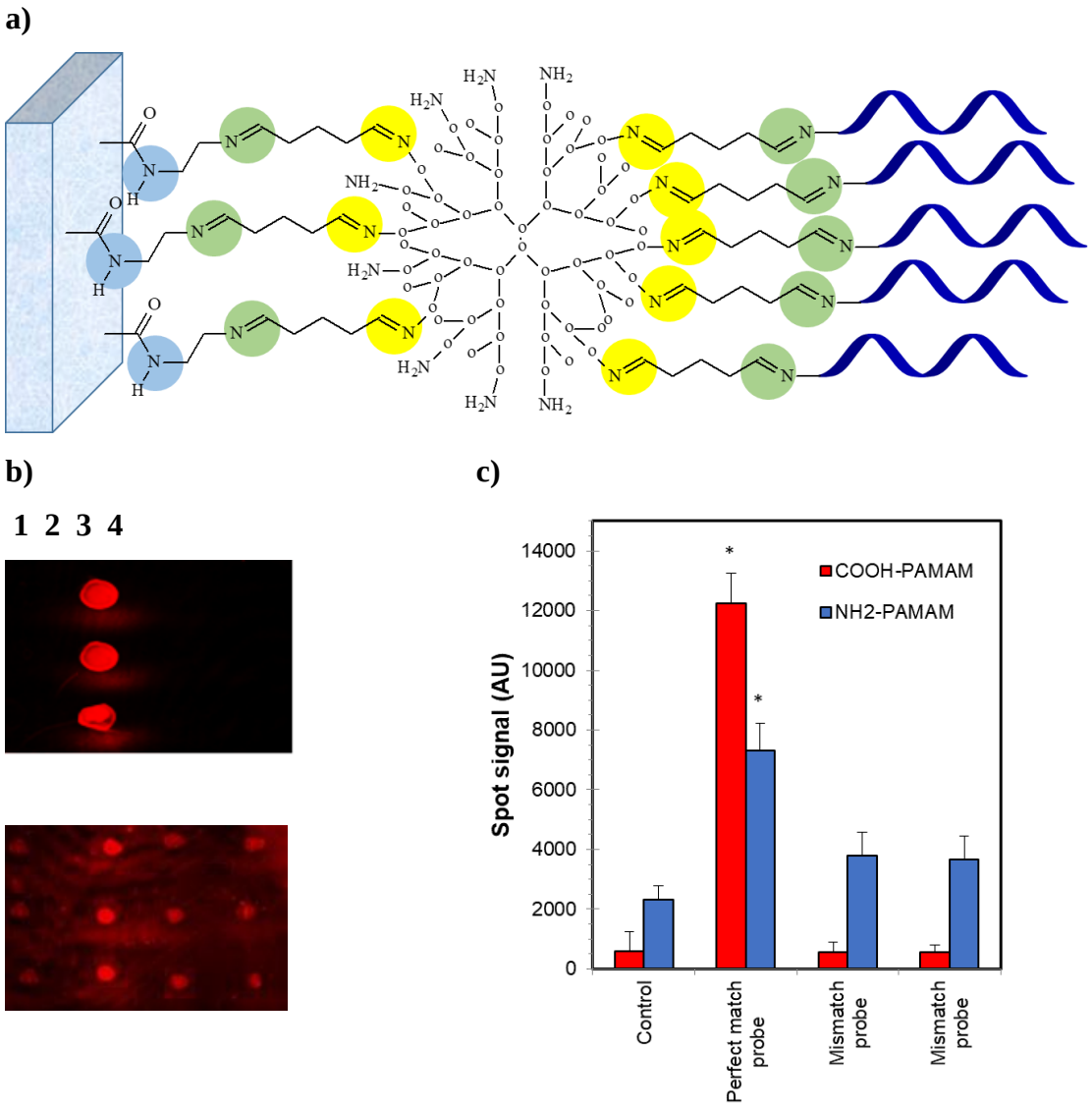

Fig. S3.4. Nature of dendrimer. **(**a) Reaction scheme of immobilization of amine-dendrimer/probe. (b) Array images for carboxyl-dendrimer/probe hybrids (top) and amine-dendrimer/probe hybrids (bottom). 1: control, 2: perfect-match probe; 3: mismatch probe; 4: mismatch probe. (c) Spot intensity in hybridization assay depending on the coupling chemistry and probe sequence. DNA target: $1.8 \cdot 10^{11}$ copies.

Table S3. Comparison of PC and COP chips based on contact angle measurements.

	PC	COP
Raw material	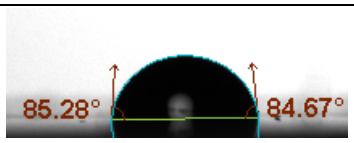	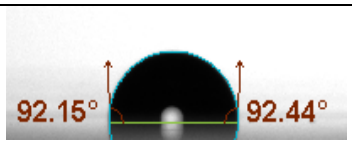
Photoactivation	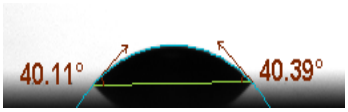	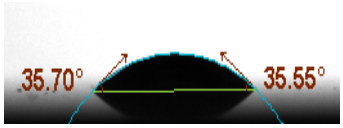
EDA functionalization	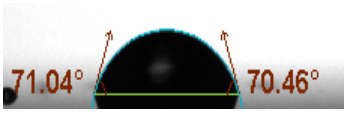	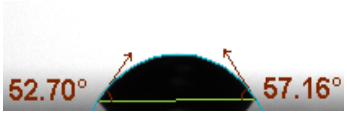
Final chip		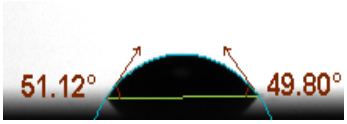

Table S3.4. Comparison of DNA chips based on dendrimer approaches. Material: PC.

	Dendrimer-mediated immobilization	**Oligo-conjugated dendrimers**
Reagents	COOH-PAMAM	Oligo-functionalized PAMAM
Dendrimer amount*	30 mL/chip	12 μL/chip (2,500 times less)
Protocol	Step 1. Dendrimer film formation by spin coating Step 2. Immobilization of amino probes	Direct synthesis and immobilization
Equipment	Spin coater Arrayer	Arrayer
Time	150 min	110 min (reduction of 26 %)
Image	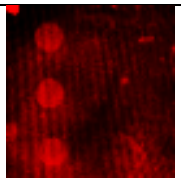	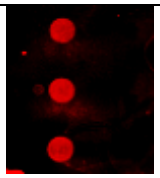
Spot signal	19,600	21,800
Background signal	12,000±1,000	6,000±200 (reduction of 50%)

* Chip: 25 mm × 75 mm (18.75 cm^2), 300 spots/chip, spot diameter 350 μm, dispensation volume 40 nL.

Table S3.5. Dendrimer-mediated immobilization of oligonucleotides. Effect of dendrimer concentration for film formation on surface morphology and roughness (±0.05 nm). Spin-coating: 3,000 rpm for 60 s. Rq: root mean square deviation of assessed profile.

[PAMAM]	0 M	10^{-8} M
Image	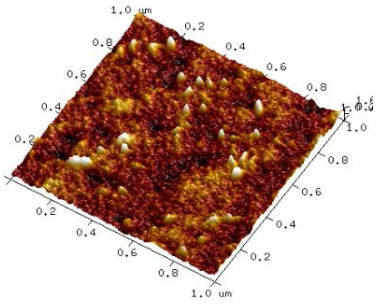	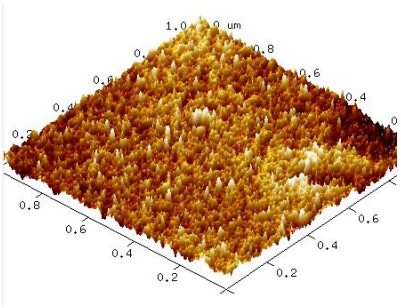
	Depth range = 4 nm Rq = 0.66 nm	Depth range = 8 nm Rq = 1.17 nm
[PAMAM]	10^{-6} M	10^{-4} M
Image	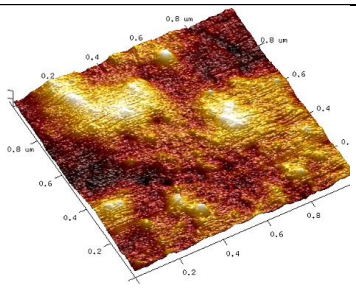	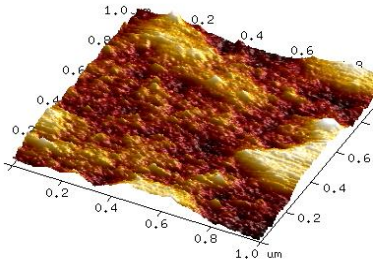
	Depth range = 10 nm Rq = 1.89 nm	Depth range = 10 nm Rq = 1.59 nm

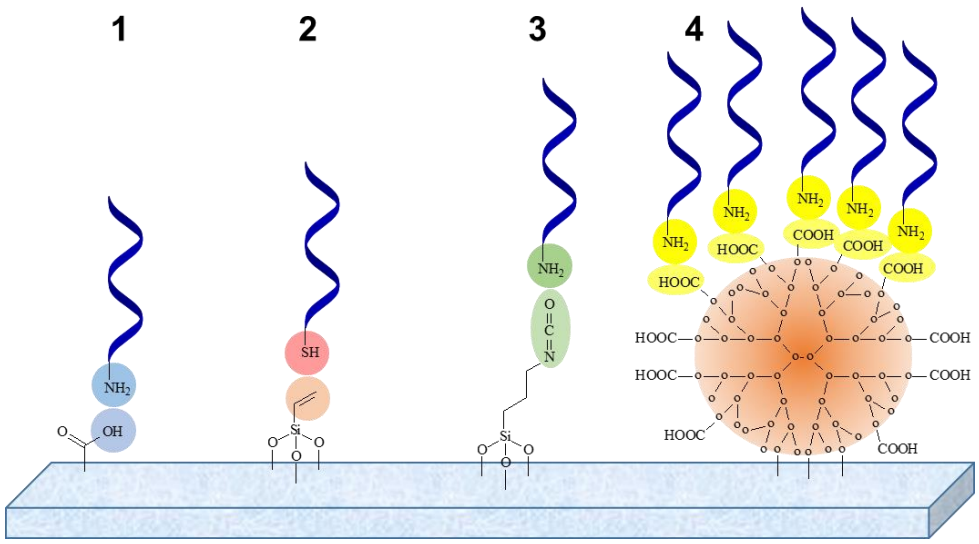

Fig. S3.5. 2D strategies for immobilization of oligonucleotide probes. 1: Direct EDC coupling. 2: Silanization by ICPTS and EDC coupling. 3: Silanization by VTES and photoclick-chemistry. 4: Dendrimer-mediated EDC coupling.

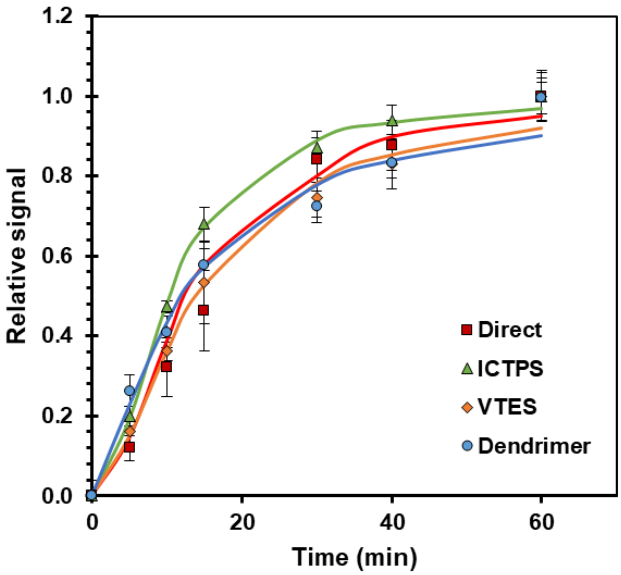

$S = 1 - \frac{1}{1 + \left(\frac{t}{a}\right)^{b}}$	Direct	ICPTS	VTES	Dendrimer
A	14.87	10.41	14.08	12.16
B	2.13	1.96	1.68	1.38
R^2	0.992	0.998	0.988	0.975

Fig. S3.6. Comparison of DNA immobilization chemistries on hybridization kinetics at 37 ºC. Assay: Hybridization in array format. Target: complementary oligonucleotide. Model: logistic equation obtained from relative spot intensity (S) and hybridization time (t). Replicates: 3 spots.

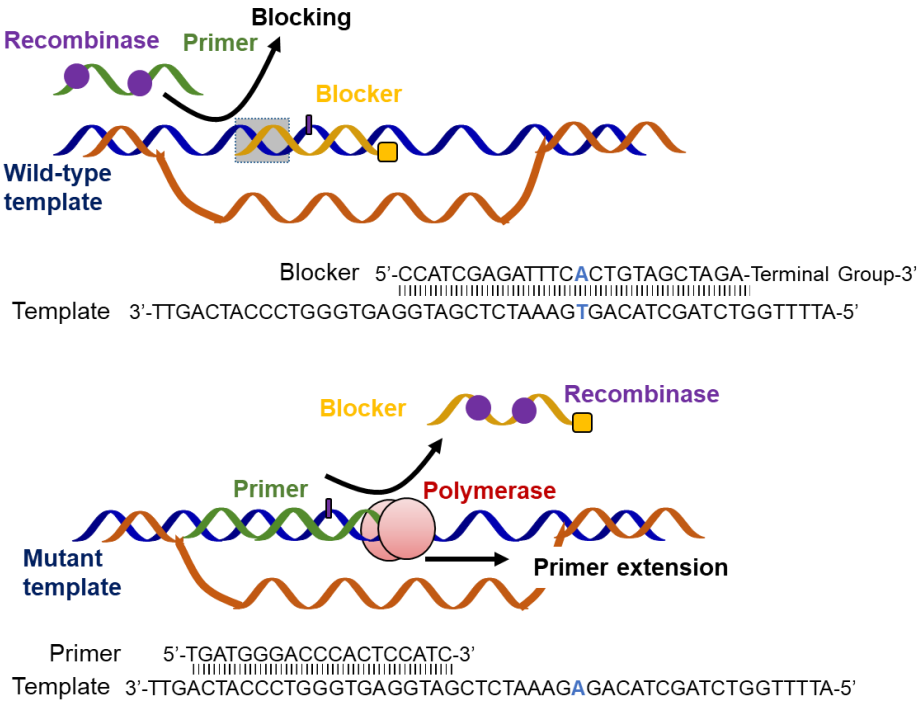

Fig. S3.7. DNA amplification mechanism of blocked RPA: wild-type variant (top) and mutant variant (bottom). Grey rectangle indicates the overlapping region between primer and blocker for enhancing the clamping effect

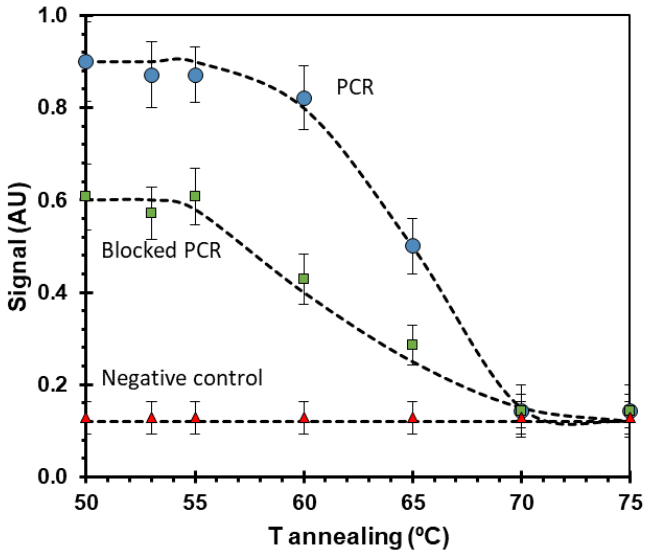

Fig. S3.8. Effect of annealing temperature on PCR clamp of *BRAF* gene using the selected oligonucleotide set (primers and blocker). Sample: Wild-type genomic DNA. (wild-type base: thymine).

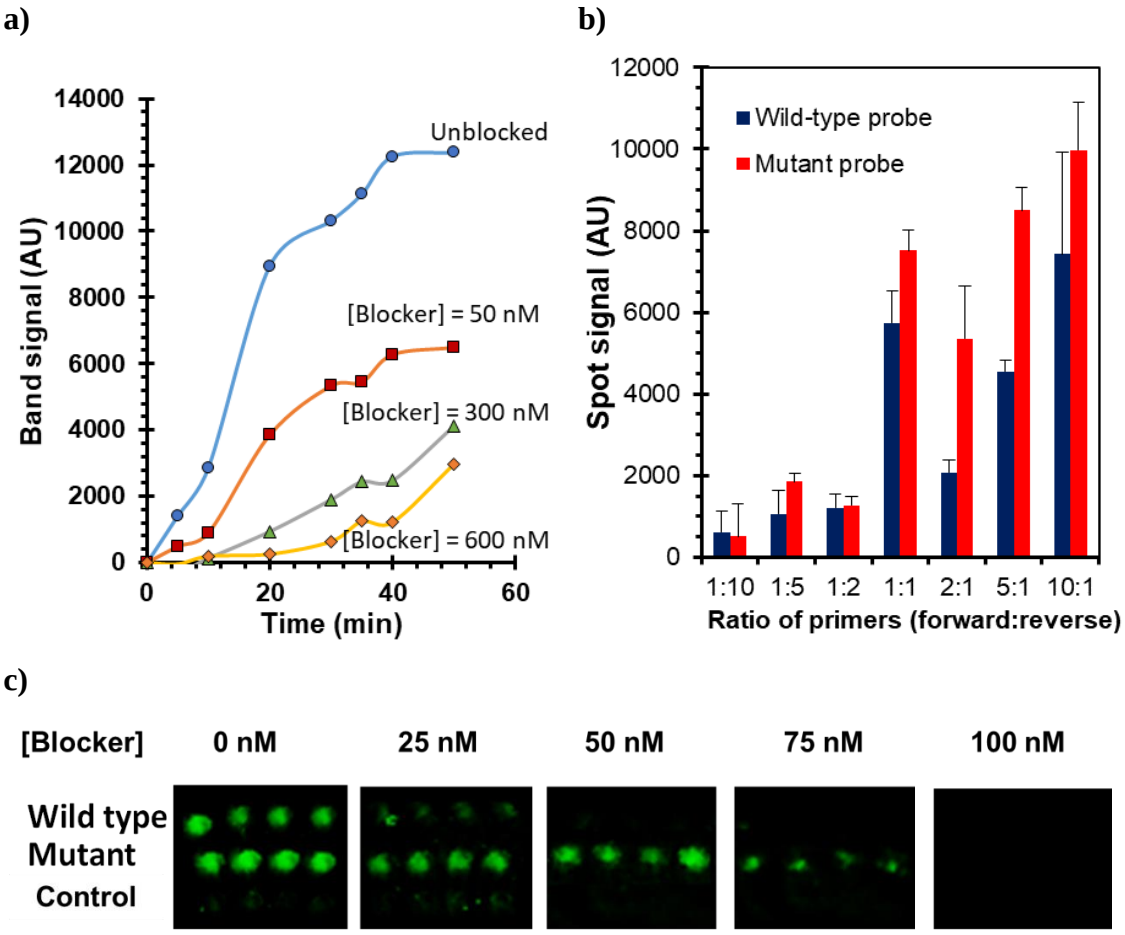

Fig. S3.9. Optimization of blocked RPA. (a) Amplification kinetics at different amounts of ddC blocker. Sample: Wild-type genomic DNA. Technique: Agarose gel electrophoresis (b) Effect of forward primer:reverse primer stichometry (asymmetric amplification. Sample: Wild-type genomic DNA. Technique: Chip hybridization assay. (c) Array images depending on blocker concentration. Sample: Mutant genomic DNA. Technique: Chip hybridization assay.

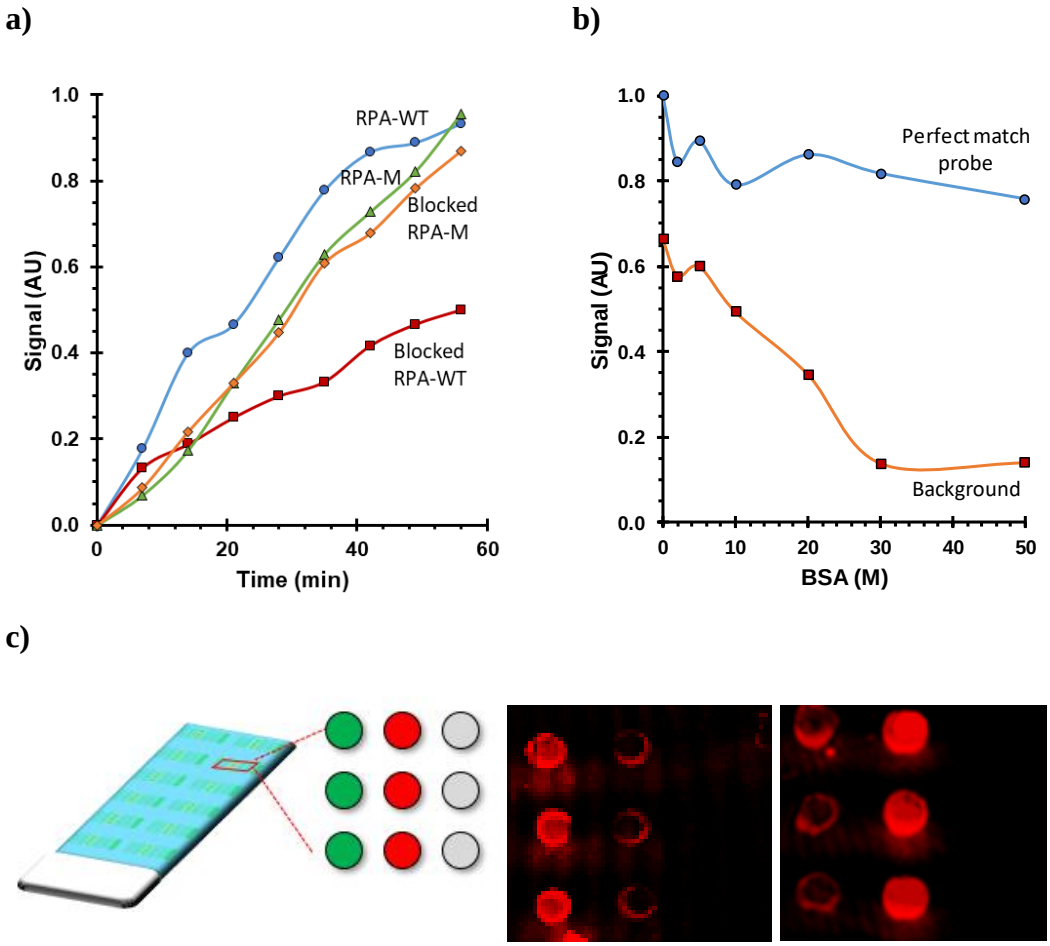

Fig. S3.10. Detection of *BRAF* p.V600E mutation (c.1799T>A) based on blocked RPA. (a) Kinetic curve for standard RPA and blocked RPA from wild-type and mutant patients. (b) Spot intensity at different concentration of BSA used for chip treatment. (c) Array assay for blocked RPA products: chip layout (left), wild-type patient (central), and mutant patient (right). Probes: wild-type (green), p.V600E (red) and negative control (grey).

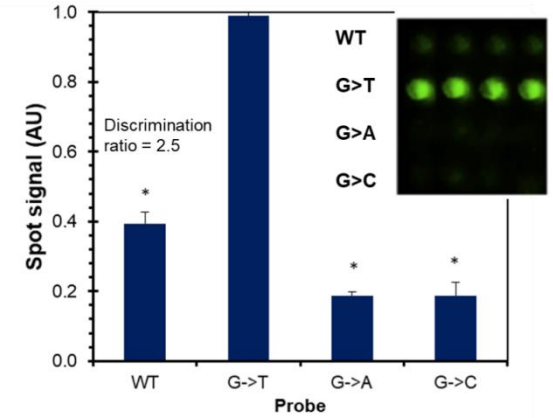

Fig. S3.11. Mutation discrimination based on blocked RPA and chip hybridization assay from a cancer patient sample. Insert: Array image for discrimination wild type and mutant bases of *KRAS* gene at hybridization assay. Genotype patient:mutant base: thymine (confirmed by sequencing technique). Student t-test: * indicates p<0.00

Capítulo 4

Genosensor para la detección de la mutación PIK3CA^{H1047R}basada en amplificación por recombinasa-polimerasa bloqueada en chips dendronizados

Resumen

El capítulo 4, se centra en el desarrollo de un genosensor integrado para la detección de la mutación puntual *PIK3CA^{H1047R}*, combinando los elementos desarrollados a lo largo de la presente tesis doctoral. Para ello, se han desarrollado chips de policarbonato con microcanales fluídicos de alta densidad, mediante el anclaje covalente de híbridos dendrón-DNA, obteniendo así, un genosensor que permite la detección sensible y rápida de productos selectivos procedentes de la RPA-bloqueada.

Estos sistemas 3D basados en híbridos DNA-dendrón fueron comparados con los desarrollados en el capítulo anterior basados en híbridos DNA-dendrímeros y con sistemas 2D. Ambas moléculas dendriméricas presentaron mejores prestaciones analíticas que los sistemas lineales, dada la mayor densidad superficial de sitios de unión a sondas alelo-específicas, la gran flexibilidad de las ramas que conforman su estructura, la reducción de impedimentos estéricos y la distancia superficie-sonda.

La plataforma desarrollada ha permitido la detección sensible (10-100 veces superior que los sistemas lineales), selectiva (95%) y multiplexada de producto de RPA-bloqueada procedente de tejido parafinado de pacientes patológicos de CCR. El desarrollo del genosensor presentado, contribuye a la generación de plataformas integradas con requisitos ASSURED: asequible, sensible, específico, fácil de usar, rápido y robusto, sin equipo y en punto de atención.

Genosensor for *PIK3CA*^{H1047R}single point mutation detection based on blocked recombinase polymerase amplification in dendron-chip

Abstract:

An integrated genosensor was developed for selective and sensitive *PIK3CA*^{H1047R} mutation detection based on the combination of selective isothermal blocked-RPA amplification and high-density dendron polymer chip. To reach the detection limit of *PIK3CA*^{H1047R} blocked-RPA products, DNA-dendron hybrids were conjugated by fast click chemistry and immobilized onto active polymer surface to create forest-array chips with multipoint-sites. The sensitive, versatile, multiplex and easy to read colorimetric dendritic platform exhibit multi-attaching sites for blocked-RPA recognition in comparison with linear surfaces (10-100 folds). This portable and low cost genosensor is sensitive (detection limit genomic DNA: 0.02ng/µL), specific (single-base differentiation (95%)), and isotherm (37ºC).

Introduction

PIK3CA (phosphoinositide-3-kinase, catalytic alpha polypeptide) gene mutation has been located in colorectal, breast, glioblastoma, gastric, ovary, lung, and skin human cancers (Wang, 2014). Concretely, *H1047R* is a hotspot mutation that lies within the kinase domain of *PIK3CA*, and results in increased phosphorylation of AKT, growth factor-independent cell survival, and transformation in cell culture. The selective and sensitive detection of this single nucleotide variation from heterogeneous pathological samples is critical for early diagnosis, individualized therapy and prognosis (Wang, 2014). Although conventional methods such as PCR or sequencing as been applied for *PIK3CA*^{H1047R} gene mutation detection, *point-of-care* testing (POCT) in decentralized laboratories to expand testing capacity is demanded (Zarei, 2017).

In this context, recombinase polymerase amplification (RPA) has emerged as a novel sensitive, selective and isothermal technique for molecular diagnosis, with excellent operational conditions for integrated devices (Li, 2018). Compared to PCR-

based assay and loop-mediated isothermal amplification (LAMP), RPA is faster (20-40 min), simpler to perform, due requires a lower temperature (25-37°C) and previous denaturation step or expensive equipment is not nedded, which results in lower energy consumption (Lei, 2020). Furthermore, this technology has been applied in automated microfluidic devices, reducing the volume reaction (Yin, 2020) and combined with integrated POCT devices. For instance, RPA has been integrated recently in electrochemical (Khaliliazar, 2020), surface Raman scattering (SERS) (Wang, 2017), microarray based biosensors (Lázaro, 2019) and lateral flow assay (LFA) (Ivanov, 2020). All these features, position RPA as a potencial candidate for the exploitation and commercialization of kits and consumables with affordable, easy-to-use, fast, robust and equipment-free solutions in descentralized laboratories and low-resource environments (Mondal, 2016).

Despite RPA mechanism is highly selective (Lobato, 2018), the detection of single point mutations in heterogeneous specimens, where the concentration of mutant alleles is presented in low proportions in a native matrix is a complex challenge. For that purpose, Blocked-RPA approach as been applied for selective amplification based on the enrichment of minority alleles in *PIK3CA*^{H1047R} mutation. This RPA variant is based on the addition of ddC-blocking agent that overlaps partially with native complementary sequence from the 5' end (Martorell, 2018). Blocked-RPA amplification mechanism only uses 3 oligonucleotides (2 primers and a dideoxycytidine blocking agent) compared to other isotherms that need 4 or 6 primers such as LAMP or SDA technique (Lei, 2020). Moreover, this selective method is fast and no-expensive equipment is required compared with PNA-PCR based method developed previosly for selective *PIK3CA* gene detection (Zeng, 2017).

To reach the detection limit required for detection of *PIK3CA*^{H1047R} blocked-RPA products, dendritic molecules were conjugated with allele-specific probes for the construction of sensitive, versatile, multiplex and easy to read colorimetric microarray chip. Those dendritic structures (dendrimers and dendrons) are hiperbranched polymers with multiattaching sites and are capable of self-organizing into surfaces (Erdem, 2018). Concretely, dendrons are monomers of dendrimers and can be covalent bonded

through the focal point and by the hiperbranched peripheral groups (Kawauchi, 2015) onto solid surfaces. Those dendronized surfaces has been constructed in conventional surfaces such as gold and glass (Caminade, 2006), just a minority of authors have developed integrated plataforms with polymeric surfaces in PDMS or PMMA (Hao, 2019) (Akers, 2017), here, we develop a forest-array biosensor onto polycarbonate chip. For that purpose, DNA-dendron conjugates were photochemically bounded by smart click chemistry and immobilized in activated polymer. This reaction consists of the radical addition of the sulfur atom to the unsaturation, generating a C-S bond, and it is activated by UV photons. So, it can be considered as a click one, because it takes place in few minutes or even seconds with high yields, it does not require additional reagents or catalyst, solvents and it is clean because no subproducts are generated (Bañuls, 2017).

The development of the presented *PIK3CA*^{H1047R} genosensor contributes to the generation of integrated platforms with ASSURED requirements: Affordable, Sensitive, Specific, User-friendly, Rapid & robust, Equipment-free, and Delivered.

Materials and methods

Materials

PC (polycarbonate, Makrolon®) was used as polymer substrate (dimensions 75 mm × 25 mm). Polyester bis-MPA dendron, 8 acetylene, 1NHBoc core (generation 3), N-hydroxysuccinimide (NHS), bovine serum albumin (BSA), 2-(N-morpholino) ethanesulfonic acid (MES), 1-ethyl-3-(3-dimethylaminopropyl) carbodiimide (EDC) were purchased from Sigma-Aldrich. The reagents used for genomic DNA extraction were GeneRead DNA FFPE Kit (Qiagen, Hilden, Germany) and PureLink extraction kits (Invitrogen). DNA amplification kits for PCR and RPA were DNA Amplitool kit (Biotools, Spain) and TwistAmp Basic RPA kit (TwistDx, UK), respectively. The array printing solution was EDC at 50 mM and NHS 50 mM in MES 0.1 M. The hybridization buffer was saline-sodium citrate (SSC) 1×: sodium chloride at 150 mM, sodium citrate at 15 mM, formamide 25% (pH 7.0). The hybridization washing solution was composed by NaCl 15 mM and trisodium citrate 1.5 mM. The developing buffer (pH 7.4) was a solution of Tween 20 (0.05%) in phosphate buffered saline (PBS), containing 137 mM NaCl, 12 mM

phosphate and 2.7 mM KCl. Monoclonal anti-Dig antibody and monoclonal antisheep-HRP antibody were supplied by Abcam. The HRP-substrate was 3,3',5,5'-tetramethylbenzidine solution (ep(HS)TMB-mA, SDT Reagents). DNA oligomers were purchased from Eurofins (Table SI.1).

Fabrication of planar chip

The amino-protected dendron (10 mg/mL) was mixed in 10% methanol in the presence of chloridric acid (3M) during 3 hours by end-over-rotation to favor the homogeneous deprotection reaction and neutralized with sodium hydroxide (1.5 M). The conjugation of the deprotected alkyne-dendron (10^{-8}M) terminated in amino groups with the thiolated DNA probes (100 nM) was carry out in 0.05 M EDC/NHS/MES buffer by click chemistry using UV light at 254 nm for 30 seconds. The dendron-DNA conjugate solution was stored at 4 ºC until use. Polycarbonate substrates were functionalized by plasma UV/ozone oxidation and incubated with sodium hydroxide as previously described (Martorell, 2018) to generate carboxylic acid groups. The dendron-DNA conjugates were immobilized onto the polycarbonate substrates by the carbodimide chemistry. For that, the dendron-DNA conjugate solution was spotted by non-contact printing onto the functionalized surface (drop volume 30 nL, room temperature and 70 % humidity) (1500 AD, Biodot). After 60 min, the surface was washed with PBST and destilled water and dry with air flusing.

Fabrication of micro-cavity array chip

The chip compromised of three layers: two PC sheets (1.0 mm thickness) with an intermediate pressure-sensitive adhesive (PSA) with channels and holes patterned. Chip dimensions were 75 mm x 25 mm x 2.028mm. On bottom layer, the immobilization of DNA-dendron hybrids was performed as described above. Thus, the bottom plate contained seven line-test-arrays of thiol-allele-specific probes conjugated with alkyl dendron, including 6 replicates per target probe. Top layer of PC includes aligned 0.3 cm holes constructed by milling machine (Bungard Elektronik CCD/ATC GmbH & Co.KG). PSA layers were cutted with Grapfhtec Pro equipment (parameters of force: 18 units; velocity: 20 units). Autodesk inventor (CAD-3D) model was used as fluidic chamber chip

design. Each microfluidic chamber is constituted by 7 inputs and outputs (0.3 cm of diameter) connected with 7 hybridization cameras (20µl, 0.5x1 cm^2). The microstructures within the air control layer (chambers and holes) were aligned carefully for uniform liquid channels in order to prevent droplets and air bubles. No linking were observed**.**

DNA-extraction

Genomic DNA was extracted from 5-µm thick FFPE sections using deparaffinization solution and GeneRead DNA FFPE Kit (Qiagen, Hilden, Germany) according to manufacturer's protocol. This isolation kit contains uracil-DNA glycosylase (UDG) that leads to the reduction of C > T sequence artefacts. DNA extraction from human cell HCT 116 (ATCC CCL-247) and buccal cells was performed using PureLink kits (Invitrogen). Concentration of the DNA extracts (ng/µL) was obtained by spectrophotometry using NanoDrop 2000c, and by fluorimetry using Qubit dsDNA HS Assay Kit (ThermoFisher Scientific).

Blocked-RPA amplification

The reaction mixtures for blocked RPA amplification were prepared with rehydrated buffer, 14 mM of magnesium acetate, 480 nM of upstream primer and downstream digoxigenin-labeled primer, 50 nM of blocking oligonucleotide, 4 ng of genomic DNA, and the enzyme pellet. The heating system was a simple laboratory heater (Memmert) at 37°C for 40 min.

Hybridization assay and detection

Amplification products were detected by hybridization assay on the selective DNA probes-conjugates immobilized on chips. Blocked-RPA products (2 µL) were mixed with hybridization buffer (18 µL) and heated (95 °C, 5 min). Then, the solutions were dispensed onto sensing areas and incubated at 37 °C for 60 min. The arrays were rinsed with progressive dilutions of hybridization washing buffer. For chip staining, an immunoreaction was performed. The reagents were anti-dig antibody (1:2500) and HRP-labelled secondary antibody (1:400) in developing buffer. After substrate dispensation, a dark blue solid deposit was formed in positive spots. Polymer-dendronized chips were

directly scanned (Epson Perfection 1640SU office scanner), producing monochromatic images (Tagged Image File Format, color depth 16 bit, scale 0–65535). The optical intensity signals of each spot (230 µm diameter) were quantified using in-home software.

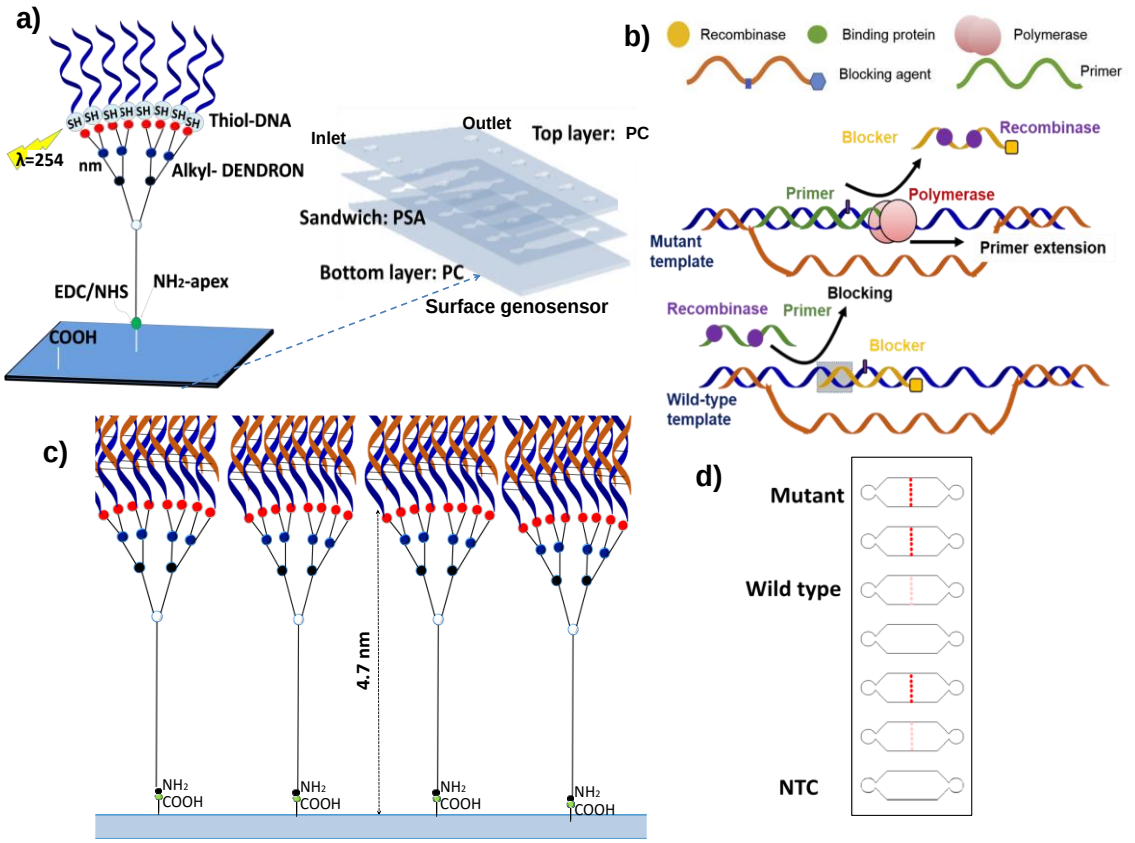

Fig. 4.1: Scheme assay of *PIK3CA*^{H1047R} integrated genosensor. **a**) Dendron-chip fabrication. **b**) Blocked-RPA assay. **c**) On- dendron chip allele specific hybridization. **d**) Colorimetric detection

Results

On-chip assay

The first challenge was to develop an integrate platform to detect low concentration of RPA product. For that, dendron-forest surfaces were building in polymer chip for increasing the disposable anchoring sites per area. Due dendritic structures can be conjugated previously with DNA before immobilized onto planar surfaces (Warner, 2020), here, we conjugate alkyl-hyperbranched dendrons with thiol probes by click chemistry, prior to immobilization onto active polycarbonate surface. For that purpose, DNA-dendron hybrids were conjugated during 0 to 180 seconds and immobilized onto active polymer chip by nanospotting deposition (Fig.S4.1). Background signal was detected at 0 seconds, due the non-specific absorption of DNA-blackbone amino groups with residual carboxylic acid groups of active thermoplastic surface. Denaturation of probes explains the decreasing of spot signal at times up to 50 seconds of UV irradiation. Selected conditions were founded at 30 seconds of irradiation time. Varyng concentrations of alkyl dendron (10^{-5} M to 10^{-10} M) were conjugated with fixed concentration of thiol-probe and, in parallel, different amounts of thiol-probe (10^{-6}M-10^{-12}M) were conjugated by click chemistry with fixed concentration of alkyl dendron (10^{-8} M). The conjugates were immobilized onto active polycarbonate surface and hybridized with complementary target. Saturation curve was observed for concentrations up to 10 nM of allele specific probe (LOD=0.01 nM) and reproducible results (95%) were obtained for replicates intraday-interchip. Selected conditions were founded for 10^{-8} M alkyl-dendron for 10^{-7} M of oligo-DNA.

DNA-Dendron arrays were compared in terms of sensitivity and selectivity with DNA-dendrimer and VTES arrays too. For that purpose, synthetic targets were hybridized with complementary and no-complementary probes. Although 3D and 2D platforms discriminated 100% of the targets, forest surfaces exhibit higher responses (30%) than VTES platform at 100 nM of mismatch/perfectmatch probe concentration (Fig.4.2). Moreover, a calibration assay with complementary target was performance, for that, a concentration range of 0 to 100 nM of target was hybridized with 100 nM of complementary probe and similar responses were obtained for dendronized platforms,

while a reduction of 25±5% was observed for silane surface. The detection limit was founded at 0.005 and 0.05 nM for dendronized and no dendronized platform respectively.

The reduction signal of linear surfaces besides on the disposable sites for anchoring target molecules. While silane platform only has one point site for covalent binding, dendrons and dendrimers exhibit a large number of sites in the same area. Moreover, the flexibility of the branches, the reduction of the steric hindrance and the distance surface-probe promotes higher efficiency in terms of immobilization and hybridization in forest surfaces. Although dendrimers (64 carboxylic acid groups) were conjugated previously with probes in homogeneous media, when the conjugated is immobilized onto plastic surface, the bottom side was not accessible due the free carboxylic acid groups were bounded with amino radical groups of active polycarbonate, but the top of conjugated dendrimer (4.5 nm of diameter; ≈32 oligomers) remains accessible. For dendronization process with dendron architecture, 2 occupied the same area than one dendrimer, generating analogous number of disposable sites for DNA hybridization, showing similar responses for both platforms. The efficiency of click chemistry compared with carbodiimide coupling, mainly less aggregation and higher distance surface-branches of dendron promotes the equal responses with dendrimer array too.

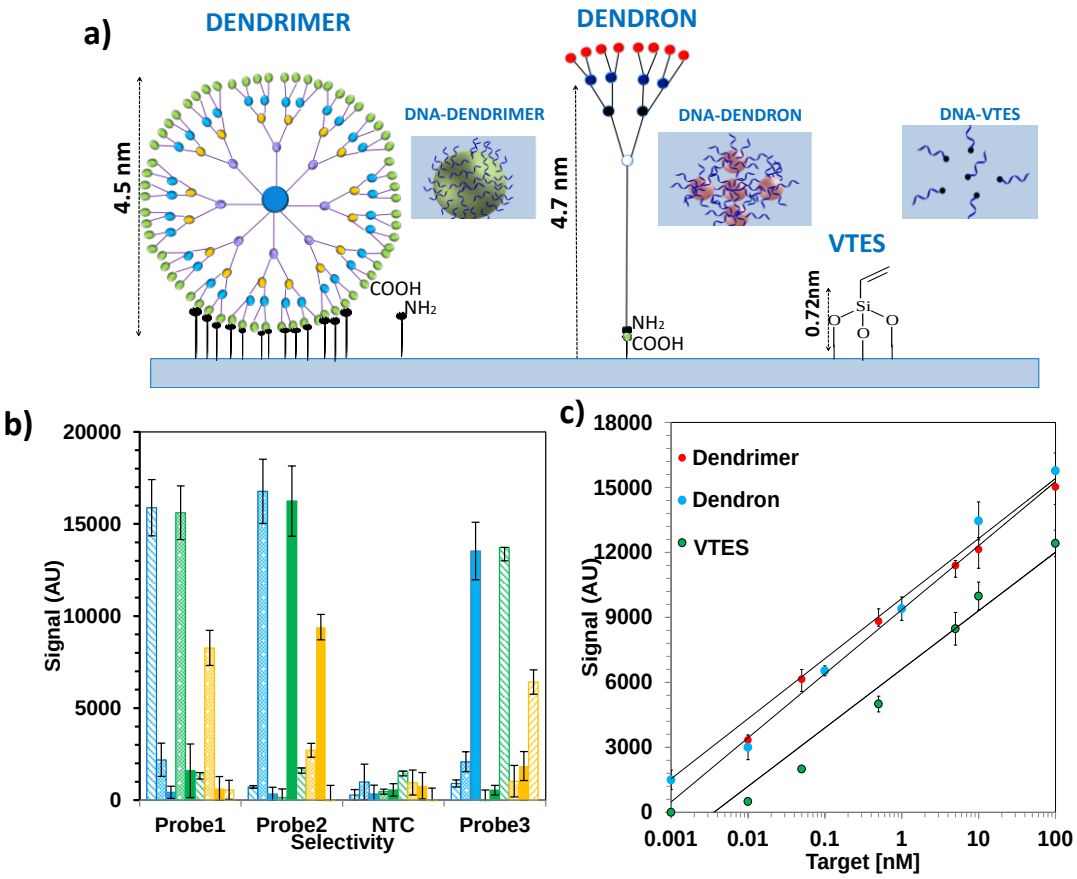

Fig. 4.2. 3D and 2D chips. **a**) Scheme of functionalized polycarbonate chips: vertical view of dendrimer with 64 carboxylic-branches, dendron with 8 alkyl-branches (3D-surfaces) and VTES silane (2D-linear surfaces). Top view of DNA immobilized surface with dendrimer, dendrons and VTES for the same occupied area. **b**) Spot signal for selective hybridization assay with complementary and no-complementary target. **c**) Spot intensity for calibration concentration of target (0.001-100 nM) hybridized with 100 nM complementary oligo.

Integration assay

For the integration of blocked-RPA mechanism in forest-array polymer chip, we firstly tested the blocked-RPA parameters. For that, CRC cell line HCT116 wich harbours a heterozygous H1047R mutation (Hao, 2016) has been applied, the reaction was conducted under isothermal conditions between 15 and 50 ºC, and the incubation time was extended from 0 to 60 min, respectively. Altought RPA amplification assay can operate at varying temperatures (22-45ºC) and reaction times (20-40 min) (Li, 2018),

here, for *PIK3CA*^{H1047R} blocked-RPA amplification, the selected conditions were founded at 37ºC and 40 min, according with previous studies (Martorell, 2018) (Fig.S4.2). Then, a serial concentration of ddC blocker (0-100 nM) was added to RPA mastermix and detected by allele-specific hybridization with restrictive conditions (formamide 25%, low ionic strength). As shown in Fig.S4.3, the addition of blocker oligonucleotide exhibit a dose-dependent suppression of wild type *PIK3CA* RPA-product signal.These results were compared with blocked-PCR approach and similar data were obtained, however, a signal increase of 15±5% was observed for blocked-RPA product hybridization**.** These results demonstrated that the competition between the upstream primer and the blocker reduced the percentage of amplified wild-type allele, promoting selective detection of *PIK3CA*^{H1047R} mutation. Furthermore, the method enables the discrimination between mutants in the same locus of *PIK3CA* gene in exon 20 (p.H1047R (G), p.H1047L (T), p.H1047P (C)) and even in different exon of the same gen (p.E542K (A)). After amplification process, mutant *PIK3CA*^{H1047R} blocked products were purified and hybridized with wild type RPA mixed products in order to corroborate the product formation and the selectivity of the approach (Fig.S3. 4).

For the optimization of analytical capabilities of dendronized *PIK3CA*^{H1047R} integrated platform, hybridization kinetics and sensitivity assays were evaluated. For that purpose, the hybridization process was runed at varying times (0-70 min), for 20 minutes of reaction, 50% of signal was observed, while for signal saturation, 60 minutes were needed. Moreover, in order to determine the LOD of the system, a calibration curve at varying amounts of genomic DNA (0.005-16 ng/ µL) from CRC cell line HCT116 was tested. Saturation signal was obtained for concentration up to 8 ng/µL and LOD of method was found at 0.02ng/ µL (65 genomic DNA copies) (Fig. 4.3).

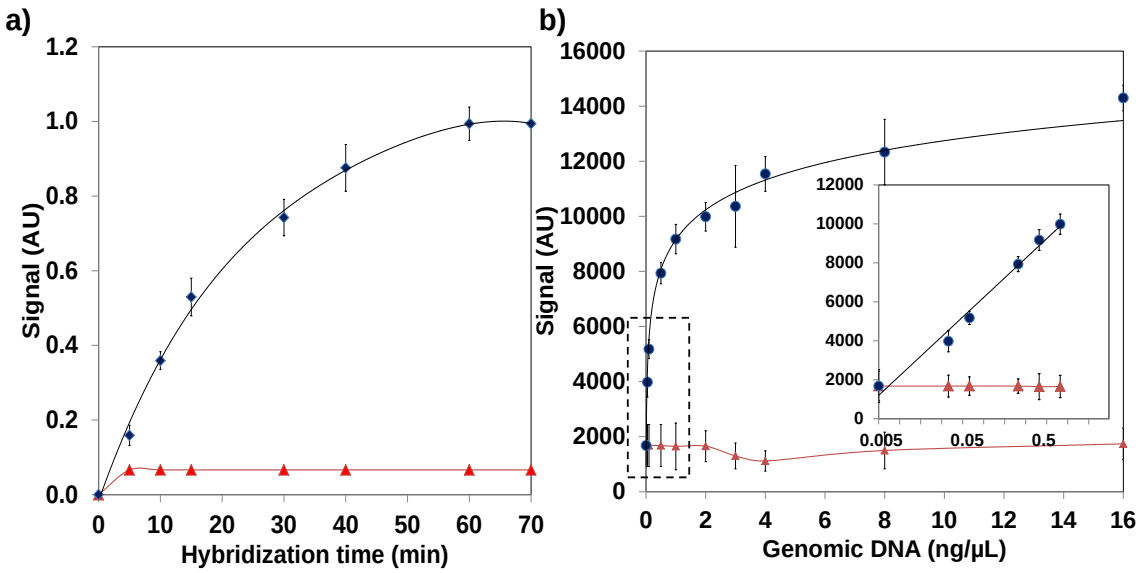

Fig. 4. 3. Analytical capabilities of dendro-polymer chip. **a**) Influence of hybridization time in registered signal. **b**) Calibration curve of genomic DNA hybridized in forest-array 0.005-16 ng/ µL.

Performances on chamber-chip

For miniaturization of integrated platform, sealed chips with microfluidic channels were fabricated. This chamber-chip enables the reduction of the volume reaction and prevents the contamination of the sample than the planar chip. Each aligned hybridization camera contains a dendron-spot-line for sensitivity enhancement and possess 20 µL of capacity. Just 2 µL of blocked RPA product were needed for test-line detection in comparison with 4 µL needed for planar chip assay. Moreover, the washing and detection buffers volumes were reduced at 50% for each sample too. This platform it was made from simple, inexpensive, and low cost plastic materials, no pumps were required and eight hybridization reactions were loading in parallel per chip. Equal experimental conditions were implemented for fluidic and no-fluidic chips for mutation detection of *PIK3CA*^{H1047R} human samples, similar responses with no significate differences were achieved for both assay formats (**Fig. 4**).

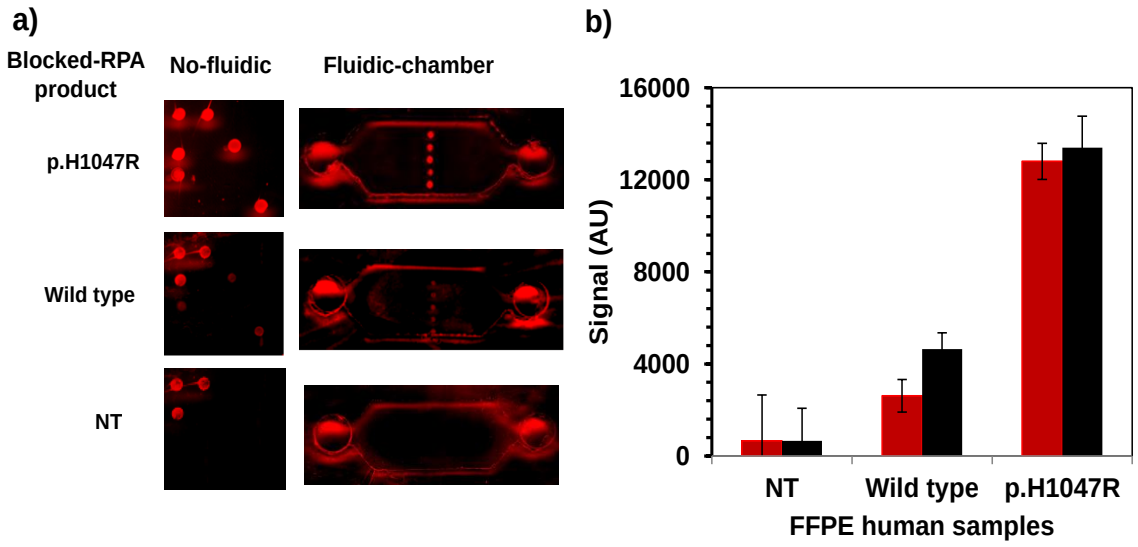

Fig. 4.4. Detection of mutation *PIK3CA*^{H1047R} after blocked RPA amplification in fluidic and no fluidic dendron chip. **a**) Comparative capture array-images for *PIK3CA* detection (mutant (p.H1047R), wild type and no human negative template (NT)) in no fluidic and fluidic-chamber chip. **b**) Spot signals of comparative formats for mutation discrimination assay.

Aplication

The developed method was evaluated for *PIK3CA*^{H1047R} mutation detection of human samples from formalin-fixed paraffin-embedded tissues. Those extracts exhibited high degradation due to fixation. Moreover, these clinical samples possess an elevate wild type proportion and low concentration of mutated DNA. Six samples were classified as wild-type and six samples as p.H1047R mutant (Fig. 4.5). Those results are in concordance with the results reported by the reference method (NGS).

The displayed results exhibit powerful abilities to detect the rare mutated alleles in heterozygous tissue specimens of human cancers. The selectivities and sensitivities achieved with integrated RPA-blocked forest genosensor are comparable to those obtained by selective isothermal approaches such as PE-RCA (Li, 2019) or by LAMP approaches, like, USS-sbLAMP (Kalofonou, 2020) or PE-LAMP (Ding, 2019),with the advantges that requires less time and oligonucleotides in the amplification process.

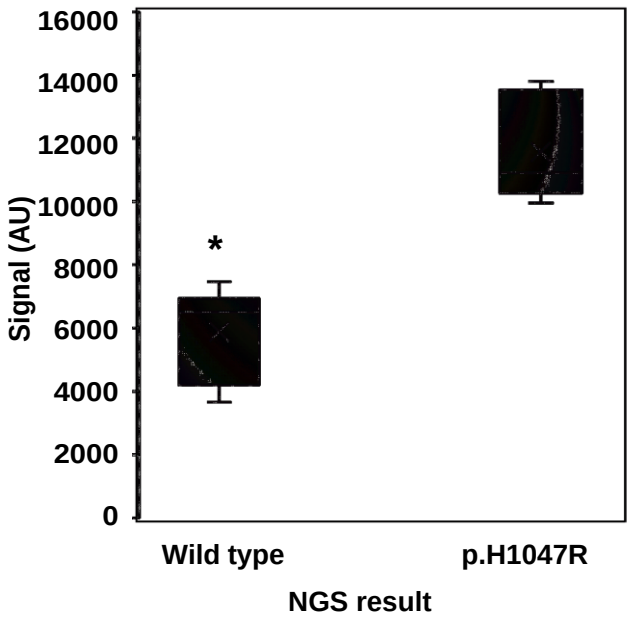

Fig. 4.5: Patients discrimination of *PIK3CA*^{H1047R} mutation with blocked-RPA dendron-polymer chip integrated genosensor. T-test:*p-value<.05.

Conclusions

Here, we presented an integrate platform for *PIK3CA*^{H1047R} mutation detection based on the combination of RPA isothermal amplification with high density dendron polymer-chip for easy colorimetric detection.This genosensor enables the single point mutation detection in heterogeous human samples with higher concentration of wild type genomic DNA. The selectivity of the approach is reached thanks to the addition of a ddC blocker, wich promotes the enrichment of minority alleles. The Blocked-RPA amplification operates at 37ºC (no expensive equipment is required), only requires 3 oligonucleotides and 40 minutes for amplification process compared to other isotherms amplification techniques, wich is correlated with lower energy consumption.

The fabrication of polymer integrated platforms represents a clear advantage in terms of prototyping, cost, portability, as well as the ability to generate 3D and µfluidic systems for the construction of closed and fast-reading consumables. Here, we developed a dendron-polymer chip by fast and clean click chemistry on functionalized thermoplastic polycarbonate surface for enhancement the sensitivity and detect low concentration of blocked-RPA products. The presented integrated *PIK3CA*^{H1047R}

genosensor exhibit higher analytical capabilities than linear surfaces due to the large number of allele-specific probe binding sites per surface area, the great flexibility of hiperbranches structure, the reduction of steric impediments and the surface-probe distance. This genosensor contributes to new generation of biomedical devices analyses on site, point-of-care and low cost diagnostics.

References

1. Zarei, M. (2017). Portable biosensing devices for point-of-care diagnostics: Recent developments and applications. *TrAC Trends in Analytical Chemistry*, *91*, 26-41.
2. Ravi, N., Cortade, D. L., Ng, E., & Wang, S. X. (2020). Diagnostics for SARS-CoV-2 detection: A comprehensive review of the FDA-EUA COVID-19 testing landscape. Biosensors and Bioelectronics, 165, 112454.
3. Li, J., Macdonald, J., & von Stetten, F. (2018). A comprehensive summary of a decade development of the recombinase polymerase amplification. Analyst, 144(1), 31-67.
4. Lei, R., Wang, X., Zhang, D., Liu, Y., Chen, Q., & Jiang, N. (2020). Rapid isothermal duplex real-time recombinase polymerase amplification (RPA) assay for the diagnosis of equine piroplasmosis. *Scientific reports*, *10*(1), 1-11.
5. Yin, J., Zou, Z., Hu, Z., Zhang, S., Zhang, F., Wang, B., ... & Mu, Y. (2020). A "sample-in-multiplex-digital-answer-out" chip for fast detection of pathogens. Lab on a Chip, 20(5), 979-986.
6. Mondal, D., Ghosh, P., Khan, M. A. A., Hossain, F., Böhlken-Fascher, S., Matlashewski, G., ... & Abd El Wahed, A. (2016). Mobile suitcase laboratory for rapid detection of Leishmania donovani using recombinase polymerase amplification assay. Parasites & vectors, 9(1), 281.
7. Lobato, I. M., & O'Sullivan, C. K. (2018). Recombinase polymerase amplification: basics, applications and recent advances. Trac Trends in analytical chemistry, 98, 19-35.
8. Wang, L., Hu, H., Pan, Y., Wang, R., Li, Y., Shen, L., ... & Chen, H. (2014). PIK3CA mutations frequently coexist with EGFR/KRAS mutations in non-small cell lung cancer and suggest poor prognosis in EGFR/KRAS wildtype subgroup. *PloS one*, *9*(2), e88291
9. Martorell, S., Palanca, S., Maquieira, Á., & Tortajada-Genaro, L. A. (2018). Blocked recombinase polymerase amplification for mutation analysis of PIK3CA gene. *Analytical biochemistry*, *544*, 49-56.

10. Zeng, Q., Xie, L., Zhou, N., Liu, M., & Song, X. (2017). Detection of PIK3CA mutations in plasma DNA of colorectal cancer patients by an ultra-sensitive PNA-mediated PCR. Molecular diagnosis & therapy, 21(4), 443-451.
11. Wang, J., Koo, K. M., Wee, E. J., Wang, Y., & Trau, M. (2017). A nanoplasmonic label-free surface-enhanced Raman scattering strategy for non-invasive cancer genetic subtyping in patient samples. Nanoscale, 9(10), 3496-3503.
12. Ivanov, A. V., Safenkova, I. V., Zherdev, A. V., & Dzantiev, B. B. (2020). Nucleic acid lateral flow assay with recombinase polymerase amplification: Solutions for highly sensitive detection of RNA virus. Talanta, 210, 120616.
13. Lázaro, A., Yamanaka, E. S., Maquieira, A., & Tortajada-Genaro, L. A. (2019). Allele-specific ligation and recombinase polymerase amplification for the detection of single nucleotide polymorphisms. Sensors and Actuators B: Chemical, 298, 126877
14. Roy, D., & Park, J. W. (2015). Spatially nanoscale-controlled functional surfaces toward efficient bioactive platforms. *Journal of Materials Chemistry B*, *3*(26), 5135-5149.
15. Caminade, A. M., Padie, C., Laurent, R., Maraval, A., & Majoral, J. P. (2006). Uses of dendrimers for DNA microarrays. Sensors, 6(8), 901-914.
16. Hao, X., Yeh, P., Qin, Y., Jiang, Y., Qiu, Z., Li, S., ... & Cao, X. (2019). Aptamer surface functionalization of microfluidic devices using dendrimers as multi-handled templates and its application in sensitive detections of foodborne pathogenic bacteria. Analytica chimica acta, 1056, 96-107.
17. Akers, P. W., Hoai Le, N. C., Nelson, A. R., McKenna, M., O'Mahony, C., McGillivray, D. J., ... & Williams, D. E. (2017). Surface engineering of poly (methylmethacrylate): Effects on fluorescence immunoassay. Biointerphases, 12(2), 02C415.
18. Erdem, A., Eksin, E., Kesici, E., & Yaralı, E. (2018). Dendrimers Integrated Biosensors for Healthcare Applications. In Nanotechnology and Biosensors (pp. 307-317). Elsevier
19. Kawauchi, T., Oguchi, Y., Nagai, K., & Iyoda, T. (2015). Conical Gradient Junctions of Dendritic Viologen Arrays on Electrodes. *Scientific reports*, *5*(1), 1-11.

20. Warner, C. N., Hunter, Z. D., Carte, D. D., Skidmore, T. J., Vint, E. S., & Day, B. S. (2020). Structure and Function Analysis of DNA Monolayers Created from Self-Assembling DNA–Dendron Conjugates. *Langmuir*, *36*(19), 5428-5434
21. Carlmark, A., Malmström, E., & Malkoch, M. (2013). Dendritic architectures based on bis-MPA: functional polymeric scaffolds for application-driven research. *Chemical Society Reviews*, *42*(13), 5858-5879
22. Paez, J. I., Martinelli, M., Brunetti, V., & Strumia, M. C. (2012). Dendronization: A useful synthetic strategy to prepare multifunctional materials. *Polymers*, *4*(1), 355-395
23. Öberg, K., Ropponen, J., Kelly, J., Löwenhielm, P., Berglin, M., & Malkoch, M. (2013). Templating gold surfaces with function: A self-assembled dendritic monolayer methodology based on monodisperse polyester scaffolds. *Langmuir*, *29*(1), 456-465
24. Anavi, D., Popowski, Y., Slor, G., Segal, M., Frid, L., Amir, R. J., ... & Amir, E. (2018). Covalent functionalization of solid cellulose by divergent synthesis of chemically active dendrons. *Journal of Polymer Science Part A: Polymer Chemistry*, *56*(18),
25. Kim, D. H., Kang, H. S., Hur, S. S., Sim, S., Ahn, S. H., Park, Y. K., ... & Lee, J. H. (2018). Direct detection of drug-resistant hepatitis B virus in serum using a Dendron-modified microarray. Gut and liver, 12(3), 331.
26. Escorihuela, J., Banuls, M. J., Grijalvo, S., Eritja, R., Puchades, R., & Maquieira, A. (2014). Direct covalent attachment of DNA microarrays by rapid thiol–Ene “Click” chemistry. Bioconjugate chemistry, 25(3), 618-627.ints by thiol–ene or thiol–yne coupling chemistry. Bioconjugate chemistry, 28(2), 496-506.
27. Bañuls, M. J., González-Martínez, M. Á., Sabek, J., García-Rupérez, J., & Maquieira, Á. (2019). Thiol-click photochemistry for surface functionalization applied to optical biosensing. *Analytica chimica acta*, *1060*, 103-113
28. Jiménez-Meneses, P., Bañuls, M. J., Puchades, R., & Maquieira, A. (2018). Fluor-thiol photocoupling reaction for developing high performance nucleic acid (NA) microarrays. *Analytical chemistry*, *90*(19), 11224-11231. microarraying of half-antibodies. *Chemical Communications*, *54*(48), 6144-6147.

29. Hao, Y., Samuels, Y., Li, Q., Krokowski, D., Guan, B. J., Wang, C., ... & Wang, Z. (2016). Oncogenic PIK3CA mutations reprogram glutamine metabolism in colorectal cancer. Nature communications, 7(1), 1-13.
30. Kalofonou, M., Malpartida-Cardenas, K., Alexandrou, G., Rodriguez-Manzano, J., Yu, L. S., Miscourides, N., ... & Toumazou, C. (2020). A novel hotspot specific isothermal amplification method for detection of the common PIK3CA p. H1047R breast cancer mutation. Scientific reports, 10(1), 1-10
31. Ding, S., Chen, R., Chen, G., Li, M., Wang, J., Zou, J., ... & Tang, Z. (2019). One-step colorimetric genotyping of single nucleotide polymorphism using probe-enhanced loop-mediated isothermal amplification (PE-LAMP). Theranostics, 9(13), 3723.
32. Li, X. H., Zhang, X. L., Wu, J., Lin, N., Sun, W. M., Chen, M., ... & Lin, Z. Y. (2019). Hyperbranched rolling circle amplification (HRCA)-based fluorescence biosensor for ultrasensitive and specific detection of single-nucleotide polymorphism genotyping associated with the therapy of chronic hepatitis B virus infection. Talanta, 191, 277-282

Supplementary Information

Complementary experiments

For optimization and comparison purposes in terms of sensitivity and selectivity, additional chips were fabricated. In all cases, the substrates were activated by plasma UV/ozone oxidation, as previously described.

EDA/COOH-PAMAM chips. Amine functionalized dendrimers (COOH-PAMAM dendrimer, generation 3.5, Sigma Aldrich) were immobilized in active-amino-plastic chip. The treatment of activated chips consisted in incubation of cross-linker solution (EDA 1%, EDC 50 mM). Non-contact printing of COOH-dendrimer conjugated with NH_2-probe via EDC/NHS was fabricated.

VTES chips (Thiol-reaction). Thiol-probes were grafted on activated plastic chips by thiol-ene click chemistry reaction without Dendron mediated. After photo-activation, a solution of vinyltriethoxysilane (VTES, Sigmal Aldrich) at 3% in isopropanol was incubated for 1 h at room temperature. Chips were washed several times with isopropanol, air-dried and heated at 110 °C for 1 h. Thiol-DNA probes in PBS buffer were dispensed on the activated surface (40 nL). Finally, chips were irradiated during 30 s by UV-ozone at 254 nm, washed and air dried.

Table S4.1. List of used oligonucleotides.

Synthetic perfect match

Target	Use	Sequence 5'-3'
A	Thiol-probe	TTGCTGATTTTCAACATCAGTCTGATAAGCTA-T_{10}-SH
	Amine-probe	GATTTTCAACATCAGTCTGATAAGCTATTTTT-NH_2
	Target	TAGCTTATCAGACTGATGTTGAAAATCAGCAA-DIG
B	Thiol-probe	TTGCTGATTTCAGCTGCTTTTGGGATTCCGTTG-T_{10}-SH
	Amine-probe	GATTTCAGCTGCTTTTGGGATTCCGTTGTTTTT-NH_2
	Target	CAACGGAATCCCAAAAGCAGCTGAAATCAGCAA-DIG
C	Thiol-probe	TTGCTGATTTACCCCTATCACGATTAGCATTAA-T_{10}-SH
	Amine-probe	GATTTACCCCTATCACGATTAGCATTAATTTTT-NH_2
	Target	TTAATGCTAATCGTGATAGGGGTAAATCAGCAA-DIG

PIK3CA gene

Exon	use	Sequence 5'-3'
20		
	FP-c	TTTGGAGTATTTCATGAAACAAATG
	RP	DIG-TGTGTGGAAGATCCAATCCATT
	Blocker	TGAATGATGCACATCATGGTGGCT-23ddC
	Wild-type	NH_2-C6-TTTTTTTTTT-AATGATGCACATCATGGTGGCT
	p.H1047R	NH_2-C6-TTTTTTTTTT-ATGATGCACGTCATGGTGGC
	p.H1047L	NH_2-C6-TTTTTTTTTT-AATGATGCACTTCATGGTGGCT
	p.H1047P	NH_2-C6-TTTTTTTTTT-ATGATGCACCTCATGGTGGC
	p.H1047R	SH-C6-TTTTTTTTTT-ATGATGCACGTCATGGTGGC

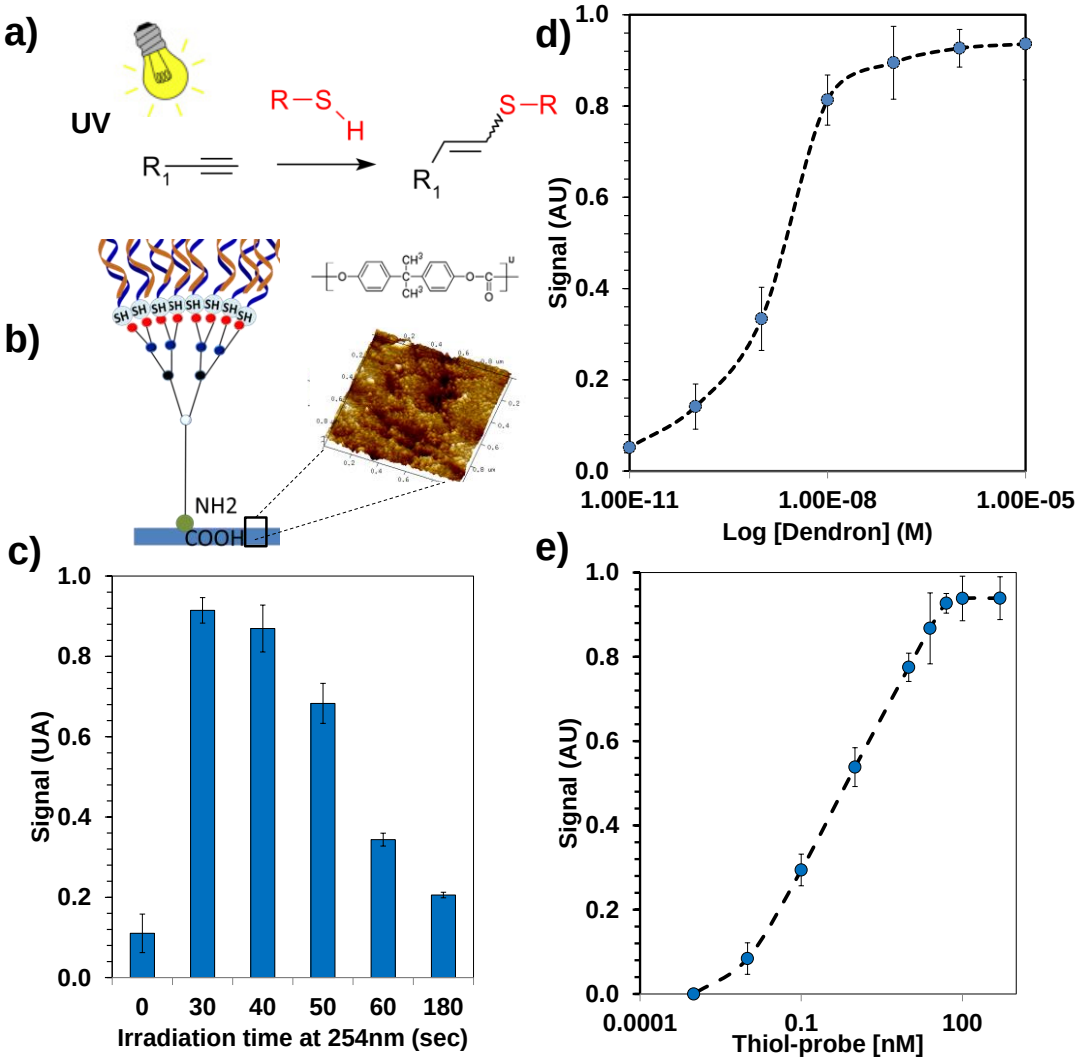

Fig. S4.1: Optimization of DNA-dendron conjugation by click chemistry. **a**) Scheme assay of thiol-yne reaction by photoactivation. **b**) Hybridization of target with DNA-dendron conjugate onto active PC polymer. **c**)Spot signal for thiol-probe immobilization via click chemistry at different irradiation times (λ=254nm). **d)** Signal intensities at different concentration of alkyne-dendron (10^{-5}M to 10^{-10}M) at 100 nM of thiol DNA probe in hybridization assay. **e)** Signal intensities at different concentration of thiol DNA probe with 10^{-8} M of alkyne-dendron in hybridization assay.

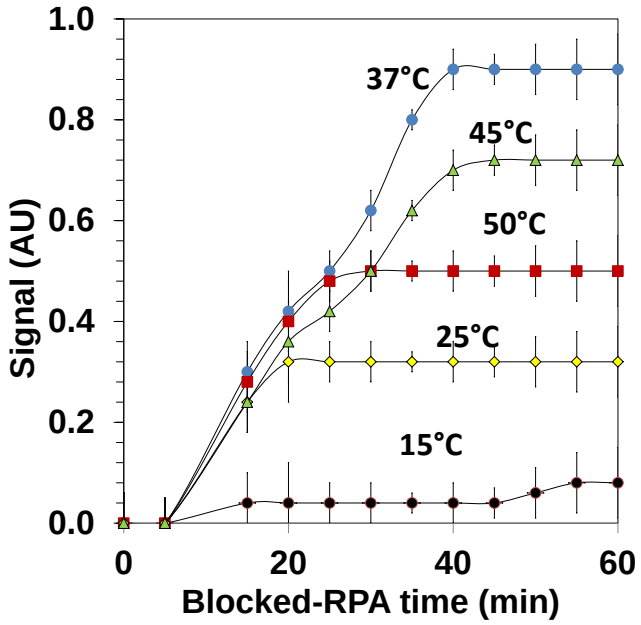

Fig. S4.2. Influence of isothermal temperature and reaction time at blocked-RPA amplification for *PIK3CA*^{H1047R} mutation detection

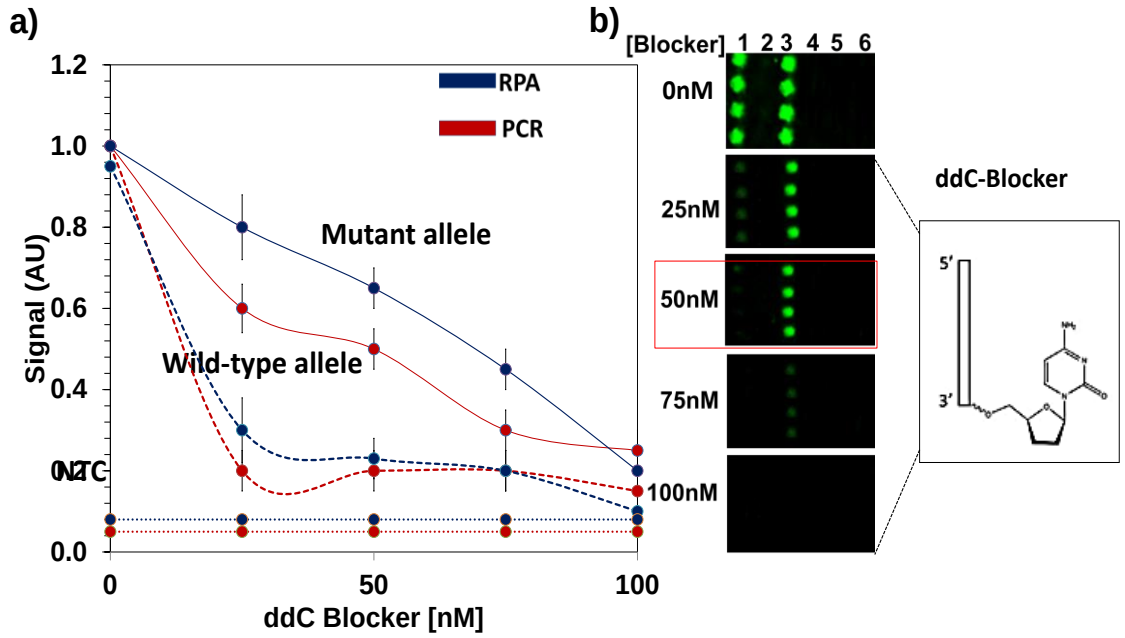

Fig. S4.3: **a**) Hybridization signal of mutant *PIK3CA*^{H1047R} sample by blocked-RPA and blocked-PCR approach at varying concentration of ddC Blocker. **b**) Capture array image for different amounts of blocking agent correlated with loss signal of wild type probe signal (1:Wild type; 2: p.E542K (A); 3: p.H1047R (G); 4: p.H1047L (T); 5: p.H1047P; 6: NTC)

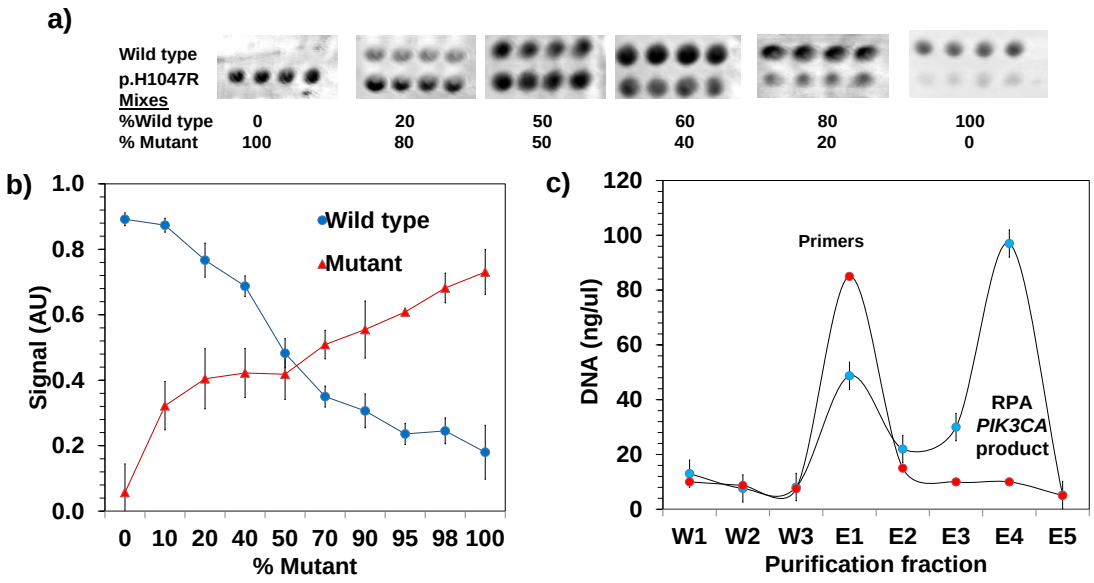

Fig. S4.4: **a)** Capture-array image of hybridization mixes in allele-specif chip of blocked-RPA *PIK3CA*^{H1047R} mutant/wild-type products at varyng concentrations. **b)** Hybridization mixes of mutant RPA blocked products with wild-type products at varyng concentrations. **c)** Purification of blocked-RPA product (Red: Blocked-RPA mix without template, blue: Blocked-RPA *PIK3CA*^{H1047R} product.

Conclusiones

Conclusiones

Como resultado de las investigaciones llevadas a cabo en esta tesis, se ha demostrado, por primera vez, que es posible la amplificación isoterma bloqueada por recombinasa-polimerasa (RPA-bloqueada). Además, esta estrategia ha permitido la amplificación selectiva de los alelos mutantes de los genes *PIK3CA, KRAS* y *NRAS* en presencia de los alelos nativos y, en consecuencia, detectar mutaciones puntuales minoritarias. Por otro lado, se han señalado las ventajas que presenta frente a otras reacciones de amplificación.

(i) Trabaja a temperatura constante (entre 25 y 40ºC) evitando la necesidad de un termociclador de PCR.

(ii) Utiliza sólo 3 oligonucleótidos sin funcionalización de alto costo (2 cebadores y un agente bloqueante tipo ddC) frente a técnicas que utilizan 4 o 5 cebadores (ej. LAMP o SDA) o funcionalizaciones tipo PNA o LNA.

(iii) La técnica RPA-bloqueada es más rápida (20-40 min) que la PCR (60-120 min) y que otros ensayos isotermos (ej. LAMP 60 min).

(iv) No requiere de una etapa previa de desnaturalización y opera a temperatura constante, lo que es una gran ventaja al no requerir de termociclador ni regulación exacta de la temperatura.

Las plataformas desarrolladas en esta tesis consiguen reducir en un 50 % la señal procedente de los alelos nativos, detectando bajas proporciones del alelo mutante (5%). Se ha demostrado la efectividad de la RPA bloqueada en el enriquecimiento de alelos minoritarios, discriminando selectivamente (95%) los alelos mutantes en muestras heterogéneas, procedentes de tejido biopsiado, las cuales presentan una elevada proporción de alelos nativos. Los resultados obtenidos han sido comparados en todas las plataformas con la PCR-bloqueada, observándose selectividades equiparables y sensibilidades ligeramente superiores (±15%) utilizando la variante RPA bloqueada.

Respecto a otras tecnologías de discriminación de mutaciones puntuales, las aproximaciones desarrolladas en la presente tesis doctoral han proporcionado respuestas semejantes a las de la pirosecuenciación (5-10% mutante), PCR a tiempo real (10% mutante) o PCR-RFLP (5%). Aunque métodos como COLD-PCR o PNA-LNA PCR, también basados en enriquecimiento de alelos, consiguen selectividades ligeramente superiores (1% mutante), las plataformas desarrolladas ofrecen ciertas ventajas. Así, tienen mayor capacidad de multiplexado, disminución de consumo energético y coste, así como, reducción de los tiempos de respuesta. Además, mejoran la portabilidad y no requieren de equipos sofisticados ni infraestructuras costosas, lo que permite realizar test en punto de atención.

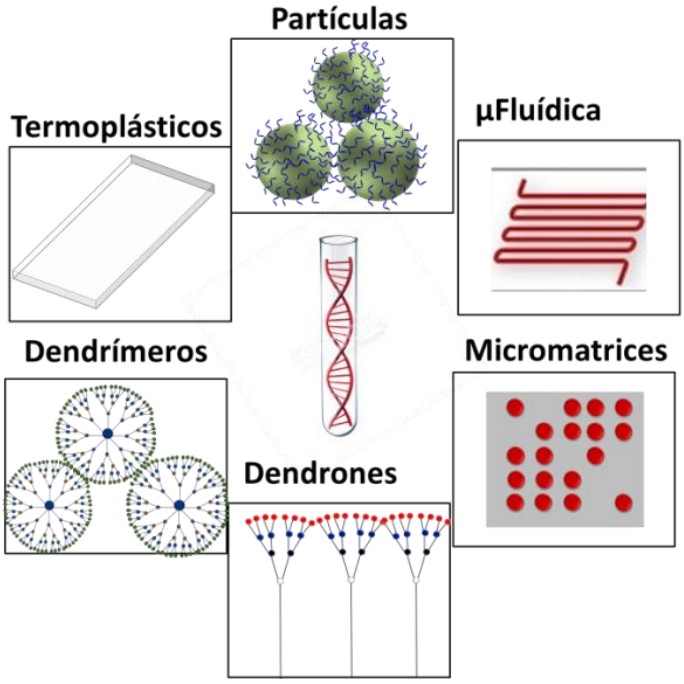

Además, los productos de la amplificación isoterma RPA-bloqueada se han detectado con ensayos de hibridación en formatos que combinan materiales como partículas magnéticas, dendrímeros o dendrones y polímeros termoplásticos para desarrollar genosensores de altas prestaciones.

Con la plataforma desarrollada en el capítulo dos, se ha logrado la hibridación homogénea de producto RPA-bloqueado con micropartículas magnéticas conjugadas a

sondas alelo específicas, discriminando mutaciones de un único nucleótido en el codón 12 de gen *KRAS*, de manera selectiva (95%) y sensible (250 copias). El sistema integrado por chips con canales fluídicos y una plataforma de imanes, ha permitido reducir los tiempos de hibridación (20 min), volúmenes de reacción (50%) e interferencias. Este sistema es muy novedoso frente a otros desarrollos que combinan partículas magnéticas con la amplificación RPA para cribado de fármacos, o detección de patógenos. En el área de cáncer, únicamente se comunicaronen 2019 los resultados de un biosensor electroquímico para la detección la mutación $BRAF^{V600}$ en células tumorales (CTC).

Las plataformas desarrolladas en los capítulos tres y cuatro, utilizan chips planos donde las sondas han sido inmovilizadas mediadas con polímeros orgánicos hiperramificados de dendrímeros y dendrones, para generar superficies de alta densidad. Ambas plataformas ofrecen ventajas en términos de sensibilidad, puesto que consiguen reducir el límite de detección a 64 copias de ADN genómico y 0.001 nM de ADN sintético frente a la plataforma 1, mejorando los límites de detección entre 10 y100 veces. Esta respuesta se debe a la capacidad que tienen dichas estructuras dendríticas para generar superficies 3D, lo cual incrementa los sitios de anclaje por unidad de superficie y mejora la densidad de inmovilización (13 pmol/cm^2) en comparación con superficies planas 2D (6 pmol/cm^2).

Si bien es cierto que ambas aproximaciones ofrecen respuestas similares en términos de selectividad y sensibilidad, la plataforma 4 presenta ventajas en términos de velocidad de reacción, puesto que sólo requiere de 30 segundos para la conjugación covalente tiol-ino de sondas tioladas a dendrones con grupos alquilo frente a los 60 minutos requeridos para la conjugación de dendrímeros carboxílicos. Además, los tiempos de activación de los grupos presentes en la superficie de estos materiales también se ven reducidos (20 min) así como el volumen de muestra (20 µL frente a 50 µL). Aunque estas estructuras fractales han sido aplicadas para la detección de mutaciones a partir de producto de PCR, este trabajo es el primero que combina el mecanismo de amplificación isoterma de RPA con moléculas dendriméricas, dirigido a

la detección de mutaciones puntuales en los oncogenes *BRAF*^{V600} y *PIK3CA*^{H1047R}, a partir de muestras complejas procedentes de tejido tumoral.

De acuerdo con los resultados obtenidos, tanto en prestaciones analíticas como su aplicación en el análisis de muestras procedentes de pacientes oncológicos, permite afirmar que se han alcanzado los objetivos planteados en la tesis. Además, las plataformas, metodologías y aplicaciones desarrolladas en la presente tesis doctoral representan una nueva generación de genosensores que cumplen con las prestaciones ASSURED, indicadas por la Organización Mundial de la Salud, para sistemas de apoyo al diagnóstico y exigidos por la sociedad del siglo XXI.

Publicaciones

1. Martorell, S., Palanca, S., Maquieira, Á., & Tortajada-Genaro, L. A. (2018). Blocked recombinase polymerase amplification for mutation analysis of *PIK3CA* gene. Analytical Biochemistry, 544, 49-56.
2. Martorell, S., Tortajada-Genaro, L. A., & Maquieira, Á. (2019). Magnetic concentration of allele-specific products from recombinase polymerase amplification. Analytica Chimica Acta, 1092, 49-56.
3. Martorell, S., Tortajada-Genaro, L. A., González-Martínez, M. A., & Maquieira, A. (2021). Surface coupling of oligo-functionalized dendrimers to detect DNA mutations after blocked isothermal amplification. Microchemical Journal, 106546.
4. Genosensor for *PIK3CA*^{H1047R} mutation detection after blocked recombinase polymerase amplification in dendron plastic chip. (En redacción)

Congresos

1. Título del trabajo: Plastic substrates as platforms for mutational analysis of oncogenes Nombre del congreso: X International Workshop on Sensors and Molecular Recognition Ciudad de celebración: Valencia, España, Fecha de celebración: 08/07/2016 Sara Martorell Tejedor; Ángel Maquieira Catalá; S. Palanca; Luis Antonio Tortajada Genaro. "Libro de artículos". pp. 293 - 296.

2. Luis Antonio Tortajada Genaro; Sara Martorell Tejedor; Ana Lázaro Zaragozá; Sarai Palanca; Ángel Maquieira Catalá. Detección de mutaciones en oncogenes en el tratamiento dirigido al cáncer colorrectal. Actualidad Analítica. 60, pp. 21 - 24. 2017. ISSN 2340-8006

3. Título del trabajo: DNA-based assay of mutation hotspots using magnetic beads. Nombre del congreso. Valencia, España, Fecha de celebración: 07/07/2017 Sara Martorell Tejedor; Luis Antonio Tortajada Genaro; Ángel Maquieira Catalá. "XI International Workshop on Sensors and Molecular Recognition". pp. 166 - 169.

4. Título del trabajo: mutational analysis of braf oncogene in colorectal cancer patients. Nombre del congreso. Valencia, España, Fecha de celebración: 07/07/2017 Irene Jiménez Romero; Ana Lázaro Zaragozá; Sara Martorell Tejedor; Luis Antonio Tortajada Genaro; Ángel Maquieira Catalá. "XI International Workshop on Sensors and Molecular Recognition". pp. 121 - 125.
5. Título del trabajo: Estabilidad de ácidos nucleicos: análisis termodinámico para el bio-reconocimiento de mutaciones y polimorfismos Nombre del congreso: XXXVI Reunión Bienal de la Real Sociedad Española de Química (RSEQ 2017) Ciudad de celebración: Sitges, Spain, Fecha de celebración: 29/06/2017 Luis Antonio Tortajada Genaro; ERIC SEITI YAMANAKA; Sara Martorell Tejedor; Ana Lázaro Zaragozá; Rosa Puchades Pla; Ángel Maquieira Catalá. pp. 0 - 0.
6. Título del trabajo: DNA biosensor base don chitosan film. Valencia, España, Fecha de celebración: 07/07/2019 Sara Martorell Tejedor; Luis Antonio Tortajada Genaro; Ángel Maquieira Catalá. "XII International Workshop on Sensors and Molecular Recognition".
7. Título del trabajo: Biosensado en formato micromatriz para la detección de miRNA. Ciudad de celebración: Valencia, España, Fecha de celebración: 07/07/2019 Belén Sirera Conca; Sara Martorell Tejedor; Luis Antonio Tortajada Genaro; Ángel Maquieira Catalá. "XIII International Workshop on Sensors and Molecular Recognition".
8. Título del trabajo: Dendron-mediated chip for integrated genosensing. Valencia, España, Fecha de celebración: 08/07/2021 Sara Martorell Tejedor; Luis Antonio Tortajada Genaro; Ángel Maquieira Catalá. "XIV International Workshop on Sensors and Molecular Recognition". (En redacción)

Tabla resumen. Comparativa entre las plataformas desarrollas en la tesis.

	Plataforma 1	**Plataforma 2**	**Plataforma 3**	**Plataforma 4**
Biomarcador diana	*PIK3CA e9, e20*	*KRAS c12*	*BRAF v600*	*PIK3CA e20*
Amplificación	RPA bloqueada	RPA bloqueada	RPA bloqueada	RPA bloqueada
[oligo bloqueante]	50 nM	70 nM	40 nM	50 nM
Reducción señal nativa con bloqueo	50%	50%	50%	50%
Reducción señal mutante con bloqueo	7%	6%	5%	6%
Formato hibridación	Heterogéneo	Homogéneo	Heterogéneo	Heterogéneo
Sistema microfluídico	No	Sí	No	Sí
V muestra (µL)	5	2	5	2
Nanoherramienta	-	Partículas MNPs	Dendrímeros	Dendrones
Superficie	PC	Partícula/COP	PC/COP	PC
Química de anclaje	Covalente Carbodiimida	Covalente Carbodiimida	Covalente Carbodiimida	Covalente Tiol-ino (Click)
$\rho_{inmovilización}$	6 pmol/cm^2	5 pmol/cm^2	13 pmol/cm^2	13 pmol/cm^2
Absorción inespecífica	5%	30%	10%	5%
Detección	Colorimetría	Fluorescencia	Colorimetría	Colorimetría
Multiplexado	Sí	-	Sí	Sí
Amplificación (min)	40	40	40	30
Activación+inmovilización (min)	70	-	90	70
Conjugación (min)	-	60	60	0.3
Hibridación (min)	60	20	60	60
Selectividad	95%	95%	95%	95%
LOD DNA genómico	500 copias	250 copias	65 copias	65 copias
Reproducibilidad	85-95%	75-85%	85-95%	85-95%
LOD (%mutante)	5%	5%	5%	5%